CHARACTERIZATION OF NS1 GLYCOSYLATION MUTANT VIRUSES AS A POTENTIAL VACCINE CANDIDATE FOR WEST NILE VIRUS

Thesis submitted in accordance with the requirements of the University of Liverpool for the degree of Doctor in Philosophy

by

Melissa Christine Whiteman

February 2008

ABSTRACT

West Nile virus (WNV) is a mosquito-borne flavivirus that has N-linked glycosylation sites on the premembrane (prM) envelope (E) and nonstructural 1 (NS1) proteins. NS1 contains three glycosylation (asparagine-X-threoine [NXT]) sites at $NS1_{130}$, $NS1_{175}$, and $NS1_{207}$. The first aim of the thesis was to attenuate WNV through the ablation of the NS1 glycosylation sites, individually and in all combinations, initially by replacing the asparagine (N) with alanine (A) in the glycosylation motif using site-directed mutagenesis of a WNV infectious clone. Two of the mutants were greatly attenuated, up to 50,000-fold, for lethal neuroinvasiveness in mice, had reduced viraemia at two and three days post-infection relative to the parental strain, but multiplied similarly to the parental strain in Vero cells. Although these viruses were highly attenuated, the most attenuated NS1 mutant virus reverted to virulence and reversion at the first NS1 glycosylation site ($NS1_{130}$) was seen in mice that succumbed to infection. The second aim was to diminish reversion. Thus, the first NS1 glycosylation site was mutated such that it contained two or three amino acid substitutions in the $NS1_{130}$ glycosylation motif (NNT→SVT; NNT→QQA), while the second and third glycosylation sites remained a single N to A amino acid change. These viruses were highly attenuated for mouse neuroinvasiveness and neurovirulence, >100,000-fold and 3,000-fold, respectively, compared to the parental strain and did not revert to virulence. Multiplication kinetics of the attenuated viruses in mice showed a decrease in multiplication compared to the parental strain and a small plaque phenotype. The third aim was to examine a functional role for the NS1 protein using these mutant viruses. Electron microscopy studies of the most attenuated NS1 glycosylation mutant virus revealed changes in the virus-induced structures compared to the parent virus-infected Vero cells that may suggest involvement of the NS1 protein in the formation of these structures. Cytokine expression experiments showed several down-regulated cytokines in the sera of parent and attenuated NS1 mutant virus-infected mice compared to mock-infected serum suggesting that immune evasion by the suppression of cytokines may contribute to the WNV virulence phenotype. Therefore, mutations in the NS1 glycosylation sites were hypothesized to modify virus replication and the host response to infection leading to a mouse attenuated phenotype. Construction of a virus with mutations ablating the glycosylation site in the E protein together with the ablation of the three NS1 glycosylation sites completely attenuated this virus for mouse neuroinvasiveness with an $ipLD_{50}$ >100,000 PFU. It was hypothesized that the ablation of the prM glycosylation site would also attenuate WNV. Contrary to previous studies, however, the ablation of the prM glycosylation site did not attenuate the virus and multiplication kinetics in cell culture revealed that this mutant virus multiplied to higher titres at all time points when compared to the parental strain. Utilization of the mutant viruses generated in this thesis may have potential as effective components of future vaccine candidates.

CONTENTS

LIST OF FIGURES

LIST OF TABLES

ACKNOWLEDGMENTS

I wish to thank my mentors Professor Alan Barrett and Professor Tom Solomon. I would certainly not have completed this thesis if it were not for the dedication and effort of Dr. Barrett. Your faith in me and guidance through the not so straight and narrow path gave me the confidence to persevere. I cannot thank you enough. Thank you also to Dr. Solomon who so graciously agreed to co-mentor and support me through this journey.

I would also like to thank Dr. Rich Kinney and Dr. Claire Huang at the Centres for Disease Control. I am grateful to have had such great technical training. Your patience, guidance and technical skills helped to make me a better scientist. Your kindness towards me transcended the workplace and I am thankful to have your friendship. I would also like to thank my other friends at the CDC, Mel and John Liddell. You took me in as your own and always made me feel happy. I could always count on you to put a smile on my face, even on the really bad days.

To all members of the Barrett Lab, past and present: Shuilu Zhang, Jana Vonlindern, Amber Engel, Greg Gromowski, Sareen Galbraith, Mike Holbrook, Monica McArthur and Fiona May, thanks for making a great work environment. Special thanks to Li Li for your technical support and to you and your husband for letting me borrow all the tools for my house. They helped me to get out some of the frustration I had from the lab! Also thanks to Jason Wicker for helping me with all those mice and not complaining about it, even if it was payback. Thanks to David Beasley for technical

support, especially in training me with the mice. Many thanks also to the members of the Solomon Lab; Allison German and Wipa Tangkananond, thank you for making me feel at home in Liverpool. Special thanks to Jenny Collett for opening your home to me on my visits.

I would also like to thank those at the University of Texas Medical Branch that have helped teach and guide me with various techniques. Thanks to Dr. Vsevolod Popov, Violet Han, Julie Wen, Yvette Girard and Ted Whitworth for EM support, Dr. Thomas Albrecht and Eugene Knutson for confocal support, Gavin Bowick for densitometer support and Dr. Juan Olano, Mike Woods and Robert Baskerville for Bioplex support. Thank you also to Dr. Mike Diamond and Dr. Kyung Min Chung from Washington University in St. Louis for kindly providing the NS1 antibodies.

This thesis is dedicated to my family. I would not have made it this far without your love and support. To my mother who was always there for me and gave me the strength and courage to do anything, nothing I could ever say would express my gratitude to have you as a mother. To my father, whom I'm sure my slightly scattered, sometimes misunderstood yet creative brain comes from. There's always a method to our madness, even if others may not see it right away. And to my talented brother, you were there for me when I needed you the most and I thank you for that.

LIST OF ABBREVIATIONS

Å	angstrom
A	alanine
ADE	antibody-dependent enhancement
ALF	Alfuy
AST	average survival time
BSA-G	Bovine serum albimin-glycine
BGS	Bovine growth serum
C	cysteine
C protein	capsid protein
C6/36	mosquito (*Aedes albopictus*) cell line
cDNA	complementary DNA
CDC	Centres for Disease Control
CSF	cerebral spinal fluid
CM	convoluted membrane
CNS	central nervous system
CPE	cytopathic effect
CRD	carbohydrate recognition site
DAPI	4',6-diamidino-2-phenylindole
DC	dendritic cell
DEN	dengue
DHF	dengue hemorrhagic fever
dNTP	deoxyribonucleotide triphosphate
dsDNA	double-stranded RNA
DTT	dithiothreitol
E protein	envelope protein
EDTA	ethylenediaminetetraacetic acid
EIA	enzyme immunoassay
EM	electron microscopy
ENT	Entebbe bat
ER	endoplasmic reticulum
FITC	Fluorescein
g	gram
GA	gluteraldehyde
GCSF	granulocyte colony-stimulating factor
GMCSF	granulocyte macrophage colony-stimulating factor
GTE	glucose-tris-EDTA
H	histadine
HCl	hydrochloric acid
HCV	hepatitis C virus
hpi	hours post-infection/inoculation

HRP	horseradish peroxidase
ic	intracerebral
ICAM	intercellular adhesion molecule
IFN	interferon
Ig	immunoglobulin
IL	interleukin
ip	intraperitoneal
IRES	internal ribosome entry site
IRF	interferon regulated factor
JAK	Janus kinase
JE	Japanese encephalitis
kb	kilobase
KC	neutrophil chemoattractant
kD	kilodalton
KOK	Kokobera
KUN	Kunjin
L	litre
L-selectin	lymphocyte adhesion molecule
LB	Luria-Bertani
LD_{50}	lethal dose 50
M	molar
M protein	membrane protein
M-CSF	macrophage colony-stimulating factor
MCP	monocyte chemoattractant protein
MEM	modified eagle medium
Mi	mitochondria
MIG	monokine induced by interferon gamma
MIP	macrophage inflammatory protein
moi	multiplicity of infection
µl	microlitre
ml	millilitre
mm	millimetre
mM	milimolar
mRNA	messenger RNA
MTase	methyltransferase
MVE	Murray Valley encephalitis
N	asparagine
Neuro 2A	mouse neuroblastoma cell line
nm	nanometre
NS	nonstructural
nt	nucleotide
NTPase	nucleoside triphosphatase
NY99	New York 1999
Nu	nucleus
P388 D1	murine macrophage cell line

PAGE	polyacrylamide gel electrophoresis
PBS	phosphate buffered saline
PC	paracrystalline array
PCR	polymerase chain reaction
PD_{50}	protective dose 50
PFGPA	paraformaldehyde glutaraldehyde picric acid
PFU	plaque forming unit
RIPA	RadioImmuno Precipitation Assay buffer
prM protein	premembrane protein
$PRNT_{50}$	plaque reduction neutralization test 50
Q	glutamine
RdRp	RNA-dependent RNA polymerase
RNA	ribonucleic acid
RNase	ribonuclease
rpm	revolutions per minute
RT	reverse transcription
S	serine
SD	standard deviation
SDS	sodium dodecyl sulfate
SEP	Sepik
SIGN	specific intercellular adhesion molecule 3-grabbing nonintegrin
SLE	St. Louis encephalitis
SMS	smooth membrane structure
sp	species
STAT	signal transducer and activator of transcription
SVP	subviral protein
TBE	tick-borne encephalitis
TBS	tris buffered saline
TE	Tris-EDTA
TEM	transmission electron microscopy
TIEM	transmission immuno-electron microscopy
Th	T-helper
TLR	Toll-like receptor
TM	transmembrane
TMS	tubular membrane structure
TNF	tumor necrosis factor
ts	temperature sensitive
Tyk	tyrosine kinase
UA	uranylacetate
UK	United Kingdom
US	United States
USU	Usutu
UTR	untranslated region
VLP	virus-like particle
VEGF	vascular endothelial growth factor

Vero	African green monkey kidney cell line
VP	vesicle packet
WNV	West Nile virus
WNF	West Nile fever
X	amino acid
YF	yellow fever

CHAPTER 1 : INTRODUCTION

1.1 General introduction to West Nile virus

West Nile virus (WNV) was discovered in the 1930's when it was isolated from the blood of a febrile woman in Africa (Smithburn *et al.,* 1940). This virus was originally classified as a group B arbovirus due to its cross neutralization with Japanese encephalitis (JE), St. Louis encephalitis (SLE), Murray Valley encephalitis (MVE), Kunjin (KUN), Kokobera (KOK), Stratford and Alfuy (ALF) viruses (De Madrid and Porterfield, 1974). Subsequently, the group B arboviruses have been classified as the genus *Flavivirus* in the family *Flaviviridae*. The *Flaviviridae* is a diverse family, including three genera: *Pestivirus* that includes Bovine virus diarrhea and classical swine fever viruses, *Hepacivirus* that includes hepatitis C virus (HCV) and the genus *Flavivirus*. The latter consists of more than 70 viruses, including mosquito-borne viruses such as dengue (DEN) and yellow fever (YF), tick-borne viruses such as tick-borne encephalitis (TBE) and no known vector-borne viruses such as Entebbe bat (ENT). Currently, WNV is classified in the JE group, which contains ALF, Cacipore, Koutango, JE, MVE, Usutu (USU), WN and Yaounde viruses. Kunjin virus, found in Australia, is classified as a subtype of WNV.

Following the initial isolation in Uganda, the next isolates of WNV were obtained over a decade later from healthy children (Melnick *et al.,* 1951). After this time, isolates collected from several outbreaks suggested that the virulence of this virus varied somewhat. In 1997, one study examined the phylogenetics of 20 WNV isolates collected from several outbreaks in Africa and France and showed that WNV strains were divided in to two separate lineages (lineage I and lineage II) and that the Australian KUN virus belonged to lineage I as a WN subtype (Berthet *et al.,* 1997; Lanciotti *et al.,* 1999) (Figure 1-1). While many WNV strains cause asymptomatic to

mild infections in humans, recent outbreaks, since the mid-1990s, in Europe and the Americas were associated with severe neuroinvasive disease resulting from highly virulent strains. Currently, WNV is found in Africa, Asia, Europe, the Middle East, Australia (KUN) and recently in North and South America (Figure 1-2). In the United States (US) all 48 contiguous states, except Maine, have documented human WNV infections. Since its introduction into the US in 1999, WNV has been responsible for at least 1,045 human fatalities and almost 11,000 cases of diagnosed neuroinvasive (encephalitis/ meningitis) disease (CDC, Arbonet). There are currently four lisenced equine vaccines in the US: a whole cell formalin inactivated vaccine (Ng *et al.*, 2003), a recombinant canarypox containing the prM and E of WNV (Minke *et al.*, 2004; Siger *et al.*, 2004), a recombinant plasmid DNA containing the prM and E of WNV (Davis *et al.*, 2001) and a WNV/YF17D chimera containing theprM and E of WNV (Arroyo *et al.*, 2004). However, to date no vaccine or antiviral is available for human use.

1.2 History of West Nile virus

1.2.1 History of disease

West Nile virus was first isolated in 1937 from a febrile woman in the West Nile district of Uganda (Smithburn *et al.*, 1940). It was nearly 15 years later that the first epidemic of WNV was reported in Israel (Bernkopf *et al.*, 1953). During this time, a four year study of the upper Nile region examined the prevalence of WNV in humans, arthropods and birds. It was concluded that of nearly 80,000 different arthropods collected, WNV was isolated from the *Culex* species of mosquitoes only and of the 420 birds examined, neutralizing antibodies were found in 65% of crows, 42% of

sparrows and virus was isolated from a sick pigeon. It was also demonstrated that approximately 60% of the human population possessed WNV antibodies (Taylor *et al.*, 1956). A serological survey of animals during these outbreaks indicated that a wide range of animals had been also infected by WNV and it was hypothesized that horses may be involved in the amplification of the virus (Murgue *et al.*, 2001). In fact, more than 50% of horses possessed WNV antibodies (Schmidt and El Mansoury, 1963), although experimentally infected horses elicited little to no viraemia (Taylor *et al.*, 1956). Based on the above, WNV was considered to be an arthropod-borne virus (arbovirus) that was transmitted by *Culex* mosquitoes to birds, who were the amplifiying vertebrate hosts. Humans and horses were considered "dead-end" hosts as the viraemia was not sufficient to infect mosquitoes.

Human cases were noted as febrile illnesses and it was not until 1957 that the first WNV cases including neurological manifestations were reported (Spigland *et al.*, 1958). During this time WNV was not commonly associated with neuroinvasive disease, rather it was associated with either asymptomatic or mild flu-like illness. Hypothesizing that the immune response to WNV infection may prevent other diseases, terminal cancer patients were infected with WNV in the hopes of inhibiting neoplasms. Ninety patients were given high doses of WNV either intramuscularly or intravenously, the patients observed and viremia was recorded (Southam and Moore, 1951; Southam and Moore, 1954). Interestingly, this study gave insight into the pathogenesis of human WNV infection. Many patients did not develop any clinical signs of infection other than fever, though a few patients developed encephalitic manifestations. Viremia was found 24 hours post-infection and lasted for six days or more. It was noted that there was a direct correlation between the longevity of the

viremia and the severity of disease. In most cases, WNV antibodies were detected three weeks post-infection.

Between 1950 and 1998, several outbreaks of WNV were documented (Figure 1-3). The first recorded outbreak of WNV occurred in 1951 in Israel. During this time 123 cases of WN fever were recognized with no fatalities. It was noted that the majority of cases were among children younger than six years with the highest morbidity in children less than three years old (Bernkopf *et al.,* 1953). Two more outbreaks occurred in Israel in 1957 and 1962 and it was at this time that the first clinical cases associated with neurological manifestations were noted (Spigland *et al.,* 1958; Pruzanski and Altman, 1962). Also in 1962, WNV appeared in France causing an epizootic resulting in 30% mortality in horses that exhibited neurological manifestations (Joubert *et al.,* 1970). Severe encephalitis in humans was also reported at this time and one human fatality occurred in 1964 (Panthier *et al.,*1968). West Nile outbreaks were seen in South Africa in 1974 and 1983-84, and WNV was isolated from the brains of children who succumbed to encephalitis in Russia, Romania, Spain and India during this time (Georges *et al.,* 1987). The first large, severe outbreak of WNV was seen in 1996 in Bucharest, which was also the first time an outbreak occurred in an urban setting, leading to a high number of cases associated with WNV infection (Tsai *et al.,* 1998). Also at this time, an outbreak in Morocco was associated with one human encephalitic case while 45% of horses clinically affected by WNV succumbed to infection (Tber, 1996; El Harrack *et al.,* 1997). In the fall of 1997 an outbreak in Tunisia resulted in eight human fatalities, this time the majority being >60 years old (Triki, 2001). Two outbreaks in 1998 occurred in Italy and Israel, which were again associated with human and animal encephalitis (Murgue *et al.,* 2001).

1.3 The summer of 1999: WNV impacts the new world

1.3.1 Introduction of WNV in to the US and expansion throughout the Americas

Until 1999, WNV was confined to the Eastern Hemisphere, including parts of Asia, Africa, Europe, Australia (KUN) and the Middle East. In the summer of 1999, the first cases of WNV were seen in New York City, including nine deaths. It was unclear what impact this newly introduced pathogen would have in subsequent years, or if this virus would be able to overwinter given the cold climate in the Northeast of the United States (US). In the years following the introduction of WNV into New York, it was clear that the virus continued to thrive by inhabiting more naïve areas while still being maintained in areas affected in the previous years (Figure 1-4). Although the initial WNV outbreak in New York was confined to the immediate area, by the next year expansion of the virus epidemic was apparent. By the summer of 2000, WNV had spread along the Eastern Seaboard of the US, including 12 states, yet only two deaths were associated with WNV infection. In 2001, 16 more states reported WNV cases, including nine deaths. Although WNV infection had spread geographically in the US, the number of deaths did not rapidly increase; however, WNV continued to be isolated from mosquitoes, birds and horses. By 2002, more than 4,000 human cases of neuroinvasive encephalitis/meningitis disease and WN fever, and 284 deaths were documented, and the virus had spread across the US to California. According to the CDC, this was the largest encephalitic arboviral epidemic in recorded history in the Western Hemisphere. In 2003, the number of WNV cases and deaths were similar to the previous year, and WNV was now found in almost every state of the US. During 2004 and 2005, the number of WNV cases and deaths was reduced by more than half compared to 2003, while 2006 saw a small

increase in the documented human cases with 177 deaths. To date (November 13, 2007), there have been 3,304 WNV cases, including 93 deaths during 2007. The decline in the incidence of WNV infection is probably due to many contributing factors, including higher prevalence of protective antibodies in the human, bird and animal populations versus the naïve population in earlier years.

1.3.2 Veterinary impact of WNV

West Nile virus also had a great impact on veterinary disease in North America. In 1999 birds, including crows, were found dead due to the virulence of this virus in birds. In fact, dead birds became an indicator of WNV activity in many areas, since high levels of the virus could be found in these animals. Thousands of dead birds tested positive for WNV infection between 1999 and 2000, including at least 75 species (Hayes, 2001). The migratory pattern of birds has been implicated in the spread of WNV across the US, into Canada, and Central and South America (Figure 1-5). In fact, a popular but unproven hypothesis for the introduction of WNV into the US proposes that a bird infected with WNV got lost on a migratory flyway, crossing the Atlantic to land in New York. It is also possible that an infected bird whose migratory route spans from regions where WNV is epidemic to the United States, such as the Arctic Tern, introduced WNV to the US (Figure 1-6). It has also been proposed that an infected human travelling from endemic areas to the US was responsible for the 1999 outbreak. However, humans may not produce the high viraemia necessary to transmit the virus to a mosquito. It has been demonstrated experimentally that the viraemia in birds may reach up to 12 log10 PFU/ml while one study found that of humans that donated blood in 2002, the highest titre was 3.2 log10 PFU/ml (Komar *et al.*, 2003; Hayes *et al.*, 2005).

Early in the US outbreak it was also apparent that many other incidental hosts succumbed to WNV disease, including horses. Horses were highly susceptible to infection and death due to exposure to virus-infected mosquitoes. Approximately 20% of horses infected with WNV presented clinical signs of encephalitis, such as hind limb paralysis and muscle tremors (Ward *et al.*, 2006). In later years, it was reported that many other animals were succumbing to WNV, possibly through non-mosquito-borne transmission, including turkeys, geese and alligators (CDC, 2003;Austin *et al.*, 2004; Jacobson *et al.*, 2005). Non-mosquito-borne transmission of WNV for alligators and birds has been shown experimentally through close contact, though not documented in nature (Komar *et al.*, 2003; Klenk *et al.*, 2004).

1.4 Epidemiology of WNV

1.4.1 Transmission cycle of WNV

West Nile virus is a mosquito-borne flavivirus transmitted primarily by various *Culex* species of mosquitoes. The WNV transmission cycle includes birds as the reservoir host, which amplifies the virus to high titres (Figure 1-7). Naïve mosquitoes feed on these birds becoming infected with the virus via the bite of the infected mosquito and subsequently pass the virus onto naïve birds and the cycle repeats. Many incidental or dead end hosts have been identified for WNV, including humans and animals such as horses. These incidental hosts are thought not to contribute to the biology of the virus since most infections do not result in high viraemia, however, high titres of the virus have been found in experimentally infected mammals (Hayes, 2001). Non-viraemic transmission of WNV has also been shown experimentally where non-infected mosquitoes that feed in close proximity to infected mosquitoes could become infected,

although the significance of this transmission in nature is undetermined (Higgs *et al.*, 2005).

1.4.2 Mosquito vectors

As mentioned in above, *Culex* mosquito species had been implicated as the major transmission vectors in early outbreaks of WNV. This was also true in the 1996 Bucharest epidemic, which included 17 human deaths where *Culex pipiens pipiens* comprised 96% of all mosquitoes that tested positive for WNV (Campbell *et al.*, 2001).

Although the major mosquito vector involved in the transmission of WNV in the US also includes *Culex spp.*, the virus has been isolated from over 60 different species of mosquitoes, 10 of which may be important in the transmission of the virus (Hayes *et al.*, 2005). After feeding on WNV-infected birds, mosquitoes harbour virus particles in the salivary gland where it can be transmitted to an amplification or dead end host when the mosquito takes a blood meal.

West Nile virus transmission has been detected in the United Kingdom (UK) where as many as 50% of birds analyzed were positive for WNV antibodies (Buckley *et al.*, 2003). Although the mosquito transmission vector and amplification bird host exist in the UK, WNV has not been implicated as a human pathogen in this part of the world presumably due to a combination of factors that may include: herd immunity of birds with previous exposure to WNV, less virulent virus and/or lack of bridging vectors.

1.4.3 Non-mosquito transmission of WNV

Although humans are most commonly infected with WNV by the bite of a virus-infected mosquito, non-mosquito transmission of WNV has proved to be an important route of transmission, especially for immunocompromised individuals in the US. Non-vector-borne transmission of WNV was first recognized in 2002 when transplant patients became particularly susceptible to serious infection. It was estimated that 40% of transplant patients infected with WNV were at risk of developing serious neuroinvasive disease versus approximately 1% for the general public (Kramer *et al.*, 2007). Other non-vector-borne transmission routes of WNV infection for humans include: blood transfusions, breast milk and intrauterine transmission (Kramer *et al.*, 2007). Nonetheless, non-mosquito transmission of WNV is rare. Increased screening reduces the risk of WNV infection for transfusion and transplantation patients, and the vast majority of cases remain vector-borne.

1.4.4 Risk factors

As noted above, children appeared to be more at risk for WNV infection until the 1990's, when it was evident that WNV infections had become more associated with neurological involvement among the elderly. Chilren were more susceptible than adults in past outbreaks probably because many children had not yet been exposed to the virus and therefore, did not possess antibodies towards the virus. However, it was noted during an outbreak in Isreal that children presented mild clinical signs such as fever, lymphadenopathy and rash, while the immunocompromised, or elderly, had increased neurologic involvement (Goldblum, 1959; Spigland et al., 1958). In this

case, age appeared to be a risk factor for severe WN disease. Similarly in the US, the elderly, or immunocompromised, have the greatest risk for neuroinvasive disease, while children and healthy adults are at a low risk of acquiring severe clinical manifestations (Hayes and O'Leary, 2004).

The greatest risk factor for WNV infection is increased exposure to infected mosquitoes due to areas of residence and the seasons. In the US, all states have experienced WNV cases since 1999, while outbreaks in Europe and Africa have continued to occur in specific regions. The seasons also contribute as a risk factor in that temperate climates typically seen in the summer months correspond to greater increases of cases seen worldwide. This is due, in part, to the transmission cycle of the virus. As mentioned above, the virus is transmitted by mosquitoes, which may accumulate not only at times of mild weather, but also may be highest in the rainy seasons.

1.5 Pathology of WNV

1.5.1 Clinical symptoms of WNV

Humans infected with WNV exhibit a range of disease manifestations from asymptomatic to severe morbidity and mortality. Asymptomatic cases account for about 80% of human infections (Mostashari *et al.,* 2001). A mild infection or West Nile fever (WNF) consists of a febrile illness including: fever, headache, fatigue, malaise, muscle pain and weakness and may involve gastrointestinal symptoms and macular rash on extremities (Hayes *et al.,* 2005; Hayes, 1989; Watson *et al.,* 2004).

In some instances (<1% of those infected), neuroinvasive disease occurs (Hayes *et al.*, 2005). In these cases patients develop meningitis, encephalitis or paralysis, and symptoms involve a range of clinical manifestations, including: mild disorientation, severe tremors, asymmetric flaccid paralysis, respiratory failure, coma and death (Pepperell *et al.*, 2003; Sejvar *et al.*, 2003a; Jeha *et al.*, 2003; Sejvar *et al.*, 2003b; Li *et al.*, 2003; Hayes *et al.*, 2005).

1.5.2 Gross pathology of human WNV infection

West Nile encephalitis infection causes inflammation, necrosis and loss of neurons mostly in the brainstem and spinal cord (Kleinschmidt-Demasters *et al.*, 2004; Guarner *et al.*, 2004). West Nile virus was not isolated from human post-mortem tissues until 2001 and only isolated from immunocompromised patients containing a high viral load (Hayes *et al.*, 2005). Viral antigen was seen within the neurons and throughout the CNS in immunocompromised patients (Guarner *et al.*, 2004), yet the virus was rarely seen by EM and only detected in the ER of neurons. Depletion of the motor neurons of the anterior horn of the spinal cord was commonly found upon autopsy caused by WNV infection and may be linked to paralysis (Kramer *et al.*, 2007). Lack of damage to other sections of the spinal cord may provide clues into the pathogenesis of neuroinvasive infection (Kramer *et al.*, 2007).

1.5.3 Diagnosis of WNV

Infection of WNV may be identified in the serum or CSF by enzyme immunoassays (EIA) that detect immunoglobulin (Ig) M (Hayes *et al.*, 2005). West Nile virus IgM antibody is typically detected by eight days post-infection in the serum or CSF of patients with neuroinvasive disease (Martin *et al.*, 2002). Although persistent

infections are rare, IgM may be detected in the serum or CSF at one year post-infection and a positive result may not exclude previous infections (Campbell *et al.*, 2002; Roehrig *et al.*, 2003; Kapoor *et al.*, 2004). Due to the cross-reactivity of antibodies to the envelope (E) glycoprotein of related flaviviruses, EIA may not be accurate and, therefore, other assays such as a microsphere assay incorporating a nonstructural protein appear to discriminate between WN antibodies and antibodies from SLE, dengue (DEN), JE vaccine and YF vaccine infection (Wong *et al.*, 2004). West Nile virus can also be detected in the serum, CSF and tissues by RT-PCR, which can be used for diagnostic purposes to distinguish between flaviviruses (Bhatnagar *et al.*, 2007). The most specific test to date remains the plaque reduction neutralization assay, which is used to detect four-fold or greater differences between acute and convalescence phase in serum samples. This assay is often used in combination with other serological assays.

1.5.4 Treatment of WNV infection

To date there are no antiviral therapies to combat WNV infection. Reduced viral replication has been seen in cell culture studies with some candidate WNV treatments, although many therapies have not been effective in preclinical studies in animal models or human trials (Kramer *et al.*, 2007). Potential therapeutics include phosphorodiamidate-morpholino-oligomers (PMO's), which have been shown to inhibit WNV replication in cell culture (Deas *et al.*, 2005) and show some protection in mice against WNV disease (Kramer *et al.*, 2007). Interferon-α2β treatment of patients with WNV meningoencephalitis demonstrated considerable recovery of neurologic functions in the small number of patients that received this treatment, yet the efficacy in a large study has not been determined (Sayao *et al.*, 2004). Another

treatment that has shown some efficacy in humans is the administration of intravenous immunoglobulin containing high titers of WNV antibody; however, this treatment has also not been widely studied in humans (Shimoni *et al.,* 2001).

1.6 Molecular Virology

1.6.1 Virion

West Nile virus is a small enveloped positive sense RNA virus whose genome is approximately 11kb in length. The surface of the virion contains the envelope (E) and membrane (M) proteins surrounding the nucleocapsid and core that encompasses the nonstructural proteins (Figure 1-8). The mature virus appears as a smooth spherical particle, icosohedral symmetry, that measures approximately 500 Å in diameter (Kuhn *et al.,* 2002; Nybakken *et al.,*2006). The outer layer of the virion contains 180 copies of the E protein arranged in a herringbone pattern and the same amount of M protein anchored by the C-terminal ends (Kuhn *et al.,* 2002). In contrast, the immature virus particle is larger in size (600 Å) due to the precursor premembrane protein (prM) and E heterodimers (Zhang *et al.,* 2003).

The genome encodes 10 genes; three structural proteins (capsid (C), prM/M and E) in the 5' quarter of the genome and the remainder of the genome encodes the seven nonstructural (NS) proteins (NS1-NS5). The gene order is 5'-C-M-E-NS1-NS2A-NS3-NS4A-NS4B-NS5-3'. The genome is flanked by a short 117 nucleotide 5' untranslated region (5'UTR) and a longer but variable (300-600 nucleotides) 3'UTR. The genome is translated as one polyprotein that is co- and post-translationally modified by viral and cellular enzymes to yield the 10 proteins (Figure 1-9).

1.6.2 WNV structural proteins

West Nile virus contains three structural proteins including the C, prM/M and E proteins. The structural proteins are involved in various steps of the replication cycle and comprise the virion.

Capsid protein

The flavivirus nucleocapsid core contains the C protein and viral RNA. The electron dense core displays differential symmetry by cryoelectron microscopy suggesting that the C protein and viral RNA assemble randomly (Patkar *et al.*, 2007). Also, the viral membrane shows no apparent connectivity with the nucleocapsid suggesting the C protein does not interact with the M and E proteins. The C protein is a small (~12 kD) basic protein that binds viral RNA and is not highly conserved among flaviviruses (Khromykh and Westaway, 1996; Patkar *et al.*, 2007). The C-terminal end of the C protein serves as a signal sequence involved in the translocation of the prM protein to the lumen of the endoplasmic reticulum (ER), which is proteolytically cleaved by the NS2B-NS3 viral protease (Amberg *et al.*, 1994; Yamshchikov and Compans, 1994; Zhang *et al.*, 2003). This mature form of the C protein is found in the virion and associated with intracellular membranes by a conserved internal hydrophobic sequence (Markoff *et al.*, 1997). The C protein has been found associated with the ER, within the cytoplasm and in the nucleus (Wang *et al.*, 2002). Kunjin virus-infected Vero cells showed C protein interactions with the perinuclear membranes and within the nucleus (Westaway *et al.*, 1997). The translocation of the C protein to the nucleus has an undetermined role in the replication cycle of the virus.

prM/M protein

The larger prM protein is the precursor to the small M protein. The prM and E proteins form heterodimers that translocate to the ER. The C-terminal sequence of the C protein is required for prM translocation, and the processing of the prM protein occurs with the cleavage of this signal sequence (Amberg *et al.*, 1994). The flavivirus prM protein contains one to three putative N-linked glycosylation sites in the N-terminal region (Chambers *et al.*, 1990). The glycosylation sites, as well as six conserved cysteine residues involved in disulfide formation, are cleaved to form the mature M protein (Nowak and Wengler, 1987). The C-terminal end of the prM protein is involved in membrane anchoring, containing two transmembrane domains (Markoff *et al.*, 2003).

The prM protein is associated with immature virus particles and is likely to protect E protein from inactivation due to the low pH during transport through the intracellular vesicles (Heinz and Allison, 2000). The prM protein also elicits a chaperone-like function preventing conformational changes in the E protein within the low pH secretory pathway (Guirakhoo *et al.*, 1992). The prM protein is cleaved by furin or a furin-like protease after the virus leaves the trans-Golgi network, but before the release of the virus, to reveal the mature form of the virus (Murray *et al.*, 1993; Stadler *et al.*, 1997).

The M protein is much smaller than the prM protein that existis in the mature form of the virus after prM cleavage. Few studies have investigated the role of the M protein. A single mutation at M_5 for JE virus increased plaque size and infectivity in cell culture, but did not affect virulence in mice. Since this mutation was shown to inactivate the virus at low pH, it has been hypothesized that the M protein may

function to stabilize the E protein dimers at neutral pH from forming trimers (Maier *et al.*, 2007).

E protein

The E protein is the major surface viral protein involved in receptor binding and fusion. The X-ray crystallographic structure of the E protein for TBE, DEN-2 and WN viruses revealed some similarities including three domains; the N-terminal domain 1, elongated dimerization domain II containing the fusion peptide and an immunoglobulin-like domain III (Rey *et al.*, 1995; Modis *et al.*, 2003; Zhang *et al.*, 2004; Nybakken *et al.*, 2006) (Figure 1-10). Flavivirus E protein may contain up to four N-linked glycosylation sites and WNV strains have either one or no glycosylation sites. The crystal structure for WNV is based on the NY99 strain, which contains one glycosylation site at E_{154} (Nybakken *et al.*, 2006). A mutation at the N-linked glycosylation site affects the virulence of WNV in mice, decreases infectivity in cell culture and influences particle assembly (Beasley *et al.*, 2005; Hanna *et al.*, 2005). The glycosylation sites for DEN viruses have been proposed to modulate receptor binding through intercellular adhesion molecule (ICAM)-3 mediated adhesion (Navarro-Sanchez *et al.*, 2003). The putative receptor binding domain III for mosquito-borne flaviviruses, including JE, YF and WN viruses, contain an RGD/RGE integrin binding recognition motif yet mutations in this motif did not abolish YF virus binding to the cell, suggesting the use of a non-integrin receptor (van der Most *et al.*, 1999).

The E protein is involved in fusion utilizing a class II fusion process (Figure 1-11). After receptor-mediated endocytosis, a pH change occurs that triggers a

conformational change of the E dimers and the domain II moves toward the host cell membrane. The hinge region, now exposed, inserts into the host cell membrane resulting in the formation of E protein trimers followed by the movement of domain III resulting in the hemifusion of the lipid membrane. This enables a trimer formation bringing the transmembrane regions and fusion peptide in close proximity (Mukhopadhyay *et al.,* 2005).

The E protein undergoes yet another conformational change in its replication cycle during maturation. Before the release of the virus, 60 trimers of the prM and E heterodimer on the surface of the virus disassociate to 90 E homodimers after the furin-mediated cleavage of the prM protein in a low pH induced manner. This dissociation causes a conformational change in the E protein from the hinge between domains I and II (Mukhopadhyay *et al.,* 2005).

The E protein also elicits neutralizing antibodies. Neutralizing antibodies against the E protein are important for protective immunity and are involved in the clearance of viral infection.

1.6.3 WNV nonstructural proteins

West Nile virus synthesizes seven nonstructural (NS) proteins inside virus-infected cells, including NS1, NS2A, NS2B, NS3, NS4A, NS4B and NS5. These proteins are necessary for virus replication.

NS1 protein

The flavivirus NS1 protein is highly conserved and all members contain conserved N-linked glycosylation sites (asparagine-X-serine/threonine [NXS/T]). For the JE

serogroup, all members, except JE virus, contain three glycosylation sites with the asparagine residue at $NS1_{130}$, $NS1_{175}$ and $NS1_{207}$ (Bakonyi *et al.*, 2004; Blitvich *et al.*, 2001; Chambers *et al.*, 1990; Sumiyoshi *et al.*, 1987). Other mosquito-borne flaviviruses contain two glycosylation sites at $NS1_{130}$ and $NS1_{207}$ ($NS1_{208}$ YF) while non-vector-borne ENT bat virus has four predicted N-linked glycosylation sites (Dalgarno *et al.*, 1986; Pryor and Wright, 1994; Flamand *et al.*, 1992; Kuno and Chang, 2006). The glycosylation sites have been linked with virulence of the virus and showed attenuation in mice and reduced infectivity in cell culture for DEN-2 and YF viruses (Crabtree *et al.*, 2005; Pryor and Wright, 1994; Pletnev *et al.*, 1993).

The NS1 protein forms dimers and is found in different forms within the cytoplasm, associated with the plasma membrane, and is secreted (Blitvich *et al.*, 2001; Flamand *et al.*, 1999; Mason, 1989; Schlesinger *et al.*, 1990; Post *et al.*, 1991; Winkler *et al.*, 1988; Winkler *et al.*, 1989; Crooks *et al.*, 1994). Although the function of this protein has yet to be identified, the NS1 protein has been identified as essential for replication as large in-frame amino acid deletions within NS1 were deficient in negative-strand RNA synthesis; however, replication could be restored by supplying this protein in *trans* (Lindenbach and Rice, 1997). The NS1 protein has extensive identity and homology between different flaviviruses, yet the NS1 protein functions in a virus-specific manner (Lindenbach and Rice, 1999). The NS1 protein interacts with other proteins necessary for replication, including the NS2A and NS4A proteins (Lindenbach and Rice, 1999; Kummerer and Rice, 2002).

The NS1 protein has been implicated to possess immunomodulatory capabilities. High levels of circulating NS1 protein has been linked to serious DEN infection,

which may lead to potentially lethal DHF infection (Alcon *et al.,* 2002; Young *et al.,* 2000, Libraty *et al.,* 2002; Macdonald *et al.,* 2005; Avirutnan *et al.,* 2006). The role of secreted NS1 protein is unclear, but it is thought to be involved in the immune complex formation (Young *et al.,* 2000), induction of autoreactive antibodies against extracellular matrix proteins (Chang *et al.,* 2002), and enhanced viral production (con-LePoder *et al.,* 2005). Recently, the cell surface associated NS1 protein for WNV has been shown to bind regulatory protein factor H, inhibiting complement activation, which may prevent complement-dependent lysis of infected cells (Chung *et al.,* 2006). This is contrary to studies with DEN virus where NS1 appears to activate complement (Avirutnan *et al.,* 2006), suggesting a novel function for WNV NS1. Finally, antibodies to NS1 have no neutralizing activity but do induce protective immunity, probably by antibody dependent cellular cytoxicity and elicit passive protection in mouse and monkey models (reviewd by Gibson *et al.,* 1988)

The NS1 protein forms a hexamer, heat-labile homodimer and a short-lived monomer and can be found inside the cell, associated with membranes, and as a soluble secreted protein (Blitvich *et al.,* 2001; Flamand *et al.,* 1999; Mason, 1989; Schlesinger *et al.,* 1990; Winkler *et al.,* 1988; Winkler *et al.,* 1989; Crooks *et al.,* 1994). Many forms of the protein have been shown to exist due to alternative cleavage sites, formation of heterodimers with E or NS2A, or differences in glycosylation status (Blitvich *et al.,* 1995; Blitvich *et al.,* 1999; Falgout & Markoff, 1995; Mason *et al.,* 1987; Nestorowicz *et al.,* 1994). Previous studies with other flaviviruses have established that glycosylation of NS1 is not required for dimerization but does affect dimer stability (Pryor and Wright, 1993; Pryor and Wright, 1994). Furthermore, it has been

suggested that dimerization may not be necessary for either the secretion of NS1 or viral replication (Hall *et al.*, 1999).

The NS1 protein has been shown to contain two distinct isoforms in cell culture, referred to as NS1° and NS1' (Mason, 1989; Blitvich *et al.*, 1995; Poidinger *et al.*, 1996). Although the cleavage site generating these isoforms is unclear, studies have found that the NS3 protease is not required, and that the NS1' isoform contains a portion of the NS2A protein (Mason *et al.*, 1987; Chambers *et al.*, 1990; Blitvich *et al.*, 1999). The function(s) of these isoforms are unclear and it is not understood if the internal cleavage of the protein is required for NS1 function. A study with JE virus-infected cells showed that NS1' may be involved in RNA dependent RNA polymerase activity and that NS3 coprecipitated with NS1' (Satchidanandam *et al.*, 2006).

NS2A protein

The NS2A protein is a small (~22 kD), hydrophobic protein. The N-terminus is located within the endoplasmic reticulum (ER) and C-terminus within the cytoplasm (Preugschat *et al.*, 1990). The C-terminus of the NS2A is cleaved by the viral protease (Preugschat *et al.*, 1990) while the N-terminus is cleaved in the ER by an unidentified host protease (Falgout and Markoff, 1995). An internal viral cleavage site resulting in the formation of NS2Aα and NS1' is necessary for the production of infectious virus (Kummerer and Rice, 2002).

The NS2A protein is required for assembly and has been shown to contribute to the virulence of the virus in mice (Liu *et al.,* 2003; Liu *et al.,* 2006). An isoleucine to asparagine mutation at $NS2A_{59}$ for KUNV resulted in a complete block of virus production, but wild-type NS2A supplied *in trans* restored the replication of infectious virus. This same study found that packaging of replicon RNA was impaired due to this mutation (Liu *et al.,* 2003). A single mutation in the NS2A protein, changing an alanine to a proline at $NS2A_{30}$, reduced the inhibition of interferon-beta promoter-driven transcription in cell culture and was highly attenuated for neuroinvasiveness and neurovirulence in 3-week-old mice (Liu *et al.,* 2006). Surprisingly, this mutant was also partially attenuated in IFN-αβγ receptor knockout mice suggesting it may play an additional immunomodulatory role (Liu *et al.,* 2006).

NS2B protein

The NS2B protein is a hydrophobic protein that contains a 40 residue central region that is a cofactor of the NS3 serine protease and is necessary for the activation of the protease (Mastrangelo *et al.,* 2007; Chambers *et al.,* 1993; Leung *et al.,* 2001). Cleavage of the NS2B/NS3 complex is necessary for replication (Chambers *et al.,* 1995). The NS2B protein also may be involved in the cleavage of the C protein (Amberg and Rice, 1999).

NS3 protein

NS3 protein contains an N-terminal serine protease and C-terminal helicase, with nucleoside 5′-triphosphatase (NTPase) and 5′-terminal RNA triphosphatase (RTPase) activities (Mastrangelo *et al.,* 2007). It is thought that the NTPase may be required for the helicase to unwind viral RNA and the RTPase may be involved in the formation of

the 5' cap (Brinton, 2002). The protease is responsible for the proteolytic cleavage of the N-terminal/C-terminal regions of the C protein, NS2A/NS2B, NS2B/NS3, NS3/NS4A, NS4A/NS4B and NS4B/NS5 junctions (Nowak *et al.,* 1989; Speight and Westaway, 1989).

Both positive- and negative-stand RNA transcripts contain highly structured secondary structures especially in the 5'UTR and 3' UTR. Therefore, it is a necessary function of the helicase to unwind nascent transcripts during transcription. The helicase aids in the initial negative strand synthesis by unwinding the polyprotein at the highly structured 3'UTR (Takegami *et al.,* 1995).

The NS3 protein may also be involved in host cell apoptosis through the recruitment of caspase-8 (Ramanathan *et al.,* 2006).

NS4A protein

The NS4A protein is a small hydrophobic protein, approximately 16kD in size, involved in the replication complex. Cleavage of this protein may be regulated since two precursors, NS3/NS4A and NS4A/NS4B, are found within the cell (Chambers *et al.,* 1990; Preugschat *et al.,* 1990). The cleavage of the NS4A/NS4B junction liberates a transmembrane signal peptide from the N-terminus of NS4B named 2K (Lin *et al.,* 1993; Preugschat and Strauss, 1991). The NS4A interacts with the NS1 protein in an undetermined fashion possibly essential for replication (Lindenbach and Rice, 1999).

The NS4A protein function has been recently implicated in the formation of virus-induced replication structures. The NS4A protein, in the absence of the 2K fragment, was shown to induce vesicle formation similar to the convoluted membrane/paracrystalline array (CM/PC) structures for KUN NS4A synthesized via the Semliki Forest virus expression system. However, the structures lacked the tightly dense structure appearance seen in virus-infected cells suggesting other factors are involved in the formation of virus-induced structures (Roosendaal *et al.,* 2006). In addition, the NS4A protein has been implicated in the formation of virus-induced structures for an NS4A DEN-2 T7 polymerase based expression system. Different from the KUN study, the NS4A protein lacking the 2K fragment induced internal structural changes similar to those seen in virus-infected cells (Miller *et al.,* 2007). Both these studies were limited in their findings and suggested the NS4A protein may be involved in the formation of virus-induced structures necessary for replication, although the NS4A protein function may differ between flaviviruses.

NS4B protein

The NS4B is a small hydrophobic protein of approximately 27 kD, which may participate in the replication cycle and immune evasion. The NS4B protein shows only 35% homology between DEN, WN and YF viruses (Umareddy *et al.,* 2006), however, members of the family *Flaviviridae* share common ER and cytoplasmic regions and transmembrane domains (Miller *et al.,* 2006) that may indicate similarities in the function of this protein between viruses.

The NS4A/NS4B precursor is cleaved by the viral protease and the resulting 2K/NS4B protein is further cleaved by a host signalase to generate the mature NS4B

protein (Chambers *et al.*, 1989; Lin *et al.*, 1993; Cahour *et al.*, 1992; Preugschat and Strauss, 1991). The NS4B protein for HCV and DEN-2 viruses localize in the ER within foci that may represent the viral replication complex (Lundin *et al.*, 2003). The expression of mature NS4B protein, but not NS4A/NS4B, leads to the formation of membranous webs in cell culture suggesting its involvement in ultrastructural membrane changes (Egger *et al.*, 2002; Konan *et al.*, 2003).

The NS4B protein contains three to five transmembrane domains with an N-terminus portion that localizes to the lumen of the ER and a C-terminus portion in the cytoplasm in DEN-2- and HCV-infected cells (Lundin *et al.*, 2003; Miller *et al.*, 2006). A portion of the NS4B protein has also been shown to translocate to the nucleus in KUN virus-infected Vero cells (Westaway *et al.*, 1997).

Mutations within the central hydrophobic region of the NS4B protein have been identified in several attenuated and passage-adapted flavivirus strains, including: chimeric WN/DEN-4 and DEN-2/DEN-4 viruses, passage adapted DEN-4 virus, JE vaccine strain, YF vaccine strain and hamster passage adapted YFV strain, and a WNV mouse attenuated strain (Pletnev *et al.*, 2002; Blaney Jr., 2003; Ni *et al.*, 1995; Hahn *et al.*, 1987; Wang *et al.*, 1995; McArthur *et al.*, 2003; Wicker *et al.*, 2006).

The NS4B protein also elicits immunomodulatory capabilities, specifically the inhibition of interferon. The first 125 amino acids of the mature NS4B protein have been shown to be crucial in the inhibition of STAT1 phosphorylation for DEN-2, YF and WN viruses (Munoz-Jordan *et al.*, 2003; Munoz-Jordan *et al.*, 2005). Mutations within the NS4B protein have also been identified in interferon-resistant HCV

replicons (Namba *et al.*, 2004). Therefore, immune evasion may be a conserved function of the NS4B protein.

NS5 protein

The NS5 protein is approximately 100 kD in size and the largest flaviviral protein. This protein is highly conserved among flaviviruses, containing a methyltransferase activity in the N-terminus, which is utilized in 5' capping, and a 3' viral RNA-dependent RNA polymerase (RdRp) required for replication (Khromykh *et al.*, 1999). The phosphorylation of serine residues of the DEN-2 virus NS5 leads to the formation of the NS3/NS5 complex, which is also required for polymerase activity (Kapoor *et al.*, 1995). The NS5 protein is found within the cytoplasm but translocates to the nucleus via a signal sequence in conjunction with a host cellular nuclear import receptor (Johansson *et al.*, 2001). Approximately 20% of the RdRp activity resides in the nucleus of WN, DEN or JE virus-infected cells (Uchil *et al.*, 2006).

Recently, the NS5 protein has been shown to elicit immunomodulatory capabilities, specifically in interferon inhibition. The NS5 protein of Langat and JE virus inhibits Jak-STAT phosphorylation via activation of cellular protein tyrosine phosphatases (Best *et al.*, 2005; Lin *et al.*, 2006).

1.6.4 WNV untranslated regions

The WNV genome contains 5' and 3' untranslated regions (UTR) located at the extreme 5' and 3'ends of the virus genome. The 5' and 3'UTR form secondary structures that are essential for replication and translation. Mosquito-borne flaviviruses including DEN, YF and JE viruses, show similar 5' stem loop structures

whereas TBE virus shows somewhat different 5'UTR secondary structure (Thurner *et al.,* 2004). The 5'UTR is not conserved among members of the family *Flaviviridae* as the hepaciviruses contain an internal IRES, while the flaviviruses contain a type 1 cap structure for translation (Brinton and Dispoto, 1988; Pestova *et al.,* 1998). The 3'UTR contains three cyclization sequences that interact with the 5' cyclization sequence, located in the N-terminal portion of the C protein, approximately 40 nucleotides downstream of the start codon (Markoff, 2003). In the absence of a poly A tail, the 3'UTR is essential for viral replication (Markoff, 2003) and may be involved in translation or genome packaging (Li and Brinton, 2001; Mandl, 2005). It has been shown for DEN virus that the cyclization of the 5' and 3'UTR's , but not the RNA cap-dependent mechanism, are required for translation (Edgil and Harris, 2006). Highly conserved regions of the 3'UTR contain two stem loop regions, however, the regions downstream of the stop codon are variable (Brinton *et al.,* 1986).

Mutations or deletions in the 3'UTR have been shown to reduce RNA replication (Khromykh *et al.,* 2003; Lo *et al.,* 2003; Elghonemy *et al.,* 2005; Hanley *et al.,* 2004). A DEN virus vaccine candidate has been proposed based on a mutant virus containing a 30 nucleotide deletion within the 3'UTR, which shows reduced replication in monkeys and induces a protective immune response (Hanley *et al.,* 2004).

1.6.5 Viral life cycle and replication

As with other flaviviruses, the WNV life cycle begins with binding of the virus to the host cell through the interaction of the E protein on the surface of the virus with cellular receptors. Although these cellular receptors have yet to be identified, attachment factors, such as heparin sulfate, alpha-v-beta-3 integrin and DC-SIGN may

be involved in the entry of the virus (Mandl *et al.,* 2001; Kroschewski *et al.,* 2003; Chu and Ng, 2004; Davis *et al.,* 2006).

Virus is taken up into the cell via receptor mediated endocytosis into clathrin-coated pits before subsequent transport of the virus to prelysosomal endocytic compartments (Chu and Ng, 2004). A rearrangement of E dimers to trimers, which occurs due to the low pH within these compartments (Allison *et al.,* 1995) is necessary for the fusion of the viral membrane with the endosomal membrane (Heinz and Allison, 2003). This results in the release of the viral nucleocapsid into the cytoplasm of the cell and uncoating of the viral RNA genome. The input RNA is translated to yield a polyprotein that is subjected to co-and post-translational processing to generate the individual proteins. Replication of the viral genome is initiated through transcription of the input positive-strand genomic RNA to produce a negative-strand RNAs, which serves as a template for synthesis of new positive-strand RNA that are used for further translation of viral proteins and progeny genomes. The next steps in the replication cycle are not as well understood, but involve packaging of genome RNA by the capsid protein and assembly of the virus through the budding of the nucleocapsid into the ER (Figure 1-12). This immature particle results from the association of the prM and E heterodimers and is not infectious (Elshuber *et al.,* 2003). Transport of the immature virus particles occurs via the host secretory pathway and cleavage of the prM in acidic vesicles of the late trans-Golgi network by host cell protease furin, which produces the mature form of the virus (Stadler *et al.,* 1997). The mature particles are released from the cell following fusion of the transport vesicles to the plasma membrane (Figure 1-13).

1.7 Immunology

1.7.1 Immune response to WNV

The use of rodent models has provided insight into the immune response to WNV infection. Early post-infection, WNV replicates in the Langerhan dendritic cells, which migrate to the draining lymph node causing viremia and subsequent infection of organs such as the kidney and spleen (Samuel and Diamond, 2006). Although the mechanism of invasion of the CNS is unknown, viral load and a cytokine involvement may facilitate the virus crossing the blood brain barrier (Figure 1-14).

Innate and humoral immune responses to WNV infection have been elucidated using rodent models. Interferons have been shown to inhibit WNV replication when given before infection, although the same is not true after infection (Anderson and Rahal, 2002; Crance *et al.,* 2003; Samuel and Diamond, 2005). Gene knockout mice lacking IFN-γ showed increased viral burden, earlier entry into the CNS, and a higher mortality rate suggesting IFN-γ has an antiviral function in controlling WNV infection (Shrestha *et al.,* 2006; Wang *et al.,* 2003). Complement, a group of proteins in the serum involved in the destruction of non-self particles, has also been shown to be essential for protection from lethal WNV infection in mice (Mehlhop and Diamond, 2006).

Although the role of cellular immunity is less well characterized, it is thought that macrophages may control WNV infection through production of nitric oxide intermediates, direct viral clearance, enhanced antigen presentation and the secretion of cytokine and chemokines (Ben-Nathan *et al.,* 1996; Kreil and Eibl, 1996; Lin *et al.,* 1997). Helper T cells play an important role in antiviral immunity, especially

cytotoxic T cell response, which are important in controlling WNV infection through cytokine production and T-cell priming (Samuel and Diamond, 2006). Although the E protein elicits a T-cell response, the nonstructural proteins, especially NS1 and NS3, have shown to be primary targets of protective T-cells (Aihara *et al.,* 1998; Kurane *et al.,* 1991; Mathew *et al.,* 1996,1998; Zeng *et al.*, 1996; Co *et al.,* 2002; Kumar *et al.,* 2003). In fact, when a dominant T-cell eliciting antigen, such as NS1, is present, the E protein does not enduce a strong cell-mediated response (Konishi *et al.,* 1995; Desai *et al.,* 1995; Kumar *et al.,* 2003). The NS1 protein has been shown to stimulate cytolytic antibodies in mice (Lin *et al.,* 1998) and were found to be the major target of IFN-γ-producing T-cells in humans (Co *et al.,*2002).

Humoral immunity has also proved to be a critically important aspect of the immune systems response to WNV infection, and neutralizing antibody is considered the key component of protective immunity. Recent studies showed B-cell deficient mice died from WNV infection but passive transfer of immune sera was able to protect mice from infection (Diamond *et al.,* 2003).

1.7.2 Immune evasion of WNV

The efficiency of WNV replication may, in part, be permitted through evasion of the host immune system. The nonstructural NS2A, NS4A and NS4B proteins for DEN-2 virus have been shown to suppress the host immune response through the down regulation of IFN-β gene expression (Munoz-Jordan *et al.,* 2003). Similarly, the nonstructural proteins of KUN virus, the Australian subtype of WNV, inhibit viral spread through the activation of the IRF-3 pathway (Fredericksen *et al.,* 2004). In this case, when the NS2A, NS2B, NS3, NS4A and NS4B proteins were individually

expressed, STAT2 translocation into the nucleus was inhibited. Recently, the NS5 protein has also been shown to inhibit Jak-STAT phosphorylation (Best *et al.,* 2005). Inhibition of the IFN-α pathway was not inhibited when NS1 was expressed (Liu *et al.,* 2005). It has also been shown that WNV replication hinders the phosphorylation and activation of Tyk2 and JAK1 (Guo *et al.,* 2005).

1.7.3 Antibody-dependent enhancement

Following infection, neutralizing antibodies, mainly against the E protein, are important for the clearance of the viral infection. However, subneutralizing antibodies, which may enhance infection, has been implicated in DHF. Referred to as antibody-dependent enhancement (ADE), concentrations of antibodies below the neutralization threshold may enhance infection through Fc-γ receptor engagement and enhancement of Fc-γ receptor-expressing cells (Mehlhop *et al.,* 2007; Pierson *et al.,* 2007). Previously, ADE had been shown experimentally *in vitro* for several flaviviruses including JE, YF, WN and DEN viruses (Cardosa *et al.,* 1986; Gould and Buckley., 1989; Halstead, 1989; Wallace *et al.,* 2003). Recently, evidence of this phenomenom has been demonstrated in mice infected with Murray Valley encephalitis and WNV (Mehlhop *et al.,* 2007; Wallace *et al.,* 2003), however, ADE has not been verified in humans.

A recent study examined ADE in mice given subneutralizing antibodies of JE and subsequent challenge with MVE (Wallace *et al.,* 2003). This study found that vireamia and mortality was increased in these mice. This study, and others like it,

suggest the possibility of ADE and is a concern for vaccines. Since ADE has yet to be shown in humans, this hypothesis remains controversial; however, severe infections subsequent to the administration of some formalin-inactivated viral vaccines have been attributed to ADE (Iankov *et al.,* 2006; Ponnuraj *et al.,* 2003; Porter *et al.,* 1972; Prabhakar and Nathanson,1981). It is important to consider the possibility of ADE when designing a vaccine candidate and therefore, a robust antibody response to vaccine should be achieved.

1.7.4 Vaccine development

Currently, no WNV vaccine or antiviral is available for human use. Three vaccines are currently licensed for equine use in the United States: a whole virus formalin inactivated vaccine (Ng *et al.,* 2003), a recombinant canarypox virus containing the WN prM and E proteins (Minke *et al.,* 2004; Siger *et al.,* 2004) and a recombinant plasmid DNA containing the WN prM and E proteins, which is also in human clinical trials (Davis *et al.,* 2001). Various other vaccine candidates have been evaluated in mice or monkeys including live-attenuated strains, live-attenuated chimeric virus strains and recombinant virus strains (Yamshchikof *et al.,* 2004; Ledizet *et al.,*2005; Qiao *et al.,*2004; Arroyo *et al.,* 2004 ; Monath *et al.,* 2006 ;Pletnev *et al.,* 2003; Despres *et al.,* 2005; Iglesias *et al.,* 2006).

A preclinical trial of a chimeric WN/DEN-4 virus has been evaluated in mice and non-human primates (Pletnev *et al.,* 2003). This live-attenuated virus was derived using reverse genetics from the DEN-4 Dominican Republic strain lacking 30 nucleotides in the untranslated region and contains the prM and E protein from the WNV NY99 strain. This recombinant virus showed decreased infectivity titres in

neuroblastoma cells compared to the parental strains and following inoculation with the vaccine virus, WN/DEN4Δ30, monkeys displayed little to no viraemia. Although all monkeys elicited neutralizing antibodies, a two-fold reduction in the neutralizing antibody titre was seen in monkeys that had previous immunity to DEN virus.

Recently, an attenuated recombinant WNV vaccine candidate was evaluated in a small clinical trial (Monath *et al.,* 2006). This vaccine was derived by reverse genetics from the YF17D vaccine strain, replacing the prM and E proteins with the corresponding WNV proteins containing attenuating mutations in the E protein. The resulting recombinant vaccine virus, ChimeriVax-WN02, has been tested for safety and immunogenicity in preclinical and clinical trials in non-human primates and humans (Monath *et al.,* 2006). Neutralizing antibody titres after the first dose were low with plaque reduction neutralization assay ($PRNT_{50}$) values in mice and monkeys of <50 four weeks post- infection and <100 14-days post-infection, respectively. After challenge, the neutralizing antibody titres in monkeys increased with $PRNT_{50}$ values $\geq$ 640 (Arroyo *et al.,* 2004). Of the 45 subjects in the phase I clinical trial, one did not seroconvert, while the others displayed neutralizing titres by 28 days post-subcutaneous inoculation of the vaccine. The vaccine was well tolerated in healthy women and men aged 18-40 years old (Monath *et al.,* 2006). A larger Phase II trial investigation of the safety, immunogenicity and efficacy of this vaccine has yet to be performed.

Although several vaccine candidates exist for WNV, some lacked high neutralizing antibody titres and the efficacy of these candidates has not proceeded beyond preclinical development.

1.8 Aims of the thesis

The impact of WNV and lack of a vaccine for human use represents the need for additional vaccine candidates to control this disease. A cDNA infectious clone exists for this virus (Beasley *et al.,* 2005) that provides an important tool to investigate molecular determinants of attenuation that may be used to generate a live-attenuated vaccine candidate.

The NS1 protein is a unique viral protein in that this nonstrucutural protein is glycosylated and is found within the cell as well as secreted through the secretory pathway. Studies have yet to identify the function(s) of this protein although it is thought be involved in several aspects of the viral replication cycle and may affect the host immune response to infection. Since the glycosylation sites of the NS1 protein are highly conserved, these sites are hypothesized to contribute to the function of the protein and therefore, may affect the virulence of the virus. Previous studies of the NS1 glycosylation sites with DEN-2 and YF viruses revealed reduced infectivity in cell culture and attenuation in mice (Pryor and Wright, 1994; Muylaert *et al.,*1996; Pletnev *et al.,* 1993; Crabtree *et al.,* 2005), however, these studies were limited to mouse neurovirulence studies. Also, these viruses possessed only two of the three glycosylation sites that WNV contains, lacking the $NS1_{175}$ site.

The objective of this thesis was to investigate a rational approach to utilizing NS1 mutations to contribute towards generation of a candidate live-attenuated WNV vaccine while investigating a functional role for the NS1 protein. The following specific aims were undertaken to achieve these objectives.

Specific Aim 1: Attenuation of WNV through the deglycosylation of the NS1 protein. Hypothesis: *The ablation of one or more NS1 N-linked glycosylation site(s) will attenuate the mouse virulence phenotype of WNV.*

Rationale: This was accomplished through site-directed mutagenesis to generate mutant viruses lacking the NS1 glycosylation site(s) in all possible combinations. These viruses were used to compare infectivity in cell culture and attenuation in mice compared to the parental strain. The mouse model for WNV mimics natural infection of neuroinvasive disease, therefore, may be used to study the neuroinvasiveness of NS1 glycosylation mutant viruses.

Specific Aim 2: Derive a candidate live-attenuated vaccine candidate virus for WNV including multigenic attenuating mutations. Hypothesis: *Attenuating mutations in the NS1 combined with attenuating mutations in other proteins will attenuate the mouse virulence phenotype, be replication competent in cell culture and elicit protective antibodies.*

Rationale: Mutations in the glycosylation sites of prM and E proteins and a conserved residue in NS4B were examined, together with attenuating NS1 glycosylation mutations, to determine if these mutations, alone or in combination, would enhance attenuation of a live-attenuated vaccine candidate.

Specific Aim 3: Utilize the NS1 protein mutant viruses to examine a functional role for the NS1 protein. Hypothesis: *Mutations in the conserved NS1 glycosylation sites will alter the function of the protein affecting various steps of the replication cycle and immune response to infection.*

Rationale: The ultrastructure of cells infected with the NS1 mutant virus was hypothesized to differ from cells infected with the parental virus due to the NS1 protein being involved in the formation of virus-induced replication structures inside infected cells. Also, the immune responses to the mutant viruses were assessed in mice with the hypothesis that infection with the attenuated viruses would alter the immune response to infection compared to mice inoculated with the parental strain.

Figure 1-1. Phylogenetics of WNV strains. Sequencing of WNV strains from across the world fell into two distinct lineages (Lineage I and Lineage 2). Lineage 1 included the New York 1999 strain and the Australian Kunjin virus among others. (Adapted from Lanciotti *et al.*, 1999).

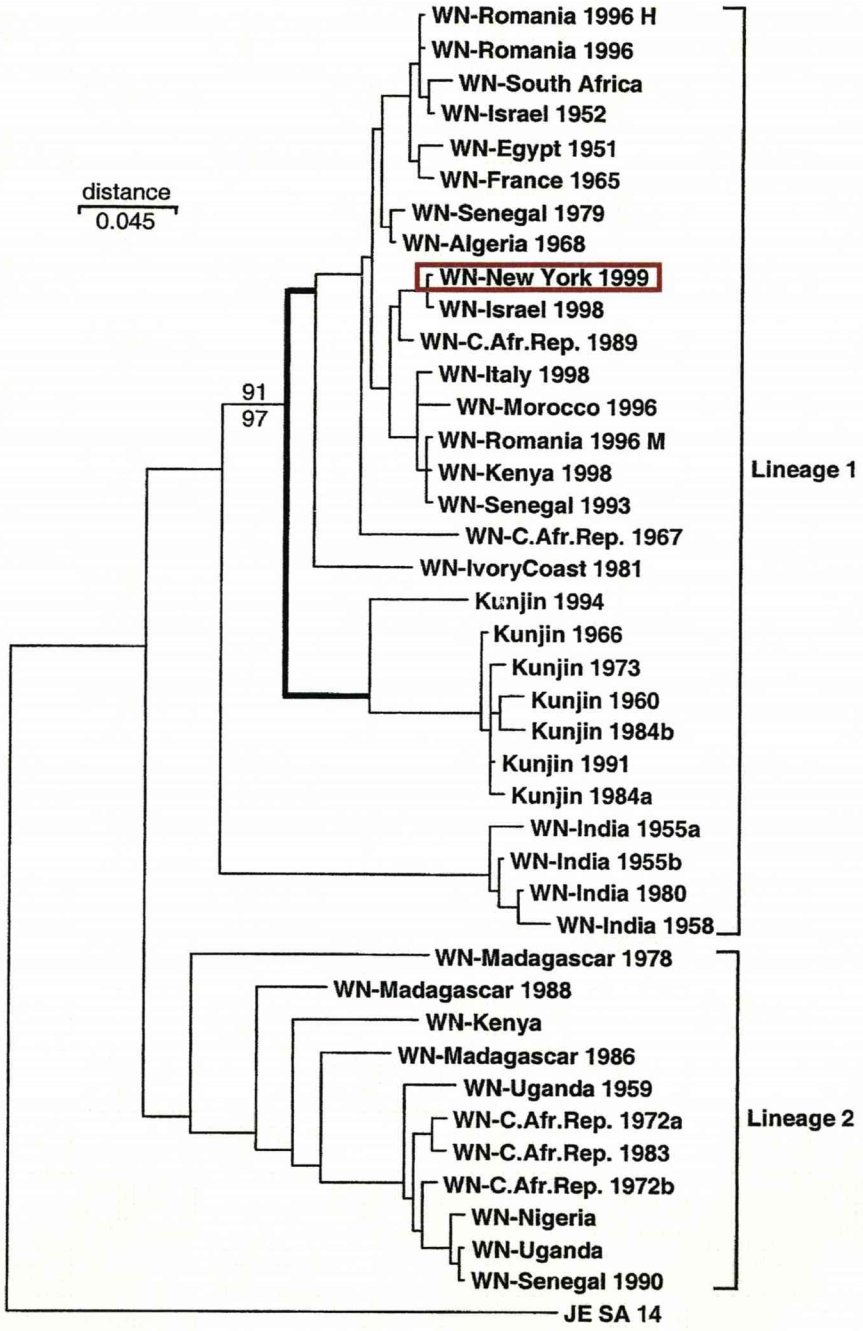

Figure 1-2. Approximate geographic distribution of West Nile virus. Blue indicates areas current or previous epidemics. Circle in Australia indicates the presence of KUN strain. (Adapted from CDC, Arbonet)

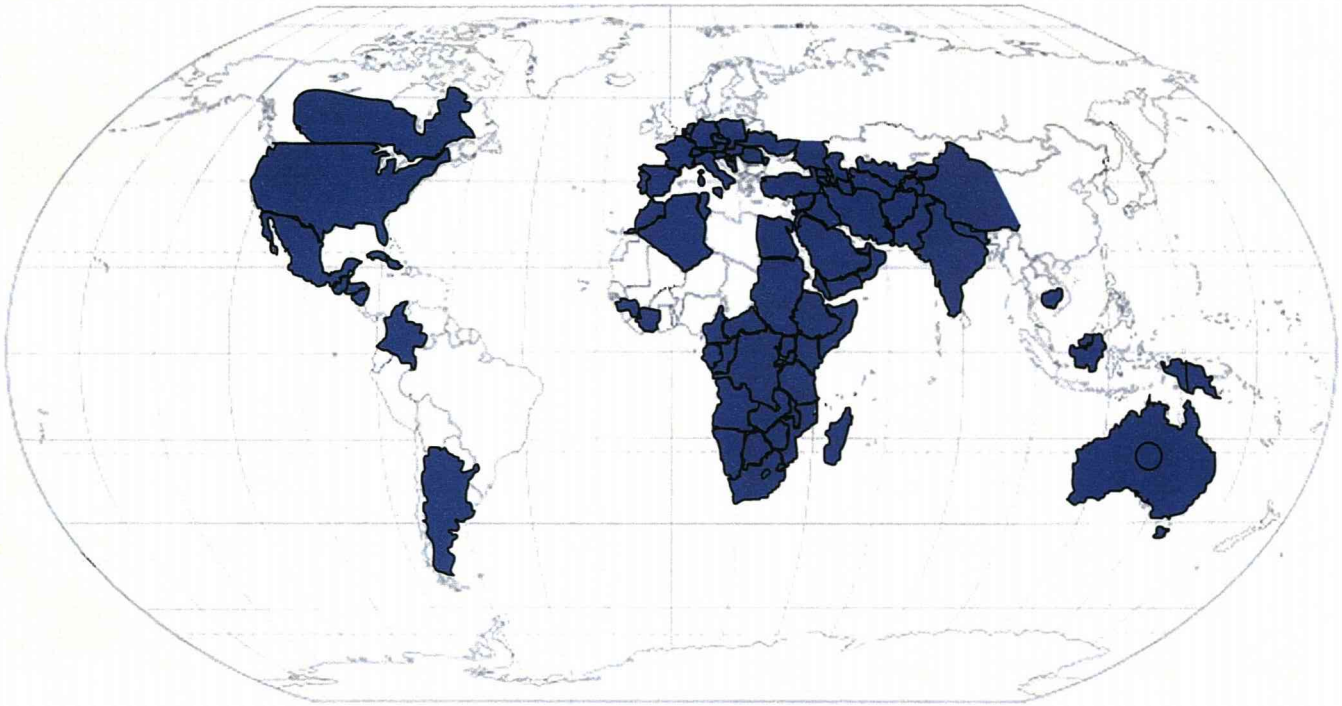

Figure 1-3. Outbreaks of WNV from 1951-2000. (Adapted from Murgue *et al.*, 2001)

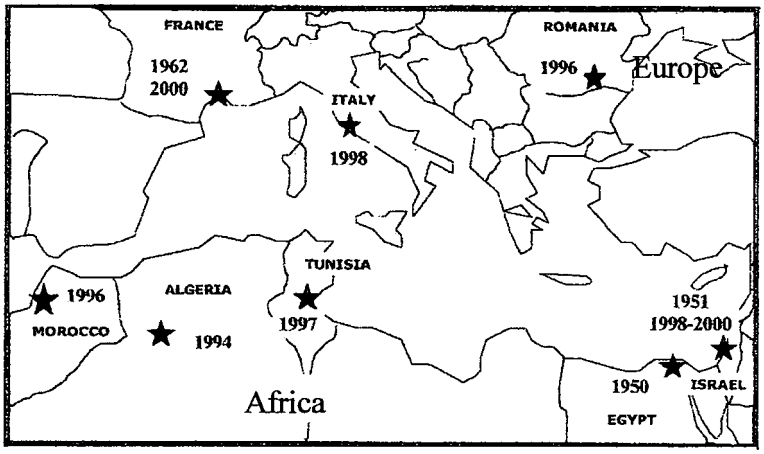

Figure 1-4. Distribution of human WNV cases in the US 1999-2006. (Adapted from CDC, Arbonet)

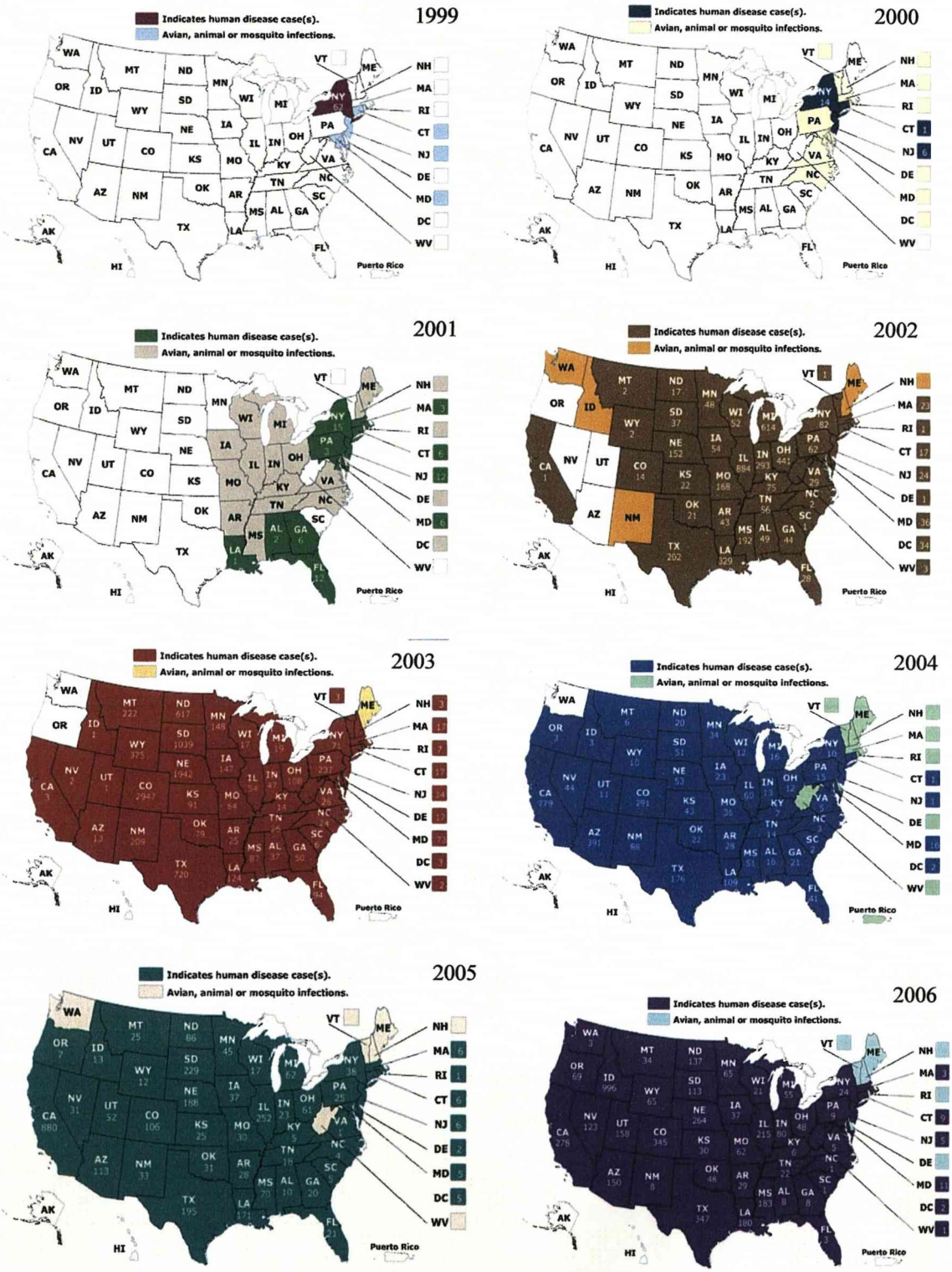

Figure 1-5. Migratory flight patterns of birds. The flyways in the Americas shows how different routes travel across the US, Canada and South America (Adapted from Gubler, 2007).

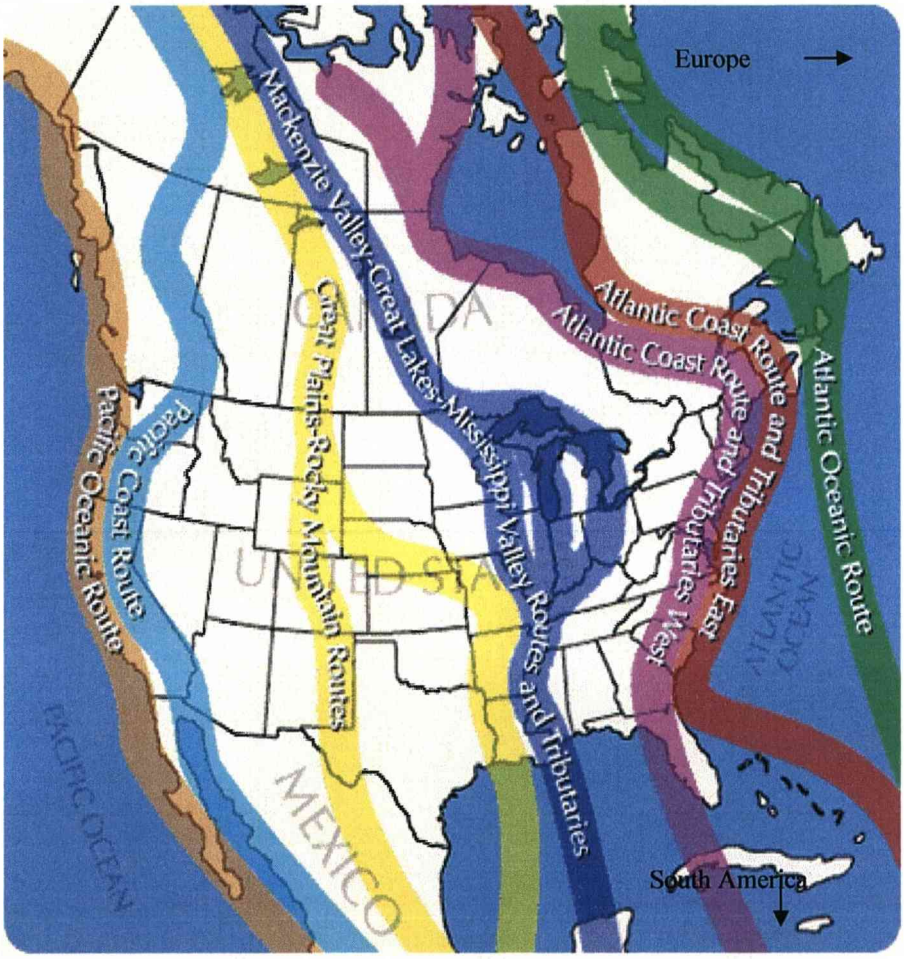

Figure 1-6. Distribution and migratory route of the Arctic Tern. The Arctic Tern nests around the world including Europe and the United States (Adapted from Reed *et al.*, 2003).

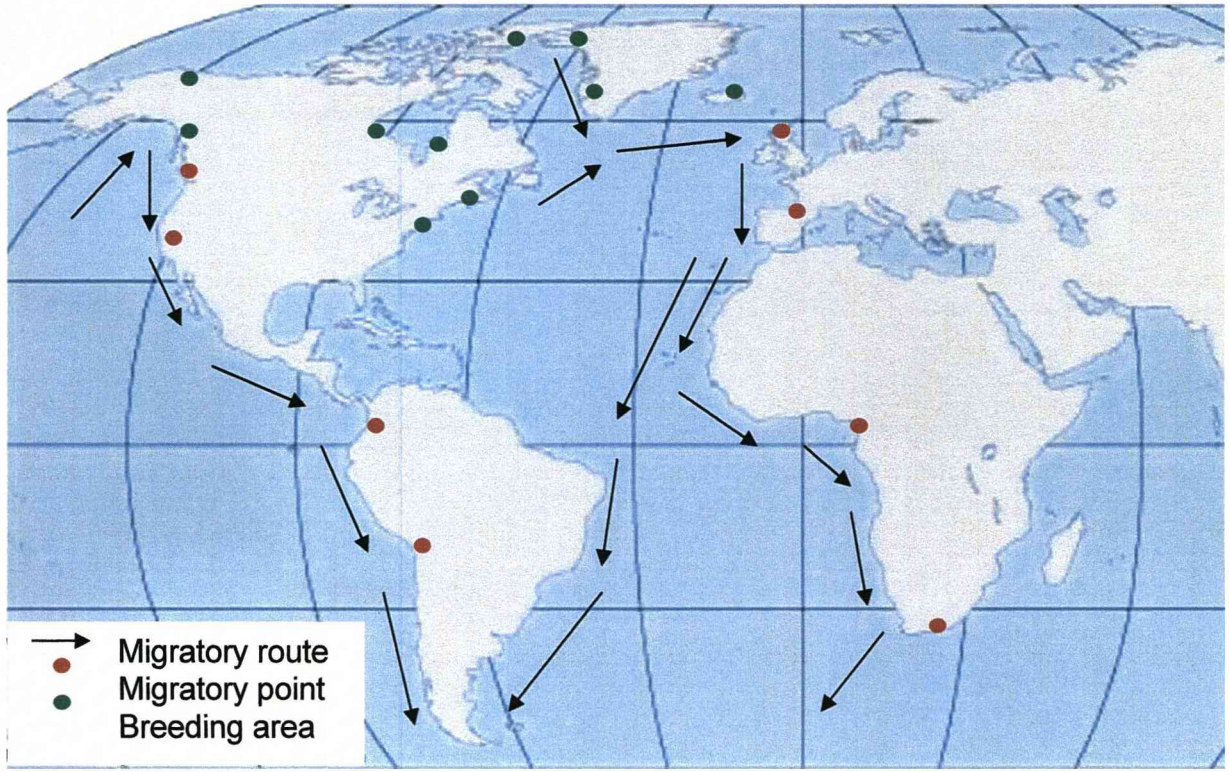

Figure 1-7. Transmission cycle of WNV. (Adapted from CDC, Arbonet)

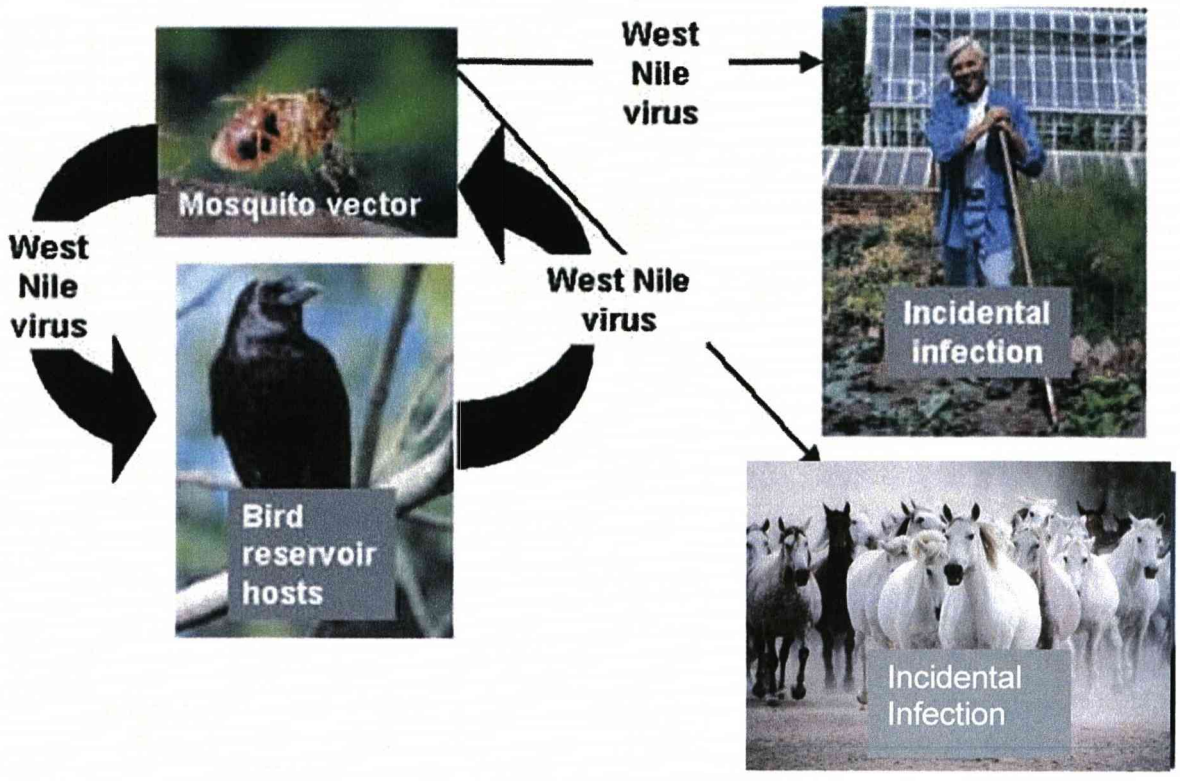

Figure 1-8. Structure of West Nile virus. West Nile virus structure appears as a round, spherical shape with iscosohedral symmetry. The E and M protein reside on the surface of the protein that contains the nucleocapsid and core containing the viral RNA (Adapted from Mukhopadhyay *et al.*, 2003)

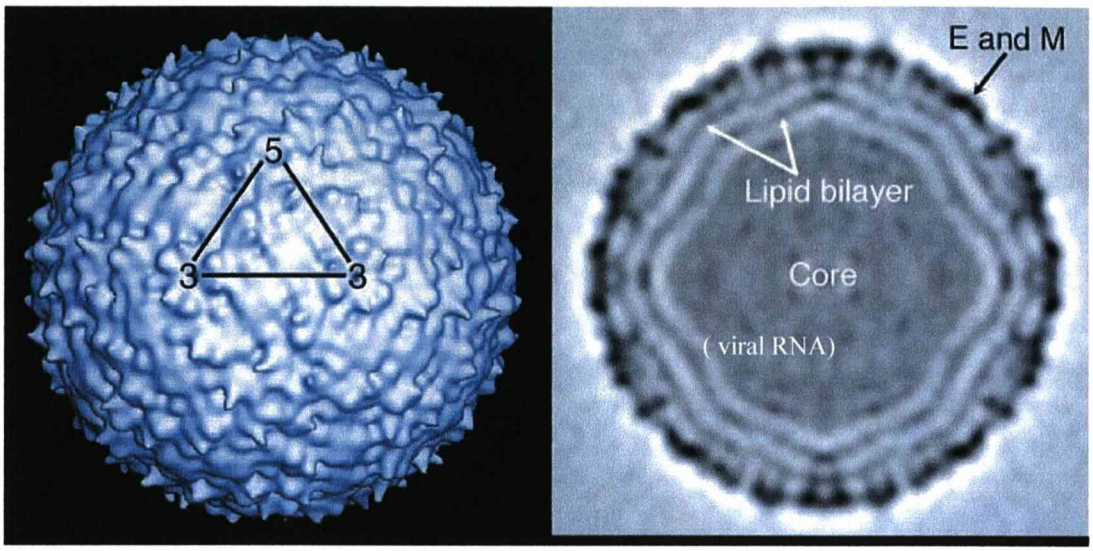

Figure 1-9. Schematic of West Nile virus genome. (Provided by ADT. Barrett)

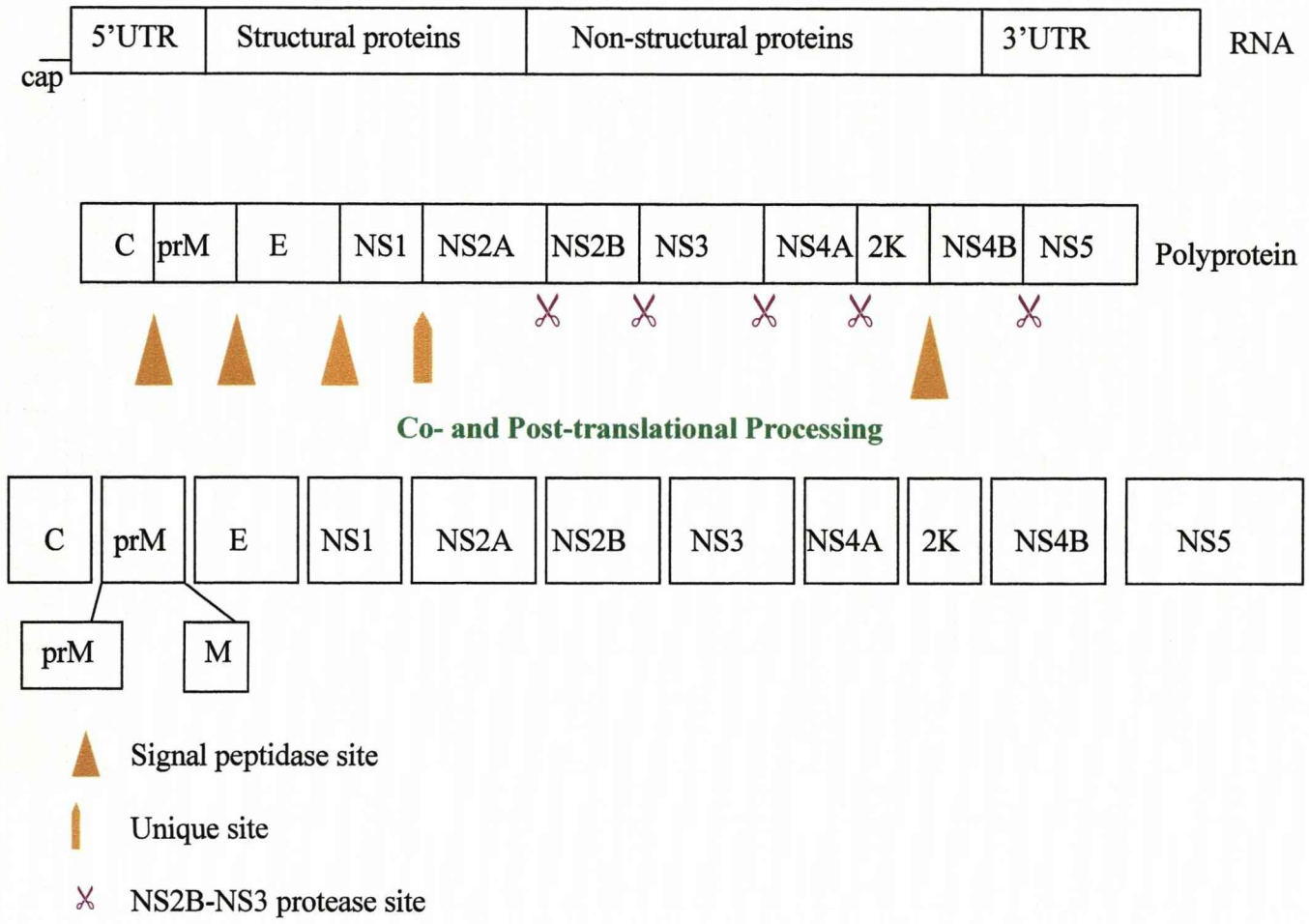

Figure 1-10. X-ray crystallographic structure of West Nile virus E protein. The E protein is comprised of three domains: domain I in red, domain II in yellow and domain III in blue. West Nile virus E contains one N-linked glycosylation site at E154. (Adapted from Kanai *et al.*, 2006)

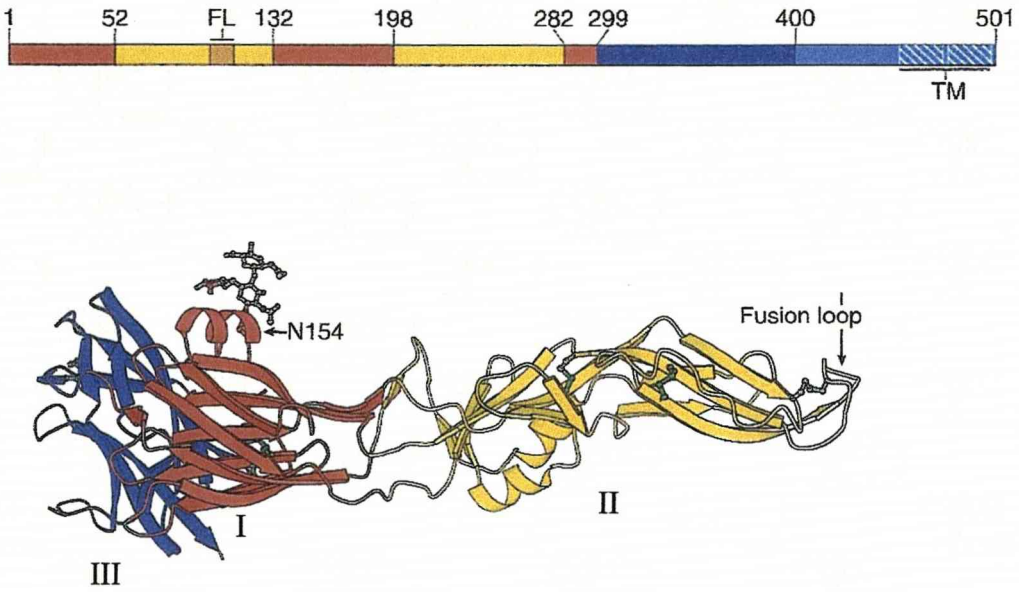

Figure 1-11. Class II fusion process. The fusion peptide of the E protein is buried within the dimer (1) the E protein binds via the receptor and is internalized in the endosome (2) a conformational change is caused by low pH. The fusion peptide, now exposed, inserts itself into the host membrane (3) The E protein folds back bringing the viral membrane closer to the host membrane (4) Domain III moves closer to domain II resulting in hemifusion of the membrane (5) where the trimer forms moving the transmembrane and the fusion peptide are in close proximity (6). (Adapted from Mukhopadhyay *et al.*, 2005)

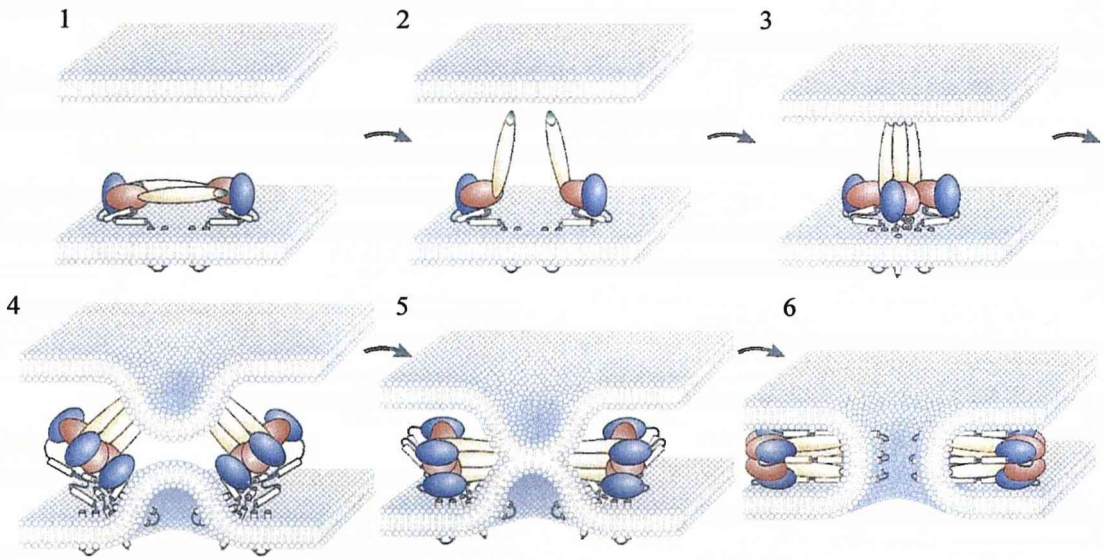

Figure 1-12. Flavivirus life cycle overview. The steps involved in the assembly of the virus remain vague, although proposed to be within the Golgi. (Adapted from Mukhopadhyay *et al.*, 2005).

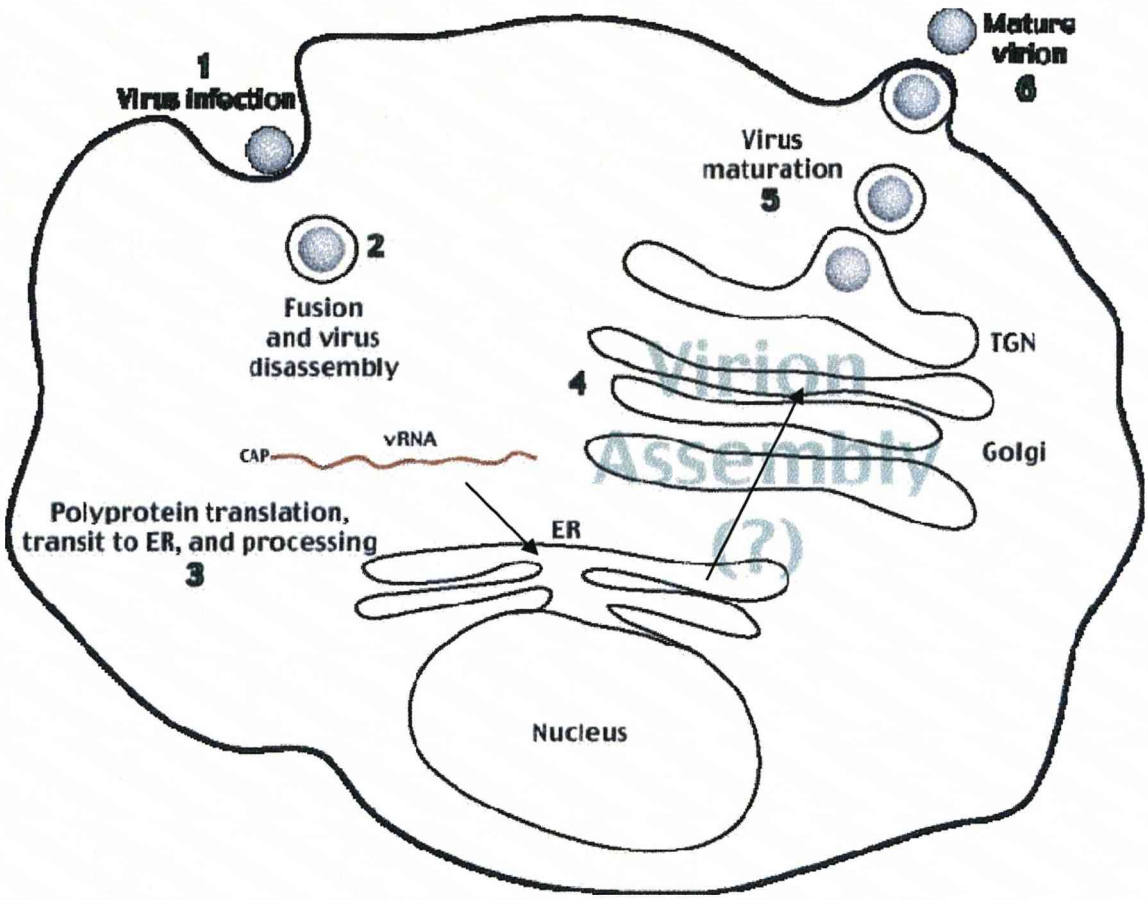

Figure 1-13. Flavivirus replication cycle. After binding and fusion, the capsid and viral RNA are exsposed leading to RNA replication begining with translation and polyprotein processing followed by the synthesis of a negative strand RNA intermediate. Newly synthesized positive RNA leads to viral morphogenesis in intracellular vesicles before maturation and release (Adapted from Solomon and Barrett in Nash and Burger (Eds) Clinical Neurovirology Marcel Decker 2003).

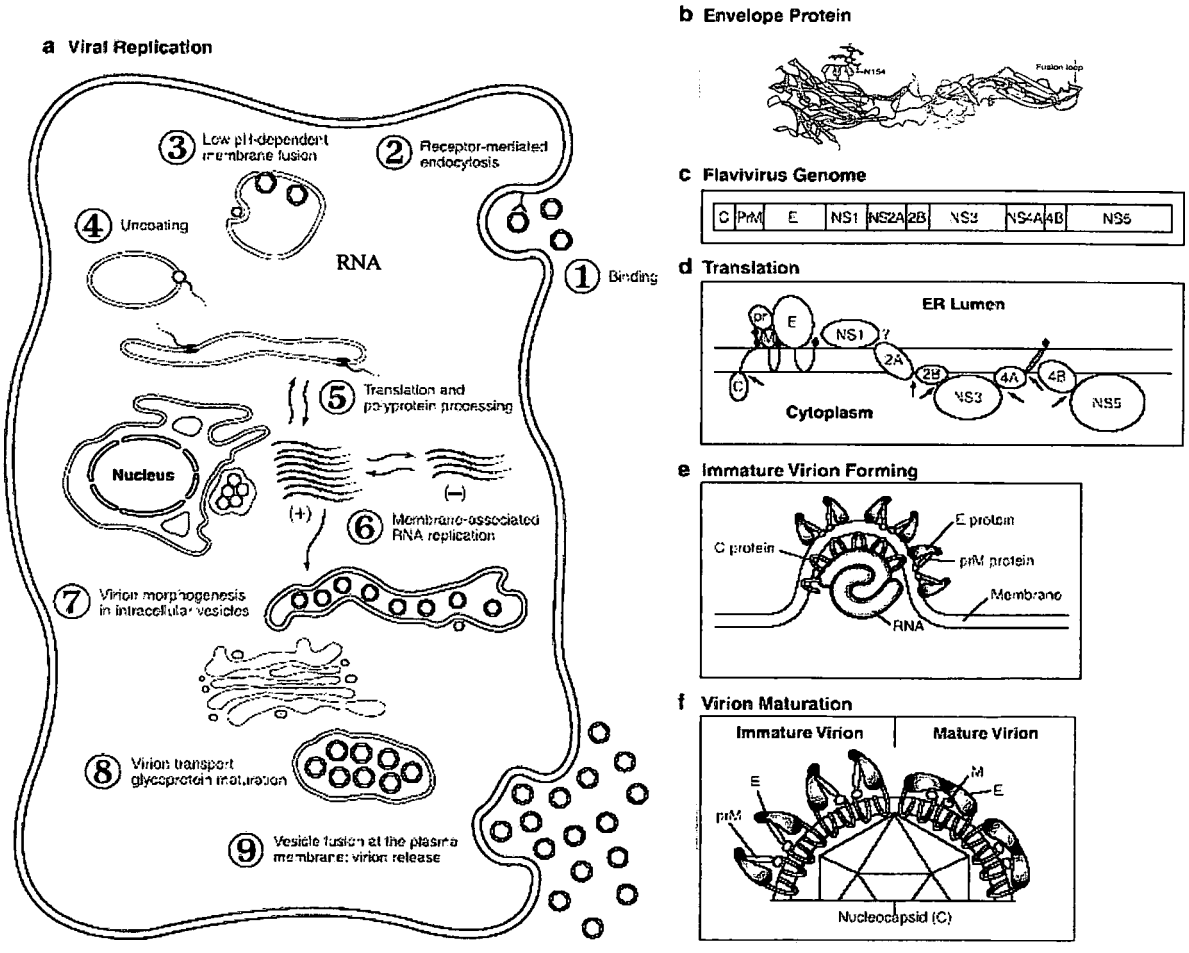

Figure 1-14. Dissemination of West Nile virus from mosquito bite to neuroinvasion. West Nile virus from the saliva of a mosquito travels from Langerhans dendritic cells to the draining lymph node resulting in viraemia. Virus crosses the blood brain barrier possibly aided by TNFα and infects the neurons. (Adapted from Samuel and Diamond, 2006).

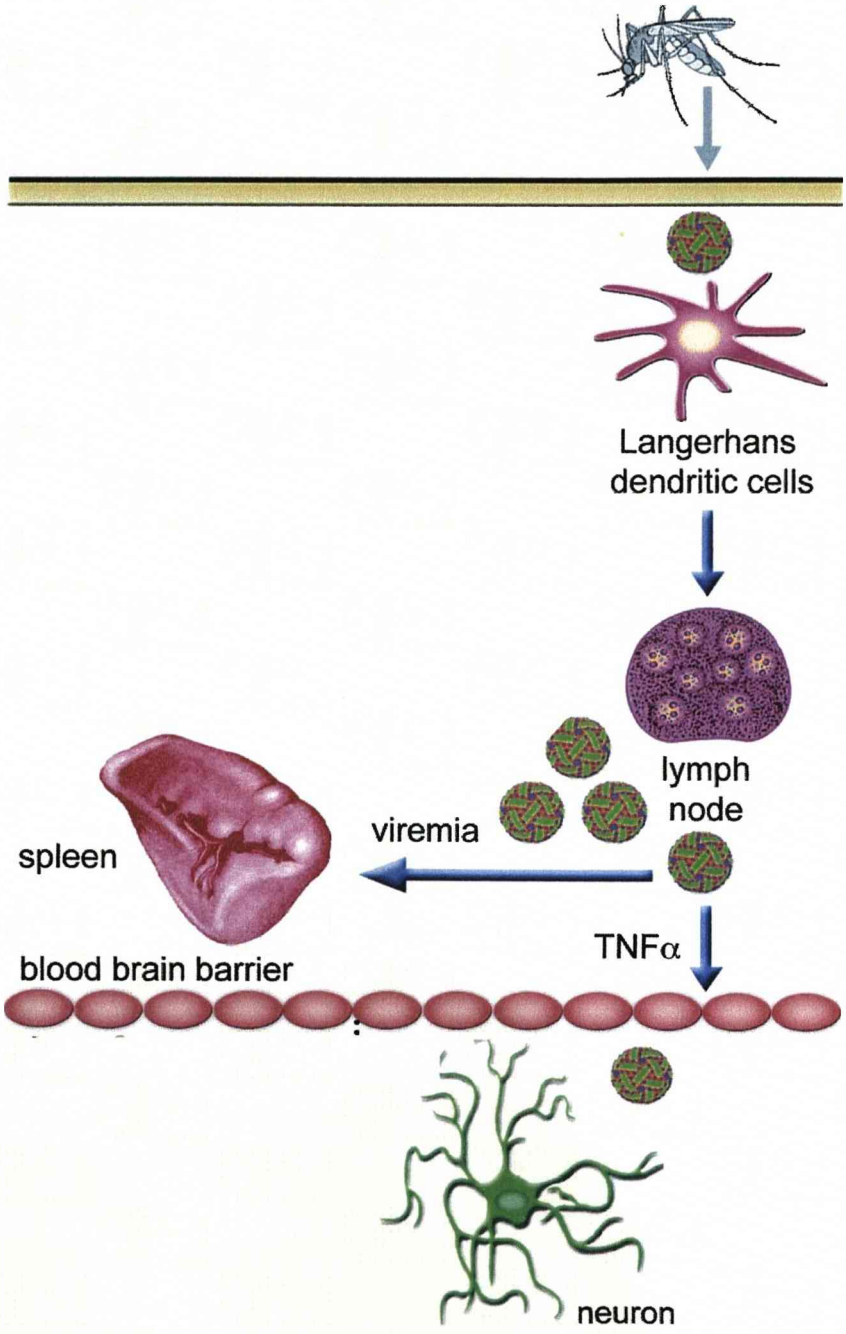

CHAPTER 2 : MATERIALS AND METHODS

2.1 Buffers and reagents

GTE resuspension buffer

50mM Glucose

25mM Tris-Cl

10 mM EDTA

Alkaline lysis buffer (SDS/NaOH)

0.2 N NaOH

1% SDS

3M KOAc pH 4.8

60ml 5M KOAc

11.5 ml glacial acetic acid

28.5 ml dH_2O

TE-RNase A buffer

10ul of stock RNase A (10mg/ml)

0.5ml TE buffer

PAGE running buffer (10x)

Glycine 144g

Tris 30g

SDS 20g

1L dH_2O

Western blot wet transfer buffer (10x)

Tris 30.3g

Glycine 144g

1L dH_20

Luria-Betani (LB) broth and agar

20g LB powder

Add dH_2O to 1L

For agar add 15g Bacto agar per liter

0.1 M cacodylate buffer

Dissolve 21.4 g sodium cacodylate trihydrate in ca. 800 ml deionized water

Titrate with 12N HCL to pH 7.2

Add water to total volume 1,000 ml

Filter and store

PFGPA stock solution

200ml 0.1 M cacodylate buffer heat to 60°C for 10 min

Add 12g paraformaldehyde powder, cover with aluminum foil and continuing heating while stirring until solution becomes clear

Remove from hot plate and cool at least 15 minutes

Add 0.04g trinitrophenol (picric acid)

Adjust pH to 7.3

PFGPA.1 fixative (100ml)

To 40ml stock solution add 0.2 ml 50% glutaraldehyde

Add 59.8 ml dH_20

Add 0.03g $CaCl_2$

Adjust pH to 7.3

PFGPA.1 fixative (final concentration)

2.5% formaldehyde

0.1% glutaraldehyde

0.03% picric acid (trinitrophenol)

0.03% $CaCl_2$

0.05 M cacodylate buffer pH 7.3-7.4

0.1 M maleate buffer (1000 ml)

Dissolve 5.8g maleic acid in ca. 900ml dH_2O

Add 2.2g NaOH

Titrate pH to 5.2 with 1N NaOH

Add dH_2O to 1000 ml

1% uranylacetate (UA) in 0.1 M maleate buffer (100ml)

Dissolve 0.58g maleate acid in ca. 90 ml dH_2O

Add 0.2g NaOH

Adjust pH to 6.0 with 1N NaOH

Dissolve 1g UA

2.2 Site-directed mutagenesis

A cDNA infectious clone designed from WNV NY99 (382-99) was used for these experiments (Beasley *et al.*, 2005). Briefly, the clone consists of a two plasmid system containing the WNV 5'untranslated region (UTR), the structural genes and the natural nt-2495 *NgoMIV* site of the NS1 gene in one plasmid (designated pWN-AB), and the *NgoMIV* through the 3' UTR in the second plasmid (pWN-CG). An *XbaI* site was engineered after the *NgoMIV* site of the 5' plasmid and at the end of the 3'UTR in the second plasmid. The vector plasmid (Kinney *et al.*, 1997) is a modification of plasmid pBR322 containing a T7 bacteriophage promotor upstream of the WNV 5' UTR.

The NS1 glycosylation mutants were derived using site-directed mutagenesis (Stratagene QuikchangeII XL). Nucleotide AA to GC mutations were engineered at genomic nucleotide positions 2857-2858, 2292-2293 and 3088-3089 in pWN-CG to change the asparagine to an alanine (N→A) for $NS1_{130}$, $NS1_{175}$, and $NS1_{207}$ (Table 2-1). Nucleotide A to G mutation was engineered in pWN-CG at 2858 to change the asparagine to serine (N→S) at $NS1_{130}$, 2858-2862 ACAAC→GCGTG to change asparagine, asparagine to serine, valine (NN→SV) at $NS1_{130-131}$, 2857-2859 AAC→CAG to change the asparagine to glutamine (N→Q) at $NS1_{130}$ and 2857 to

2865 AACAACACC→CAGCAGGCG to change asparagine, asparagine, threoine to glutamine, glutamine, alanine (NNT→QQA) at $NS1_{130-132}$ (Table 2-1). The prM and E glycosylation sites were also ablated by changing the asparagine to serine (N→S) with nucleotide changes at 508-510 (TCG→AAT) for the prM_{15} mutant and at 1427 (A→G) for the E_{154} mutant (Table 2-1).

2.3 Large scale plasmid DNA extraction

Plasmid DNA of the WN cDNA infectious clone was extracted using a large scale plasmid extraction protocol. Either broth containing a bacterial colony or the bacterial colony from a plate streaked with bacterial culture broth was used to grow the bacteria in 200 ml LB broth with 200 µl of a 50 mg/ml stock of ampicillin overnight. The culture broth was centrifuged for five minutes at 6,000 rpm to pellet the cells. Next, the cells were resuspended in 6 ml of cold GTE, the cells lysed with 9 ml SDS/NaOH for five minutes on ice before the addition of 9 ml of 3M KOAc. The cellular debris and chromosomal DNA was then pelleted by centrifugation for 10 minutes at 10,000 rpm. The liquid was aspirated and added to 16 ml ispropanol, mixed, and centrifuged for 15 minutes at 10,000 rpm to reveal a pellet. The liquid was discarded and 500 µl TE buffer was added to dissolve the pellet and RNase A was added. This mixture was placed at 37°C for 30 minutes to one hour before phenol chloroform and chloroform extractions. Ethanol was added to the tube and a pellet was formed after centrifugation for 10 mintues at 14,000 rpm at 4°C. The ethanol was discarded and 500 µl of TE was added to dissolve the pellet. This crude DNA prep was further purified using the Qiagen PCR purification kit. Concentrations of DNA were

determined by running one microliter of sample on a gel with DNA loading buffer (NEB).

2.4 In vitro ligation

The two plasmids (Fig. 2-1) were prepared for *in vitro* ligation by digesting approximately 1μg of each 5' pWN-AB and 3' pWN-CG plasmid with *NgoMIV* and *XbaI*. The 5' and 3' DNA fragments were purified by agarose gel electrophoresis and ligated using T4 DNA ligase (NEB) overnight at 4°C, after which the ligase was heat inactivated for 10 minutes at 70°C. Ligated DNA containing full-length WNV genome was linearized by *XbaI*, treated with proteinase K, extracted twice with phenol/chloroform/isoamyl alcohol and once with chloroform, and then ethanol precipitated. The pelleted DNA was rehydrated in 10 μl of TE buffer pH 8.0 (Invitrogen) and used as template for transcription, incorporating A cap analog (NEB) and using the Ampliscribe T7 transcription kit (Epicentre). After two hours of incubation at 37°C, 2 μl of the transcription reaction was analyzed by agarose gel electrophoresis to ensure that transcription had taken place. The remaining transcription reaction was mixed with $3.3x10^6$ Vero cells in 500 μl of phosphate buffered saline (PBS; Gibco), placed in a 0.2-cm electrode gap cuvette (Bio-Rad), and pulsed twice at 1.5 kV, 25μF, and ∞ ohms using a Gene Pulser electroporator (Bio-Rad). The electroporated cells were incubated at room temperature for 10 minutes, then added to 35 ml of minimal essential medium (MEM-Gibco) supplemented with 8% BGS (Hyclone), 100 units/ml of penicillin and 100 μg/ml of streptomycin (Gibco), 0.1 mM non-essential amino acids (Sigma), and 2 mM L-glutamine (Gibco) in a 75-cm^2 tissue culture flask (Costar), and incubated in 5% CO_2 at 37°C. Virus was

harvested when cytopathic effects (CPE) were apparent. The cell debris was pelleted by centrifugation, and the supernatant medium was stored in 1 ml aliquots at -80°C.

2.5 RT-PCR

RNA was extracted from a sample of each mutant virus using the QiaAmp Viral RNA Mini kit (Qiagen), and a cDNA fragment containing the NS1 gene was amplified by RT-PCR (Roche Titan One Step RT-PCR kit) and sequenced to confirm the presence of the introduced mutation(s). Primers used for genome and protein fragment sequencing are outlined in Table 2-2 and the RT-PCR conditions used are as follows:

Reverse transcriptase	50°C	30 min	
Denaturing	94 °C	2 min	x1
Annealing	55 °C	30 sec	
Extension	68 °C	2 min	
Denaturing	94 °C	15 sec	x9
Annealing	55 °C	15 sec	
Extension	68 °C	2 min	
Denaturing	94 °C	15 sec	x25
Annealing	60 °C	15 sec	
Extension	68 °C	2 min Δ 5sec	
Hold	4 °C		

2.6 Cell culture

2.6.1 Passaging virus

Viruses were passaged in Vero cells before subsequent use. Supernatant from transfected cells were added to a confluent monolayer of Vero cells, left for 30 minutes at room temperature before adding maintenance media containing 2% BGS (Hyclone) MEM supplemented with glutamine, penicillin/streptomycin and non-essential amino acids. Supernatant was collected two days later, centrifuged and frozen at -80 °C.

2.6.2 Plaque titration

Infectivity of each virus was measured by plaque titration using 6-well tissue culture plates (Costar-3506) containing confluent Vero cell monolayers. The virus was added to the cells in ten-fold dilutions and left at room temperature for 30 minutes, rocking the plates every five minutes. After this time, 4 ml of 2% agarose/MEM overlay was added to the cells and the plates were placed at 37 °C. For temperature sensitivity assays, an additional plate was prepared in parallel and incubated at 39.5 °C. Two days later, a second 2 ml overlay containing 2.4% neutral red (Sigma) was added. Plaques were visualized over the next two days. A temperature-sensitive phenotype was evidenced by reduced viral plaque titre at 39.5 °C compared to 37°C.

2.6.3 Plaque reduction neutralization tests

Neutralizing antibody titres were determined by $PRNT_{50}$. Mice inoculated intraperitoneally (ip) with either NY99 or attenuated mutant viruses were bled 21 days

post-inoculation and the serum collected. Serum was diluted 1:5 in PBS and heat inactivated at 56°C for 30 minutes. The serum was then diluted 1:5 in PBS before preparing two-fold dilutions in 100 µl of 2% MEM. The NY99 virus was diluted to 200 PFU/100 µl and 100 µl of virus was added to 100 µl of serially diluted serum, mixed and placed at 4°C overnight. One hundred microlitres of the serum/virus mixture was added to confluent Vero cells in 6 well plated (Costar). Back titrations of the virus were also plated at 10^{-1} to 10^{-2}, or 100, 10, and 1 PFU respectively, to test the dilutions. Plaques were counted and the $PRNT_{50}$ was determined by a 50% reduction in plaques.

2.7 Multiplication in cell culture

Viral replication kinetics were analyzed in monkey kidney Vero (ATCC CCL 81) mouse macrophage-like P388 D1 (ATCC CLL-46) and mouse neuroblastoma Neuro 2A (ATCC CCL-131) cells. Virus was adsorbed at a moi of 0.1 to confluent monolayers of cells for 45 minutes at room temperature. The inoculum was aspirated, cells washed with PBS and maintenance MEM medium containing 2% BGS was added. Triplicate monolayers were infected for each virus, and samples were collected at 12, 24, 36, 48, 60, 72 and 96 hours post-infection for Vero and P388 D1 cells and at 12, 24, 48, 72, and 96 hours for Neuro 2A cells, centrifuged to pellet cell debris, and frozen at -80°C until analyzed by plaque titration in Vero cells. Some of the mutant viruses were combined into one large experiment and the data was subsequently separated; therefore, the NY99 replication curve may be repeated in more than one chapter.

2.8 Western Blot

Confluent Vero cells in 100 mm tissue culture petri dishes were inoculated with mutant virus or the parental strain. After adsorbing for 30 minutes, the virus inoculum was removed, the cells were washed twice with PBS, and 10 ml of MEM containing 2% BGS and supplemented as above was added. The plates were incubated for two days at 37°C, after which the culture medium was collected, concentrated to 250 µl by using an Amicon 10kd filter, and mixed with an equal volume of RIPA lysis buffer (Eliceiri *et al.*, 1998). Whole cell lysates were also collected. Laemmli loading dye containing 0.5M Tris pH 6.8, 6% glycerol and bromophenol blue was added to the culture medium extract, and samples were boiled for five minutes. Similarly, Laemmli loading dye containing 0.6 M DTT (Sigma) was added to the whole cell lysate samples. Five to 25 µl of each sample was loaded onto a 10% polyacrylamide gel (Bio-Rad), and western blotting was performed by using a transblot (Bio-Rad) according to the manufacturer's instructions. After wet transfer, the blots were blocked overnight in 5% milk (Sanalac) in Tris buffered saline (TBS). Next, the blocking buffer was removed, anti-NS1 monoclonal antibody (Chung *et al.*, 2006) was added at a dilution of 1:200, and the blots were incubated for 30 minutes at 37°C. The primary antibody was removed by three five- minute washes with TBS. Secondary anti-mouse whole IgG antibody containing horseradish peroxidase (HRP-Sigma) and diluted 1:5,000 in blocking buffer was added for 30 minutes at room temperature. The secondary antibody was removed with three five-minute washes of TBS, and chemiluminescent reagent was added (Super Signal - Pierce). Audoradiographs were developed to visualize the protein.

Some western blots used to visualize the NS1 protein were re-probed in order to visualize the E protein. In these cases, the blots were stripped using Restore Western Blot Stripping Buffer (Pierce). Approximately 25 ml of buffer was added to the blot with rocking for 10 minutes to remove the chemiluminescence and antibodies. The blot was then washed with TBS three times to remove the stripping buffer before blocking in milk. The primary (anti-EDIII) and secondary (anti-mouse-HRP) antibody and chemiluminescence were added as described above for the NS1 antibody.

2.9 Confocal microscopy

In vitro fluorescent conjugate antibody probing was used to examine differences in the E and NS1 protein staining pattern of the attenuated E_{154S}, $NS1_{130\text{-}132QQA/175A/207A}$ and $E_{154S}/NS1_{130A175A/207A}$ mutant versus the parental NY99 strain and mock-infected cells. A coverslip containing a confluent monolayer of Vero cells was infected with either mutant or parental WNV at a moi of 0.1. The viruses were left to adsorb for 30 minutes at room temperature, the inoculum removed and the coverslips washed with PBS twice before 2% serum containing medium was added and left at 37°C for 48 hours. The coverslips were then fixed in acetone and dried. A double staining technique was used to probe the E and NS1 protein by adding a rabbit anti-E domiain III antibody to the coverslips, left for one hour at 37°C, then wash three times with PBS. The second primary antibody, a mouse anti-NS1, was added and left at 37°C for 45 minutes, then wash three times with PBS. The two secondary anti-rabbit and anti-mouse alexoflour conjugate antibodies were then added (Molecular Probes) diluted to 10 μg/ml and left at 30 minutes at 37°C then washed three times with PBS. The coverslips were mounted on slides with DAPI containing Prolong Gold mounting

media (Molecular Probes). The slides were viewed using a Ziess confocal and the images visualized using Zeiss LSM image browser. All slides were analyzed using the same gain.

A similar technique was used to visualize the endoplasmic reticulum (ER). A confluent monolayer of Vero cells was infected with either $NS1_{130\text{-}132QQA/175A/207A}$ or parental NY99 strain at an moi of 0.1 or mock-infected as above. Cells were fixed, stained and visulaized as above, except the primary antibody, mouse anti-ER antibody diluted 1:200, was used (Molecular Probes).

2.10 Electron microscopy

The parental NY99, attenuated NS1 glycosylation mutant viruses and mock-infected cells were used for electron microscopy (EM) to visualize the virus within the cell. T25 flasks containing a confluent monolayer of Vero cells were infected with a moi of 0.1, virus left to adsorb for 30 minutes and then washed with PBS before adding 2% MEM media. Forty-eight hours post-infection the cells were washed with PBS and fixed with PFGPA.1 fixative (see reagents) for two hours at room temperature. Next, the cells were washed with 0.1 M cacodylate buffer three times for 10 minutes at room temperature. After washing the cells were scraped, placed into an eppendorf tube and centrifuged for 10 minutes at 8,000 rpm to pellet cells. At this time the cell pellet was divided into two separate tubes to complete the procedure for transmission electron microscopy (TEM) and transmission immuno-EM (TIEM).

2.10.1 TEM post-fixation and embedding procedure

Post-fixation, 1% OsO4 in 0.1 M cacodylate buffer was added to the cell pellet and left for 1 hour at room temperature followed by three washes with 0.1 M cacodylate buffer for 10 minutes each, then one wash in 0.1 M maleate buffer at pH 5.2 for 10 minutes. Next, *en bloch* staining consisting of 1% UA in 0.1 M maleate buffer was performed for 30 minutes at 60°C followed by four 10 minute washes with 0.1 M maleate buffer at a pH of 5.2 at room temperature, then the pellet was left in 0.1 M maleate buffer overnight at 4°C. The next day the pellet was dehydrated with several ethanol washes including 50% ethanol wash for 10 minutes, 75% ethanol for 10 minutes, 95% ethanol for 10 minutes and three washes with 100% ethanol for 10 minutes each. Infiltration of the pellet with propylene oxide (PO) was performed next two times for 10 minutes each followed by two 1 hour infiltration steps, PO:Poly/Bed 812= 50:50 and 25:75 , with rocking and then pure Poly/Bed 812 was added twice for one hour with rocking. Embedding followed by placing the cell pellet in Poly/Bed 812 into polyethylene capsules to polymerize overnight at 60°C. The embedded cell pellet was then cut into thin sections and placed on disks for visualization on the electron microscope.

2.10.2 TIEM post-fixation and embedding procedure

Post-fixation, *en bloc* staining for TIEM consisted of one wash in 1% UA in 0.1 M maleate buffer, making sure the pellet was away from the wall of the tube, for 20 minutes at 60°C. Four consecutive washes with 0.1 M maleate buffer at a pH of 5.2 for 10 minutes each was followed by one wash in the same buffer overnight at 4°C. Dehydration of the pellet was performed by two 10 minute washes with 50% ethanol,

two 10 minutes washes with 75% ethanol and one 1 hour wash in the dark with a 1:2 dilution of 75% ethanol and LR white. Three more consecutive washes with LR white were performed first for 1 hour at room temperature and then overnight followed by one more 1 hour wash. The cell pellet LR white mixture was embedded into small gelatin capsules for polymerization for 24 hours at 60°C. Following polymerization, thin sections were cut and placed onto disks.

2.10.2.1 Antibody staining

Petri dishes lined with parafilm were used to wash and stain the disks. The buffers and antibodies were syringe filtered, drops were added to the parafilm and the disks were placed face down onto the drops. The cells were blocked in BSA-G buffer for 15 minutes before placed onto the primary antibody. The primary antibodies were diluted 1:2 for the rabbit α-EDIII and 1:10 for the mouse α-NS1 (17 NS1: Chung *et al.* 2006) in BSA-G, combining both, and left for one hour in a moist chamber and then overnight at 4°C. The next day the unbound primary antibodies were removed with five washes in BSA-G for three minutes each and then placed onto 20 µl of the secondary antibodies containing a 1:20 dilution of the α-rabbit and α-mouse gold particles in 1% BSA for one hour at room temperature in a moist dark chamber. The unbound secondary antibodies were then removed by another five washes of BSA-G for three minutes each and followed by three TBS buffer washes for five minutes each and one wash with water for five minutes. Next 2% aqueous GA was added for five minutes and then washed with water three times for five minutes each. A five minute staining in 2% UA followed and was washed three times for five minutes each in water and then left to air dry before the final Pb-citrate step for 30 seconds. The disks were then visualized in the electron microscope.

2.11 Mouse studies

2.11.1 Ip and ic inoculations

To determine the mouse virulence phenotype of the mutant viruses, groups of five 3-4, 3- or 5-week-old female NIH Swiss mice (Harlan Sprague-Dawley) were inoculated via intraperitoneal (ip) and intracerebral (ic) routes with serial 10-fold dilutions of virus. Due to the lack of availability of mice, some experiments contained 3-5 week-old-mice. Differences in the LD_{50} of weanling- and adult-infected mice were undertaken in Chapter 9. The parental NY99 strain derived from the infectious clone was used as a positive control in each experiment, and PBS was used as a negative control. Mice were observed for 21 days and 50% lethal dose was calculated for each group. Some of the mutant viruses were combined into larger experiments and the data subsequently separated; therefore, the parental NY99 control may be repeated in more than one chapter.

2.11.2 Multiplication kinetics

To study the *in vivo* replication kinetics of the attenuated viruses compared to the parental strain, groups of mice were inoculated ip with 100 PFU of either $NS1_{130A/207A}$, $NS1_{130A/175A/207A}$, or clone-derived parental NY99 virus. Three mice were sacrificed each day post-infection for six days, and brains and blood were collected. Blood samples were centrifuged in a microtainer tube containing a serum separator before collecting the serum and storing at -80°C. Each brain was homogenized in 500 µl of 2%MEM and frozen at -80°C. All samples were plaque titrated in Vero cells.

2.11.3 Serum collection

Whole blood was collected from mice via tail bleeds. Blood was collected in mictrotainer tubes containing a serum separating gel (BD- 365956) and left at room temperature for at least 30 mintues to coagulate. After this time the tubes were centrifuged at 6,000 rpm for 90 seconds and serum was transferred to a new tube. The serum was stored at -80 °C until subsequent use.

2.11.4 Isolating and sequencing virus from the brain

Brains from moribound and dead mice were collected and homogenized in 2% BGS MEM. The RNA was extracted either from the brain homogenate or from culture supernatant from Vero cells infected with brain homogenate.

2.12 Cytokine/chemokine analysis

2.12.1 Cytokine membrane

Whole blood was collected at one and three days post-infection from mice inoculated ip with the parental NY99 strain or PBS inoculated mice. The blood was allowed to coagulate, the serum separated (see serum collection section) and frozen before use with RayBiotech's Mouse Cytokine Antibody Array III membranes (Fig. 2-2). The protocol supplied with the kit was followed and the membranes were analyzed using a densitometer.

2.12.2 Bioplex

Serum collected from 3-, 5- and 3-5-week-old mice inoculated ip with the parental NY99, $NS1_{130A/175A/207A}$, $NS1_{130\text{-}132QQA/175A/207A}$ or PBS on days one and three post-

infection was used for cytokine/chemokine expression anlysis using the Bioplex kit and equipment (BioRad). The mouse 23- and/or 9-plex beads (Table 2-3) and the standard controls were utilized according to manufacturer's instructions. Triplicate samples were analyzed on 96-well plates read using the Plex-200 machine. Student's t-test was used to determine the significance of up- or down-regulation compared to the mock-infected samples.

2.13 Statistical significance

Statistical significance was determined for mouse average survival time and the cytokine assays. Significance was determined by Student's t-test ($p<0.05$) for all experiments. The mouse average survival time significance was determined by comparing the parental NY99 strain to the mutant strains and the significance of the cytokine data was determined by comparing the virus-infected samples to the mock-infected samples. No outliers were visualized by a box and whiskers plot.

Significance was also determined for the immuno-EM studies. Six fields were counted for the mock and NY99-infected cells for both E and NS1 gold particles. The background staining for the mock-infected cells was significantly less than the infected cells ($p<0.01$) by Student's t-test.

2.14 Research statement

The experimental work contained in this thesis was the work of the author. The laboratory research in this thesis was conducted at the University of Texas Medical

Branch in Galveston,TX under the supervision of Professor Alan Barrett (UTMB) and Professor Tom Solomon (Liverpool).

Table 2-1. Mutagenesis primers

prM_{15S}	CTAACTTCCAAGGGAAGGTGATGATGACGGTATCGGCTACTGACG
E_{154S}	GTCGCACGGAAGCTACTTCCACACAGGTTGG
$NS1_{130A}$	CCAGAACTCGCCGCCAACACCTTTGTGG
$NS1_{175A}$	GGTCAGAGAGAGCGCCACAACTGAATGTGACTCG
$NS1_{207A}$	GGATTGAAAGCAGGCTCGCTGATACGTGGAAGC
$NS1_{130Q}$	GCACCAGAACTCGCCCAGAACACCTTTGTGGTTGATGGTCCGG
$NS1_{130S}$	CCAGAACTCGCCAGCAACACCTTTGTGGTTG
$NS1_{130\text{-}131SV}$	CAGAACTCGCCAGCGTGACCTTTGTGGTTG
$NS1_{130\text{-}132QQA}$	GCACCAGAACTCGCCCAGCAGGCGTTTGTGGTTGATGGTCCGG

Figure 2-1. Drawing of WNV genome: mutagenesis to transfection. The WNV cDNA infectious clone exists as a two plasmid system. Mutagenesis was performed to either plasmid according to the location of the desired mutation. The two plasmids were ligated together before transfection into Vero cells.

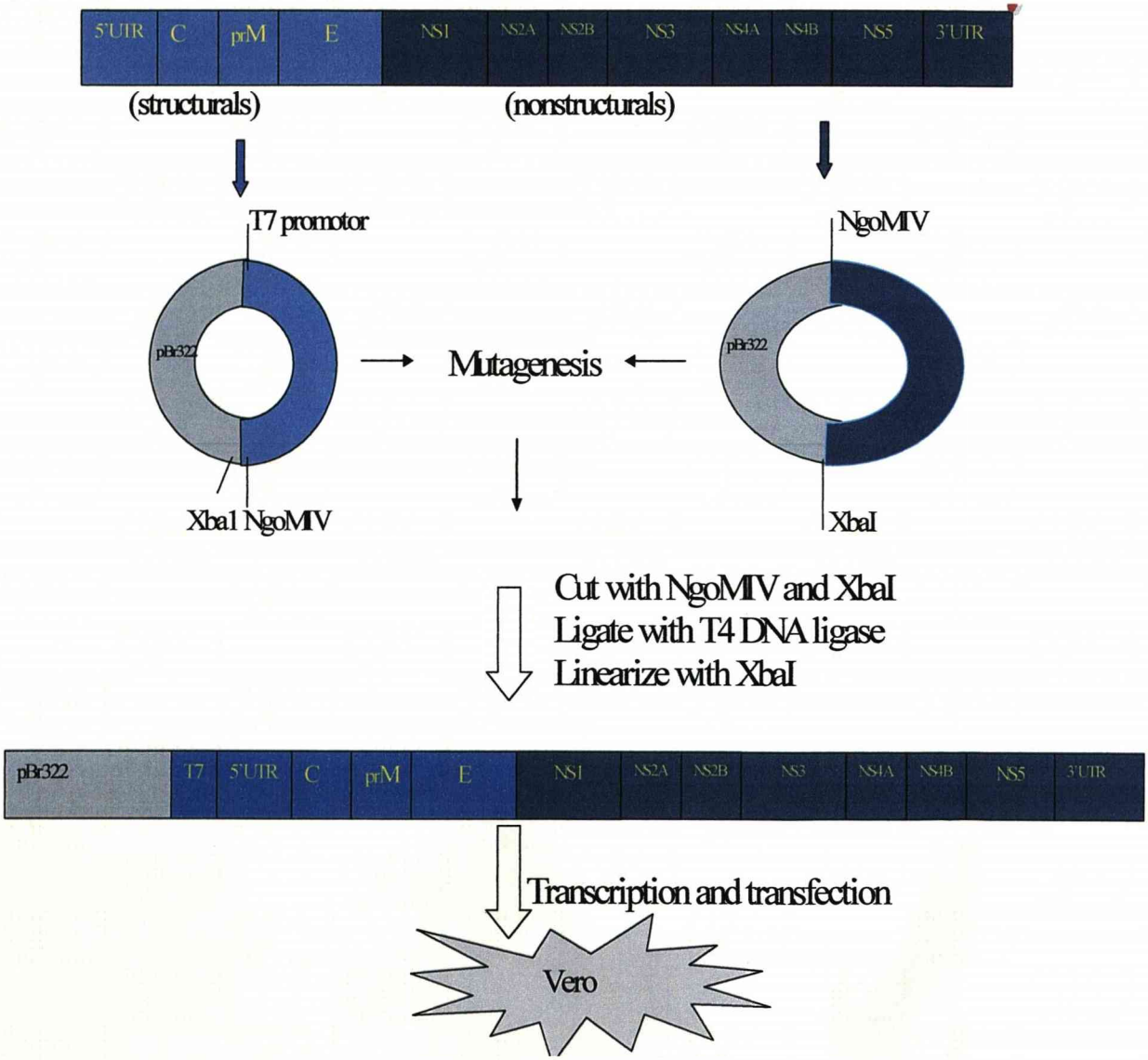

Table 2-2. NY99 infectious clone primers

WN-1272-	CAACGGCTGCGGACTATTTGG
cWN-2500-	GCCGGCTGATGTCTATGGCAC
WN-2495-	GCCGGCAAGAGCTGAGATGTG
cWN-3795-	CGCTTTGAGAAACGATGCCACC
WN-3739-	GGAGACGTGGTACACTTGGCGC
cWN-5248-	GGCCTCTTTGATGATCTGTGGCAG
WN-5199-	CGGCGCCGGTAAAACAAGG
cWN-6701-	CCAATGCCCTTCCGCTGC
WN-6640-	GCCTTATTGAGTGTGATGACCATGG
cWN-8155-	GCTCTTCAACCTCAGCACTTGACG
WN-8086-	CCTTCTGAGTGTTGTGACACCCTCC
cWN-9592-	CCACATCATCTGGGCCAATCAC
WN-9511-	GCCCTAAACACTTTCACCAACCTGG
cWN-11029-	AGATCCTGTGTTCTCGCACCACC

WN=sense primer
cWN=antisense primer

Figure 2-2. RayBio mouse cytokine antibody array III (Adapted from RayBioTech)

	A	B	C	D	E	F	G	H	I	J	K	L	M	N
1	POS	POS	POS	POS	Blank	Axl	BLC	CD30 L	CD30 T	CD40	CRG-2	CTACK	CXCL16	Eotaxin
2	NEG	NEG	NEG	NEG	Blank	Axl	BLC	CD30 L	CD30 T	CD40	CRG-2	CTACK	CXCL16	Eotaxin
3	Eotaxin-2	Fas Ligand	Fractalkine	GCSF	GM-CSF	IFN γ	IGFBP-3	IGFBP-5	IGFBP-6	IL-1α	IL-1 beta	IL-2	IL-3	IL-3 Rb
4	Eotaxin-2	Fas Ligand	Fractalkine	GCSF	GM-CSF	IFN γ	IGFBP-3	IGFBP-5	IGFBP-6	IL-1α	IL-1 beta	IL-2	IL-3	IL-3 Rb
5	IL-4	IL-5	IL-6	IL-9	IL-10	IL-12 p40/p70	IL-12 p70	IL-13	IL-17	KC	Leptin R	Leptin	LIX	L-Selectin
6	IL-4	IL-5	IL-6	IL-9	IL-10	IL-12 p40/p70	IL-12 p70	IL-13	IL-17	KC	Leptin R	Leptin	LIX	L-Selectin
7	Lymphotactin	MCP1	MCP-5	M-CSF	MIG	MIP-1α	MIP-1γ	MIP-2	MIP-3 β	MIP-3α	PF-4	P-Selectin	RANTES	SCF
8	Lymphotactin	MCP1	MCP-5	M-CSF	MIG	MIP-1α	MIP-1γ	MIP-2	MIP-3 β	MIP-3α	PF-4	P-Selectin	RANTES	SCF
9	SDF-1α	TARC	TCA-3	TECK	TIMP-1	TNFα	sTNF RI	sTNF RII	TPO	VCAM-1	VEGF	Blank	Blank	Blank
10	SDF-1α	TARC	TCA-3	TECK	TIMP-1	TNFα	sTNF RI	sTNF RII	TPO	VCAM-1	VEGF	Blank	POS	POS

Table 2-3. List of mouse cytokine/chemokines used for Bioplex. Experiments included the use of either the 23-plex or both 9-plex and 23-plex

9-plex				23-plex						
MIP-2	LIF	IL-15	IL-1α	IL-1β	IL-2	IL-3	IL-4	IL-5	IL-6	IL-9
PDGF	M-CSF	IL-18	IL-10	IL-12(p40)	IL-12(p70)	IL-13	IL-17	KC	IFN-γ	MCP-1
VEGF	MIG	FGF	MIP-1α	MIP-1β	GM-CSF	TNF-α	Eotaxin	G-CSF	RANTES	

CHAPTER 3 : REMOVING THE GLYCOSYLATION MOTIF(S) IN THE NS1 PROTEIN BY CHANGING THE ASPARAGINE TO ALANINE

3.1 Introduction

The flaviviral NS1 protein contains two to four highly conserved N-linked glycosylation motifs. All members of the JE serogroup, with the exception of JE virus, contain three glycosylation motifs at asparagine (N) residues $NS1_{130}$, $NS1_{175}$, and $NS1_{207}$ (Bakonyi *et al.*, 2004; Blitvich *et al.*, 2001; Chambers *et al.*, 1990; Sumiyoshi *et al.*, 1987) . Other mosquito-borne flaviviruses, including JE and DEN viruses, contain two glycosylation motifs at positions $NS1_{130}$ and $NS1_{207}$, while YF, SEP and YOK viruses have two motifs at positions $NS1_{130}$ and $NS1_{208}$, and ENTV contains four potential sites at $NS1_{106}$, $NS1_{130}$, $NS1_{208}$ and $NS1_{326}$ (Dalgarno *et al.*,1986; Pryor & Wright, 1994; Flamand *et al.*, 1992, Kuno and Chang, 2006). Although the functions of NS1 are not well defined, it appears to be involved in multiple steps of the replication cycle (Lindenbach & Rice, 1997; Mackenzie *et al.*, 1996; Westaway *et al.*, 1997). It has also been suggested that the NS1 protein of DEN-2 virus induce autoreactive antibodies against extracellular matrix proteins, which may play a role in the development of dengue hemorrhagic fever (Chang *et al.*, 2002; Falconar, 1997).

Studies involving the ablation of NS1 glycosylation sites have been performed for other mosquito-borne flaviviruses, including DEN-2, DEN-4 and YF viruses (Crabtree *et al.*, 2005; Muylaert *et al.*, 1996; Pletnev *et al.*, 1993; Pryor & Wright, 1994 ;Pryor *et al.*, 1998). In contrast to WNV, these viruses contain only two glycosylation sites in NS1 ($NS1_{130}$ and $NS1_{207}$) and phenotypic studies were limited to replication in cell culture and mouse neurovirulence studies. Overall, these published studies showed that nonglycosylated NS1 mutant viruses have impaired replication and, with a couple of exceptions, displayed a decrease in mouse neurovirulence.

In this chapter, ablation of the WNV NS1 glycosylation sites was achieved by changing the asparagine of the glycosylation motif to an alanine by site-directed mutagenesis. Alanine was chosen due to its small size and ability to reside inside or outside of the protein. The mutation of a specific amino acid is denoted by the single letter amino acid code after the amino acid in question. A total of seven glycosylation mutants were generated using all possible combinations of mutations including: $NS1_{130A}$, $NS1_{175A}$, $NS1_{207A}$, $NS1_{130A/175A}$, $NS1_{130A/207A}$, $NS1_{175A/207A}$ and $NS1_{130A/175A/207A}$.

3.2 Results

3.2.1 In vitro characterization of mutant viruses

The studies in the PhD utilize an infectious clone of prototype strain New York 1999 (NY99) of WNV. This infectious clone has the WNV genome contained in two plasmids; the 5' half and 3' half and was obtained from Dr. Richard Kinney of the United States Centres for Disease Control and Prevention in Fort Collins Colorado. The details of the infectious clone can be found in Chapter 2, Materials and Methods, section 2.2. The mutant viruses were generated by site-directed mutagenesis of the infectious clone, as described in Materials and Methods, section 2.2-2.4. All studies compare mutant viruses generated by site-directed mutagenesis to the "parental" NY99 strain generated from the infectious clone via transfection of Vero cells with *in vitro* generated RNA. Previous studies (Beasley *et al.,* 2005) have shown that the phenotype of the NY99 virus appears identical to that generated from the NY99 infectious clone.

Seven glycosylation mutants were rescued as infectious virus following transfection of Vero cells with *in vitro* generated RNA as described in Materials and Methods section 2.4. Neither the parental NY99 strain nor any of the mutant viruses derived from it were temperature sensitive at 39.5° C except for $NS1_{130A,}$ which was slightly temperature sensitive (20-fold reduction in infectivity titre at 39.5° C; Table 3-1) and the plaque morphology of each of the mutants was not altered from that of parental NY99 virus.

The NS1 gene of each mutant was sequenced and confirmed the integrity of the introduced mutation(s) and that no additional, possibly compensatory, mutations had arisen in the gene. Full length genome sequencing was performed for the $NS1_{130A/207A}$ and $NS1_{130A/175A/207A}$ mutant viruses, which showed the greatest attenuation in mice (see below). The $NS1_{130A/207A}$ mutant contained one unexpected silent change at nucleotide 10221 in the NS5 gene, while $NS1_{130A/175A/207A}$ contained only the engineered mutations compared to the NY99 cDNA infectious clone.

3.2.2 Western Blot

NS1 is normally a secreted protein. Accordingly, polyacrylamide gel electrophoresis and western blot analysis were performed on concentrated culture media collected from NY99 and NS1 mutant virus-infected Vero cells, at 48 hours post-infection. This was undertaken to determine whether or not the NS1 protein of each glycosylation mutant was secreted, and to assess the difference in the apparent molecular weight of each mutated NS1 protein, compared to that of the parental NY99 virus, resulting from the loss of single or multiple NS1 glycosylation sites (Fig. 3-1A). Anti-NS1 monoclonal antibody 17NS1 (Chung *et al.*, 2006) detected NS1 protein in the culture medium of cells infected with clone-derived WNV NY99 and all of the

mutants, indicating that the loss in glycosylation did not significantly affect NS1 protein secretion. Variable levels of glycosylation were putatively confirmed by the observed differences in migration between the parental NY99 NS1 protein and the NS1 of each single, double, and triple glycosylation mutant (Fig. 3-1A). The monomeric form of the NS1 triple mutant $NS1_{130A/175A/207A}$ migrated faster than that of the double mutants $NS1_{130A/175A}$, $NS1_{175A/207A}$ and $NS1_{130A/207A}$, which in turn migrated faster than the monomeric NS1 of single mutants $NS1_{130A}$, $NS1_{175A}$ and $NS1_{207A}$. Samples separated in the absence of reducing agent revealed E-NS1 dimers and monomeric states of NS1, as has been previously documented for other flaviviruses (Blitvich *et al.,* 1995; Flamand, *et al.,*1999; Mason, 1989). The NS1-NS1 dimer is readily converted to monomer after boiling, and therefore was not detected (Winkler *et al.,* 1988; Blitvich *et al.,* 1995). The NS1 monomer appeared as a cluster of bands, probably due to the different cleavage products of this protein (Mason, 1989; Blitvich *et al.,* 1995). The presence of multiple NS1 bands was likely more pronounced in the glycosylation mutant samples because of the decrease in NS1 size due to the loss of glycosylation at one, two, or three sites (Fig. 3-1A). Western blotting was also performed for whole cell lysate samples of $NS1_{130A/175A/207A}$, NY99, $NS1_{130A}$, $NS1_{175A}$, and $NS1_{207A}$ mutant virus-infected cells boiled in the presence of dithiothreitol (DTT) to analyze the reduced form of the NS1 protein (Fig. 3-1B). Two major isoforms of NS1, a larger NS1' band and a smaller NS1° band, were detected by anti-NS1 monoclonal antibody 17NS1. These two NS1 isoforms have been described previously for JE and MVE viruses (Mason, 1989; Blitvich *et al.,* 1995; Blitvich *et al* 1999.) (Fig. 3-1B).

3.2.3 Multiplication kinetics of mutant viruses in cell culture

Multiplication characteristics of the parental clone-derived NY99 virus and mutant viruses were compared in mouse neuroblastoma Neuro 2A, monkey kidney Vero cells and mouse macrophage-like P388 D1 cells. Confluent monolayers were infected at an moi of 0.1, the supernatant collected in triplicate at 12,24,48,72 and 96 for Neuro 2A cells and 12, 24, 36,48, 60, 72 and 96 hours post-infection for Vero and P388 D1 cells. The infectivity titres were determined in Vero cells.

3.2.3.1 Neuro 2A cells

No differences were seen between the parental NY99 infectious clone virus and the triple glycosylation mutant $NS1_{130A/175A/207A}$ virus in the Neuro 2A cells (Fig. 3-2A). Other NS1 mutant viruses were not studied.

3.2.3.2 Vero cells

The triple ($NS1_{130A/175A/207A}$) and the double ($NS1_{130A/207A}$) mutant viruses and the parental NY99 strain were compared in Vero cells to determine the multiplication kinetics in cell culture. No differences were seen in multiplication kinetics of the parental virus and the double or triple NS1 glycosylation mutants in Vero cells (Fig. 3-2B)

3.2.3.3 P388 D1 cells

Multiplication curves in P388 D1 cells exhibited modest differences in infectivity titres, with the double and triple NS1 glycosylation mutant viruses ($NS1_{130A/207A}$ and

$NS1_{130A/175A/207A}$) having a lower infectivity titre compared to the parental strain at the 12 and 48 hour time points (Fig. 3-2C).

3.2.4 Mouse virulence phenotype of mutant viruses

All seven NS1 glycosylation mutant viruses were examined for mouse neuroinvasiveness through inoculation by the ip route. Glycosylation mutant viruses ($NS1_{130A/207A}$ and $NS1_{130A/175A/207A}$) were also examined for neurovirulence through inoculation by the ic route. Attenuation was determined by the LD_{50} comparison of the mutant viruses to the parental NY99 strain.

3.2.4.1 Neuroinvasiveness and neurovirulence of mutant viruses

The mouse neuroinvasive phenotype (i.e., the ability to invade the brain following inoculation by a peripheral route) was examined following ip inoculation of 3-4 week old female NIH Swiss mice. Only one of the single glycosylation mutants, $NS1_{175A}$, was attenuated (500-fold) compared to clone-derived parental NY99 virus, while the double mutants $NS1_{130A/175A}$ and $NS1_{175A/207A}$ were attenuated 800- and 200-fold, respectively (Table 3-2). The two most attenuated mutants by this route were $NS1_{130A/207A}$ and $NS1_{130A/175A/207A}$, which was attenuated 3,200-fold and 50,000-fold, respectively, compared to the parental NY99 strain.

Mouse neurovirulence (i.e., the ability of virus to cause disease following direct inoculation into the brain) was assessed for three of the viruses: clone-derived parental NY99 virus and glycosylation mutants $NS1_{130A/207A}$ and $NS1_{130A/175A/207A}$ (Table 3-2). Following ic inoculation, the $NS1_{130A/207A}$ and $NS1_{130A/175A/207A}$ mutants were attenuated 50-fold and 160-fold, respectively, compared to NY99 virus.

3.2.4.2 Sequence analysis of viral RNA isolated from mouse brains

RNA was isolated from the brains of mice that succumbed to ip inoculation with 1,000, 100 or 10 PFU of each of the seven mutant viruses, and the WNV NS1 gene was amplified by RT-PCR and sequenced. In one study, all five mice that succumbed to infection following ip $NS1_{130A/175A/207A}$ inoculation, and two mice that succumbed to infection following ip inoculation of each $NS1_{130A}$, $NS1_{175A}$, $NS1_{207A}$, $NS1_{130A/175A}$, $NS1_{130A/207A}$ or $NS1_{175A/207A}$ mutant were analyzed. Only the $NS1_{130A/175A/207A}$ virus showed a mutation in the NS1 gene and this was a reversion, which occurred only at the asparagine (N) of the $NS1_{130}$ site (i.e., A → N). The full-length genomic consensus sequence was determined for one $NS1_{130A/175A/207A}$ mutant virus isolated from the brain of a mouse that succumbed to infection following ip inoculation with 1,000 PFU. A reversion to N at the $NS1_{130}$ site, as well as two additional mutations in domain II of the E protein at $E\text{-}_{M204V}$ and $E\text{-}_{E237G}$ were identified (Fig 3-3). This "revertant" virus was observed to have a highly neuroinvasive phenotype of <0.1 PFU/LD_{50}, following ip inoculation. The mutations at E_{204} and E_{237} were introduced individually into the NY99 infectious clone, and a variant virus was generated for each mutation. Mice infected with these viruses showed an $ipLD_{50}$ of 20 PFU for the E_{204} mutant and 2 PFU for the E_{237} mutant.

In a second study, viral RNA was isolated from the brains of a total of 6 mice that succumbed to $NS1_{130A/175A/207A}$ virus infection during different experiments, and the E and NS1 genes were amplified by RT-PCR and sequenced. Viral RNA from two of these mice contained the same two $E\text{-}_{M204V}$ and $E\text{-}_{E237G}$ mutations as well as the reversion at $NS1_{130}$. Three of the six viruses contained no mutations in either E or

NS1 other than the engineered mutations. One of the six had no mutations in E but the $NS1_{130}$ changed to Aspartic acid.

In a third study, viral RNA was isolated from the brains of four mice that succumbed to infection with mutant virus $NS1_{130A/175A/207A}$ containing reversion at $NS1_{130}$ (A → N) plus $E\text{-}_{M204V}$ and $E\text{-}_{E237G}$ mutations ($E_{204V/237G}$-$NS1_{175A/207A}$). Analysis of these four brains showed that the reversion at $NS1_{130}$ and the E_{204} and E_{237} mutations were retained in viral RNA from the brains of all four mice.

3.2.4.3 Multiplication in vivo

Examination of the multiplication of clone-derived parental WNV and the two most attenuated mutant viruses, $NS1_{130A/207A}$ and $NS1_{130A/175A/207A}$, following ip inoculation (three mice per group per time point) of 100 PFU revealed all three viruses were cleared from the serum after the third day post-infection (Fig. 3-4A). The attenuated strains encoding the mutations at $NS1_{130A/207A}$ and $NS1_{130A/175A/207A}$ showed a delay in the onset of viraemia when compared to the parental NY99 virus. The parental NY99 virus was detected in the brain of one mouse at day 4 post-inoculation and in all mice by the fifth day post-inoculation, whereas neither $NS1_{130A/207A}$ nor $NS1_{130A/175A/207A}$ mutant viruses were detectable in the brain by 6 days post-infection, as determined by plaque titration (Fig 3-4B). The level of detection was 50 PFU/brain. This result was confirmed by RT-PCR of the NS1 gene where both $NS1_{130A/207A}$ and $NS1_{130A/175A/207A}$ groups were negative for detection of viral RNA in the brains of all three mice on days 4, 5 and 6 post-inoculation, while the NY99 samples that showed infectious virus were also positive by RT-PCR (Fig 3-5).

In an effort to investigate a possible correlation between level of viraemia and mortality of the animals, groups of 5 mice were inoculated ip with one of the two attenuated mutants, $NS1_{130A/207A}$ or $NS1_{130A/175A/207A}$, at a dose of either 1,000 or 100 PFU in order to achieve groups of mice that either succumbed to or survived infection, respectively. Additional groups of mice were inoculated ip with either 100 or 10 PFU of infectious clone-derived NY99 virus. Mice were bled on days 2 and 3 post-infection to measure viraemia. Brains were harvested from moribund mice following euthanasia and from mice that died, and homogenized before passaging once in Vero cells for isolation and sequencing of the virus. In general, a peak viraemia $\geq$ 200 PFU/ml at 2 or 3 days post-inoculation correlated with a fatal outcome (Table 3-3). The level of viraemia was significantly reduced on both day 2 and day 3 post-infection in the mice infected with either of the two attenuated viruses, compared to mice infected with the parental NY99 strain. The highly attenuated phenotype of the $NS1_{130A/175A/207A}$ mutant virus correlated with the greatest reductions in viraemia, morbidity, and mortality. In the case of the parental NY99 strain, only one mouse, given 10 PFU of virus, showed no detectable viraemia and did not succumb to infection. However, this surviving mouse did not survive secondary ip challenge with 100 PFU of the NY99 virus. This is consistent with the lethal dose of NY99 virus being approximately equivalent to the infectious dose (i.e., $LD_{50} = ID_{50}$).

Only one mouse survived infection with the $NS1_{130A/207A}$ mutant at each inoculum of 100 or 1,000 PFU (Table 3-3). However, the apparent survivor at the 1,000 PFU dose had a viraemia of 3,500 PFU/ml on day three, which was higher than most mice that succumbed to infection in this group, and this mouse exhibited encephalitic manifestations of permanent hind limb paralysis, and was euthanized. In the case of

the $NS1_{130A/175A/207A}$ group given 1,000 PFU, two animals had a viraemia greater than 1,000 PFU/ml and subsequently died. Viral RNA isolated from the brains of these mice encoded a reversion to N at $NS1_{130}$, as had been observed in the original experiments to investigate reversion (section 3.2.4.2.). Another mouse in the 100 PFU dose $NS1_{130A/175A/207A}$ group succumbed to infection without detectable viraemia. However, viral RNA isolated from the brain of this mouse also showed the reversion to N at the $NS1_{130}$ site.

3.3 Discussion

Previous studies of the attenuating effects of mosquito-borne flavivirus NS1 deglycosylation have focused on YF, DEN-2 and DEN-4 viruses, which have two glycosylation sites in NS1. West Nile virus NS1 contains three glycosylation sites, and this study determined that WNV utilizes all three glycosylation sites in the NS1 protein (see Figure 3-1). The NS1 glycosylation sites were ablated in various combinations to generate seven mutants, and phenotypic properties of these mutants were investigated.

Despite ablation of all three NS1 glycosylation sites of WNV, the triple $NS1_{130A/175A/207A}$ mutant exhibited apparent genetic stability *in vitro*, as demonstrated by its containing the expected genomic nucleotide sequence and its robust multiplication in cell culture (Fig. 3-2). This contrasts with the NS1 glycosylation mutant viruses for DEN-2 virus where the dual (complete) deglycosylation of the NS1 protein of a DEN-2 virus was unable to produce infectious virus and the engineered mutation at $NS1_{207}$ acquired secondary mutations to enable replication in mosquito C6/36 or monkey kidney LLC-MK2 cell culture (Crabtree *et al.*, 2005).

The triple NS1 glycoslyation mutant ($NS1_{130A/175A/207A}$) that included three amino acid changes and the parental NY99 virus were initially chosen to compare multiplication kinetics in Neuro 2A cells. Plaque titration in Vero cells of triplicate samples per time point revealed similar infectivity titres for both the parental strain and the mutant containing the most amino acid mutations, despite attenuation for neuroinvasiveness and neurovirulence of this mutant virus. Similar multiplication kinetics were also seen in Vero cells for the parental NY99 strain, double $NS1_{130A/207A}$ and triple $NS11_{30A/175A/207A}$ mutant viruses. Unlike Neuro 2A and Vero cells, the triple glycosylation mutant ($NS1_{130A/175A/207A}$) showed some reduction in multiplication in the mouse macrophage-like derived P388 D1 cell line compared to the parental NY99 strain, particularly at the 12 and 48 hour time points. The double ($NS1_{130A/207A}$) mutant virus showed a reduction in infectivity titre similar to the triple $NS1_{130A/175A/207A}$ mutant virus in the P388 D1 cells. This is consistent with a previous report of delayed replication for NS1 glycosylation mutants of YF virus (Muylaert *et al.,* 1996). Since macrophages are infected early after inoculation of mice by the ip route, this impediment to multiplication may explain, in part a reduced viraemia, earlier clearance of the virus from the blood, and the observed inability of this virus to replicate to high enough titres to invade the brain.

The data in this chapter indicated that all three NS1 glycosylation sites contribute to the mouse virulence phenotype of WNV, with the triple mutant virus showing the greatest attenuation of the mutants that were engineered. The additional $NS1_{175}$ glycosylation site that is found only in WNV and other viruses belonging to the JE serogroup, except JE virus, was shown to play an important role in the mouse neuroinvasive phenotype of WNV NY99. Ablation of glycosylation at $NS1_{175}$

attenuated this mutant compared to the parental strain, whereas ablation of either the $NS1_{130}$ or $NS1_{207}$ site alone had much less effect on the neuroinvasive phenotype. The degree of attenuation that was observed depended on the particular NS1 mutation or combination of NS1 mutations incorporated into the viral mutant. The $NS1_{130A/207A}$ and $NS1_{130A/175A/207A}$ mutants were consistently attenuated more than 200-fold, compared to the parental NY99 virus when inoculated ip into 3-4 week-old mice. Interstingly, the double $NS1_{175A/207A}$ mutant was not as attenuated as the single $NS1_{175A}$ mutant virus in mice. Disparate phenotypic effects of deglycosylation at different NS1 loci have been previously reported for a chimeric TBE/DEN-4 virus in which deglycosylation of the DEN-4 $NS1_{130}$ site attenuated the mouse neurovirulence of the chimeric virus, whereas deglycosylation of the $NS1_{207}$ site actually increased mouse virulence (Pletnev *et al.,* 1993).

Previous studies with other flaviviruses have shown that mutation of the first ($NS1_{130}$) or both ($NS1_{130/207\text{-or-}208}$) glycosylation sites by replacing the asparagine with an alanine, isoleucine or glutamine in the NS1 protein cause variable attenuation of mouse neurovirulence (Crabtree *et al.,*2005; Muylaert *et al.,* 1996; Pletnev *et al.,* 1993). Although for WNV the ablation of the first $NS1_{130}$ glycosylation site alone did not attenuate the virus, this site appeared to be important for the ability of the virus to replicate efficiently *in vivo* when the other two glycosylation sites were ablated as well ($NS1_{130A/175A/207A}$ mutant). Many of the viruses that were isolated from the brains of mice that had succumbed to infection with the $NS1_{130A/175A/207A}$ mutant showed an A → N reversion at the $NS1_{130}$ site. Given the high frequency of occurrence of this reversion in viruses recovered from the brains of mice infected ip with the $NS1_{130A/175A/207A}$ mutant, the increased neuroinvasiveness of the $NS1_{130A/175A/207A}$

mutant virus in certain instances of virus-induced mouse morbidity and mortality was partially attributed to reversion at the $NS1_{130}$ site, which rendered the virus neuroinvasive. Although both $NS1_{130A/207A}$ and $NS1_{130A/175A/207A}$ mutants replicated to measurable viremic titres in virus-infected mice, neither virus replicated to detectable levels in the brain, suggesting that in the absence of reversion at $NS1_{130}$ or the absence of other virulence enhancing mutations, these viruses generally lacked neuroinvasiveness. The decreased $icLD_{50}$ values of the $NS1_{130A/207A}$ and $NS1_{130A/175A/207A}$ mutants, relative to the NY99 virus, indicated that attenuation of neurovirulence also contributed to the overall attenuated phenotypes of these two viruses, despite the similarities of their multiplication kinetics compared to the parental NY99 virus in mouse neuroblastoma cells.

Interestingly, some $NS1_{130}$ revertants had two additional substitutions at residues 204 and 237 in domain II of the E protein (Fig 3-3). The role of these E protein mutations is not clear. However, their presence in the revertants suggested a possible interaction between E and NS1 under the selective pressure of replication *in vivo*. The amino acid at E_{204} appears to reside buried inside the protein while E_{237} is a surface accessible amino acid (VIPERdb http://viperdb.scripps.edu/) and resides close to an antibody epitope (Oliphant *et al.,* 2006). Individually, each of these E mutations either did not significantly alter (E_{237}) or slightly attenuated (E_{204}) the mouse neuroinvasive phenotype of parental WNV. Although it is not understood why the $NS1_{130}$ site was the only site of reversion observed in this study, it has been shown for the related MVE virus that this glycosylation site contains a complex carbohydrate and is suggested to lie outside the interface of the NS1 dimer (Blitvich *et al.,* 2001; Hall *et al.*, 1999). N-linked carbohydrate groups have been implicated to function in

several ways such as protein folding, secretion rates and stability in the endoplasmic reticulum (Varki 1998). This study demonstrated that glycosylation of at least one of the glycosylation sites of the NS1 protein was important for viral multiplication *in vivo*. The $NS1_{130}$ glycosylation site, which exhibited significant attenuation in synergy with the other two glycosylation loci in the $NS1_{130A/207A}$ and $NS1_{130A/175A/207A}$ mutants, appears to play a critical role in the function of the protein and the biology of the virus.

Finally, this study showed that the removal of the three glycosylation sites of the NS1 protein generated a viable WNV that replicated robustly in cultures of several mammalian cell types, and the triple mutant was significantly attenuated for both neuroinvasiveness and neurovirulence in a mouse model. Overall, this study is consistent with previous studies suggesting that the structural protein genes are not the only genes that contribute to the neuroinvasive phenotype of flaviviruses (Pletnev *et al.*, 1993). However, this is the first study to clearly demonstrate that mutations in the nonstructural NS1 protein are sufficient to attenuate the neuroinvasive phenotype in the mouse model.

Table 3-1. Temperature sensitivity of all seven NS1 alanine mutant viruses and parental NY99 virus.

Virus	37°C (Log_{10}PFU/ml)	39.5°C (Log_{10}PFU/ml)	Δ 37°C- 39.5°C (Log_{10}PFU)
NY99	6.6	6.5	0.1
$NS1_{130A}$	6	4.7	1.3
$NS1_{175A}$	8.1	7.4	0.7
$NS1_{207A}$	7	6.6	0.4
$NS1_{130A/175A}$	7.9	7.6	0.3
$NS1_{130A/207A}$	7.9	7.5	0.4
$NS1_{175A/207A}$	7.8	7.3	0.5
$NS1_{130A/175A/207A}$	8.2	8.3	-0.1

Figure 3-1. Non-reducing western blot of NS1 protein from supernatant of all seven alanine mutants and NY99 (A), and from cell lysates of the single and triple mutants and NY99 treated with a reducing agent (B) collected from Vero-infected cells at an moi of 0.1.

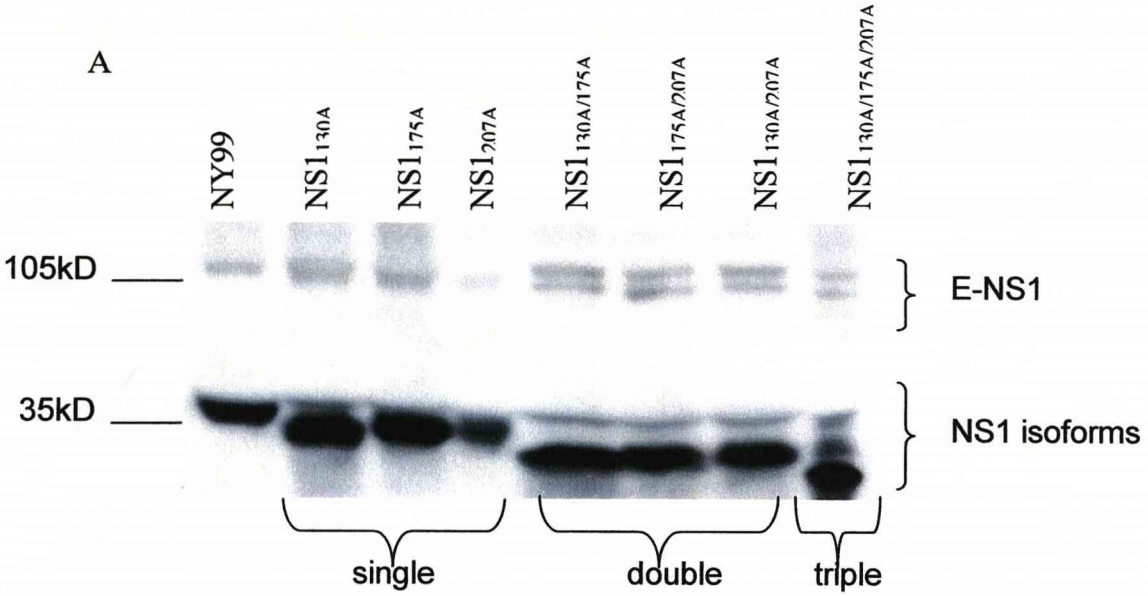

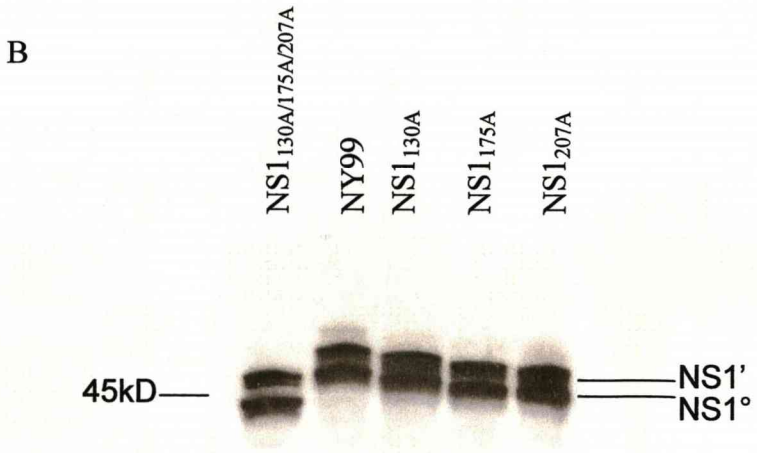

Figure 3-2. Multiplication kinetics of parental NY99 and $NS1_{130A/175A/207A}$ mutant viruses in mouse neuroblastoma Neuro 2A cells (A) and parental NY99, $NS1_{130A/207A}$ and $NS1_{130A/175A/207A}$ mutant viruses in monkey kidney Vero cells (B) and mouse macrophage-like P388 D1 cells (C) at an moi of 0.1. Each time point represented by mean $\pm$ SD of triplicate samples.

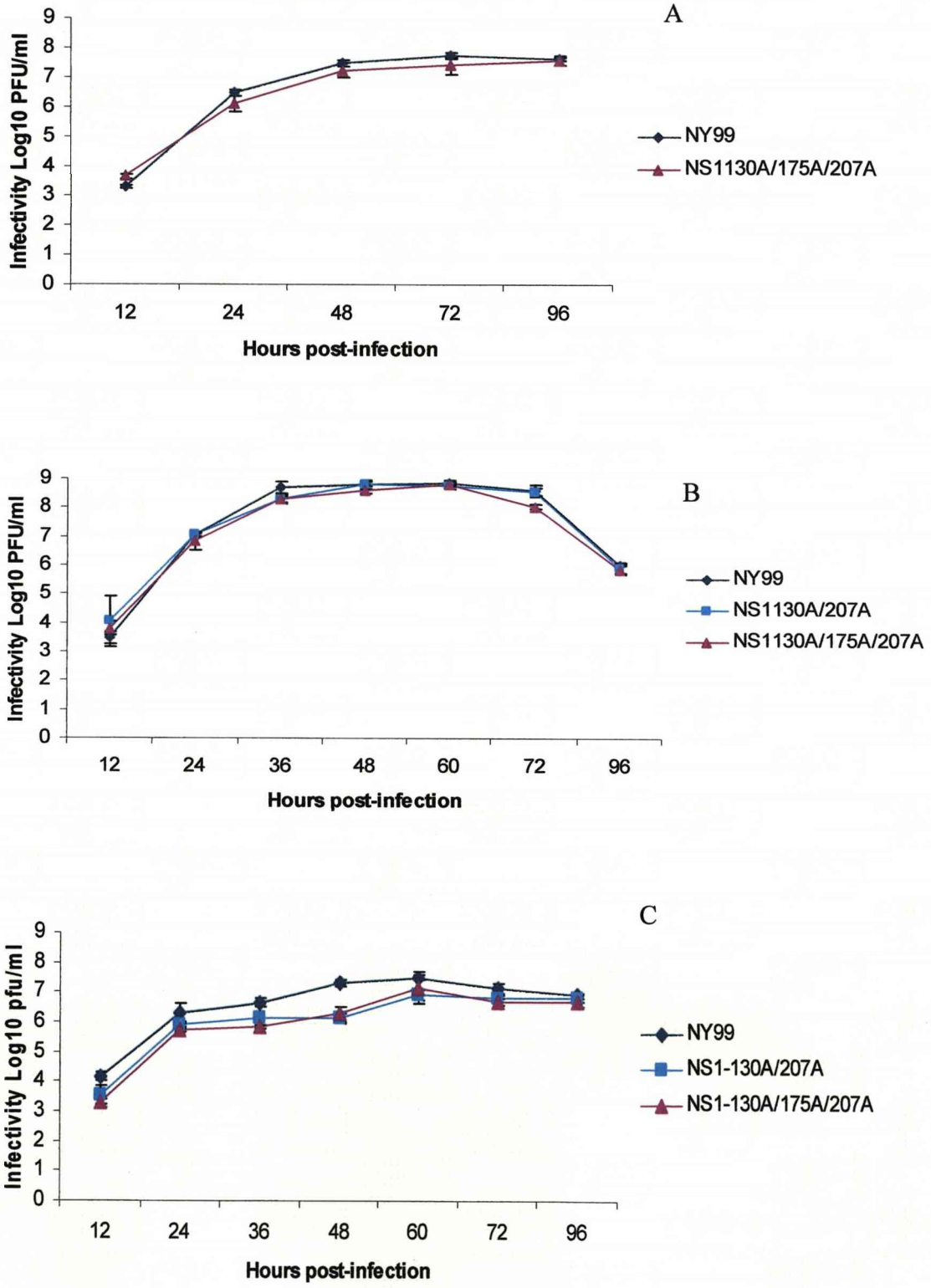

Table 3- 2. Mouse neuroinvasiveness (ip) and neurovirulence (ic) of NS1 glycosylation alanine mutant viruses and the parental NY99 strain.

Virus	$ipLD_{50}$ (PFU)	AST ± SD*	p-Value†	$icLD_{50}$ (PFU)
NY99	0.1	7.7 ± 0.8	NA	0.5
$NS1_{130A}$	2	10.0 ± 1.9	<0.05	nd
$NS1_{175A}$	50	10.0 ± 1.2	<0.05	nd
$NS1_{207A}$	1.3	7.4 ± 0.9	>0.05	nd
$NS1_{130A/175A}$	80	9.0 ± 1.2	>0.05	nd
$NS1_{130A/207A}$	320	9.5 ± 1.7	>0.05	25
$NS1_{175A/207A}$	20	7.8 ± 1.0	>0.05	nd
$NS1_{130A/175A/207A}$	5,000	9.0 ± 1.4	>0.05	80

*=Average standard survival time (days) at dose of 1,000 PFU
p-value†= significance of difference between AST of mutant virus and that of the NY99 virus (Student's t-test)
nd = not determined

Figure 3-3.Top view of WNV E glycoprotein showing the E_{204} and E_{237} mutations. Colors represent different domains: Red-Domain I, Yellow-Domain II, Blue-Domain III

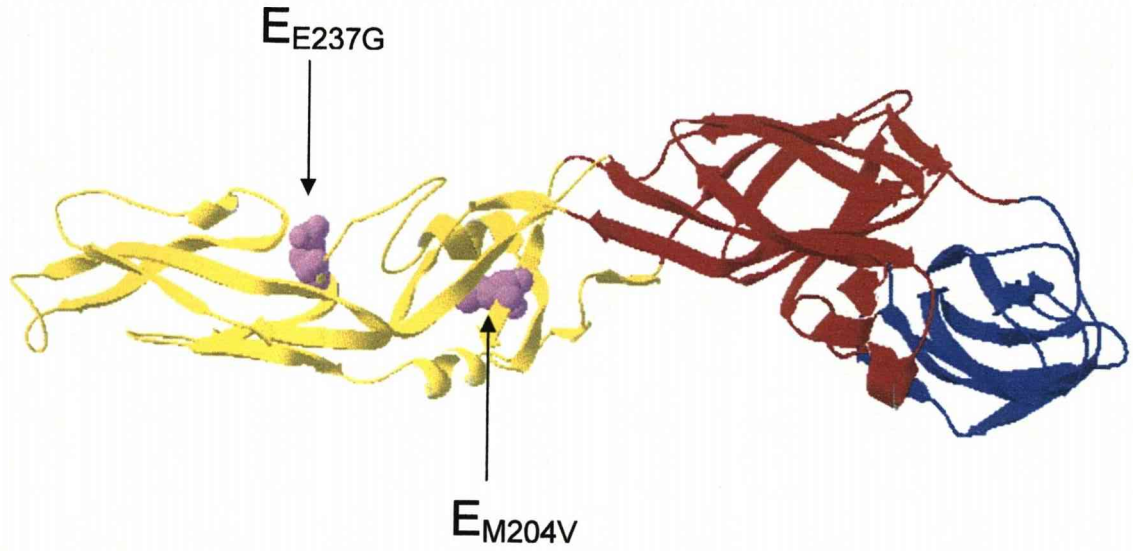

Figure 3-4. Multiplication kinetics of parental NY99 and attenuated NS1 glycosylation alanine mutant viruses in mouse serum (A) and brain homogenates (B) 1-6 days post-inoculation. Each time point is mean of three mice ± SD.

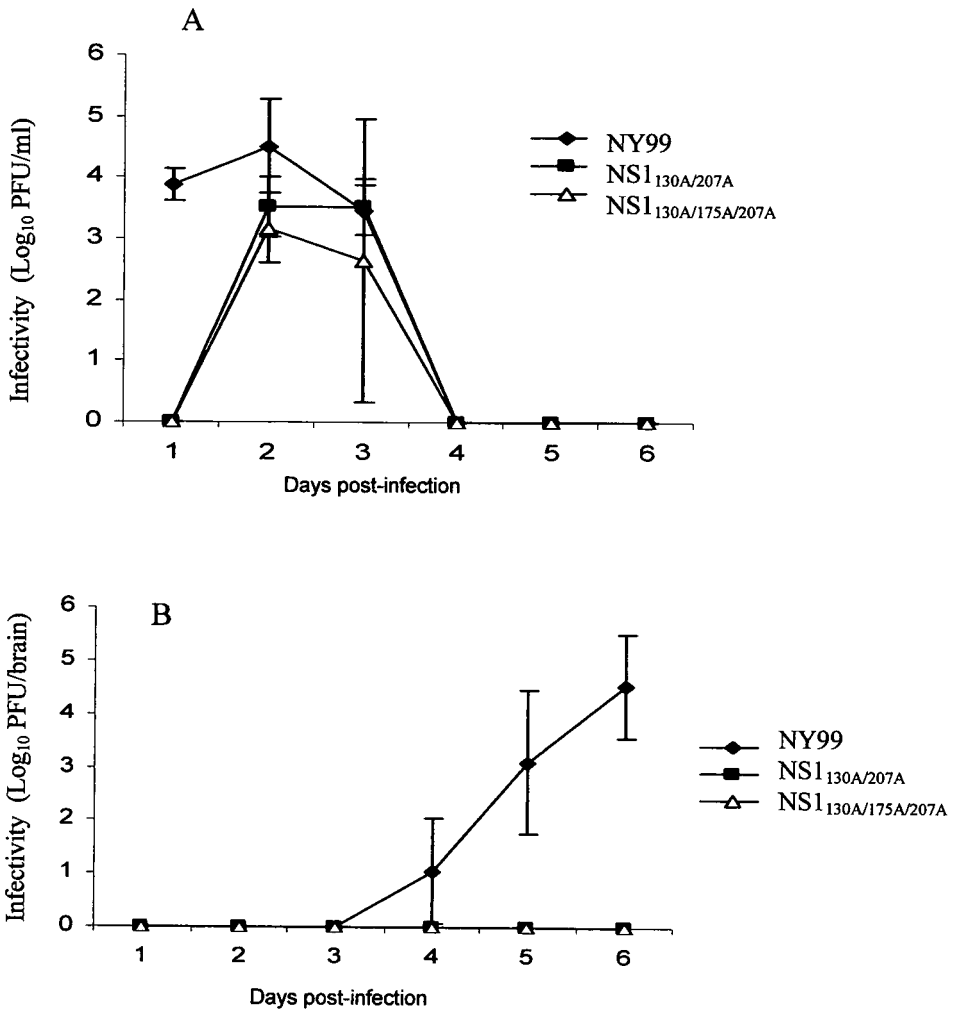

Figure 3-5. Conformation of the WNV NS1 gene by RT-PCR of viral RNA present in brain homogenates in the parental NY99-infected mice but not in the attenuated NS1 mutant-infected mice from samples 4-6 days post-ip inoculation used in Fig. 3-4 .

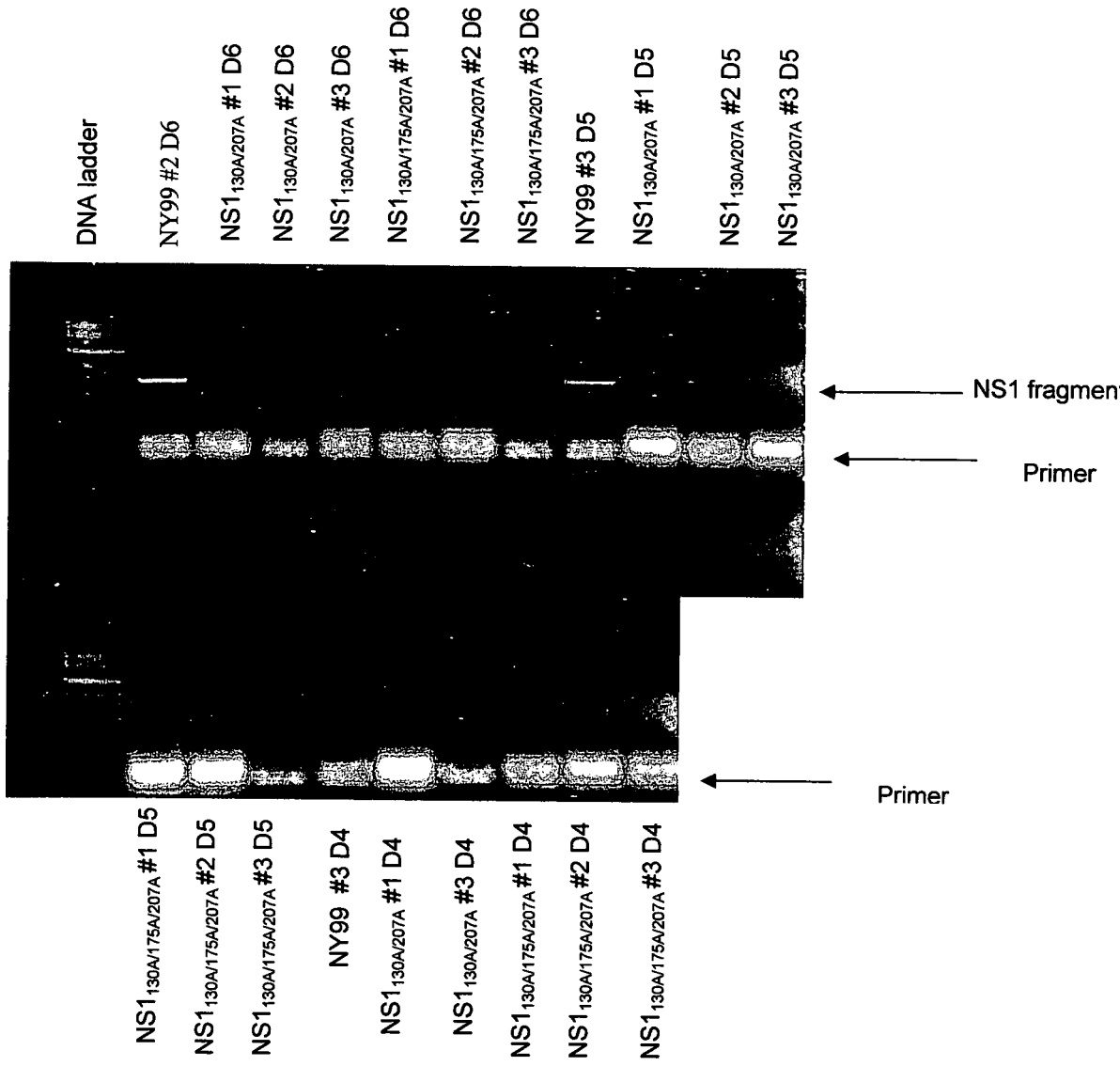

Table 3-3. Infectivity titre of mouse serum collected two and three days post-inoculation by the ip route with either parental NY99 or attenuated NS1 glycosylation mutant viruses

	NY99 (10 PFU ip)		**$NS1_{130A/207A}$ (100 PFU ip)**		**$NS1_{130A/175A/207A}$ (100 PFU ip)**	
Mouse	2 dpi (PFU/ml)	3 dpi (PFU/ml)	2 dpi (PFU/ml)	3 dpi (PFU/ml)	2 dpi (PFU/ml)	3 dpi (PFU/ml)
1	<50	15,000*	50	600*	<50	<50
2	<50	<50	<50	<50	<50	<50*‡
3	2,000	150,000*	1,000	5,000*	<50	<50
4	4,000	50,000*	2,000	5,000*	<50	<50
5	2,500	300,000*	50	200*	<50	<50

	NY99 (100 PFU ip)		**$NS1_{130A/207A}$ (1,000 PFU ip)**		**$NS1_{130A/175A/207A}$ (1,000 PFU ip)**	
Mouse	2 dpi (PFU/ml)	3 dpi (PFU/ml)	2 dpi (PFU/ml)	3 dpi (PFU/ml)	2 dpi (PFU/ml)	3 dpi (PFU/ml)
1	5,000	2,000*	1,500	600*	50	<50
2	6,500	3,000*	100	3,500†	100	100
3	10,000	5,000*	100	1,100*	<50	<50
4	4,000	10,000*	500	600*	50	4,500*‡
5	<50	12,500*	250	1,000*	400	1,500*‡

*Mice that succumbed to infection

†Partially paralyzed and euthanized

‡Reversion of Ala to Asn at $NS1_{130}$

CHAPTER 4 : CHANGING $NS1_{130}$ TO A SERINE AND TWO AMINO ACIDS IN THE GLYCOSYLATION MOTIF

4.1 Introduction

In Chapter 3, the three NS1 N-linked glycosylation sites (NXT) of WNV were ablated by changing the asparagine of the glycosylation motif to an alanine (NXT → AXT). Alanine was chosen because it is a small uncharged amino acid that is hypothesized to not disrupt the conformation or function of the protein. It was demonstrated in Chapter 3 that the triple glycosylation mutant ($NS1_{130A/175A/207A}$) was unstable in mice. Many viruses isolated from the brains of mice that succumbed to this virus had one or more mutations, including reversion at one of the glycosylation sites ($NS1_{130}$) plus two mutations in the E protein. Although this virus was highly attenuated, several mice that died following ip inoculation had one or more of these amino acid substitutions.

Accordingly, it was hypothesized that complete attenuation of neuroinvasiveness in mice would be achieved if the mutations incorporated in the NS1 protein would not revert the glycosylation status to wild-type at the $NS1_{130}$ site. Since the $NS1_{130}$ glycosylation motif contains two asparagines in the first and second position of the glycosylation motif (NNT), both asparagines were mutated by changing the first asparagine to a serine and the second asparagine to a valine (NNT→SVT). In this way the glycosylation site could not be restored either by reversion at $NS1_{130}$ or by shifting the glycosylation motif using the second asparagine that could result from a mutation in the fourth position to a serine or threonine (i.e. SNTF → SNTT). In addition, a mutant virus was generated containing only a single amino acid mutation at $NS1_{130}$ by changing the asparagine to a serine (NNT→SNT) in order to determine what effects, if any, the specific amino acid change would have at this site. Serine was selected because it is a mutation in the E glycosylation site of WNV isolates

found in nature (Beasley *et al.*, 2005) and its molecular structure resembles asparagine (Fig 4-1).

A total of four new mutant viruses were generated, including $NS1_{130S}$, $NS1_{130\text{-}131SV}$, $NS1_{130S/175A/207A}$ and $NS1_{130\text{-}131SV/175A/207A}$. Multiplication kinetics in cell culture and the neuroinvasiveness and neurovirulence phenotype in mice were examined by comparing the mutant viruses to the parental NY99 strain.

4.2 Results

4.2.1 In vitro characterization of mutant viruses

Five days post-transfection, all four mutant viruses were harvested, samples frozen and then passaged once in Vero cells before subsequent experiments were performed. The NS1 gene was sequenced for all mutant viruses and no mutations were identified other than the engineered mutations. Plaque titration of $NS1_{130S}$ and $NS1_{130\text{-}131SV}$ revealed a typical NY99 plaque morphology while the $NS1_{130S/175A/207A}$ and $NS1_{130\text{-}131SV/175A/207A}$ mutant viruses displayed a small plaque morphology (<1mm) compared to the parental strain (2mm) (Fig. 4-2). A temperature sensitivity (ts) assay at 39.5°C indicated that the serine mutant viruses $NS1_{130S}$, $NS1_{130\text{-}131SV}$ and $NS1_{130S/175A/207}$ were not ts (Table 4-1). The $NS1_{130\text{-}131SV/175A/207A}$ mutant virus, having a 1.6 $\log_{10}$ reduction in infectivity titre, was considered somewhat ts given that a >2 $\log_{10}$ reduction in infectivity is normally used to define a ts phenotype (Table 4-1).

4.2.2 Western blot analysis

All four mutant viruses were analyzed by western blot after infection of Vero cells at a moi of 0.1, incubation for 48 hours followed by concentration of the viral culture

supernatant. The maximum allowed volume of protein sample (25µl) was loaded on a PAGE gel following wet transfer and probing with a NS1 monoclonal antibody 17 NS1 (Chung *et al.*, 2006) and chemilumenescence (Fig. 4-3A). The NS1 protein for the single glycosylation mutant viruses ($NS1_{130S}$ and $NS1_{130\text{-}131SV}$) migrated faster than the NS1 protein for the parental NY99, and the NS1 protein for the triple glycosylation mutants ($NS1_{130S/175A/207A}$ and $NS1_{130\text{-}131SV/175A/207A}$) migrated faster than the single glycosylation mutants, indicating a loss in glycosylation (Fig. 4-3A). The western blot used to identify the NS1 protein was stripped and reprobed with a recombinant E domain III antibody as a loading control. The results from this blot indicated that the relative amounts of E protein for each sample were similar for the parental NY99 and serine glycosylation mutants $NS1_{130S}$, $NS1_{130\text{-}131SV}$, $NS1_{130S/175A/207A}$ but not $NS1_{130\text{-}131SV/175\ A/207A}$ (Fig. 4-3B).

An overlay of the E and NS1 probed blots shows the differences in migration of the two proteins (Fig. 4-3C). The larger protein, E, migrates slower than the smaller NS1 protein. Overall, the western blots indicated a reduction of secreted NS1 protein in the glycosylation mutant viruses.

4.2.3 Multiplication kinetics of mutant viruses in cell culture

Multiplication kinetics of the glycosylation mutant viruses and parental NY99 virus derived from the infectious clone were compared in mouse macrophage P388 D1, monkey kidney Vero and mouse neuroblastoma Neuro2A cells. Cells were infected at a moi of 0.1 in triplicate, cell culture supernatant was collected for each virus at 12, 24, 48, 72 and 96 hours post-infection and infectivity was determined by titration in

Vero cells. Figure 4-4A-C shows the multiplication curves with mean infectivity values for each time point and standard deviation.

4.2.3.1 Vero cells

Since no differences were seen in the mouse attenuated triple alanine mutant virus ($NS1_{130A/175A/207A}$) in Vero cells (Fig. 3-2B), only the triple serine mutant virus ($NS1_{130\text{-}131SV/175A/207A}$) and parental NY99 strain were analyzed in this cell line (Fig. 4-4A). The parental NY99 WNV increases in infectivity titre up to 48 hours post-infection in Vero cells, whereas the $NS1_{130\text{-}131SV/175A/207A}$ mutant virus increases until 96 hours post infection. At 12 hours post-infection the infectivity titre of the mutant virus compared to the parental strain were similar. However, at 24 and 48 hours post-infection there was up to a 100-fold decrease in infectivity compared to the parental NY99 strain. Infectivity levels were similar to NY99 virus at the 72 and 96 hour time points.

4.2.3.2 Neuro2A cells

Since WNV shows tropism for the brain, mouse neuroblastoma Neuro2A cells were selected to investigate differences in the multiplication of the $NS1_{130\text{-}131SV}$ and $NS1_{130\text{-}131SV/175A/207A}$ mutant viruses compared to the NY99 parental strain. Unlike multiplication in Vero cells, the parental NY99 strain and serine mutant viruses $NS1_{130\text{-}131SV}$ and $NS1_{130\text{-}131SV/175A/207A}$ increased in infectivity titre until 72 hours post-infection and subsequently began to decrease at 96 hours post-infection. Although both mutants displayed a reduction in infectivity titre at all time points compared to NY99 virus, the $NS1_{130\text{-}131SV/175A/207A}$ mutant showed the greatest reduction in

infectivity titre (approximately 70-100-fold) compared to the parental strain (Fig. 4-4B).

4.2.3.3 P388 D1 cells

As macrophages are infected early in the infection process following ip inoculation of mice, the mouse macrophage cell line P388 D1 was used to investigate differences in multiplication kinetics between the parental NY99 and serine mutant viruses, including $NS1_{130S}$, $NS1_{130\text{-}131SV}$ and $NS1_{130\text{-}131SV/175A/207A}$ mutants (Fig. 4-4C). The NY99 strain increased in infectivity titre until 48 hours post-infection followed by a small decrease in infectivity titres at subsequent time points (Fig. 4-4C). The mutant viruses followed a similar trend in multiplication with all three mutant viruses, $NS1_{130S}$, $NS1_{131\text{-}131SV}$ and $NS1_{130\text{-}131SV/175A/207A}$, showing a reduction in infectivity titre compared to the parental strain at all time points; at least 100-fold and up to 10,000-fold reduction for $NS1_{130\text{-}131SV/175A/207A}$ at 96 hours post-infection.

4.2.4 Mouse virulence phenotype of mutant viruses

To determine whether or not the serine mutants were attenuated for mouse virulence, 3-4 week female outbred NIH Swiss mice were inoculated by the ip route to determine the neuroinvasive phenotype and by the ic route to determine the neurovirulence phenotype of all four mutant viruses ($NS1_{130S}$, $NS1_{130\text{-}131SV}$, $NS1_{130S/175A/207A}$ and $NS1_{130\text{-}131SV/175A/207A}$) compared to the parental NY99 strain and the $NS1_{130A/175A/207A}$ mutant. Serial 10-fold doses of each virus were inoculated into groups of mice and lethality and survival times were calculated (Tables 4-2 and 4-3).

4.2.4.1 Neuroinvasiveness and neurovirulence of mutant viruses

As hypothesized, the $NS1_{130}$ serine mutants showed a greater level of attenuation of neuroinvasiveness than the alanine mutant viruses (Chapter 3). However, the serine mutants exhibited an unexpected level of attenuation of neuroinvasiveness as increasing the number of amino acid mutations did not necessarily correlate with attenuation. The single glycosylation mutant viruses, $NS1_{130S}$ and $NS1_{130\text{-}131SV}$ exhibited a similar level of attenuation of neuroinvasiveness with $ipLD_{50}$ values of 1,300 and 2,000 PFU respectively (Table 4-2). Interestingly, both viruses were attenuated at least 130-fold for neuroinvasiveness compared to the parental NY99 strain, which was more than the triple alanine mutant virus $NS1_{130A/175A/207A}$ (Table 4-2). The triple serine mutant viruses, $NS1_{130S/175A/207A}$ and $NS1_{130\text{-}131SV/175A/207A}$, showed inconsistent mouse neuroinvasive phenotypes in that the mutant with the most amino acid mutations, the $NS1_{130\text{-}131SV/175A//207A}$ mutant virus, was less attenuated than the $NS1_{130S/175A/207A}$ mutant virus with an $ipLD_{50}$ values of 80 and >100,000 PFU, respectively. In this experiment the $NS1_{130A/175A/207A}$ triple alanine mutant virus was attenuated 50-fold for neuroinvasiveness compared to the parental NY99 strain, which was less attenuated than three of the four serine mutant viruses, excluding $NS1_{130\text{-}131SV/175A/207A}$.

Neurovirulence was investigated by inoculating mice by the ic route. Compared to the parental NY99 strain with an $icLD_{50}$ of 30 PFU, three of the mutant viruses, $NS1_{130S}$, $NS1_{130S/175A/207A}$ and $NS1_{130\text{-}131SV/175A/207A}$ mutants did not have a significant difference in neurovirulence compared to the parental strain (i.e., $icLD_{50}$ of 80, 50 and 50 PFU, respectively) (Table 4-2). In this study the most attenuated mutant for neurovirulence was the $NS1_{130\text{-}131SV}$ mutant with an $icLD_{50}$ of 300 PFU.

The mouse virulence study was repeated in a second group of female 3-4 week old NIH Swiss mice with the $NS1_{130\text{-}131SV}$, $NS1_{130\text{-}131SV/175A/207A}$ mutant viruses and compared to the parental NY99 and $NS1_{130A/175A/207A}$ mutant virus (Table 4-3). The parental NY99 strain displayed an $ipLD_{50}$ of 10 PFU and an $icLD_{50}$ of 10 PFU while the $NS1_{130\text{-}131SV}$ mutant showed an $ipLD_{50}$ of 300 PFU and an $icLD_{50}$ of >100 PFU. The $NS1_{130\text{-}131SV/175A/207A}$ mutant showed the most attenuation with an $ipLD_{50}$ of 80,000 PFU and an $icLD_{50}$ of 500 PFU. In this study the triple alanine mutant virus, $NS1_{130A/175A/207A}$, was more attenuated for neuroinvasiveness than the $NS1_{130\text{-}131SV}$ mutant virus but less attenuated than the triple serine mutant virus, $NS1_{130\text{-}131SV/175A/207A}$, that had an $ipLD_{50}$ of 1,000 PFU. Overall, the results of the two studies confirmed a high level of attenuation of mouse virulence for the mutant viruses compared to the parental NY99 strain.

4.2.5 Sequence analysis of viral RNA isolated from mouse brains

The brains of mice that succumbed to infection following ip inoculation with the serine mutant viruses were collected, the nucleic acid extracted, and viral RNA subjected to RT-PCR and sequencing to analyze the NS1 gene for mutations. The E gene was also analyzed due to the mutations in the E gene found in the brains of mice that succumbed to $NS1_{130A/175A/207A}$ following ip inoculation. Three brain samples were analyzed for each serine mutant virus at a dose of 1,000 or 100 PFU, except the $NS1_{130S/175A/207A}$ mutant virus for which only two mice succumbed to infection. No mutations, including reversions were seen in the NS1 gene of any of the serine mutant viruses at the engineered mutation sites and no mutations in the E protein were identified. However, all three mice that succumbed to infection following ip inoculation with the $NS1_{130S}$ mutant virus contained an A→C change at nucleotide

position 2589 that resulted in a glutamine to histidine (CAA→CAC) amino acid mutation at $NS1_{40}$ (Fig 4-5).

Viral RNA isolated from the brains of mice that succumbed to ip inoculation with the $NS1_{130A/175A/207A}$ mutant virus used in these mouse virulence studies was also examined for mutations in the E and NS1 gene. All three samples analyzed showed the same reversion at the $NS1_{130}$ site and the same two mutations in the E gene (E_{204} and E_{237}) found in Chapter 3 section 3.2.4.2.

4.3 Discussion

In Chapter 3, the ablation of the three NS1 glycosylation sites consisted of changing each asparagine to an alanine. Although a high level of attenuation of neuroinvasiveness was achieved, especially with the $NS1_{130A/175A/207A}$ mutant virus, reversion at the $NS1_{130}$ site as well as compensating mutations in the E protein were seen in viruses isolated from the brains of mice that succumbed to infection following ip inoculation with this virus. Since several mice that succumbed to infection inoculated with the alanine triple mutant virus showed reversion at the $NS1_{130}$ residue, it was hypothesized that changing more than one amino acid in the first ($NS1_{130}$) glycosylation motif would result in a virus that would not readily revert to a virulent phenotype, and thus a more stable, attenuated virus. This was achieved by changing the $NS1_{130}$ asparagine to a serine and the $NS1_{131}$ asparagine to a valine (NNT→SVT).

The $NS1_{130S/175A/207A}$ and $NS1_{130\text{-}132SV/175A/207}$ serine mutant viruses showed reduced multiplication in cell culture as well as a small plaque phenotype compared to the parental strain. Reduced infectivity titre and small plaque phenotype were associated with attenuation of neuroinvasiveness in the mouse model (Fig. 4-2 and Tables 4-2

and 4-3). Unlike the alanine mutants (Chapter 3), the serine mutant viruses displayed reduced infectivity titres in all three cell types examined with the most differences in mouse macrophage P388 D1 cells.

The protein blots showed a reduction in the secreted NS1 of the serine mutant viruses. The E control protein blot showed consistent bands between the parental NY99 and serine mutant viruses indicating the reduction in secreted NS1 was not due to an overall reduction in synthesis of viral proteins. The exception to this was the $NS1_{130-131SV/175A/207A}$ mutant virus. The western blots for this protein samples indicated an overall loss of viral protein that contributed to the reduction in secreted NS1.

Neuroinvasive and neurovirulence phenotypes were determined in female 3-4 week NIH Swiss mice. All four of the serine mutants proved to be attenuated for neuroinvasiveness to some extent compared to the parental NY99 strain. This was in contrast to the alanine mutants where only two of the seven engineered mutants were highly attenuated ($NS1_{130A/207A}$ and $NS1_{130A/175A/207A}$) (Table 3-2). Interestingly, the single mutation at the $NS1_{130}$ residue, changing the asparagine to a serine ($NS1_{130S}$) attenuated the virus 200-fold for neuroinvasiveness. This was unexpected since changing the $NS1_{130}$ residue to an alanine ($NS1_{130A}$) did not significantly attenuate the virus. It is hypothesized that the serine mutation at this site is more stable than the alanine mutation and this is probably due to the similarity in molecular structure of the asparagine and serine compared to alanine. Serine differs from alanine by a hydroxyl group that replaces one methyl group (Fig. 4-1) and is similar to the naturally occurring asparagine in that they are both hydrophilic amino acids while alanine is weakly hydrophobic. This similarity may explain why no reversions were seen in these mutants and consequently more attenuated mutants were achieved.

It was noted that viral RNA isolated from the brains of mice that succumbed to infection with the $NS1_{130S}$ mutant virus contained an amino acid mutation at $NS1_{40}$, a non-conserved site among flaviviruses (Fig 4-5). None of the other virus-infected mouse brains showed this mutation. It is unclear why the $NS1_{130S}$ mutant was the only virus that showed a mutation in the NS1 protein, however, the possibility of mutations elsewhere in the genome cannot be ruled out. Due to the volume of sequencing of both the E and NS1 genes, determining the nucleotide sequence of the entire genome of viruses from several mice for all mutant viruses was not deemed feasible.

Two studies were conducted to determine the neuroinvasive and neurovirulence phenotype of these mutant viruses in mice. Although the LD_{50} for the serine mutant viruses, especially the $NS1_{130\text{-}131SV/175A/207A}$, showed variability in mice, the parental virus remained consistent between experiments. Since reversion of the NS1 glycosylation sites was not identified, restoration of the glycosylation site(s) cannot explain this variability. In fact, other than the mutation at $NS1_{40}$ for the $NS1_{130S}$ mutant virus, no other mutations were found in the E or NS1 protein genes of any mutant virus. This is in contrast to the alanine attenuated ($NS1_{130A/175A/207A}$) mutant where ablation of the glycosylation sites resulted in either compensating mutations in the E protein and/or reversion at $NS1_{130}$ indicating that one or more glycosylation sites were needed for neuroinvasiveness.

Differences in the mice utilized may explain discrepancies between the two mouse virulence studies, in particular the difference in results for the $NS1_{130\text{-}131SV/175A/207A}$ mutant virus in the two studies. Due to the lack of availability of the mice, 3-4 week old mice sets contained some weanling and post-weanling mice and varied between

experiments. Age-dependent resistance to flavivirus infection in mice has been shown previously for West Nile and JE viruses (Hunsberger and Roehrig, 2006; Ogata *et al.*, 1991) and it has been shown that weanling mice display immature immune systems relative to adult mice (Holladay and Smialowicz, 2000). Since differences in the LD_{50}'s were seen only in the $NS1_{130\text{-}131SV/175A/207A}$ mutant virus and not the parental NY99 strain, it is hypothesized that differences in the immune responses of the mice towards these NS1 glycoslyation mutant viruses may affect their survival rate. Further examination of this hypothesis was undertaken later in the thesis.

Figure 4-1. Molecular structure of asparagine and serine. Colors represent different atoms: Grey-carbon, white-hydrogen, red-oxygen and blue-nitrogen.

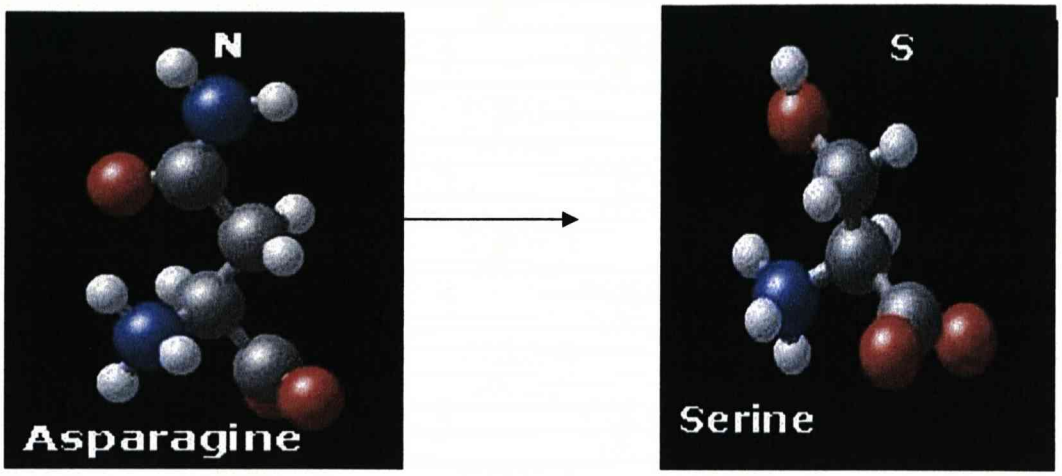

Figure 4-2. Plaque size comparison of the parental NY99 infectious clone and glycosylation serine mutant viruses in Vero cells.

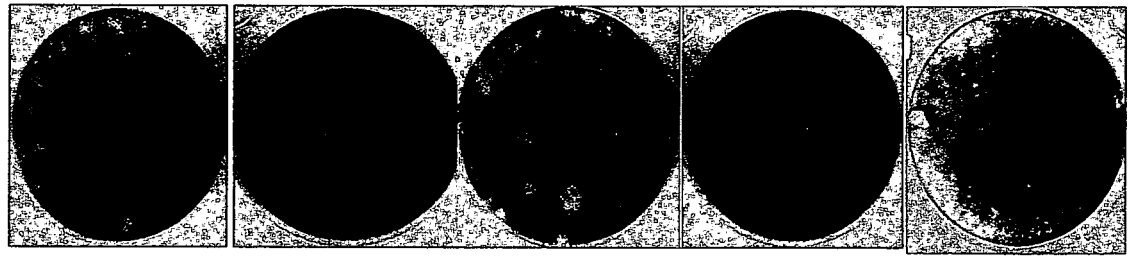

Table 4-1 Temperature sensitivity of serine mutant viruses

Virus	37°C	39.5°C	Δ (37°C-39.5°)
	Log_{10}PFU/ml	Log_{10}PFU/ml	Log_{10}PFU
$NS1_{130S}$	6.5	6.7	-0.2
$NS1_{130\text{-}131SV}$	8.2	8.0	0.2
$NS1_{130S/175A/207A}$	6.9	6.9	0
$NS1_{130\text{-}131SV/175A/207A}$	6.2	4.6	1.6

Figure 4-3. Western blots of the parental NY99 and serine mutants of the NS1 (A), E (B) and both protein blots overlaid (C).

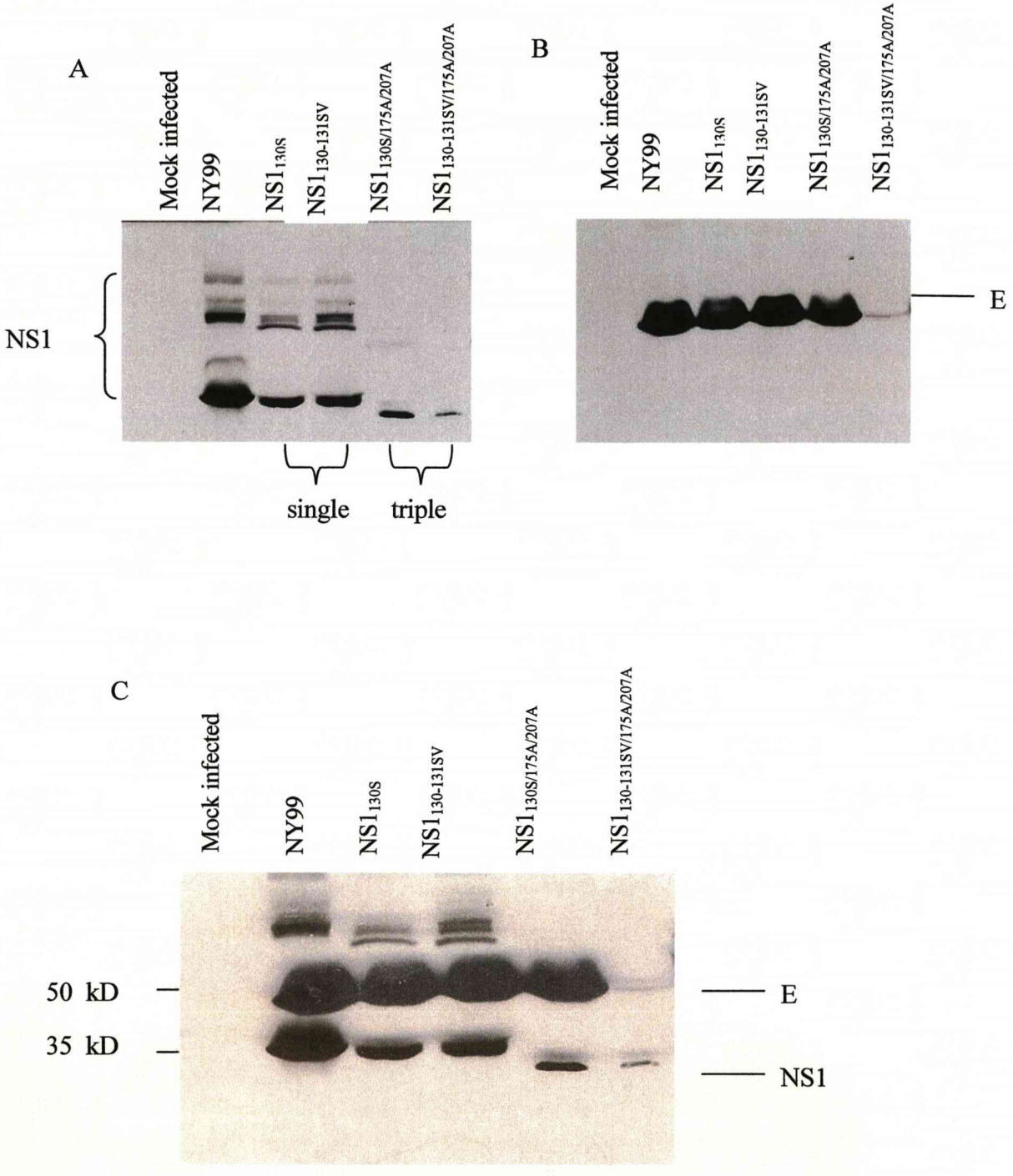

Figure 4-4 Multiplication of serine mutants and the parental NY99 strain in Vero (A) , Neuro 2A (B) and P388 D1 (C) cells. Each time point represents the mean +/- SD of triplicate samples.

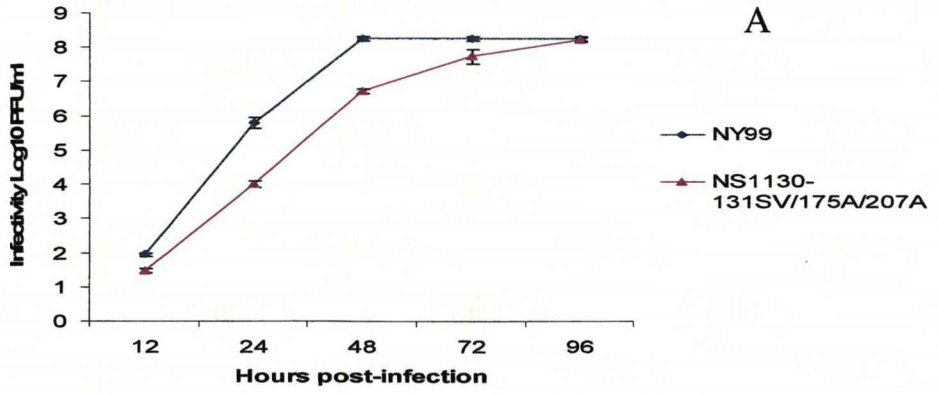

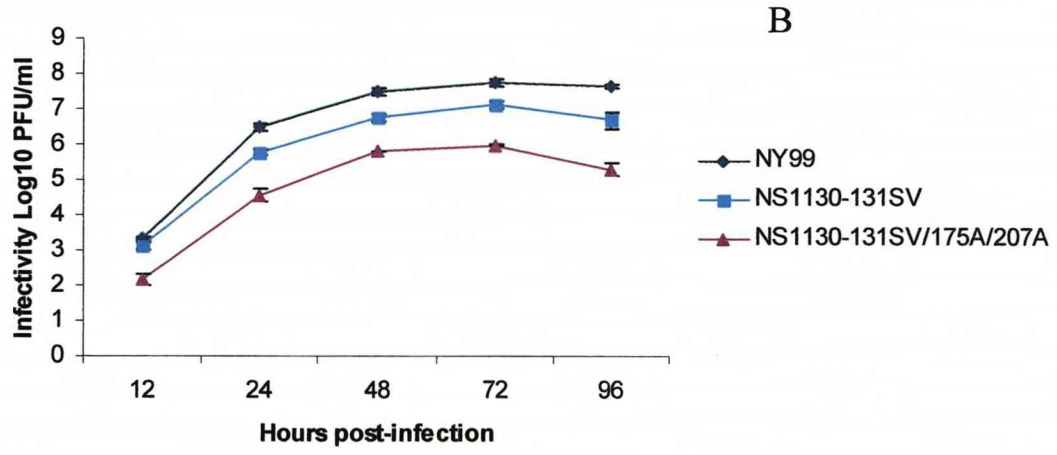

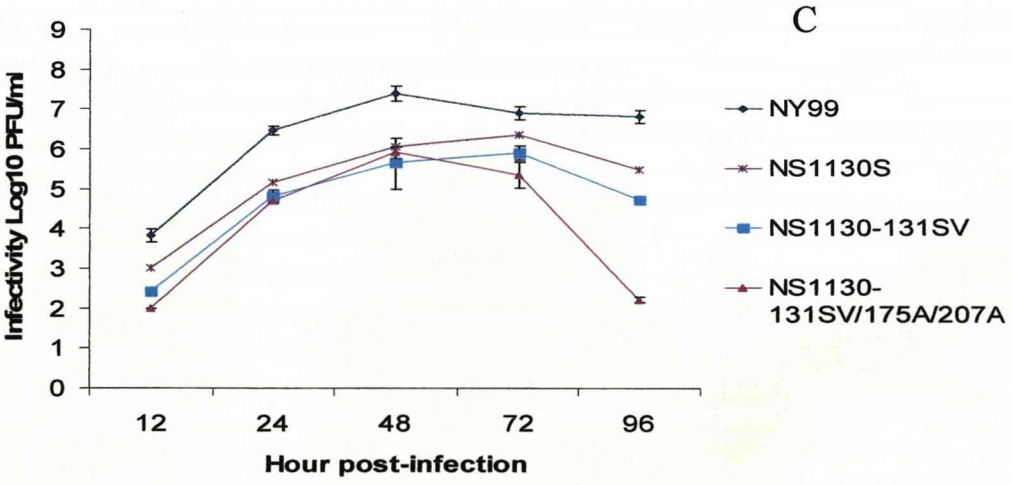

Table 4-2. Mouse virulence phenotype of serine mutant viruses and the parental NY99 strain.

Virus	$ipLD_{50}$ (PFU)	AST + SD*	p-value	$icLD_{50}$ (PFU)
NY99	10	9.2 ± 1.1	N/A	30
$NS1_{130A/175A/207A}$	500	10.5 ± 1.7	>0.05	nd
$NS1_{130S}$	2,000	9.5 ± 0.7	>0.05	80
$NS1_{130\text{-}131SV}$	1,300	9.0 ± 1.4	>0.05	300
$NS1_{130S/175A/207A}$	>100,000	>21	<0.05	50
$NS1_{130\text{-}132SV/175A/207A}$	80	9.2 ± 0.8	>0.05	50

*AST ± SD = average survival time ± standard deviation at a dose of 1,000 PFU
nd= not determined
N/A = not applicable

Table 4-3. Mouse neuroinvasiveness (ip) and neurovirulence (ic) of serine mutant viruses repeated.

Virus	$ipLD_{50}$ (PFU)	AST + SD*	p-value	$icLD_{50}$ (PFU)
NY99	10	8.0 ± 0	N/A	10
$NS1_{130A/175A/207A}$	1,000	10.5 ± 1.9	<0.05	nd
$NS1_{130S}$	nd	nd	nd	nd
$NS1_{130\text{-}131SV}$	300	10.0 ± 1.9	<0.05	>100
$NS1_{130S/175A/207A}$	nd	nd	nd	nd
$NS1_{130\text{-}132SV/175A/207A}$	80,000	>21	<0.05	500

*AST ± SD = average survival time ± standard deviation at a dose of 1,000 PFU
nd= not determined
N/A = not applicable

Figure 4-5. Amino acid alignment of the NS1 amino terminus of several flaviviruses. Highlighted amino acids represent conserved residues. The N-terminus of JE NS1 aligns downstream of the other flaviviruses represented in this figure.

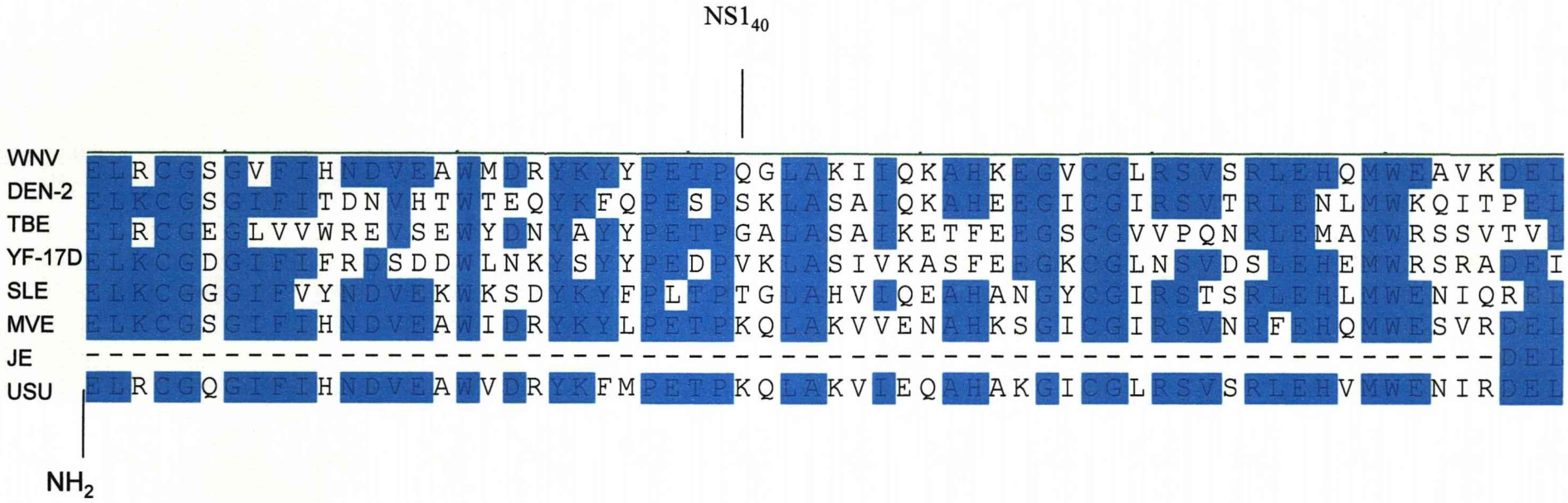

CHAPTER 5 : CHANGING $NS1_{130}$ TO A GLUTAMINE AND ALL THREE AMINO ACIDS IN THE GLYCOSYALTION MOTIF

5.1 Introduction

West Nile virus NS1 protein contains three highly conserved glycosylation sites (NXT) beginning at residues $NS1_{130}$, $NS1_{175}$ and $NS1_{207}$. The ablation of all three of these sites was examined in Chapter 3 by changing the asparagine of the glycosylation motif to an alanine and resulted in a highly attenuated phenotype for mouse neuroinvasiveness. Mice that succumbed to infection, however, contained a reversion at $NS1_{130}$ that restored the first glycosylation site as well as two amino acid mutations in the E protein (E_{204} and E_{237}).

To prevent reversion and increase mouse attenuation, the studies described in Chapter 4 reported mutating the asparagine of the $NS1_{130}$ glycosylation motif to a serine ($NS1_{130S}$, $NS1_{130\text{-}131SV}$, $NS1_{130S/175A/207A}$ and $NS1_{130\text{-}131SV/175A/207A}$). As hypothesized, the serine mutants were more attenuated than the alanine mutant viruses. Interestingly, even the single $NS1_{130}$ N→S change attenuated for mouse virulence at least as much as the most attenuated triple alanine mutant virus ($NS1_{130A/175A/207A}$). Although reversion at $NS1_{130}$ site was not detected in the serine mutants, an amino acid mutation at $NS1_{40}$ (glutamine to histadine [CAA→CAC]) was seen in all viral RNA samples isolated from the brains of mice inoculated ip with the $NS1_{130S}$ virus. No other mutations were identified in either the E or NS1 genes of the serine mutant viruses. Given that the glycosylation mutation remained, the difference in the alanine and serine mutants lies within the specific amino acid mutation. For example, the single alanine glycosylation mutant virus $NS1_{130A}$ was not attenuated in mice while the serine glycosylation mutant virus $NS1_{130\text{-}131SV}$ showed a high level of attenuation of mouse neuroinvasiveness, at least 200-fold, compared to the parental NY99 strain.

The E and NS1 gene sequences of viral RNA isolated from the brains of mice that succumbed to these viruses revealed no mutations other than those engineered, thereby suggesting that the amino acid at this site may contribute to the overall stability of the virus.

Asparagine and serine are hydrophilic amino acids whereas alanine is hydrophobic. Although serine is more similar to asparagine than alanine, serine differs from asparagine by an amide group. The amino acid glutamine also contains this amide group and differs from asparagine by only one methyl group (Fig 5-1). Due to its similarity in molecular structure, glutamine was chosen to replace the asparagine in the $NS1_{130}$ glycosylation site with the aim of preventing the mutation at $NS1_{40}$ seen in the serine mutant virus ($NS1_{130S}$) as well as reversion seen in the alanine mutants ($NS1_{130A/175A/207A}$). Furthermore, it was hypothesized that changing asparagine to glutamine at the $NS1_{175}$ and $NS1_{207}$ residues would generate a virus that was more attenuated for neuroinvasiveness in mice because of the similarity of the structure to that found in the wild type virus.

Six new mutant viruses were generated with one or more glutamine substitutions to determine the affects of changing the asparagine to glutamine. Two single site glutamine mutants were generated, $NS1_{130Q}$ and $NS1_{130Q/175A/207A}$. In addition, two mutants were generated by changing all three amino acids in the glycosylation motif such that the entire $NS1_{130}$ glycosylation motif was ablated where the two asparagines at $NS1_{130}$ and $NS1_{131}$ were both changed to glutamine and the threonine at $NS1_{132}$ was changed to an alanine (NNT→QQA), which resulted in mutants $NS1_{130\text{-}132QQA}$ and $NS1_{130\text{-}132QQA/175A/207A}$. Studies in Chapter 4 demonstrated that the serine mutation at $NS1_{130}$ attenuated the virus ($NS1_{130S}$ and $NS1_{130\text{-}131SV}$) compared to the parental NY99

strain whereas the single alanine mutation ($NS1_{130A}$) did not. Therefore, two more mutants were generated, $NS1_{175\text{-}177QQA}$ and $NS1_{207\text{-}209QQA}$.

5.2 Results

5.2.1 In vitro characterization of mutant viruses

The six mutant viruses were generated as described in Chapter 3 and harvested at five days post-transfection in Vero cells, samples frozen and then passaged once in Vero cells before subsequent experiments were performed. The viruses were titrated in Vero cells and plaque titration of the glutamine mutant viruses revealed a typical NY99 plaque morphology of about 2mm for the $NS1_{130Q}$, $NS1_{130\text{-}132QQA}$, $NS1_{175\text{-}177QQA}$ and $NS1_{207\text{-}209QQA}$ mutant viruses. However, the $NS1_{130Q/175A/207A}$ and $NS1_{130\text{-}132QQA/175A/207A}$ mutant viruses exhibited small plaque morphology of less than 1mm (Fig 5-2). A temperature sensitivity (ts) assay showed that none of the glutamine mutant viruses were ts at 39.5°C (Table 5-1). Three plaques were collected for all glutamine mutants at 39.5°C, the RNA extracted for RT-PCR and the NS1 gene was sequenced. No mutations were identified other than the engineered mutations.

5.2.2 Western blot analysis

All glutamine mutant viruses were used to infect Vero cells at a moi of 0.1, the supernatant was collected at 48 hours post-infection and concentrated before performing a western blot. The parental NY99 strain was also used to determine whether or not there was an increase in migration of the NS1 mutants, thereby putatively showing a loss of glycosylation (Fig 5-3B). The maximum amount of protein sample (25µl) was used for each, and the blots were probed with a monoclonal

NS1 antibody, 17NS1 (Chung *et al.*, 2006), before chemiluminescence and audoradiography to detect the protein. Another PAGE gel was run in the same manner, but this time the blot was probed with a rabbit anti-recombinant polyclonal E-domain III antibody as a loading control (Fig. 5-3A). Like the serine mutant viruses (Fig. 4-3), the NS1 of the single site glutamine glycosylation mutant viruses migrated faster than that of the parental NY99 virus, while the NS1 of the $NS1_{130Q/175A/207A}$ and $NS1_{130\text{-}132QQA/175A/207A}$ migrated faster than the single site mutants. In addition, the triple NS1 mutants appeared to have reduced levels of NS1 compared to the parental NY99 strain (Fig. 5-3B). The quantity of E protein for all glutamine mutant viruses, except for the $NS1_{130\text{-}132QQA/175A/207A}$ mutant virus, appeared similar to the parental NY99 strain (Fig. 5-3A).

5.2.3 Multiplication kinetics in cell culture

Multiplication kinetics of the $NS1_{130\text{-}132QQA}$ and $NS1_{130\text{-}132QQA/175A/207A}$ mutant viruses and the parental NY99 strain was determined in monkey kidney Vero, mouse macrophage P388 D1, and mouse neuroblastoma Neuro2A cells (Fig. 5-4A-C). These mutant viruses were chosen based on previous experiments where the $NS1_{130\text{-}131SV/175A/207A}$ mutant viruses showed the greatest reduction in infectivity titre compared to the parental NY99 strain (Fig. 4-4). In addition, there was little difference in multiplication kinetics between the $NS1_{130S}$, $NS1_{130\text{-}131SV}$ and $NS1_{130\text{-}131SV/175A/207A}$ mutant viruses in mouse macrophage P388 D1 cells (Chapter 4).

Cells were infected in triplicate at a moi of 0.1, cell culture supernatants were collected at 12, 24, 48, 72 and 96 hours post-infection, frozen at -80°C and then infectivity titres were determined by plaque titration in Vero cells.

5.2.3.1 Vero cells

The $NS1_{130\text{-}132QQ}$ and $NS1_{130\text{-}132QQA/175A/207A}$ mutant viruses, as well as the parental NY99 strain, showed peak infectivity titre at 48 hours post-infection with a subsequent drop in titre at later times post-infection in Vero cells. Both $NS1_{130\text{-}132QQ}$ and $NS1_{130\text{-}132QQA/175A/207A}$ mutant viruses showed a reduction in infectivity titre at 12 and 24 hours post-infection compared to the parental NY99 strain, although only the $NS1_{130\text{-}132QQA/175A/207A}$ mutant virus displayed a difference at 48 hours post-infection. $NS1_{130\text{-}132QQ}$ and $NS1_{130\text{-}132QQA/175A/207A}$ mutant viruses showed some reduction in infectivity titre at 72 and 96 hours post-infection. The $NS1_{130\text{-}132QQA/175A/207A}$ mutant virus showed the greatest difference compared to the parental NY99 strain with as much as a 3,000-fold reduction in infectivity titre at 24 hours post-infection (Fig. 5-4A).

5.2.3.2 P388 D1 cells

The parental NY99 strain increased in infectivity titre until 48 hours post-infection and subsequently reduced in infectivity titre at later times post-infection. The mutant viruses $NS1_{130\text{-}132QQA}$ and $NS1_{130\text{-}132QQA/175A/207A}$ showed reduction (up to 30-fold) in infectivity titre compared to the parental NY99 strain (Fig 5-4B). Although the infectivity titre of the $NS1_{130\text{-}132QQA}$ mutant virus was only slightly increased over $NS1_{130\text{-}132QQA/175A/207A}$, this virus did not reach peak infectivity titre until 72 hours post-infection. The $NS1_{130\text{-}132QQA/175A/207A}$ mutant virus displayed the greatest reduction in infectivity titre compared to the parental NY99 strain and followed the same curve as NY99 virus with a peak in infectivity titre 48 hours post-infection.

5.2.3.3 Neuro 2A cells

Multiplication kinetics of WNV in the mouse neuroblastoma Neuro2A cell line were slower, and did not show a rapid increase and subsequent decrease in infectivity titre, as seen in the Vero or P388 D1 cells lines. The $NS1_{130\text{-}132QQA/175A/207A}$ mutant virus showed the greatest reduction in infectivity titre with a 10-fold decrease at 24, 48, 72 and 96 hours post-infection compared to the parental NY99 strain (Fig 5-4C). Both the parental NY99 and the $NS1_{130\text{-}132QQA/175A/207A}$ viruses showed a peak infectivity titre at 72 hours post-infection, while that $NS1_{130\text{-}132QQA}$ mutant virus showed a peak infectivity titre at 48 hours post-infection; although there were little differences in the infectivity titres between the 48 and 72 hour time points.

5.2.4 Mouse virulence phenotype of mutant viruses

All six glutamine mutants were inoculated into female 3-4 week outbred NIH Swiss mice by the ip route (to determine neuroinvasiveness) and by the ic route (to determine neurovirulence). Serial 10-fold dilutions of each virus including, $NS1_{130Q}$, $NS1_{130\text{-}132QQA}$, $NS1_{175\text{-}177QQA}$, $NS1_{207\text{-}209QQA}$, $NS1_{130Q/175A/207A}$ and $NS1_{130\text{-}132QQA/175A/207A}$ were inoculated into mice. The LD_{50}'s and average survival times (AST's) were calculated and compared to two controls: the parental NY99 strain and $NS1_{130A/175A/207A}$ mutant to determine the level of attenuation (Tables 5-2 and 5-3).

5.2.4.1 Neuroinvasiveness and neurovirulence of mutant viruses

The $NS1_{130}$ glutamine mutants exhibited a high level of attenuation in mice with at least a 30-fold attenuation of neuroinvasiveness compared to the parental NY99 strain. The $NS1_{130Q}$ mutant showed an $ipLD_{50}$ of 5,000 PFU and the $NS1_{130\text{-}132QQA}$ mutant

showed an $ipLD_{50}$ of 300 PFU compared to the parental NY99 strain, which had an $ipLD_{50}$ of 10 PFU. Neither of these viruses was significantly attenuated for neurovirulence compared to the parental strain with $icLD_{50}$'s for the NY99, $NS1_{130Q}$ and $NS1_{130\text{-}132QQA}$ of 30, 50 and 20 PFU respectively. In comparison, the $NS1_{130Q/175A/207A}$ and $NS1_{130\text{-}132QQA/175A/207A}$ mutants were greatly increased in attenuation compared to the $NS1_{130A/175A/207A}$ mutant for both neuroinvasiveness and neurovirulence. The $ipLD_{50}$ for $NS1_{130Q/175A/207A}$ was >10,000 PFU with an $icLD_{50}$ of 500 PFU, while the $NS1_{130\text{-}132QQA/175A/207A}$ mutant was also highly attenuated with an $ipLD_{50}$ of >500,000 PFU and also showed the greatest attenuation for neurovirulence with an $icLD_{50}$ of 800 PFU (Table 5-2).

The $NS1_{175\text{-}177QQA}$ and $NS1_{207\text{-}209QQA}$ mutant viruses were attenuated for neuroinvasiveness but not for neurovirulence. The $NS1_{175\text{-}177QQA}$ mutant virus showed an $ipLD_{50}$ of 200 PFU while the $NS1_{207\text{-}209QQA}$ mutant virus showed a more modest attenuation with an $ipLD_{50}$ of 50 PFU compared to the parental NY99 strain that showed an $ipLD_{50}$ of 10 PFU for this experiment (Table 5-2).

In a repeat experiment (Table 5-3), the $NS1_{130\text{-}132QQA}$ and $NS1_{130\text{-}132QQA/175A/207A}$ mutants maintained a highly attenuated phenotype for both neuroinvasiveness and neurovirulence. As in the first experiment, the parental NY99 strain had an $ipLD_{50}$ and $icLD_{50}$ of 10 PFU. The $NS1_{130\text{-}132QQA}$ mutant virus displayed an $ipLD_{50}$ of 500 PFU, similar to the previous experiment and an $icLD_{50}$ of 500 PFU, which was more attenuated than seen in the previous experiment. The $NS1_{130\text{-}132QQA/175A/207A}$ mutant, on the other hand, showed consistent ip and ic LD_{50} values with an $ipLD_{50}$ of >1,000,000 PFU and an $icLD_{50}$ of 800 PFU (Table 5-3), nearly identical to the previous experiment (Table 5-2).

5.2.4.2 *Sequence analysis of viral RNA isolated from mouse brains*

The brains of mice that succumbed to ip inoculation with $NS1_{130Q}$, $NS1_{130\text{-}132QQA}$, $NS1_{130\text{-}132QQA/175A/207A}$, $NS1_{175\text{-}177QQA}$ and $NS1_{207\text{-}209QQA}$ were homogenized and viral RNA was extracted followed by RT-PCR and sequencing of the E and NS1 genes. Mice inoculated with the $NS1_{130Q/175A/207A}$ mutant virus, however, did not show morbidity or mortality, and therefore, no brains from this group were analyzed. For two viruses, $NS1_{130Q}$ and $NS1_{130\text{-}132QQA/175A/207A}$, no sequence was obtained due to the lack of RT-PCR product for these samples. For the other viruses, $NS1_{130\text{-}132QQA}$, $NS1_{175\text{-}177QQA}$ and $NS1_{207\text{-}209QQA}$, 2-5 brain samples were analyzed for each virus mutant. No mutations were identified in the E and NS1 genes, other than the engineered mutations (Table 5-4).

5.3 Discussion

Previous experiments in Chapters 3 and 4 described ablating the glycosylation sites in the NS1 protein by mutating the asparagine at the $NS1_{130}$ site to an alanine (Chapter 3) or a serine (Chapter 4), and the $NS1_{175}$ and $NS1_{207}$ sites by changing the asparagine to an alanine (Chapter 3 and 4). Although some mutants were attenuated for both neuroinvasiveness and neurovirulence in mice, it was clear that the particular amino acids in the glycosylation motif were very important and could lead to instability and/or tendencies to either revert or cause putative compensatory mutations at other residues. This led to the hypothesis that particular changes in the glycosylation motif would result in a more 'stable' virus and further attenuate the virus for mouse virulence. Therefore, the asparagine in the glycosylation motif was mutated to a glutamine due to its similarity in molecular properties to asparagines (Figure 5-1).

Western blot analyses of the glutamine mutant viruses revealed a decrease in secreted NS1 protein of all mutant viruses compared to the parental NY99 strain in Vero cells. Other than for the $NS1_{130\text{-}132QQA/175A/207A}$ mutant, this result was not due to the overall decrease in viral protein since the quantity of E protein appeared similar for all glutamine mutant viruses and the parental NY99 strain. The $NS1_{130\text{-}132QQA}$ and $NS1_{130\text{-}132QQA/175A/207A}$ mutant viruses did not show considerable differences in multiplication kinetics in Vero cells at later time points although differences were seen at all time points in P388 D1 cells and modest differenced in the Neuro2A cells . Overall these data suggests a deficiency in NS1 production and viral replication. The greatly reduced multiplication of the $NS1_{130\text{-}132QQA/175A/207A}$ mutant (Fig 5-4) is consistent with the reduced quantity of E and NS1 proteins in the western blots (Fig 5-3) compared to the other mutants and NY99 infected Vero cells.

Interestingly, changing all three amino acids in the glycosylation motif of both the $NS1_{175}$ and $NS1_{207}$ sites attenuated these viruses similar to changing each asparagine to an alanine only as undertaken in previous experiments in Chapter 3. The $NS1_{175\text{-}177QQA}$ mutant showed a 20-fold attenuation compared to the parental NY99 strain. This was not entirely surprising as the $NS1_{175A}$ mutant virus did show attenuation compared to the parental NY99 strain, although the level of attenuation was much less than some of the other mutants. The $NS1_{207A}$ mutant was not attenuated compared to the parental NY99 strain, while the $NS1_{207\text{-}209QQA}$ mutant was only weakly (5-fold) attenuated and was not considered attenuated. The $NS1_{175}$ glycosylation site is only present in the JE serogroup, except for JE virus itself, and this study indicates that this site is also important for virulence whereas the $NS1_{207}$ site alone does not appear to greatly affect the mouse virulence phenotype.

Significantly, no revertants, or any other amino acid mutations in the E or NS1 proteins, were seen in any of the mice that succumbed to infection. This was in contrast to the alanine triple mutant ($NS1_{130A/175A/207A}$ mutant) that reverted at the $NS1_{130}$ site and contained compensating mutations at E_{204} and E_{237}, and the serine mutant where a glutamine to histadine mutation at $NS1_{40}$ was found in viral RNA isolated from the brains of mice that succumbed to infection with the $NS1_{130S}$ mutant virus.

In the absence of X-ray crystallographic or NMR structure of the NS1 protein, it is unclear how these mutations affect the structure and/or conformation of this protein. Although little details are available for the structure and function of this protein, it can be surmised from these data that not only are the highly conserved glycosylation sites in the NS1 protein essential, but the specific amino acids, especially at the $NS1_{130-132}$ residues, are also very important, and may indicate a greater importance for this region such as a conformation needed for proper folding.

As hypothesized, the glutamine mutant viruses were overall more attenuated than either the alanine or serine mutant viruses and the mouse virulence phenotype of the mutant viruses was reproducible. Here it was shown that mutations in the glycosylation motif using amino acids that closely resembled those that were to be replaced, in this case asparagine to glutamine, resulted in a virus that was replication competent in cell culture yet was completely attenuated for neuroinvasiveness, highly attenuated for neurovirulence, and did not revert or cause mutations in viruses isolated from the brains of mice that succumbed to infection.

Figure 5-1. Molecular structure of asparagine and glutamine. Colors represent atoms in the amino acid; white-hydrogen, grey-carbon, blue-nitrogen, red-oxygen.

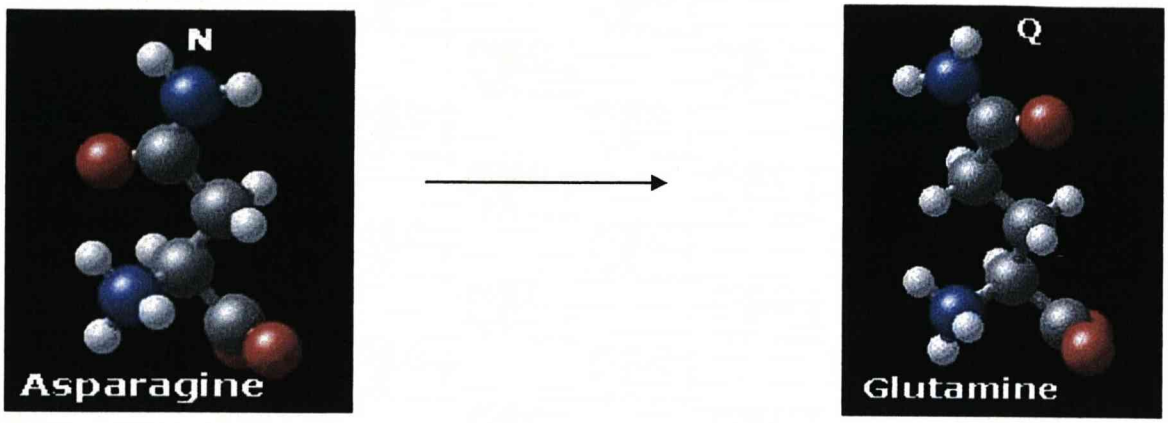

Figure 5-2. Plaque morphology of parental NY99 and all glutamine mutant viruses

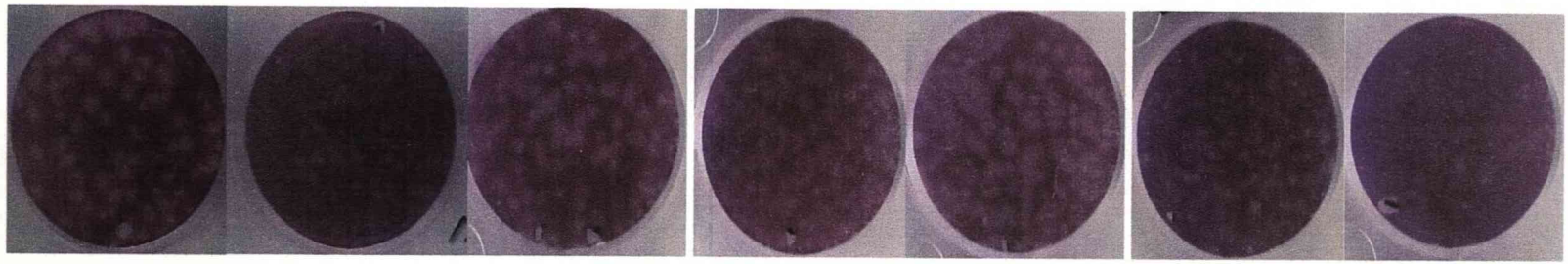

Table 5-1. Temperature sensitivity of glutamine mutant viruses

	37°C	39.5°C	Δ (37°-39.5°)
	Log_{10}PFU/ml	Log_{10}PFU/ml	Log_{10}PFU
$NS1_{130Q}$	5.1	5.1	0
$NS1_{130\text{-}132QQA}$	6.9	6.7	0.2
$NS1_{175\text{-}177QQA}$	6.2	5.8	0.4
$NS1_{207\text{-}209QQA}$	7.1	7	0.1
$NS1_{130Q/175A/207A}$	6	5.9	0.1
$NS1_{130\text{-}132QQA/175A/207A}$	6.8	5.9	0.9

Figure 5-3. Western blot of Vero-infected culture supernatant of all glutamine mutant viruses and the parental NY99 strain of the E (A) and the NS1 (B) proteins.

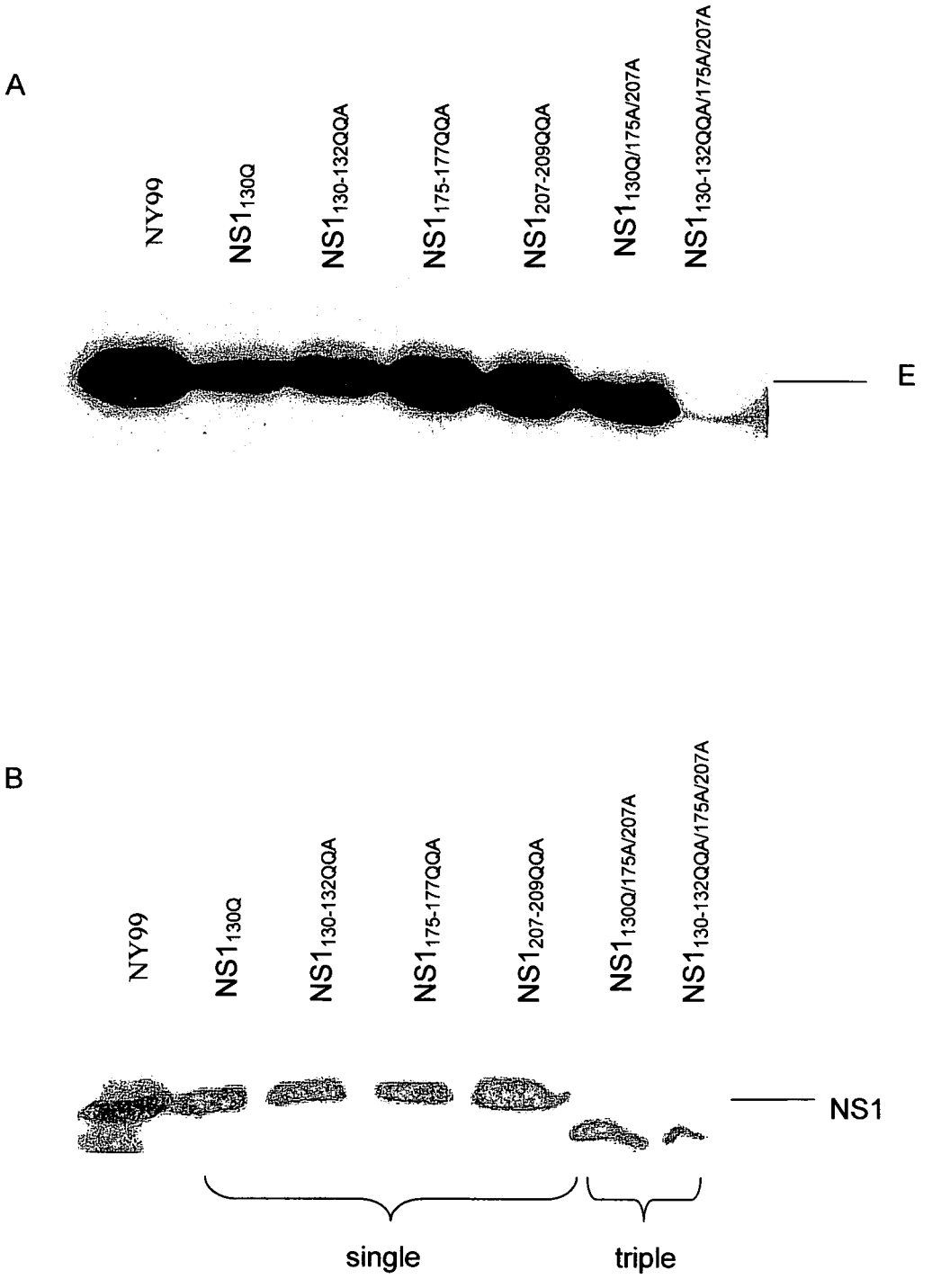

Figure 5-4 Multiplication kinetics of glutamine mutant viruses compared to the parental NY99 strain in Vero (A), P388 D1 (B) and Neuro2A (C) cells. Each time point represents the mean +/- SD of triplicate samples.

A

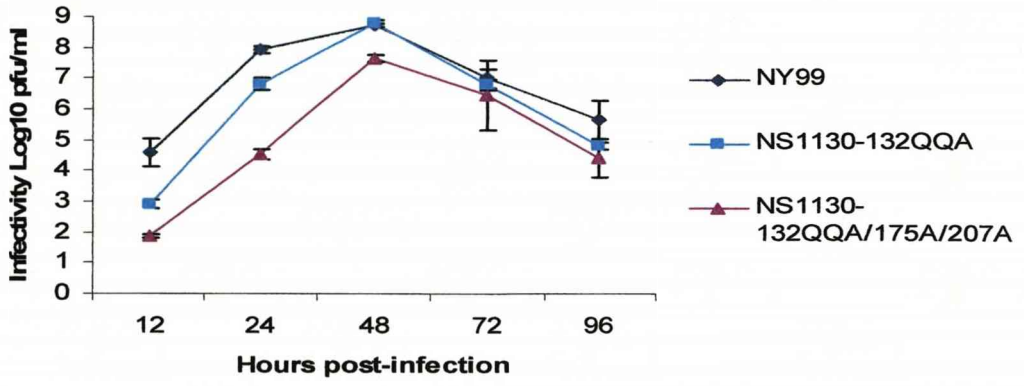

B

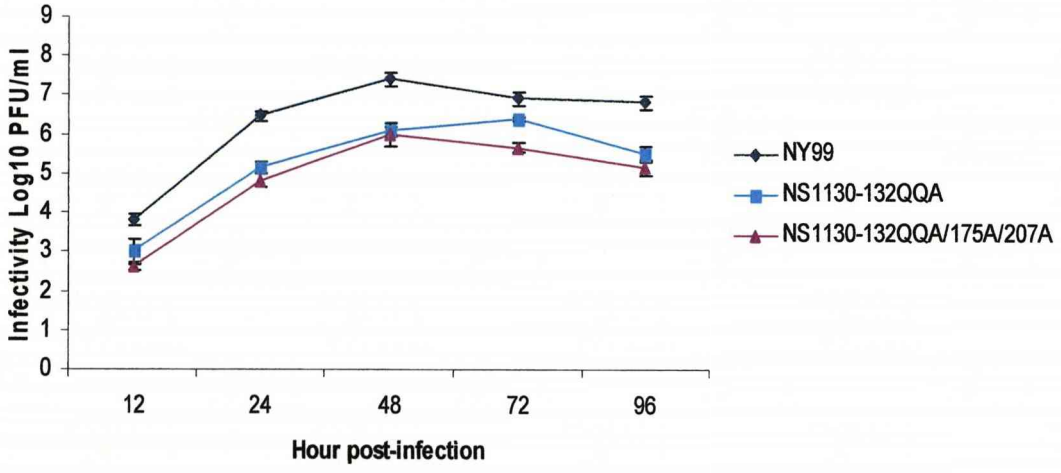

C

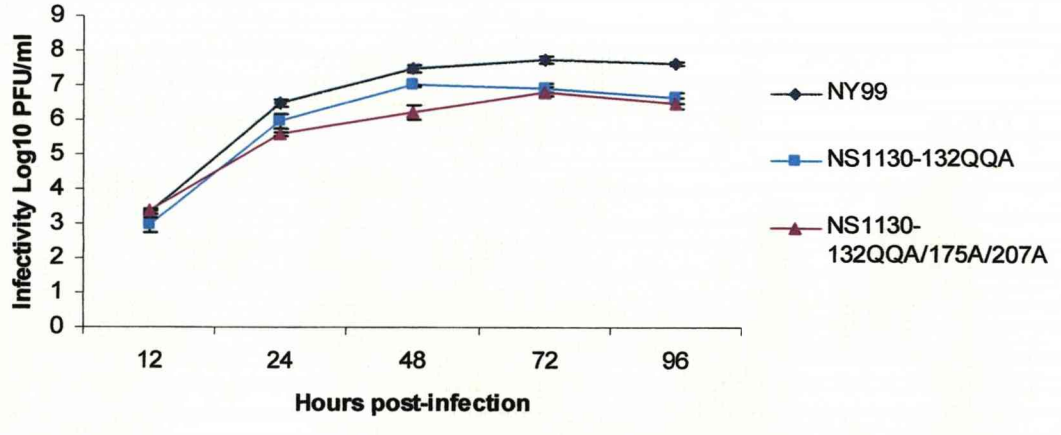

Table 5-2. Mouse virulence phenotype of glutamine mutant viruses.

Virus	$ipLD_{50}$ (PFU)	AST + SD*	p-value†	$icLD_{50}$ (PFU)
NY99	10	9.2 ± 1.1	N/A	30
$NS1_{130Q}$	5,000	>21	<0.05	50
$NS1_{130\text{-}132QQA}$	300	8.0 ± 0	>0.05	20
$NS1_{175\text{-}177QQA}$	200	9.2 ± 0.8	>0.05	50
$NS1_{1207\text{-}209QQA}$	50	8.0 ± 0	>0.05	30
$NS1_{130A/175A/207A}$	500	10.5 ± 1.7	>0.05	nd
$NS1_{130Q/175A/207A}$	>10,000	>21	<0.05	500
$NS1_{130\text{-}132QQA/175A/207A}$	>500,000	>21	<0.05	800

* Average survival time ± standard deviation at a dose of 1,000 PFU
† P-value determined by Student's T-test
nd= not determined

Table 5-3. Repeated mouse virulence study of attenuated glutamine mutant viruses.

Virus	ipLD50 (PFU)	AST + SD*	p-value†	icLD50 (PFU)
NY99	10	8.0 ± 0	N/A	10
$NS1_{130Q}$	nd	nd	nd	nd
$NS1_{130\text{-}132QQA}$	500	8.5 ± 0.6	>0.05	500
$NS1_{175\text{-}177QQA}$	nd	nd	nd	nd
$NS1_{207\text{-}209QQA}$	nd	nd	nd	nd
$NS1_{130A/175A/207A}$	1,000	10.5 ± 1.9	<0.05	nd
$NS1_{130Q/175A/207A}$	nd	nd	nd	nd
$NS1_{130\text{-}132QQA/175A/207A}$	>1,000,000	>21	<0.05	800

* Average survival time ± standard deviation at a dose of 1,000 PFU
† P-value determined by Student's T-test
nd= not determined

Table 5-4. Amino acid sequence of mutations in the E and NS1 proteins from RNA isolated from glutamine mutant- and NY99-infected mouse brains.

Virus	# of samples	Viral RNA	Sequence mutations				
			E	NS1	$NS1_{130-132}$	$NS1_{175-177}$	$NS1_{207-209}$
NY99	2	Y	None	None	NNT	NNT	NDT
$NS1_{130Q}$	1	N	nd	nd	nd	nd	nd
$NS1_{130-132QQA}$	5	Y	None	None	QQA	NNT	NDT
$NS1_{175-177QQA}$	3	Y	None	None	NNT	QQA	NDT
$NS1_{207-209QQA}$	2	Y	None	None	NNT	NNT	QQA
$NS1_{130Q/175A/207A}$	0	N	nd	nd	nd	nd	nd
$NS1_{130-132QQA/175A/207A}$	2	N	nd	nd	nd	nd	nd

nd=not determined

CHAPTER 6 : CHARACTERIZATION OF MULTIGENIC GLYCOSYLATION MUTANTS: ADDITION OF THE E GLYCOSYLATION SITE MUTATION TO THE ATTENUATED NS1 GLYCOSYALTION MUTANT VIRUSES

6.1 Introduction

Previously, Chapters 3, 4 and 5 discussed the ablation of the glycosylation site(s) in the NS1 protein and the affects of these mutations in terms of multiplication kinetics in cell culture and *in vivo,* as well as the mouse virulence phenotype compared to the parental NY99 strain. These mutant viruses proved to be replication competent in cell culture and highly attenuated in mice. However, in order to achieve a viable live-attenuated vaccine candidate, attenuating mutations in more than one gene are necessary to ensure a reversion event at one site does not lead to a vaccine revertant. Therefore, a mutation in the envelope gene, at E_{154S} (N→S), ablating the E protein glycosylation site of WNV, was added to the attenuated triple NS1 glycosylation mutant viruses.

Our laboratory has previously shown that the E_{154S} mutation attenuates WNV mouse neuroinvasiveness compared to the parental NY99 strain (Beasley *et al.,* 2005). Serine was chosen given that it is the naturally occurring mutation at this site for other WNV strains. In these studies, the E_{154S} mutant virus showed a 12-fold reduction in infectivity titre in monkey kidney Vero cells and was shown to be attenuated by 100-fold for neuroinvasiveness in mice compared to the parental NY99 strain.

A total of three new mutant viruses were generated including $E_{154S}/NS1_{130A/175A/207A}$, $E_{154S}/NS1_{130\text{-}131SV/175A/207A}$ and $E_{154S}/NS1_{130\text{-}132QQA/175A/207A}$. Multiplication kinetics in cell culture and *in vivo,* as well as mouse virulence experiments, were undertaken to determine the difference in the phenotypes of these viruses compared to the parental NY99 strain. The triple NS1 glycosylation mutant viruses, $NS1_{130A/175A/207A}$ and

$NS1_{130\text{-}131SV/175A/207A}$, were also used as control viruses in some experiments. The E_{154S} mutant virus was not utilized as the triple NS1 mutant viruses displayed greater differences, overall, compared to the parental NY99 strain in multiplication kinetics and mouse virulence in previous studies (Beasley *et al.*, 2005).

6.2 Results

6.2.1 In vitro characterization of mutant viruses

The E/NS1 mutant viruses were sequenced around the mutation sites following transfection to ensure the engineered mutations remained. Viruses were passaged once and plaqued in Vero cells before subsequent experiments were performed. Interstingly, the $E_{154S}/NS1_{130A/175A/207A}$ and $E_{154S}/NS1_{130\text{-}131SV/175A/207}$ mutants displayed high infectivity titre, but the $E_{154S}/NS1_{130\text{-}132QQA/175A/207A}$ mutant virus showed reduced infectivity with an infectivity titre of only 4 $\log_{10}$ PFU/ml, even after passage. The $E_{154S}/NS1_{130A/175A/207A}$ mutant virus displayed a minor reduction in plaque size (1.5 mm), whereas the $E_{154S}/NS1_{130\text{-}131SV/175A/207A}$ and $E_{154S}/NS1_{130\text{-}132QQA/175A/207A}$ mutant viruses showed a small plaque phenotype (<1 mm) compared to the parental NY99 strain (2 mm) (Fig. 6-1). A temperature sensitivity (ts) assay was performed with the $E_{154S}/NS1_{130A/175A/207A}$, $E_{154S}/NS1_{130\text{-}131SV/175A/207}$ and $E_{154S}/NS1_{130\text{-}132QQA/175A/207A}$ mutant viruses. None of these viruses were ts at 39.5°C (Table 6-1) and three plaques collected from each virus at 39.5°C did not reveal any mutations in the NS1 gene other than the engineered mutations after viral RNA extraction, RT-PCR and sequencing. Given that putative compensating mutations previously seen in

the E gene (E_{204} and E_{237}, Chapter 3) correlated with a reversion at $NS1_{130}$, the E gene was not sequenced.

6.2.2 Western blot analysis of mutant viruses

Western blotting was used to determine the relative amounts of E and NS1 protein, and putative loss of glycosylation, for the $E_{154S}/NS1_{130A/175A/207A}$, $E_{154S}/NS1_{130-131SV/175A/207}$ and $E_{154S}/NS1_{130-132QQA/175A/207A}$ mutant viruses. Confluent Vero cell monolayers were infected at a moi of 0.1 with either the parental NY99 or mutant viruses, the supernatant collected 48 hours post-infection and concentrated before the western blot was performed. The whole cell lysates were also collected concurrently.

The whole cell lysates showed similar E and NS1 protein levels in the NY99 and $E_{154S}/NS1_{130A/175A/207A}$ mutant viruses while the $E_{154S}/NS1_{130-131SV/175A/207A}$ and $E_{154S}/NS1_{130-132QQA/175A/207A}$ mutant viruses showed reduced levels of E and NS1 proteins (Fig 6-2A). The faster migration of the NS1 protein for the E/NS1 mutant viruses indicated a loss of glycosylation (Fig. 6-2A). The loss of glycosylation in the E protein was not as evident due to a lack of sensitivity of the PAGE to detect a migration difference from the loss of only one carbohydrate residue versus the loss of all three glycosylation sites in the NS1 protein. The E and NS1 proteins were reduced in the supernatant for the $E_{154}/NS1_{130-131SV/175A/207A}$, $E_{154S}/NS1_{130-132QQA/175A/207A}$ and to a lesser extent $E_{154S}/NS1_{130A/175A/207A}$ mutants compared to the NY99 virus (Fig. 6-2B).

6.2.3 Multiplication kinetics of mutant viruses

The multiplication kinetics in monkey kidney Vero and mouse macrophage P388 D1 cells were determined for the $E_{154S}/NS1_{130A/175A/207A}$ and $E_{154S}/NS1_{130-131SV/175A/207}$

mutant viruses and in mouse neuroblastoma Neuro 2A cells for the $NS1_{130\text{-}131SV/175A/207}$ mutant virus. The parental NY99 strain was used as a control to determine the differences in multiplication kinetics of the mutant viruses in each cell line. Since the triple serine mutant virus, $NS1_{130\text{-}131SV/175A/207A}$ showed significant differences compared to the parental NY99 strain in all three cell lines (Chapter 5, Fig 5-4), this virus was also used as a control to determine differences in the multiplication between it and the $E_{154S}/NS1_{130\text{-}131SV/175A/207}$. Due to the lack of differences of the $NS1_{130A/175A/207A}$ in Vero cells and minimal differences in P388 D1 cells compared to the parental NY99 strain (Chapter 3, Fig. 3-2) this virus was not used as a control. The $E_{154S}/NS1_{130\text{-}132QQA/175A/207}$ mutant virus was not included due to the low infectivity titre, approximately 4 $\log_{10}$ PFU/ml of this virus, even after passage in Vero cells. Cells were infected at a moi of 0.1 with either mutant virus or the parental NY99 strain in triplicate, the supernatant collected at 12, 24, 36, 48 and 72 hours post-infection for the $E_{154S}/NS1_{130A/175A/207A}$ mutant virus and at 12, 24, 48, 72 and 96 hours post-infection for the $E_{154S}/NS1_{130\text{-}131SV/175A/207A}$ mutant virus, and the infectivity titre was determined in Vero cells.

6.2.3.1 Vero cells

The parental NY99 strain displayed a peak titre at 48 hours post-infection while the $E_{154S}/NS1_{130A/175A/207A}$ mutant virus increased in infectivity titre until 72 hours post-infection(Fig 6-3A). The $E_{154S}/NS1_{130A/175A/207A}$ mutant virus showed up to a 10-fold reduction in infectivity titre compared to the parental NY99 strain at two different time points, 24 and 48 hours post infection, and notably showing a lag of multiplication at the 12 hour time point (Fig. 6-3A).

The $E_{154S}/NS1_{130\text{-}131SV/175A/207A}$ mutant virus displayed a peak in infectivity titre of approximately 8 $\log_{10}$ PFU/ml at 72 hours post-infection compared to the parental NY99 strain, which had a peak titre at 48 hours post-infection (Fig 6-4A). Differences (up to 75-fold reduction) were seen between the $E_{154S}/NS1_{130\text{-}131SV/175A/207A}$ mutant virus and the parental NY99 strain at the 24 and 48 hour time points. No differences were seen between the $NS1_{130\text{-}131SV/175A/207A}$ and $E_{154S}/NS1_{130\text{-}131SV/175A/207A}$ mutant viruses (Fig. 6-4A).

6.2.3.2 P388 D1 cells

Multiplication kinetics of the $E_{154S}/NS1_{130A/175A/207A}$ mutant virus and the parental NY99 virus in P388 D1 cells followed a similar trend, with a peak titre at 36 hours post-infection, however, the $E_{154S}/NS1_{130A/175A/207A}$ mutant virus showed reduction in infectivity titre (up to 100-fold) from NY99 virus at each time point (Fig. 6-3B).

The $E_{154S}/NS1_{130\text{-}131SV/175A/207A}$ mutant, $NS1_{130\text{-}131SV/175A/207A}$ mutant and the parental NY99 viruses showed a similar trend in multiplication kinetics (Fig 6-4B). All three viruses displayed peak titre at 48 hours post-infection. Interestingly, the $NS1_{130\text{-}131SV/175A/207A}$ mutant virus showed the greatest reduction in infectivity titre, up to 10,000- fold compared to the parental NY99 strain. The $E_{154S}/NS1_{130\text{-}131SV/175A/207A}$ mutant virus showed up to 75-fold reduction in the infectivity titre compared to the parental NY99 strain at the 24-96 hour time points. (Fig. 6-4B).

6.2.3.3 Neuro 2A cells

Since the $NS1_{130\text{-}131SV/175A/207A}$ mutant virus showed a high level of attenuation of neurovirulence (see Chapter 4, Table 4-3), the $E_{154S}/NS1_{130\text{-}131SV/175A/207A}$ virus was examined in mouse neuroblastoma Neuro 2A cells and compared to the triple serine $NS1_{130\text{-}131SV/175A/207A}$ mutant virus and the parental NY99 strain. The $NS1_{130\text{-}131SV/175A/207}$ mutant and the parental NY99 viruses showed a peak infectivity titre at 72 hours post-infection while the $E_{154S}/NS1_{130\text{-}131SV/175A/207A}$ mutant virus did not peak until 96 hours post-infection. Although the $E_{154S}/NS1_{130\text{-}131SV/175A/207A}$ mutant virus did not show any difference in the infectivity titre at 12 hours post-infection from the parental NY99 strain, this mutant showed up to a 100-fold reduction in infectivity at all other time points examined (Fig. 6-4C). Similar to the multiplication kinetics in P388 D1 cells (Fig 6-4B), the $E_{154S}/NS1_{130\text{-}131SV/175A/207A}$ mutant virus displayed a higher infectivity titre than the $NS1_{130\text{-}131SV/175A/207A}$ mutant virus at all time points (Fig 6-4C).

6.2.4 Virulence phenotype and multiplication of mutant viruses in mice

All three E/NS1 mutant viruses ($E_{154S}/NS1_{130A/175A/207A}$, $E_{154S}/NS1_{130\text{-}131SV/175A/207A}$ and $E_{154S}/NS1_{130\text{-}132QQA/175A/207A}$) were inoculated into 3-4 week female outbred NIH Swiss mice by the ip route (to determine neuroinvasiveness) and by the ic route (to determine neurovirulence) and compared to the NS1 triple mutant viruses ($NS1_{130A/175A/207A}$, $NS1_{131\text{-}131SV/175A/207A}$ and $NS1_{130\text{-}132QQA/175A/207A}$) and the parental NY99 strain. The AST's and LD_{50}'s were calculated at 21 days post-inoculation (Table 6-2).

Multiplication kinetics of the $E_{154S}/NS1_{130A/175A/207A}$ mutant, $NS1_{130A/175A/207A}$ mutant and the parental NY99 viruses in mice were examined by serial bleeds two and three day post-inoculation by the ip route. The serum collected was analyzed by plaque titration in Vero cells to determine viraemia (Table 6-3).

6.2.4.1 Neuroinvasiveness and neurovirulence of mutant viruses

The $E_{154S}/NS1_{130A/175A/207A}$, $E_{154S}/NS1_{130\text{-}131SV/175A/207}$ and $E_{154S}/NS1_{130\text{-}132QQA/175A/207A}$ mutant viruses all showed complete attenuation for neuroinvasiveness at the highest possible dose of virus with $ipLD_{50}$ values of >100,000, >100,000 and >1,000 PFU, respectively, and were at least 100-fold attenuated for neuroinvasiveness compared to the parental NY99 strain, which had an $ipLD_{50}$ value of 10 PFU (Table 6-2). Repeated experiments with the $E_{154S}/NS1_{130A/175A/207A}$ mutant virus demonstrated the same result (data not shown). Due to the low infectivity titre of the $E_{154S}/NS1_{130\text{-}132QQA/175A/207A}$ mutant virus, the highest inoculum dose was not as high as the other two viruses; therefore the $E_{154S}/NS1_{130\text{-}132QQA/175A/207A}$ mutant virus showed the least apparent attenuation of the three E/NS1 mutant viruses. The NS1 triple mutants $NS1_{130A/175A/207A}$ and $NS1_{130\text{-}131SV/175A/207A}$ that had $ipLD_{50}$ values of 1,000 and 80,000 PFU, respectfully, were further attenuated for neuroinvasiveness by the addition of the E_{154S} mutation. It was not possible to determine if the $NS1_{130\text{-}132QQA/175A/207A}$ mutant virus was further attenuated by the addition of the E_{154S} mutation as the NS1 mutant had an $ipLD_{50}$ value of >1,000,000 PFU while the $E_{154S}/NS1_{130\text{-}132QQA/175A/207A}$ mutant grew to low titer and was attenuated > 100-fold.

The addition of the E_{154S} mutation further attenuated the triple alanine mutant virus for neurovirulence; the $NS1_{130A/175A/207A}$ and $E_{154S}/NS1_{130A/175A/207A}$ mutant viruses

displaying $icLD_{50}$ values of 20 and 100 PFU, respectively while the $E_{154S}/NS1_{130A/175A/207A}$ virus was attenuated 10-fold compared to the parental NY99 strain (which had an $icLD_{50}$ value of 10 PFU). The other two E/NS1 mutant viruses, $E_{154S}/NS1_{130\text{-}131SV/175A/207A}$ and $E_{154S}/NS1_{130\text{-}132QQA/175A/207A}$, which had $icLD_{50}$ values of 126 and <100 PFU, respectively, were less attenuated for neurovirulence than the NS1 triple mutant viruses $NS1_{130\text{-}131SV/175A/207A}$ and.$NS1_{130\text{-}132QQA/175A/207A}$ that had $icLD_{50}$ values of 500 and 800 PFU, respectively (Table 6-2).

6.2.4.2 Multiplication of $E_{154S}/NS1_{130A/175A/207A}$ mutant virus in mice

Mice were bled on days two and three post inoculation to determine the viraemia (PFU/ml) in the serum (Table 6-3). The virus doses chosen for the NY99, $NS1_{130/175A/207A}$ and $E_{154S}NS1_{130A175A/207A}$ viruses were selected to contain groups that survived as well as succumbed to infection, hence the difference in the inoculum titres chosen for these viruses. Groups of five mice were inoculated with NY99 virus at doses of 10 and 100 PFU of virus, $NS1_{130A/175A/207A}$ at doses of 100 and 1,000 PFU, and $E_{154S}/NS1_{130A/175A/207A}$ virus at doses of 1,000 and 10,000 PFU. All mice inoculated with the NY99 parental strain, with one exception, succumbed to infection and revealed a viraemia of at least 2,000 PFU/ml and up to 300,000 PFU/ml on either day two or three post-inoculation. In comparison, three mice succumbed to infection inoculated with the attenuated NS1 mutant virus ($NS1_{130A/175A/207A}$) where all mice inoculated at a dose of 100 PFU showed no detectable viraemia on days 2 and 3 post-infection while two of five mice inoculated at a dose of 1,000 PFU showed vireamia at three days post-infection comparable to the NY99 inoculated mice of >1,000 PFU/ml;

however, these mice contained a reversion at $NS1_{130}$ and two mutations in the E protein at E_{207} and E_{237} (described in Chapter 3). The addition of the E_{154S} mutation reduced vireamia considerably as the $E_{154S}/NS1_{130A/175A/207A}$ infected mice exhibited little or no detectable viraemia on days 2 and 3 post-infection at a dose as high as 10,000 PFU.

6.2.5 *Induction of protective immunity in mice inoculated with the $E_{154S}/NS1_{130A/175A/207A}$ mutant virus*

Due to the phenotypes of high infectivity titre in cell culture, consistent lack of neuroinvasivess, and little to no detectable viraemia, the $E_{154S}/NS1_{130A/175A/207A}$ mutant virus was examined for induction of neutralizing antibodies and a protective immune response against challenge with NY99 virus. Groups of five mice were inoculated with serial 10-fold doses of either the mutant or parental NY99 viruses and at 21 days post-inoculation, the surviving mice were challenged ip with a lethal dose (100 PFU) of parental NY99 virus. The 50% protective dose (PD_{50}) was calculated from the mice that survived this challenge. The parental NY99 mice did not survive lethal challenge; therefore, PD_{50} was not calculable. The $E_{154S}/NS1_{130A/175A/207A}$ mutant showed a PD_{50} of 50 PFU.

In a separate experiment, the neutralizing antibody titre was determined by assaying sera collected 21 days post ip inoculation. The whole blood was left at room temperature to coagulate, the blood centrifuged and the serum collected. The serum was then stored at -80°C until a plaque reduction neutralization test was performed. Neutralizing antibody titres were represented by the dilution of the antibody able to reduce the NY99 infectivity titre by 50 percent (Table 6-4).

Since no mice succumbed to ip inoculation with the E_{154S}/$NS1_{130A/175A/207A}$ mutant virus, groups of five mice at each dose (1 to 100,000 PFU) were tested for induction of neutralization antibodies by this virus. The parental NY99 virus, on the other hand, had only two surviving mice at a dose of 1 PFU; one mouse had a low neutralization titre (80) while the other had a high titre (20,480). The five mice inoculated with 1 PFU of the E_{154S}/$NS1_{130A/175A/207A}$ mutant showed neutralization titres ranging from 20 to 1280. This variation is presumably a reflection that the mice are outbred. All five E_{154S}/$NS1_{130A/175A/207A}$ infected mice inoculated with a dose of 1,000 PFU showed high levels of neutralizing antibodies (at least 320) while mice inoculated with the highest dose of virus (100,000 pfu) had neutralization titres of 1,280 to 10,240. Interestingly, although there was no detectable viraemia for the E_{154S}/$NS1_{130A/175A/207A}$ infected mice at a dose of 10,000 PFU (see section 6.2.4.2), high levels of neutralizing antibodies were detected (320-5,120) in all five mice similarly infected (Table 6-4).

6.3 Discussion

Previously it was shown that the ablation of the glycosylation sites in the NS1 protein attenuated neuroinvasiveness, up to >100,000-fold, compared to the parental NY99 strain (Chapters 3, 4 and 5). Although highly attenuated, some mice inoculated with $NS1_{130A/175A/207A}$ virus at doses of 10 to 1,000 PFU succumbed to infection due to a reversion at the $NS1_{130}$ site. Although changing amino acids in the unstable $NS1_{130}$ site to either a serine or glutamine further attenuated the virus by preventing reversion, an attenuating mutation in more than one gene is necessary for a live-attenuated vaccine candidate; hence the mouse attenuated E_{154S} mutation was chosen for study.

The addition of the E_{154S} mutation in the $E_{154S}/NS1_{130A/175A/207A}$ and $E_{154S}/NS1_{130-131SV/175A/207A}$ mutant viruses reduced the infectivity titre compared to the parental NY99 strain. However, these viruses remained replication competent in cell culture with a peak infectivity titre up to 8 $\log_{10}$ PFU/ml. The $E_{154S}/NS1_{130-132QQA/175A/207A}$ mutant, on the other hand, showed a deficiency in multiplication with an infectivity titre of 4 $\log_{10}$ PFU/ml, even after one passage in Vero cells. Notably, the addition of the E_{154S} mutation appeared to increase the infectivity titre of the $E_{154S}/NS1_{130-131SV/175A/207A}$ mutant virus when compared to the triple serine ($NS1_{130-131SV/175A/207A}$) mutant virus indicating a stabilization of the virus due to the addition of this mutation. Interestingly, the $E_{154S}/NS1_{130A/175A/207A}$ did not display a small plaque phentotype similar to the E/NS1 ($E_{154S}/NS1_{130-131SV/175A/207A}$ and $E_{154S}/NS1_{130-132QQA/175A/207A}$) and NS1 ($NS1_{130-131SV/175A/207A}$ and $NS1_{130-132QQA/175A/207A}$) mutant viruses. Since both the $E_{154S}/NS1_{130A/175A/207A}$ and $NS1_{130A/175A/207A}$ mutant (see chapter 3) viruses resembled the parental NY99 plaque phenotype, the small plaque phenotype appeared to be due to mutations in the NS1 protein. Although all mutant viruses showed a reduction in viral infectivity titre, this reduction did not necessarily correlate with a reduction in E or NS1 protein detectable by western blotting. The $E_{154S}/NS1_{130A/175A/207A}$ mutant virus had protein levels comparable to the parental NY99 strain while the other two mutant viruses showed a reduction in both the E and NS1 proteins as detected by western blotting from the whole cell lysates. These data suggest that the asparagine to alanine change in the NS1 protein may be less disruptive than the serine or glutamine at the $NS1_{130}$ site.

Mouse virulence experiments showed that the addition of the E_{154S} mutation further attenuated the viruses for neuroinvasiveness for the $E_{154S}/NS1_{130A/175A/207A}$ and

E_{154S}/$NS1_{130\text{-}131SV/175A/207A}$, but not the E_{154S}/$NS1_{130\text{-}132QQA/175A/207A}$ mutant virus. The E_{154S}/$NS1_{130\text{-}132QQA/175A/207A}$ mutant virus showed reduced multiplication in cell culture and high titres of this virus was not available for the mouse virulence studies. Given that the $NS1_{130\text{-}132QQA/175A/207A}$ mutant virus was the most attenuated NS1 glycosylation mutant virus, the addition of the E_{154S} mutation may have caused the virus to become over-attenuated.

Interestingly, no mice succumbed to ip infection at any dose of any of the mutant viruses tested. This is in contrast to the $NS1_{130A/175A/207A}$ mutant virus where some mice did not survive infection due to a reversion at $NS1_{130}$, plus mutations at E_{204} and E_{237} seen in the viral RNA isolated from the brains of mice that succumbed following ip inoculation. The addition of the E_{154S} mutation to the $NS1_{130A/175A/207A}$ mutant virus further attenuated the virus for neuroinvasiveness and no mice succumbed to infection suggesting no reversions or compensating mutations in the E gene were generated. Although no brains were sequenced, it is hypothesized that compensating mutation or reversion did not occur since no mice succumbed to infection. Therefore, it is hypothesized that the E and NS1 mutations interact synergistically, and by adding a mutation in the E gene, the mutations in the NS1 gene were stabilized. Interstingly, however, although the addition of the E_{154S} mutation further attenuated the mouse neuroinvasuveness of the NS1 mutants, there was no further increase in the attenuation of neurovirulence. There is no obvious explanation for this result other than to confirm that neuroinvasiveness and neurovirulence appear to be encoded by different molecular determinants in the WNV genome, and that it is very likely that both phenotypes are multigenic.

Finally, the $E_{154S}/NS1_{130A/175A/207A}$ did not show detectable viraemia at two or three days post-infection in most mice inoculated ip with 10,000 PFU of the virus. Nonetheless, mice inoculated with this dose of virus were protected from subsequent lethal challenge and elicited a high neutralizing antibody response. These data, combined with the fact that no mice succumbed to infection suggests, such a mutant may have potential as a live-attenuated vaccine candidate.

Figure 6-1. Plaque morphology of E/NS1 mutant viruses compared to the parental NY99 strain

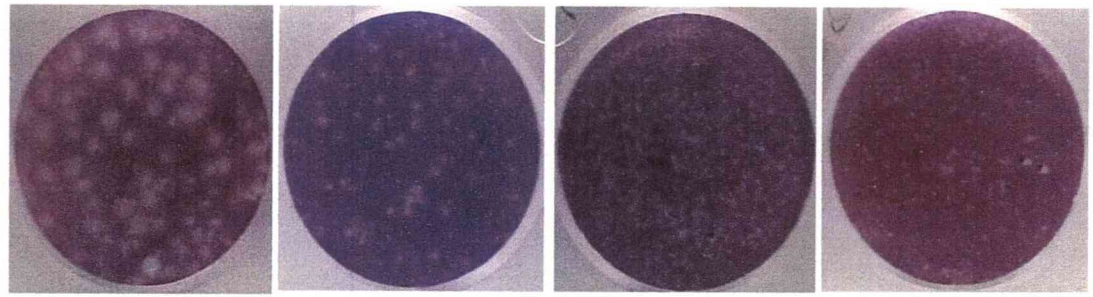

NY99 $E_{154S}/NS1_{130A/175A/207A}$ $E_{154S}/NS1_{130\text{-}131SV/175A/207A}$ $E_{154S}/NS1_{130\text{-}132QQA/175A/207A}$

Table 6-1. Temperature sensitivity of the E/NS1 mutant viruses

	37°C	39.5°C	Δ (37°-39.5°)
	Log_{10}PFU/ml	Log_{10}PFU/ml	Log_{10}PFU
$E_{154S}/NS1_{130A/175A/207A}$	7.4	7.6	-0.2
$E_{154S}/NS1_{130\text{-}131SV/175A/207A}$	6.0	6.3	-0.3
$E_{154S}/NS1_{130\text{-}132QQA/175A/207A}$	4.6	4.0	0.6

Figure 6-2. Overlay of E and NS1 western blots from virus-infected Vero lysates (A) or supernatant (B).

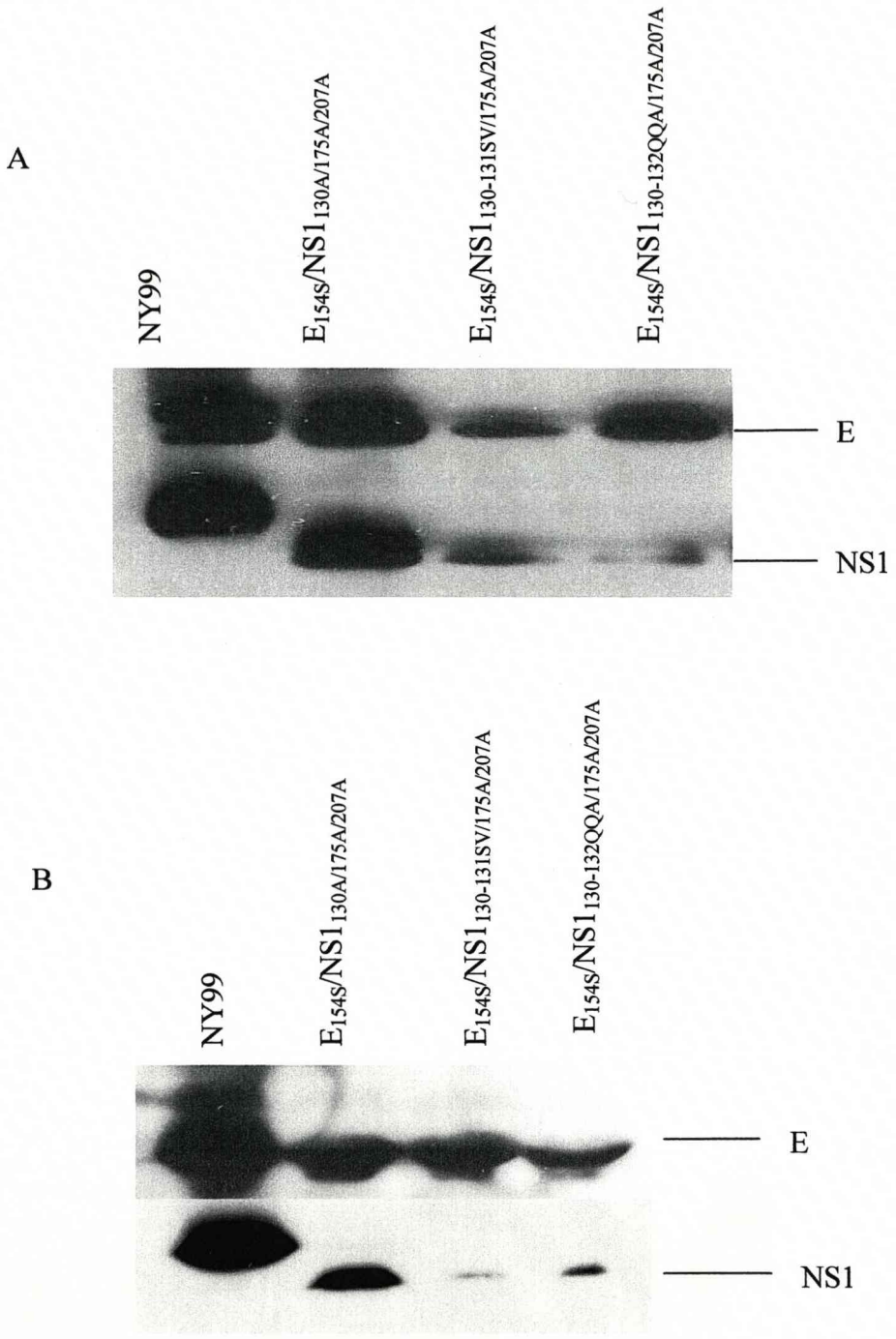

Figure 6-3. Multiplication kinetics of the $E_{154S}/NS1_{130A/175A/207A}$ mutant and parental NY99 viruses in Vero (A) and P388 D1 (B) cells. Each time point represents the mean +/- SD of triplicate samples.

A

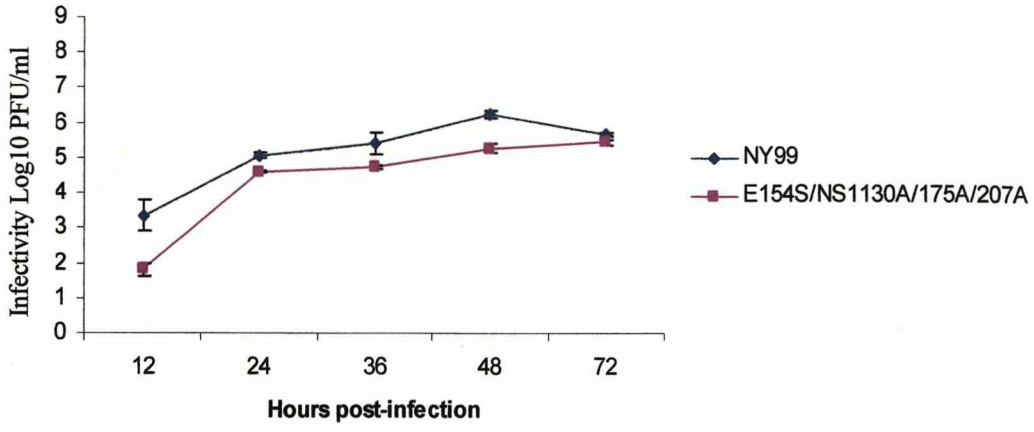

B

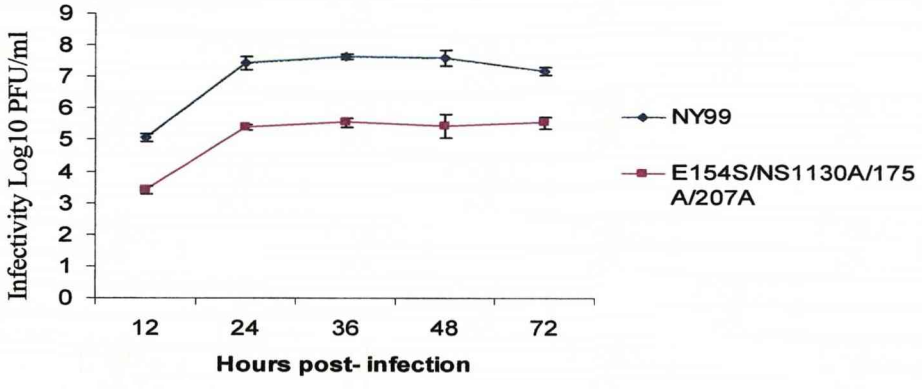

Figure 6-4. Multiplication kinetics of the $E_{154S}/NS1_{130\text{-}131SV/175A/207A}$ mutant and parental NY99 viruses in Vero (A), P388 D1 (B) and Neuro 2A (C) cells. Each time point represents the mean +/- SD of triplicate samples.

A

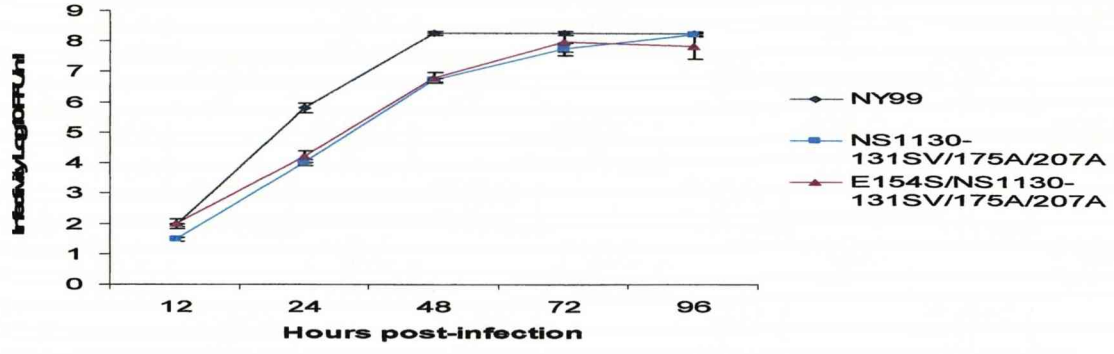

B

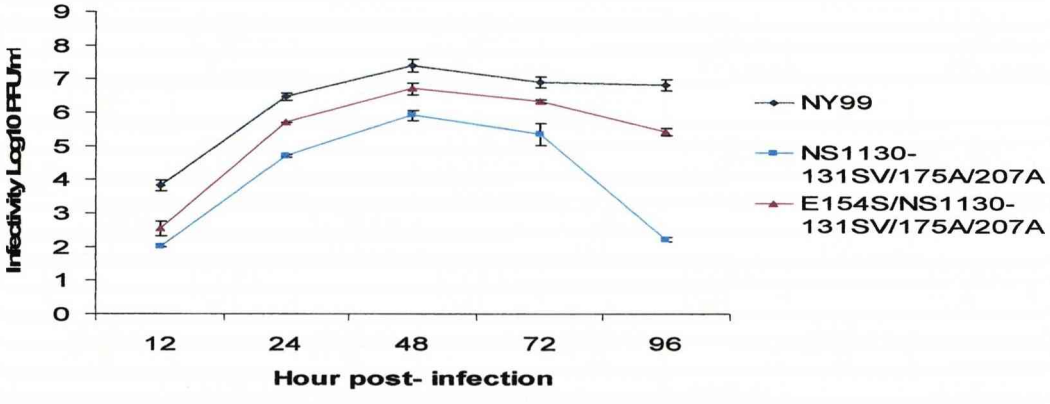

C

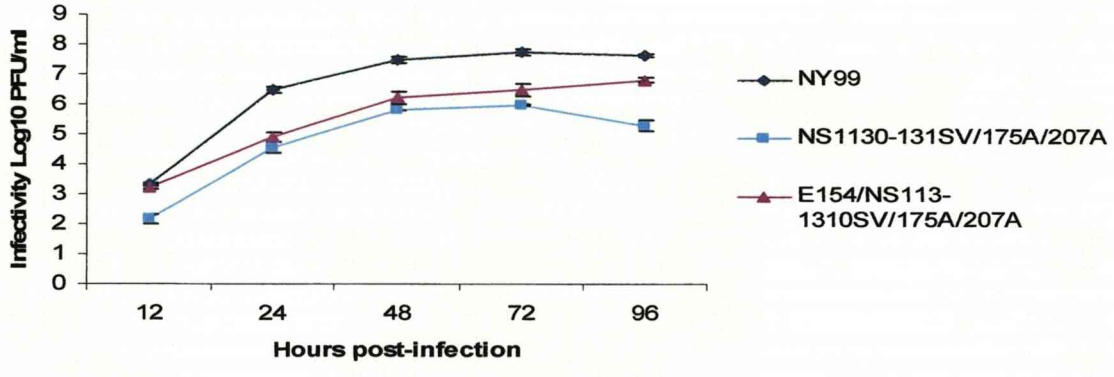

Table 6-2. Mouse neuroinvasiveness (ip) and neurovirulence (ic) of E/NS1 mutant viruses.

Virus	$ipLD_{50}$ (PFU)	AST + SD*	p-value	$icLD_{50}$ (PFU)
NY99	10	8.25 ± 0.5	N/A	10
$NS1_{130A/175A/207A}$	1,000	10.5 + 1.9	<0.05	20
$NS1_{130\text{-}131SV/175A/207A}$	80,000	>21	<0.05	500
$NS1_{130\text{-}132QQA/175A/207A}$	>1,000,000	>21	<0.05	800
$E_{154S}/NS1_{130A/175A/207A}$	>100,000	>21	<0.05	100
$E_{154S}/NS1_{130\text{-}131SV/175A/207A}$	>100,000	>21	<0.05	126
$E_{154S}/NS1_{130\text{-}132QQA/175A/207A}$	>1,000	>21	<0.05	<100

* Average survival time ± standard deviation at a dose of 1,000 PFU

p-value determined by Student's t-test

Table 6- 3. Viraemia at two and three days post-ip infection with either parental NY99, $NS1_{130A/175A/207A}$ or $E_{154S}/NS1_{130A/175A/207A}$ mutant viruses

	NY99 (10 PFU ip)		**$NS1_{130A/175A/207A}$ (100 PFU ip)**		**$E_{154S}/NS1_{130A/175A/207A}$ (1,000 PFU ip)**	
	2dpi (PFU/ml)	3dpi (PFU/ml)	2 dpi (PFU/ml)	3 dpi (PFU/ml)	2dpi (PFU/ml)	3dpi (PFU/ml)
Mouse						
1	<50	15,000*	<50	<50	<50	<50
2	<50	<50	<50	<50*‡	<50	<50
3	2,000	150,000*	<50	<50	<50	<50
4	4,000	50,000*	<50	<50	<50	<50
5	2,500	300,000*	<50	<50	<50	<50

	NY99 (100 PFU ip)		**$NS1_{130A/175A/207A}$ (1,000 PFU ip)**		**$E_{154S}/NS1_{130A/175A/207A}$ (10,000 PFU ip)**	
	2dpi (PFU/ml)	3dpi (PFU/ml)	2 dpi (PFU/ml)	3 dpi (PFU/ml)	2dpi (PFU/ml)	3dpi (PFU/ml)
Mouse						
1	5,000	2,000*	50	<50	<50	100
2	6,500	3,000*	100	100	<50	<50
3	10,000	5,000*	<50	<50	<50	<50
4	4,000	10,000*	50	4,500*‡	<50	50
5	<50	12,500*	400	1,500*‡	<50	<50

* mice that succumbed to infection

‡ Reversion at $NS1_{130}$ seen in viral RNA isolated from the brains

Table 6-4. $PRNT_{50}$ values for the parental NY99 and mutant $E_{154S}/NS1_{130A/175A/207A}$ viruses at an inoculum dose of 1-100,000 PFU. Five of five mice from each E/NS1 virus dose group survived after 21 dayasd and was analyzed, while only two mice given NY99 at an inoculum of 1 PFU survived after 21 days.

	Virus Dose (PFU)					
Mouse #	**1**	**10**	**100**	**1,000**	**10,000**	**100,000**
$E_{154S}/NS1_{130A/175A/207A}$-1	640	640	80	640	1,280	1,280
$E_{154S}/NS1_{130A/175A/207A}$-2	1,280	20	20	320	640	1,280
$E_{154S}/NS1_{130A/175A/207A}$-3	80	80	1,280	640	160	10,240
$E_{154S}/NS1_{130A/175A/207A}$-4	20	20	320	1,280	5,120	1,280
$E_{154S}/NS1_{130A/175A/207A}$-5	20	<20	5,120	2,560	320	5,120
NY99-1	20,480					
NY99-2	80					

CHAPTER 7 : LOSS OF THE PRM GLYCOSYLATION SITE AND A VACCINE CANDIDATE INCLUDING MUTATIONS IN THE PRM, E, NS1 AND NS4B PROTEINS

7.1 Introduction

West Nile virus contains one putative N-linked glycosylation site in the prM protein at asparagine prM_{15}. Other flaviviruses, including JE, SLE, YF, DEN-2, USU and TBE, contain at least one putative glycosylation site in the prM protein (Fig. 7-1). Chapters 3 to 6 described how the ablation of the E and NS1 protein glycosylation sites significantly attenuated WNV. Consequently, it was hypothesized that the loss of the prM glycosylation site would also attenuate WNV.

Although the role of this glycosylation site has not been elucidated, previous studies have investigated changes in the levels of E protein due to the loss of prM glycosylation. These studies, however, involved the use of either virus-like particles (VLP) or subviral particles (SVP), rather than infectious virus (Goto *et al.*, 2005; Hanna *et al.*, 2005). The loss of the prM glycosylation site of a TBE VLP resulted in an increase of intracellular E protein but a decrease in E protein secretion (Goto *et al.*, 2005), whereas the loss of the prM glycosylation site for a WNV SVP resulted in a decrease of E protein secretion (Hanna *et al.*, 2005). A mutation in the glycosylation site of the prM protein as it relates to the phenotype of WNV or any other flavivirus has not been previously characterized. Therefore, this chapter describes the affects of this mutation in terms of multiplication kinetics and mouse virulence phenotypes. The glycosylation site was ablated by changing the asparagine of the glycosylation motif to a serine (prM_{15} N→S). Serine was chosen since it is the naturally occurring mutation for the E glycosylation site for WNV strains.

In terms of vaccine development, to further reduce the potential of reversion to a virulent phenotype, attenuating mutations in more than two genes may prove more advantageous. Therefore, multiple mutations in up to four genes, including the prM, E, NS1 and NS4B, were examined for mouse virulence. Along with the prM_{15S} mutation, attenuating mutations in the E/NS1 mutant virus ($E_{154S}/NS1_{130A/175A/207A}$) that were described in chapter 6 were also included since this virus was replication competent in cell culture, displayed low or no detectable viremia in mice, and elicited a high neutralizing antibody response. The NS4B mutation encompasses a mutation in the central domain of the NS4B protein at $NS4B_{102}$ changing a conserved cysteine to a serine ($NS4B_{102S}$) and has been previously shown to attenuate WNV mouse neurovirulence compared to the parental NY99 strain (Wicker *et al.*, 2006). This NS4B mutation along with the mutations in the prM, E and NS1 were combined to determine mouse virulence phenotype of the mutant virus containing the mutations in all four proteins ($prM_{15S}/E_{154S}/NS1_{130A/175A/207A}/NS4B_{102S}$).

A total of three prM mutant viruses were examined for mouse virulence, including prM_{15S} to determine the affects of this mutation alone, prM_{15S}/E_{154S} to determine the virulence affects of mutations in the two structural protein glycosylation sites, and $prM_{15S}/E_{154S}/NS1_{130A/175A/207A}/NS4B_{102S}$ to determine the attenuation level of a virus containing mutations in four proteins. The prM_{15S} mutant was also examined for multiplication kinetics in cell culture to determine the affects of this mutation alone in terms of infectivity titre compared to the parental NY99 strain.

7.2 Results

7.2.1 Generation of the prM_{15S} mutant virus

As with mutant viruses described in chapters 3 to 6, the prM_{15S} mutant virus was generated by site-directed mutagenesis and transfected into Vero cells. The resulting virus was harvested and passaged once before subsequent experiments were performed. The viral RNA was extracted, RT-PCR was performed and the prM region sequenced for verification of the mutation. Due to the lack of availability of an anti-prM antibody at the time of these studies, the loss of glycosylation could not be monitored by western blotting.

7.2.2 Multiplication of the prM_{15S} mutant in cell culture

Only the prM_{15S} mutant virus was examined in cell culture to determine the multiplication kinetics compared to the parental NY99 strain, since mutations in the prM glycosylation site had not been previously characterized. Both viruses were used to infect either monkey kidney Vero cells or mouse macrophage P388 D1 cells at a moi of 0.1 in triplicate and supernatant was harvested at 12, 24, 48, 72 and 96 hours post-infection. Infectivity titres were determined by plaque titration in Vero cells.

7.2.2.1 Vero cells

Both the prM_{15S} mutant virus and the parental NY99 strain displayed similar multiplication kinetics in Vero cells with a peak infectivity titre at 48 hours post-infection and subsequent decrease. Although the prM_{15S} mutant virus and the parental NY99 strain showed similar infectivity titres at the 48, 72 and 96 hour time points, at the earlier 12 and 24 hour time points, the prM_{15S} mutant virus displayed a

higher infectivity titre, up to 10-fold, compared to the parental NY99 strain (Fig. 7-2A).

7.2.2.2 P388 D1 cells

Since the NS1 glycosylation mutant viruses (see chapters 3 to 5) showed the greatest differences in multiplication kinetics in mouse macrophage P388 D1 cells, this cell line was used to determine differences between the multiplication kinetics of the prM_{15S} mutant virus and the parental NY99 strain. Indeed, greater differences were seen in this cell line than the Vero cells between the mutant and parental viruses. The parental NY99 virus showed a peak infectivity titre at 72 hours post-infection while the prM_{15S} virus did not peak in infectivity titre until 96 hours post-infection. However, the prM_{15S} mutant virus showed up to 100-fold greater infectivity titre at all time points compared to the parental strain (Fig. 7-2B).

7.2.3 Mouse virulence phenotype of the prM_{15S} mutant viruses

Female 3-4 week old outbred NIH Swiss mice were inoculated with the mutant viruses either by the ip route to determine neuroinvasiveness or by the ic route to determine neurovirulence. The parental NY99 strain was used as a control for both the ip and ic route.

7.2.3.1 Mouse virulence phenotype of the prM_{15S} and prM_{15S}/E_{154S} mutant virus

Since previous chapters showed that NS1 glycosylation mutant viruses were more attenuated for neuroinvasiveness than neurovirulence (see chapters 3 to 6) only the neuroinvasive phenotype was initially examined for the prM_{15S} and prM_{15S}/E_{154S} mutant viruses. The prM_{15S} mutant virus displayed an $ipLD_{50}$ value of 5 PFU, which

was similar to the parental NY99 strain with an $ipLD_{50}$ value of 10 PFU. The addition of the E_{154S} mutation (prM_{15S}/E_{154S}), thereby ablating both the structural protein glycosylation sites, resulted in a mutant with an $ipLD_{50}$ value of >1,000 PFU, and was attenuated at least 100-fold compared to the parental NY99 strain (Table 7-1).

7.2.3.2 The addition of the attenuating E, NS1 and NS4B mutations

The prM_{15S} and $prM_{15S}/E_{154S}/NS1_{130A/175A/207A}/NS4B_{102S}$ mutant viruses were examined for mouse virulence and compared to several control viruses including $NS4B_{102S}$, $NS1_{130A/175A/207A}$ and $NS1_{130A/175A/207A}/NS4B_{102S}$ mutant viruses. For the neuroinvasive phenotype, the $NS1_{130A/175A/207A}$ mutant virus has an ipLD50 value of 800 PFU whereas the parental NY99 strain was 5 PFU, while the $NS1_{130A/175A/207A}/NS4B_{102S}$ showed complete attenuation for neuroinvasiveness with an $ipLD_{50}$ value of >10,000 PFU. Since the $NS4B_{102S}$ mutant was highly attenuated for neurovirulence (by the ic route) (Wicker *et al.,* 2006), this virus along with the $NS1_{130A/175A/207A}/NS4B_{102S}$ and $prM_{15S}/E_{154S}/NS1_{130A/175A/207A}/NS4B_{102S}$ mutants were examined for neurovirulence (Table 7-2). The mouse neurovirulence phenotype of the $NS1_{130A/175A/207A}/NS4B_{102S}$ mutant virus was highly attenuated with an $icLD_{50}$ of 2,000 PFU while the $NS4B_{102S}$ virus was also attenuated and had an $icLD_{50}$ of 800 PFU. In comparison, the parental NY99 virus was neurovirulent with an $icLD_{50}$ of 10 PFU. A quadruple gene mutant virus containing the prM, E, NS1 and NS4B mutations ($prM_{15S}/E_{154S}/NS1_{130A/175A/207A}/NS4B_{102S}$) was examined for mouse neurovirulence and the $icLD_{50}$ value for this virus was 30 PFU.

7.3 Discussion

The affects of the loss of prM glycosylation by changing the asparagine of the glycosylation motif to a glutamine have previously been described for West Nile and TBE viruses, however, these studies were limited and utilized either subviral particles or virus-like particles (Goto *et al.,* 2005; Hanna *et al.,* 2005). Both studies showed a decrease in either the secretion of E protein or the subviral particle, but one study found an increase in the amount of intracellular E protein. Mutations in the prM glycosylation site have not been previously described for infectious virus.

Unfortunately, there were no WNV anti-prM antibodies available at the time of these studies and therefore, the loss of glycosylation could not be monitored by western blotting. However, western blots in chapter 3 to 6 showed that the loss of E and NS1 glycosylation was achieved by mutating the asparagine in the glycosylation motif to either an alanine, glutamine or serine. There was, however, indirect evidence of an amino acid change by altered phenotype of the prM_{15S} mutant in terms of increased multiplication kinetics in cell culture, as determined by infectivity titre, compared to the parental NY99 strain (Figure 7-2). This was unexpected since previous studies showed that the loss of the glycosylation site(s) for the E and the NS1 proteins decreased the multiplication kinetics compared to parental NY99 virus (see chapters 3 to 6). Clearly, further studies are warranted to investigate this result.

A potential explanation for this result may involve an increase in the ability of the virus to attach and infect cells. The glycosylation residues for both the structural proteins (prM and E) of WNV have been shown to affect cellular tropism by increasing the susceptibility of cells to infection through the binding of the C-type

lectin attachment factor dendritic cell specific intercellular adhesion molecule 3-grabbing nonintegrin (DC-SIGN or DC-SIGNR) (Davis *et al.,* 2006). All SIGN members contain carbohydrate recognition domains (CRDs) that have been shown to bind glycosylation residues present on the surface of pathogens (Koppel *et al.,* 2005). Specifically, DC-SIGN has been shown to be a HIV-1 receptor able to capture and disseminate HIV-1 to enhance infection through the binding of the envelope glycoprotein gp120 (Getjtenbeek *et al.,* 2002). In fact, DC-SIGN and DC-SIGNR have been shown to increase infectivity *in vitro* for several viruses including Ebola, Marburg, dengue, hepatitis C, Sindbis, SARS-CoV and human cytomegalovirus (Alvarez *et al.*, 2002; Halary *et al.*, 2002; Jeffers *et al.*, 2004; Klimstra *et al.,* 2003,;Lozach *et al.,* 2004; Navarro-Sanchez *et al.,* 2003; Tassaneetrithep *et al.,* 2003). One study comparing the cellular attachment and infection rates of WNV found the N-linked glycan on the prM alone could enhance WNV infection through DC-SIGNR attachment (Davis *et al.,* 2006). Since the ability of the E glycosylation site alone to increase infection through the attachment to DC-SIGNR or DC-SIGN was not undertaken, it is unclear how the absence of the prM glycosylation residue would affect the binding of these attachment factors. Although prM is cleaved before release of the mature virus, it has been shown that significant levels of prM are associated with the infectious virus (Guirakhoo *et al.,* 1991; Keelapang *et al.,* 2004; Wengler and Wengler, 1989). One hypothesis for the increase in infectivity titre seen by the prM_{15S} mutant is that the ablation of the prM glycosylation site allowed for the increased efficiency of the E glycan binding resulting in the higher infectivity titre seen in the P388 D1 and to a lesser extent Vero cells.

Previous studies have investigated mutations in the prM at prM_{63} for TBE virus, the prM/E cleavage site for TBE virus and the C-prM signal sequence for YF virus and the affects of these mutations in cell culture and for mouse neurovirulence (Yoshii *et al.,* 2004; Elshuber *et al.,* 2003; Lee *et al.,* 2000). Overall, these studies found a reduction in infectious particles, lack of infectious particles or attenuation for mouse neurovirulence. To date, published data regarding the function of the prM protein utilizing prM mutants showed that the prM is necessary for entry, assembly and maturation of the virus and mutations in various portions of the prM protein negatively affect these functions. The mutation in the prM glycosylation site (prM_{15S}) could affect one or more of these functions, including increasing exposure of the fusion peptide. It is known that the prM masks the E protein fusion peptide (Zhang *et al.,* 2003) and therefore, it is important to consider differences for the various prM functions for future studies. In fact, one study found that a mutation in the M protein increased infectivity titre in cell culture, but not neurovirulence in mice (Maier *et al.,* 2007). This mutant virus was not inactivated at pH levels higher than those that would inactivate the parental virus suggesting enhanced replication was the result of increased fusion and uncoating. Since the prM protein may also involve in this process, fusion assays may provide useful information in understanding the affects of mutations in the prM.

The ablation of the prM glycosylation site alone did not attenuate mouse virulence and the LD_{50} was similar to the parental NY99 strain. The addition of the E_{154S} mutation (prM_{15S}/E_{154S}) resulted in a virus that was attenuated >100-fold for mouse neuroinvasiveness compared to the parental NY99 strain. These results suggest that, contrary to the results in cell culture (Fig. 7-2), the prM_{15S} mutation may not

significantly increase infectivity *in vivo*. Interestingly, the mutant containing the prM_{15S} mutation along with other established attenuating mutations in the E, NS1 and NS4B proteins ($prM_{15S}/E_{154S}/NS1_{130A/175A/207A}/NS4B_{102S}$) was not attenuated for mouse virulence suggesting that these mutations do not act synergistically. Since the NS1/NS4B ($NS1_{130A/175A/207A}/NS4B_{102S}$) mutant virus was highly attenuated for neurovirulence (Table 7- 2), it was surprising that the addition of the prM_{15S}/E_{154S} mutations resulted in the $prM_{15S}/E_{154S}/NS1_{130A/175A/207A}/NS4B_{102S}$ mutant that was not highly attenuated. Since these mice were inoculated by the ic route, brains were not collected for sequence analysis. Further analyses of these viruses, including ip inoculations and sequencing of viral RNA in the brains of mice that succumbed to infection, may prove that a combination of these mutations result in instability of the virus. Also, the loss of glycosylation of all three (prM, E and NS1) proteins may have contributed to the loss of attenuation when all four prM, E, NS1 and NS4B mutations were combined, suggesting that one or more glycosylation sites were necessary for overall stability. Previously, in chapter 3, it was shown that mutations in the E protein were found in the triple NS1 glycosylation mutant virus collected from mouse brains, but not in cell culture. This suggests selective pressure of these mutations in mice and a possible interaction between the E and NS1 proteins. It is, therefore, feasible that a functioning glycosylation site on at least one protein is necessary and the loss of all three protein glycosylation residues is not well tolerated in mice. Further experiments examining the affects of these mutations in greater detail may answer the question of how these prM mutants affect entry in to cells, assembly and release of virus from cells.

Overall, these data showed that the prM_{15S} mutation increased the efficiency of multiplication in cell culture and did not attenuate the mouse virulence phenotype of WNV. In lieu of these results, it was determined that the prM_{15S} mutation would not be advantageous to include as an attenuating mutation for a WNV vaccine candidate.

Figure 7-1. Amino acid alignment of the prM gene for several flaviviruses. Underlined amino acids indicate putative glycosylation site. Highlighted amino acids are identical for all viruses; blue and green indicate conservative and weakly similar residues, respectively.

Figure 7-2. Multiplication kinetics in Vero (A) and P388 D1 (B) for the prM_{15S} mutant virus and the parental NY99 strain. Each time point represents the mean +/- SD of triplicate samples.

A

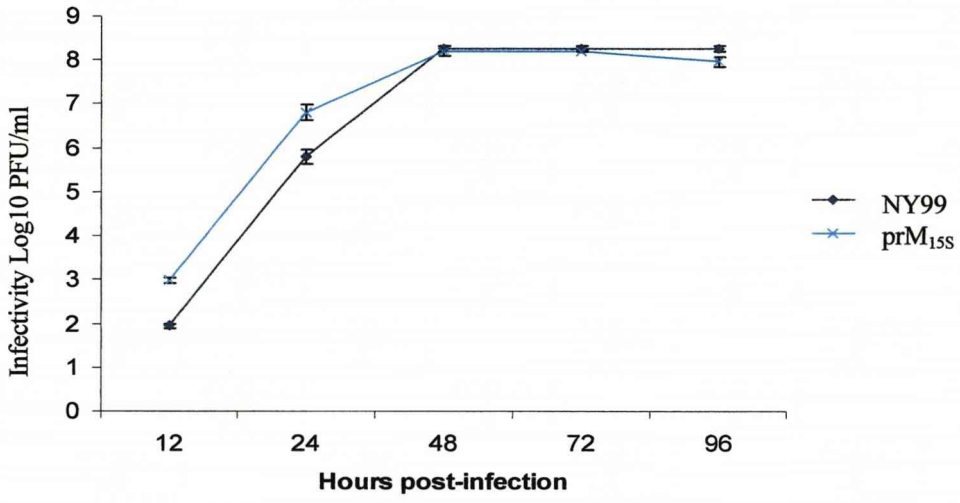

B

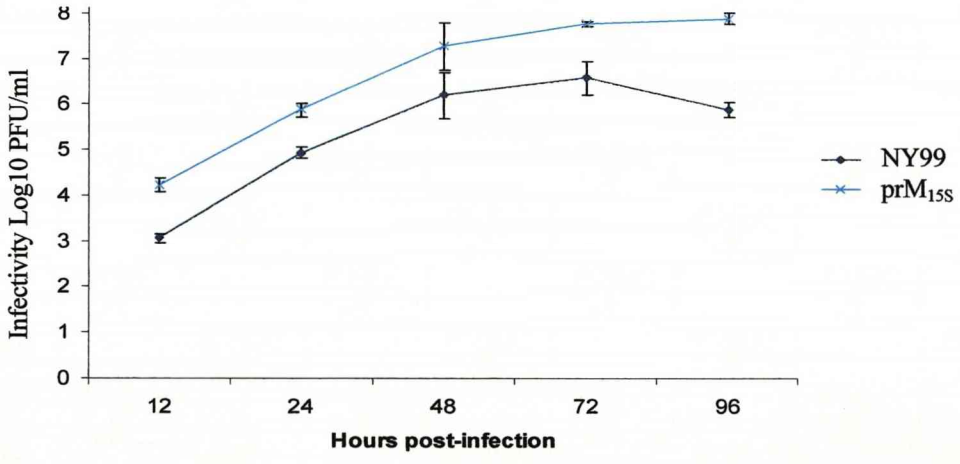

Table 7-1. Mouse virulence of the prM_{15S} mutant viruses

Virus	$ipLD_{50}$ (PFU)	AST + SD*	P-value†
NY99	10	9.2 ± 1.1	N/A
prM_{15S}	5	8.0 ± 0.8	>0.05
prM/E_{154S}	>1,000	>21	<0.05

* AST= average survival time ± standard deviation of mice inoculated with 1,000 PFU of virus
† p-value determined by Student's t-test
N/A= not applicable

Table 7-2. Mouse virulence of the viruses containing mutations in prM, E, NS1, and/or NS4B.

	ipLD50 (PFU)	AST + SD*	p-value†	icLD50 (PFU)
NY99	5	7.5 ± 0.6	N/A	10
$NS4B_{102S}$	nd	N/A	N/A	800
$NS1_{130A/175A/207A}$	800	9.0 ± 1.0	<0.05	nd
$NS1_{130A/175A/207A}$+$NS4B_{102S}$	10,000	>21	<0.05	2,000
$prM_{15S}/E_{154S}/NS1_{130A/175A/207A}$/ $NS4B_{102S}$	nd	N/A	N/A	30

nd= not determined

* AST= average survival time ± standard deviation of mice inoculated with 1,000 PFU of virus

† p-value determined by Student's t-test

N/A= not applicable

CHAPTER 8 : IN VITRO CELLULAR LOCALIZATION OF THE E AND NS1 PROTEINS AND ULTRASTRUCTURAL ANALYSIS OF THE PARENTAL NY99 AND ATTENUATED GLYCOSYLATION MUTANT VIRUS-INFECTED VERO CELLS

8.1 Introduction

Previous chapters discussed mutations within the glycosylation motifs of the NS1 protein that proved to be highly attenuated for mouse neuroinvasiveness and neurovirulence while maintaining replication competence in cell culture (see chapters 3 to 6). Many of these mutant viruses also showed attenuation markers in cell culture, such as reduced infectivity titer compared to the parental strain as well as small plaque phenotype. Also, a decrease in the level of secreted NS1 was shown by western blotting independent of E protein levels indicating the reduction in NS1 was not the result of reduced viral multiplication.

In an effort to better understand the affects of these mutations in cell culture, confocal microscopy and electron microscopy (EM) were used to visualize the localization of the E and NS1 proteins in the mutant virus-infected cells compared to the parental NY99 virus-infected cells. Colocalization of the E and NS1 proteins has been shown for MVE, KUN, JE, WN and KOK virus-infected cells by indirect immunofluorescence (Blitvich *et al.,* 1995; Mackenzie *et al.,* 1996; Westaway *et al.,* 1997). The colocalization of the E and NS1 proteins has not been previously studied by EM of virus-infected cells for any flavivirus and therefore, the colocalization of the E and NS1 proteins in WNV-infected Vero cells were visualized by transmission immuno-EM (TIEM). Furthermore, transmission EM (TEM) was also utilized for the ultrastructural analysis of the parental NY99 and attenuated $NS1_{130\text{-}132QQA/175A/207A}$ mutant virus-infected Vero cells. The $NS1_{130\text{-}132QQA/175A/207A}$ mutant virus was used since it showed the greatest attenuation for mouse neuroinvasiveness and neurovirulence of all the NS1 mutant viruses as well as having a small plaque

phenotype, and decreased infectivity titre and decreased levels of secreted NS1 protein in cell culture (see chapter 5). It was hypothesized that mutations in the NS1 glycosylation sites would alter the intracellular localization of either NS1 or E, or both proteins. In addition, it was hypothesized that comparison of the ultrastructure by TEM of parental and mutant virus-infected cells would provide further insight to the affects of the NS1 glycosylation mutations in cell culture.

8.2 Results

8.2.1 Confocal microscopy

Coverslips containing a confluent monolayer of Vero cells were infected at an moi of 0.1 with either $NS1_{130\text{-}132QQA/175A/207A}$ mutant or parental NY99 strain. At forty-eight hours post-infection the cells were fixed in a 50:50 acetone:methanol mixture, then air dried before subsequent staining. Published studies indicated that the NS1 protein colocalized with the E protein in virus-infected for several flaviruses (Blitvich *et al.*, 1995; Mackenzie *et al.,* 1996). Therefore, in an effort to better understand the mechanism of attenuation for the highly mouse attenuated NS1 glycosylation mutants; both the E and NS1 proteins were utilized to visualize the staining pattern of these two proteins for several mutant viruses. The coverslips were double-stained using mouse anti-NS1 (17NS1) monoclonal antibody and rabbit polyclonal anti-E protein domain III antiserum. Secondary anti-mouse Fluorescein (FITC) and anti-rabbit Texas Red labeled antibodies were utilized to visualize the staining pattern of each of the two proteins and the merged view to determine colocalization by confocal microscopy. Mock-infected cells were stained and appeared similar to the virus-infected cells with

very little background or nonspecific staining with either anti-E or -NS1 antibodies (Fig. 8-1).

8.2.1.1 Localization of the E and NS1 proteins for mutant and parental NY99 viruses

Similar to previous studies, the E and NS1 proteins colocalized in NY99 virus-infected Vero cells. Although these previous studies found colocalization of the E and NS1 proteins in cell culture, discrepancies in the localization of these two proteins in limited areas of the cell were noted (Blitvich *et al.,* 1995; Mackenzie *et al.,* 1996; Westaway and Goodman, 1987). Some examples of apparent lack of colocalization were also seen in this study, however, it is important to note that two different antibodies were utilized and the dilutions of these antibodies differed somewhat. Therefore, these areas can only be concluded as having differing amounts of E and NS1 protein. Overall, increased intensity of the E protein fluorescence did correlate to increased intensity of the NS1 fluorescence. Both proteins illustrated diffuse cytoplasmic staining with areas of intense fluorescence in a circularized, vesicle-like, staining pattern (Fig.8-1).

The E_{154S} mutant was used as it was previously determined to have decreased infectivity titre compared to the parental NY99 strain (Beasley *et al.,* 2005) and, therefore, was used to visualize differences in the E and NS1 proteins staining pattern for a mutant virus without changes in the NS1 protein. Interestingly, the antibody staining pattern was very similar to the parental NY99 strain, having no obvious differences and showed diffuse cytoplasmic staining of both E and NS1 proteins as

well as vesicle-like staining. Again, the E and NS1 proteins displayed overall colocalization (Fig. 8-1).

The $NS1_{130\text{-}132QQA/175A/207A}$ mutant virus showed major differences in the staining pattern of both the E and NS1 proteins compared to the parental NY99 stain. The parental NY99 strain had diffuse cytoplasmic staining, while the $NS1_{130\text{-}132QQA/175A/207A}$ mutant showed less intense vesicle-like NS1 protein staining in the absence of diffuse staining. Although areas of intense E protein staining correlated to intense NS1 protein staining in many areas, there were also significant numbers of areas of NS1 protein fluorescence without apparent E protein fluorescence (Fig. 8-1).

The attenuated $E_{154S}/NS1_{130A/175A/207A}$ mutant showed a pattern of E protein fluorescence with diffuse cytoplasmic staining, which was more similar to the parental NY99 strain and E_{154S} mutant virus than the $NS1_{130\text{-}132QQA/175A/207A}$ mutant virus. The most notable difference was the reduced fluorescence of the NS1 protein compared to the parental NY99 strain, even though cells had been infected at the same moi with both viruses (Fig. 8-1).

Since flaviviruses have been previously shown to associate with the endoplasmic reticulum (ER), virus-infected Vero cells were probed with a mouse anti-ER polyclonal antibody and visualized with a FITC conjugated antibody. Since this anti-ER antibody was only available as a mouse antibody, dual staining with the mouse derived NS1 antibody was not possible. The confocal microscopy images for the mock-infected cells showed a diffuse staining pattern indicating ER was located throughout the cell. The NY99 virus-infected cells showed many areas of circularized vesicle-like staining pattern as did the mutant $NS1_{130\text{-}132QQA/175A/207A}$ virus-infected

cells, albeit to a lesser extent, suggesting that WNV infection induced large ER vesicle formations (Fig. 8-2).

8.2.2 Electron microscopy

Since the confocal studies with the $NS1_{130\text{-}132QQA/175A/207A}$ mutant virus-infected cells showed the greatest reduction in intracellular E and NS1 proteins, this mutant virus was used to study the ultrastructural differences of mutant virus-infected cells compared to the parental NY99 strain virus-infected cells using electron microscopy. Vero cells were infected at a moi of 0.1 with one of the two viruses and cells were fixed at 48 hours post-infection before subsequent staining for EM studies. Both the attenuated and parental strains were prepared for both TEM and TIEM staining (see Materials and Methods 2.10). Immuno-staining utilized the same primary antibodies used in the confocal study, namely a rabbit anti-E protein domain III and a mouse anti-NS1 (17NS1) monoclonal antibody with secondary gold-labeled antibodies. Mock-infected Vero cells were prepared in parallel as a control to determine the ultrastructure of uninfected cells and as a background control for the TIEM experiment.

8.2.2.1 Transmission EM

Transmission EM involved the procedures of fixing, staining and embedding virus-infected and mock-infected cells before thin sections of the embedded cells were observed under high voltage and high magnification. This technique allowed for the visualization of individual compartments within the cell in detail as well as virus particles by contrast staining lipids within the cell.

Compared to the mock-infected Vero cells, the NY99 virus-infected cells showed differences in the ultrastructure within the cell characteristic of previously described flavivirus infection-induced changes including swollen endoplasmic reticulum (ER), vesicle packets (VP), smooth membrane structures (SMS), pararystalline arrays (PC) and convoluted membranes (CM) (Leary and Blair 1980; Hase *et al.*, 1987; Chu and Westaway 1992; Westaway *et al.*, 1997) (Fig 8-3). The parental NY99 virus-infected cells showed that the CMs were commonly found in close proximity to the nucleus and SMS were heavily associated around these CM structures. The small spherical shaped SMS were approximately 45-80 nm in diameter and although virus was not found within these SMS, vesicle packets (VP) containing SMS did contain virus.

Paracrystalline arrays (PC) are hexagon shaped CM-like structures, sometimes indistinguishable from CM and it has been suggested that the PC dissociates into CM late in KUN virus infection of Vero cells (Ng and Hong, 1989). The SMS were found with or without the presence of CM or PC, and differed in location in the presence or absence of the CM. The CM and PC appeared to change quite drastically in size as well as the amount of SMS associated with these structures depending on the cell. The virus induced ultrastructural changes differed from cell to cell, from cells that contained no CM or PC and generalized SMS throughout the cell, to cells with well defined CM with localized SMS near the CM. Also, some cells displayed small CM with associated PC, while others displayed multiple CM foci (Fig. 8-4).

The $NS1_{130\text{-}132QQA/175A/207A}$ mutant virus-infected cell ultrastructure was somewhat different than that of the parental NY99 virus-infected cells. First, many cells did not contain CM structures whereas these structures were found in almost every NY99 virus-infected cell. Interestingly, the SMS were frequently more abundant than the

CM structures and in fact, SMS were commonly found without the presence of CM yet virus particles in these cells were also common (Fig. 8-5). Another major difference from the NY99 virus-infected cells was the size and shape of the SMS, which varied from small round to larger tubular shape of about 20-150 nm in diameter (Fig. 8-6).

8.2.2.2 Immuno-EM

Transmission EM and TIEM differ in that TIEM involved probing with antibodies after the cells were embedded and thin sections were prepared. Gold particles were used at either 10 nm or 5 nm for the anti-mouse NS1 antibody and 15 or 5nm for the anti-rabbit E antibody. Different sized gold particles were used because the larger gold particles were easier to identify than the 5 nm particles within heavier stained areas of the cell. This technique is very different from confocal microscopy, including the use of thin sections of the cell, the ability to use higher magnification and the ability to visualize individual compartments in detail through contrast staining lipids with in the cell. Mock-infected cells were prepared in parallel to the virus-infected cells and showed minimal background staining with the anti-E and -NS1 antibodies (Fig. 8-7).

In cells infected with NY99 virus, the localization of the E protein by staining with anti-E 15 nm gold particles was determined to be throughout the cell, within vesicles, associated with virus and within the CM. The mutant $NS1_{130\text{-}132QQA/175A/207A}$ virus-infected cells showed a similar staining pattern (Fig. 8-8). An example of a tubular proliferated membrane (TPM) was also observed in the $NS1_{130\text{-}132QQA/175A/207A}$ mutant-infected cells. This structure has been previously characterized as an ER proliferated

membrane structure and was identified in WNV-infected mosquito cells at early time points (Girard *et al.*, 2005) (Fig. 8-8). Colocalization using the 5 nm anti- mouse gold particle (NS1 protein) was difficult to identify in these cells due to the difference in particle size.

In cells stained with anti-NS1 10 nm gold particles, the localization of the NS1 and E protein were more easily identified. The NY99 virus-infected cells showed NS1 protein within vesicles and throughout the cell. The NS1 protein was also found associated with virus particles and often colocalized with the E protein. Not surprisingly, much less NS1 was found in the $NS1_{130\text{-}132QQA/175A/207A}$ mutant infected cells. Nonetheless, the E and NS1 proteins appeared to colocalize within vesicles and in cells (Fig. 8-9). Interestingly, the NS1 protein often localized around the CM but not within the CM.

8.3 Discussion

Previous chapters focused on the affects of mutations in the NS1 glycosylation site(s) in cell culture and in mice. Many mutant viruses proved to be highly attenuated for neuroinvasiveness and neurovirulence, showed decreased infectivity titre and sp phenotype, although the mechanism of these affects was not clear (see chapters 3-6).

Although several of these viruses showed reduced levels of secreted NS1 compared to the parental NY99 strain, the decreased levels of NS1 protein were not consistently related with a reduction in virus infectivity as determined by plaque assay. This was evident by western blotting where the E protein levels of the NS1 mutants were comparable to the NY99 virus-infected cells although levels of NS1 protein were decreased compared to the parental NY99 strain (see chapters 4 to 6). Confocal

images confirmed this result. The E_{154S}/$NS1_{130A/175A/207A}$ mutant virus-infected cells showed intense diffuse cytoplasmic staining of the E protein but reduced, focal staining of the NS1 protein, while the E_{154S} virus-infected cells showed cytoplasmic staining of E and NS1 proteins similar to the parental NY99 strain, although both of these viruses previously showed a reduction in infectivity titre compared to the parental NY99 strain. These results suggest that a reduction in the NS1 protein was independent of the reduction in multiplication. It was previously shown (Mackenzie *et al.,* 1996; Westaway and Goodman 1987) that the E and NS1 proteins did not exclusively overlap, however, close inspection of the confocal and TIEM images in this study showed E protein was commonly found with NS1 protein in vesicles and with the virus. Interestingly, intense staining of the NS1 protein also correlated with more intense E protein staining even in the mutant-infected cells, indicative of colocalization.

In an effort to better understand and compare the differences between the parental NY99 strain and mutant infection in cell culture, TEM and TIEM were utilized and identified many differences in the structures and E and NS1 protein localization within cells infected with these viruses. Transmission EM of both the parental NY99 and $NS1_{130\text{-}132QQA/175A/207A}$ virus-infected cells showed the presence of a CM was not always present in virus-infected cells since SMS and virus particles were seen without a CM structure. It has been suggested that the CM is made up of ER (Mackenzie *et al.,* 1999). Since the SMS were often contained within ribosome studded vesicles, it is possible that the CM is made from the dissociation of the SMS containing vesicles. It is speculated that virus-infected cells without CM are at different stages of viral replication and the CM structure have not yet formed. The CMs have been proposed

as the proteolytic process site due to the colocalization of the protease NS3 and cofactor NS2B proteins (Mackenzie *et al.*, 1997). Interestingly, the E protein (but not the NS1 protein) was found associated with the CM structures indicating a wider use of these structures. Smooth membrane structures (SMS) in the absence of CMs were generally found throughout the cell whereas SMS in cells with CMs were generally found in close proximity to the nucleus, indicating a necessity of the CM to be in close proximity to the nucleus. Most cells infected with the NY99 strain showed evidence of viral infection due to a change in the ultrastructure whereas these differences were not as easily found for the $NS1_{130\text{-}132QQA/175A/207A}$ virus-infected cells. For example, there was little CM in the mutant $NS1_{130\text{-}132QQA/175A/207A}$ infected cells compared to the parental NY99 virus-infected cells. Also TPM was found in the mutant $NS1_{130\text{-}132QQA/175A/207A}$ virus-infected cells, which has been previously described for early WNV-infected mosquito cells (Girard *et al.*, 2005). From these data, it is hypothesized that the SMS are formed early in infection, relocate in close proximity to the nucleus where CM are subsequently formed. A larger experiment, including a time-course experiment with these viruses may give more insight into this hypothesis.

Besides the apparent decrease in observed CM structures, the most striking difference between the ultrastructure of the parental NY99 and $NS1_{130\text{-}132QQA/175A/207A}$ viruses in infected Vero cells was the size and shape of the SMS. The SMS in the mutant $NS1_{130\text{-}132QQA/175A/207}$ virus-infected cells differed from small spherical shape to larger tubular shape whereas the parental NY99-infected cells showed only spherical shaped SMS. Interestingly, tubular shaped SMS have been previously described for WNV-infected mosquito cells (Girard *et al.*, 2005). Mosquito cells modify N-linked glycosylation residues different from mammalian cells as mosquito cells lack the

enzymes required for the addition of complex carbohydrates (Jarvis and Finn 1996). The $NS1_{130}$ for DEN-2 and MVE viruses and $NS1_{175}$ for MVE virus glycosylation sites have been shown to contain complex carbohydrate residues while the $NS1_{207}$ site for DEN-2 virus was demonstrated as having high mannose type carbohydrate (Pryor and Wright, 1994; Blitvich *et al.,* 2001). Therefore, it is hypothesized that the discrepancy in the shape of the SMS was the result of the loss of NS1 glycosylation. Studies need to be undertaken in a second cell line to confirm the differences obtained in virus-infected monkey kidney Vero cells.

These data suggest that the NS1 protein is involved in SMS structure or formation; however, differences in the SMS were not the only dissimilarities between the parental NY99 and $NS1_{130\text{-}132QQA/175A/207A}$ mutant virus-infected cells. Many $NS1_{130\text{-}132QQA/175A/207A}$ virus-infected cells did not contain CMs but showed evidence of infection having SMS and virus. It is hypothesized that NS1 also directs the SMS towards the nucleus for subsequent function of CM/PC required for the viral replication cycle, consequently, reduced multiplication may be the result if this defect. Although only mutations in the glycosylation sites caused these results, it is possible that glycosylation residues function in many ways. In fact, N-linked chains related to glycoproteins have been shown to affect protein folding, secretion rate, intracellular trafficking, cell surface expression, intracellular stability, enzyme or cytokine activity, receptor signal transduction, susceptibility to protease or denaturants, recognition by antibodies and targeting to specific cell types (Varki, 1999). Since the NS1 protein is not expressed on the surface of the virion, some of these functions would be unlikely, such as cell surface expression or receptor signal transduction. However, the NS1 is a secreted protein and therefore many of these putative functions for the carbohydrate

residues associated with proteins cannot be dismissed. The NS1 glycosylation mutants displayed a decrease in intracellular and extracellular NS1 by confocal and western blot (see chapters 4 to 6), respectively, and well-defined rather than diffuse localization compared to the parental NY99 strain. Since nonglycosylated NS1 was still secreted from the cells, it is likely that the reduction in the secreted NS1 was a direct result of the reduction in intracellular NS1. Therefore, it is hypothesized that the NS1 protein for the nonglycosylated NS1 mutant viruses may be more susceptible to denaturation, accounting for the reduction of this protein, which directly affects the function of the protein proposed to be vesicle transport of the SMS to the nucleus where CM (which are necessary in the replication cycle) are formed .

Figure 8-1. Localization of the E and NS1 proteins by confocal microscopy in mock- (A) and WNV-infected (B-E) Vero cells. The E protein was identified by red (Texas Red) fluorescence and the NS1 protein by green (FITC) fluorescence. Both NY99- (B) and mutant E_{154S}- (C), $NS1_{130\text{-}132QQA/175A/207A}$- (D) and $E_{154S}/NS1_{130A/175A/207A}$- (E) infected Vero cells displayed a high degree of colocalization indicated by the overlap of the E and NS1 protein stains.

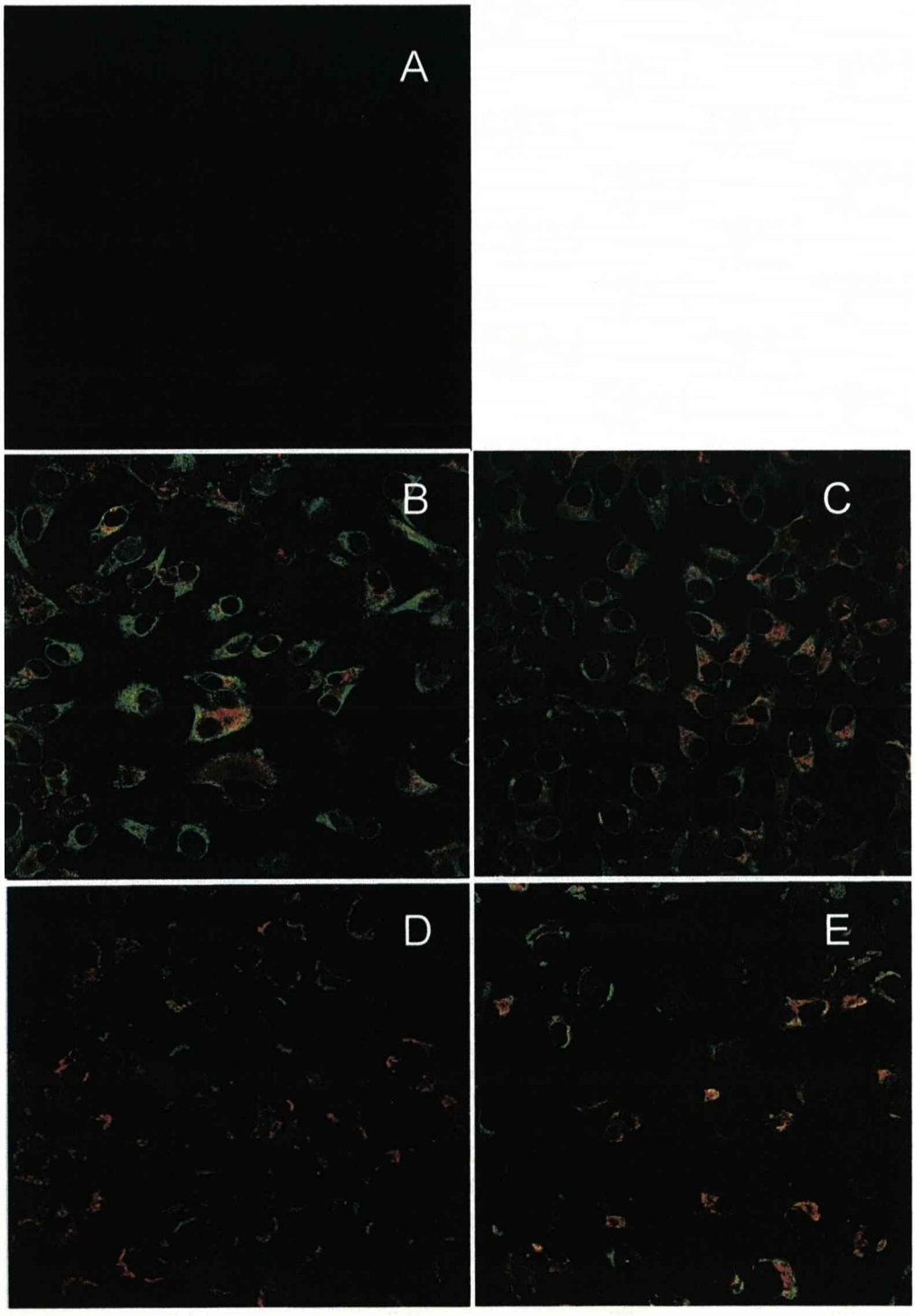

Figure 8-2. Localization of the ER by confocal microscopy in mock- versus WNV- infected Vero cells. White arrows illustrate areas of vesicle-like staining.

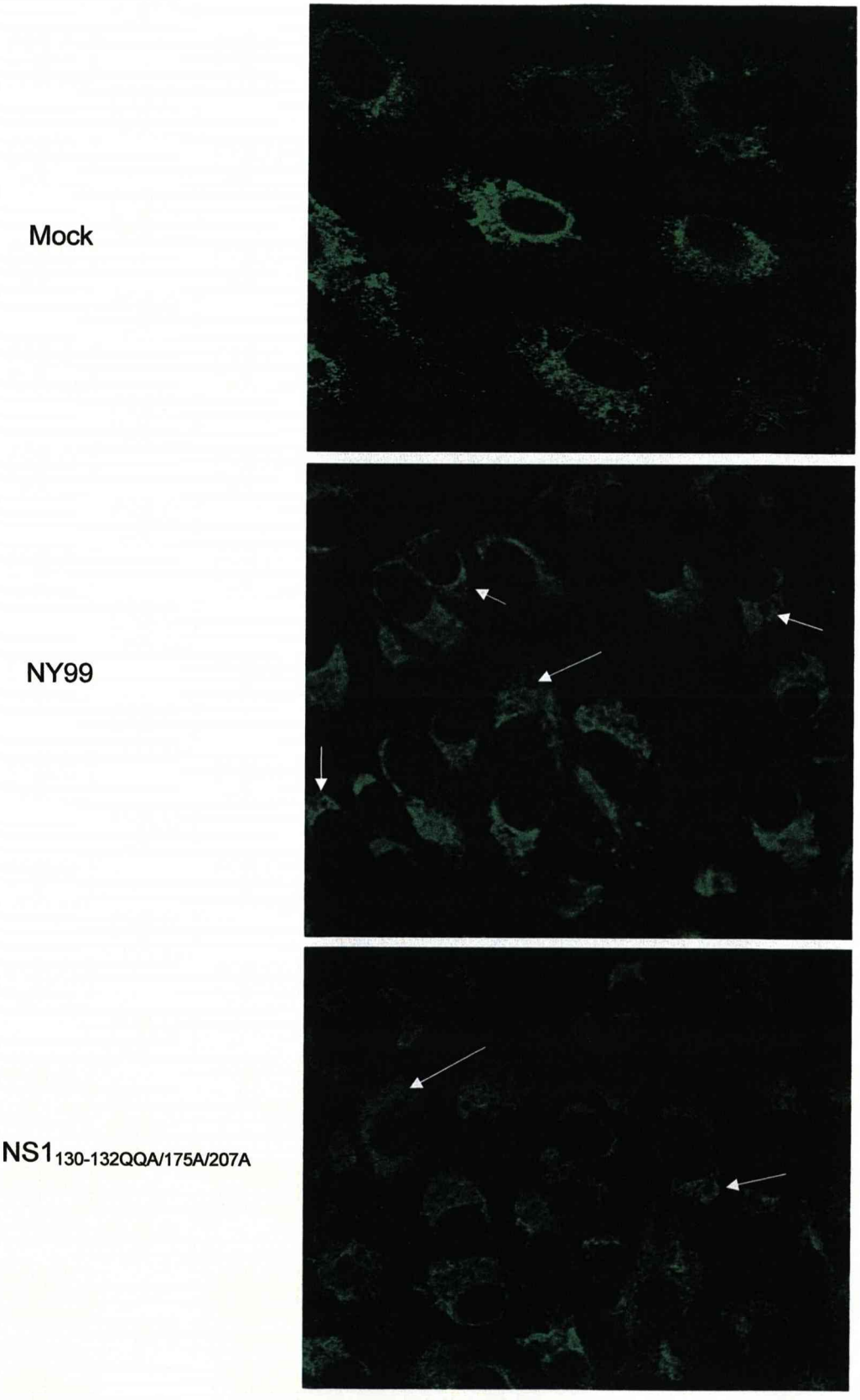

Figure 8-3. TEM ultrastructural comparison of mock- and NY99-infected Vero cells. Virus-infected cells show swollen mitochondria (Mi), smooth membrane structures (SMS), paracrystalline arrays (PC) and convoluted membranes (CM). Scale bar 500 nm for mock- and NY99-infected cells.

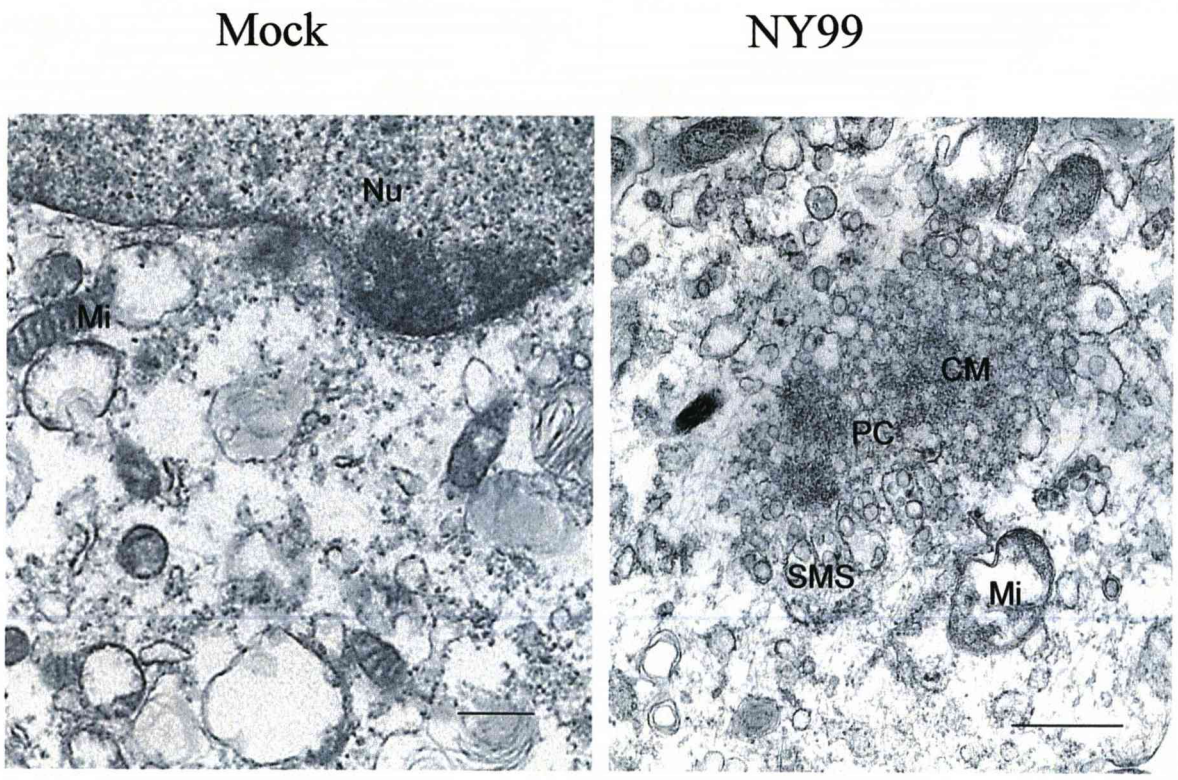

Figure 8-4. Ultrastructure differences in NY99-infected Vero cells may indicate a progression in stages of infection. TEM images of the parental NY99-infected Vero cells depicting differences in the location and arrangement of virus-induced structures cell to cell showing no apparent CM with diffuse SMS structures (A), PC and CM localized to the nucleus (B), More defined CM with SMS located between two CM foci (C) and well defined large CM structure with localized SMS (D). Scale bar 500 nm.

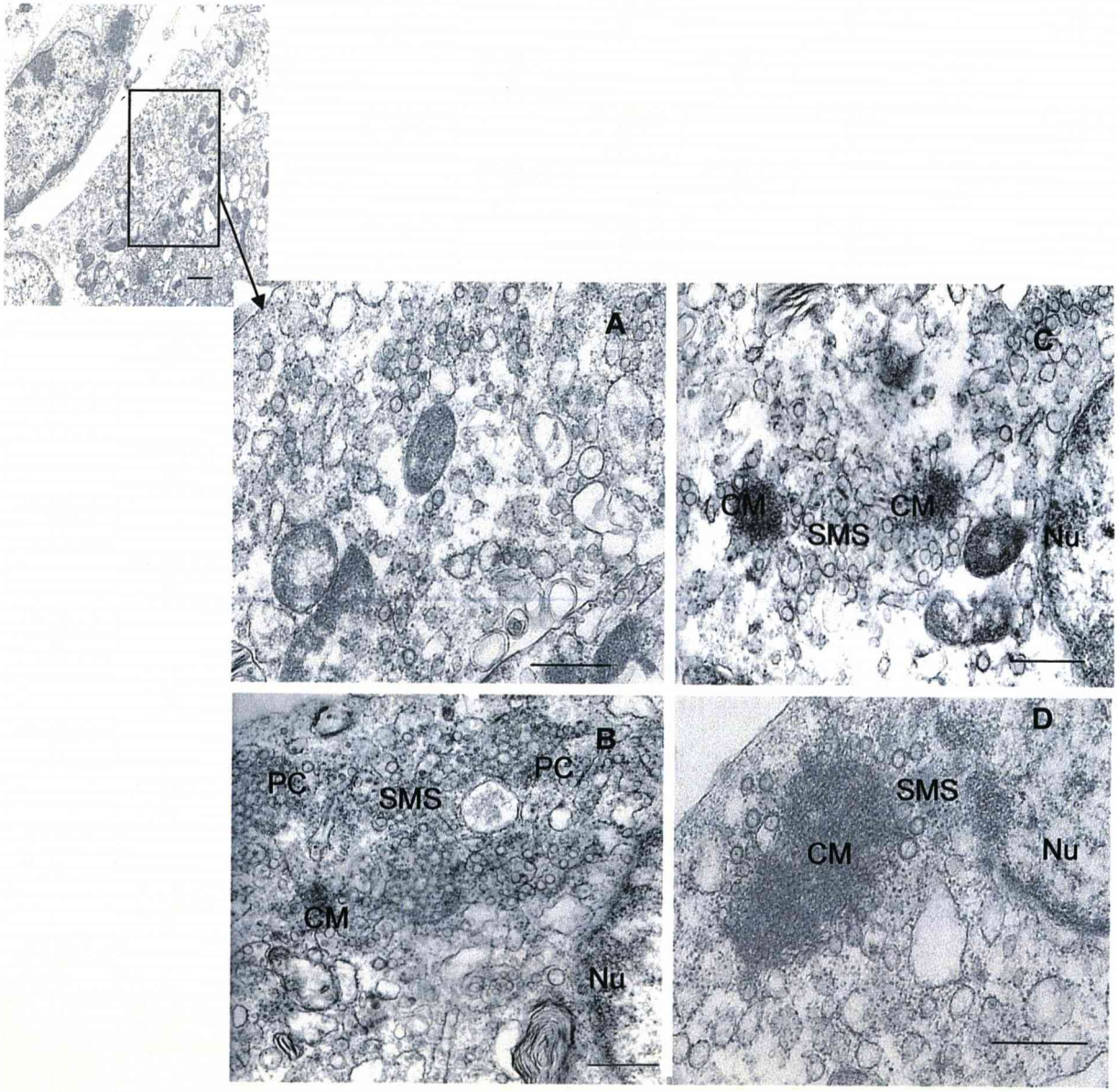

Figure 8-5. Ultrastructure comparison of the parental NY99- and attenuated $NS1_{130\text{-}132QQA/175A/207A}$ mutant virus-infected Vero cells. Both parental and attenuated infected cells show convoluted membranes (CM) near the nucleus (Nu) with associated smooth membrane structures (SMS). Swollen endoplasmic reticulum (ER) and mitochondria (Mi) evident in NY99 infected cells. Scale bar represents 500 nm.

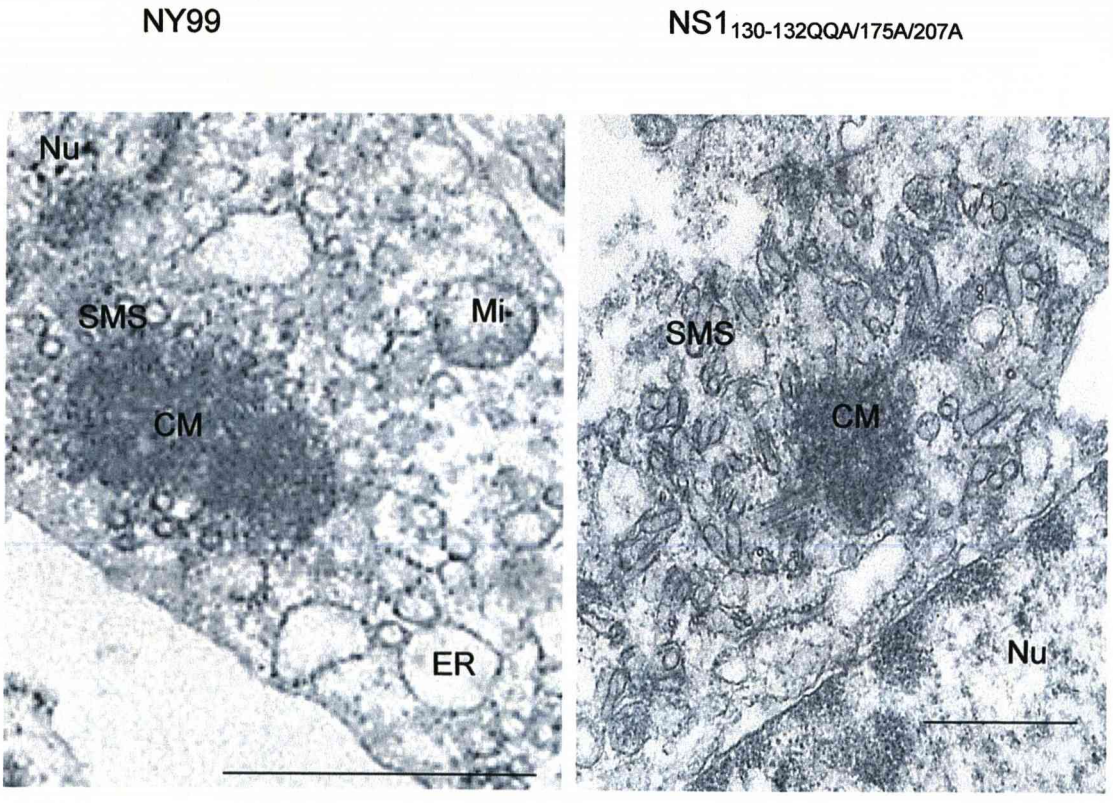

Figure 8-6. Ultrastructure of $NS1_{130\text{-}132QQA/175A/207A}$ mutant virus-infected Vero cells. Smooth membrane structures (SMS) within vesicle packets (VP) containing virus (V) throughout the cell. A paracrystalline structure (PC) also appears but no convoluted membranes (CM) were within this cell. Scale bar represents 500 nm.

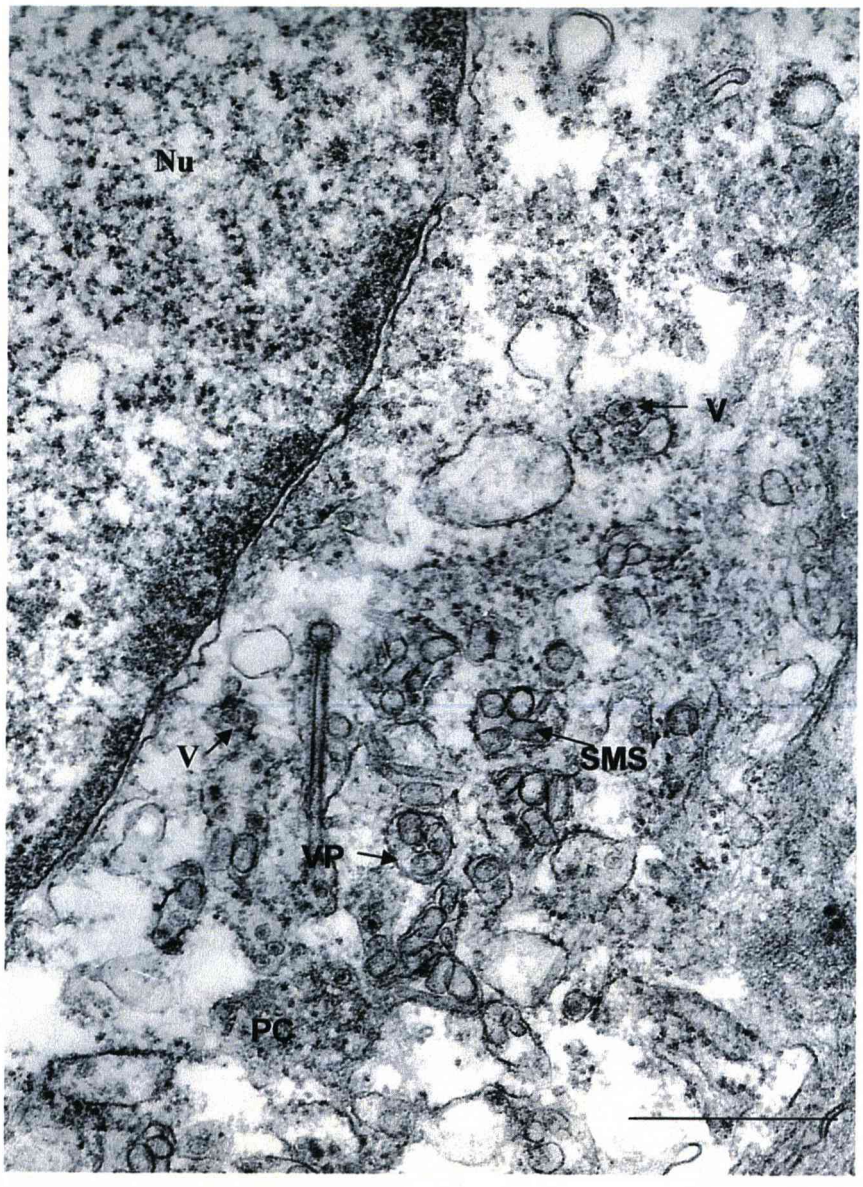

Figure 8-7. Transmission immuno-EM of mock- and NY99-infected Vero cells labeled with anti-E and anti-NS1 antibodies. Both mock- and virus-infected Vero cells labeled with 5 nm E anti-rabbit and 10 nm NS1 anti-mouse antibodies. Significant differences ($p<0.01$) in the level of E and NS1 were determined from the background of the mock-infected Vero cells compared to the NY99-infected Vero cells by Student's t-test. Scale bar 1 μm.

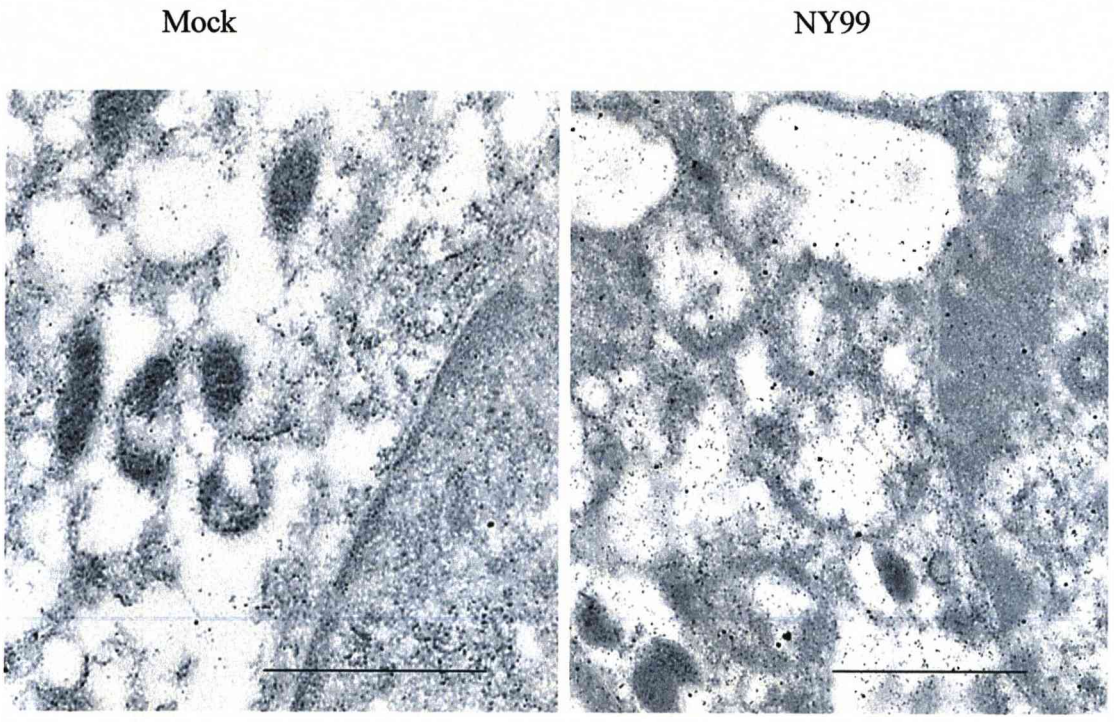

Figure 8-8. Localization of the E protein to convoluted membrane (CM) structures and vesicle associated virus. E protein localized to virus particles (V), CM and tubular membrane structures (TMS). Mitochondria (Mi). Scale bar 100 nm.

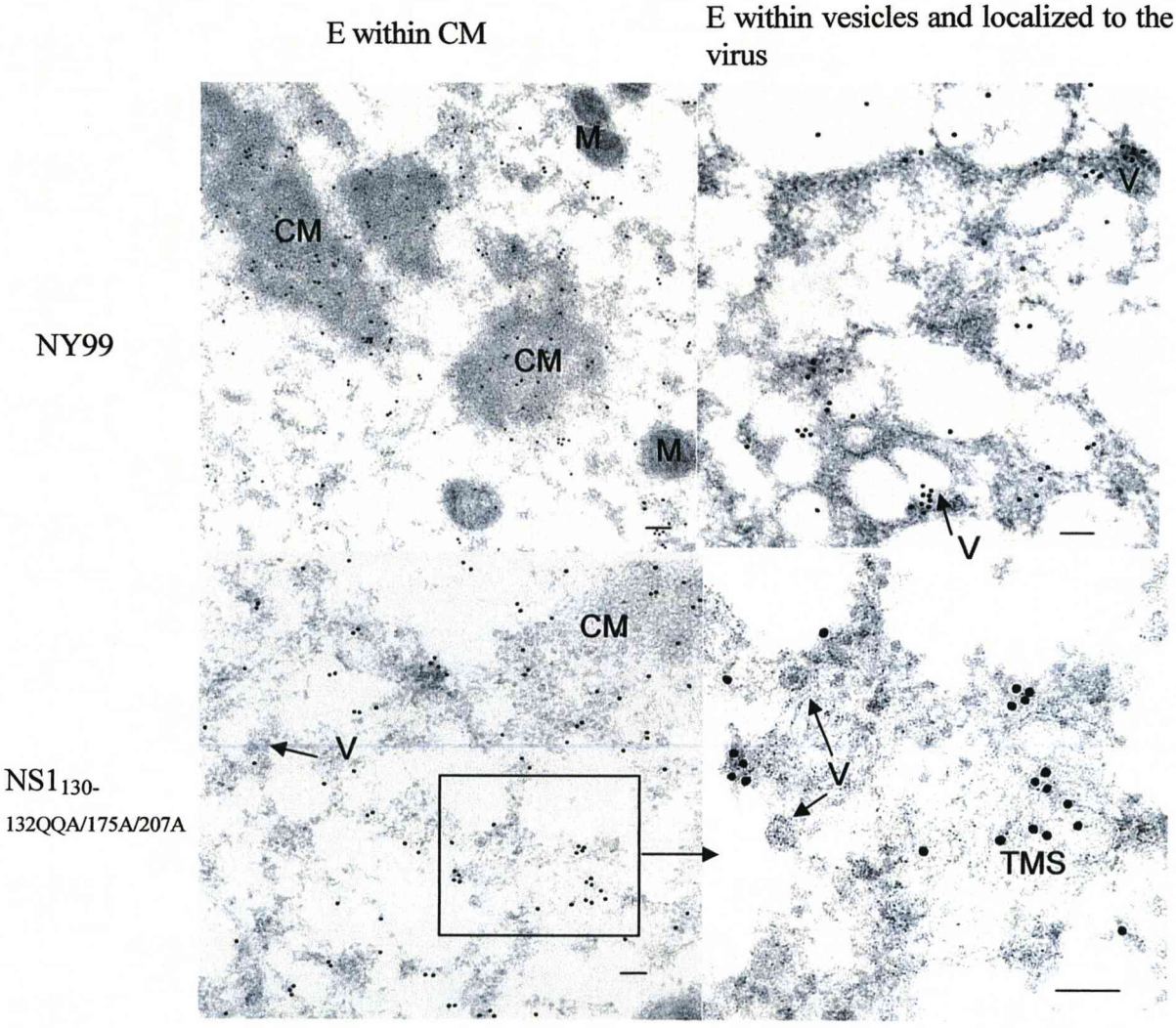

Figure 8-9 Colocalization of the E and NS1 proteins in the NY99- and $NS1_{130\text{-}132QQA/175A/207A}$ mutant virus-infected Vero cells. E protein labeled with 5 nm gold particles and NS1 with 10 nm gold particles. Scale bar 100 nm.

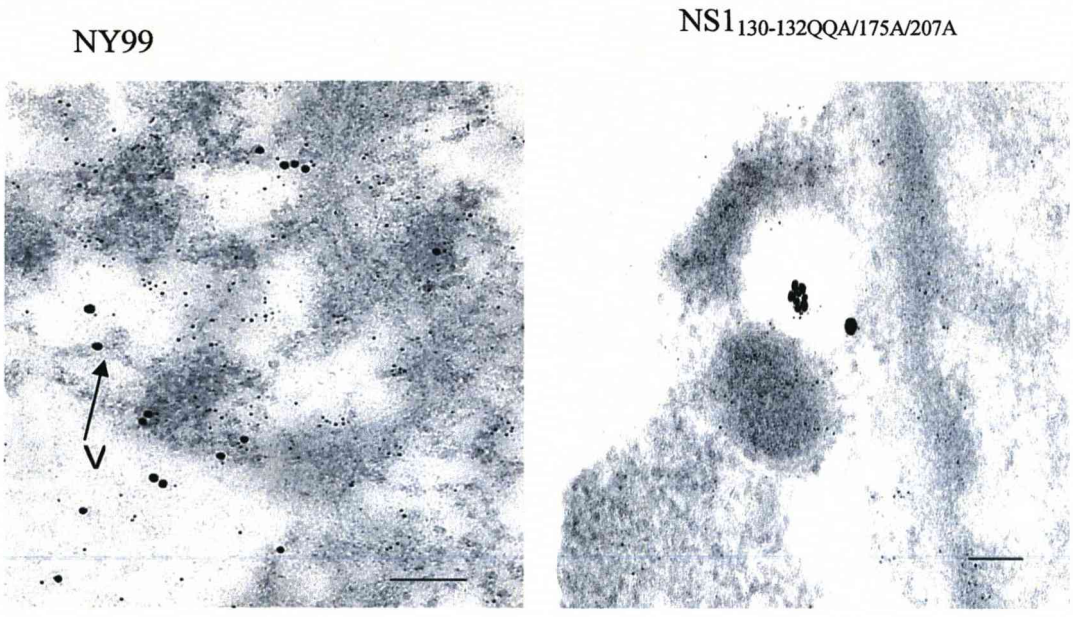

CHAPTER 9 : CYTOKINE EXPRESSION OF VIRULENT NY99 AND ATTENUATED NS1 GLYCOSYLATION MUTANT VIRUSES IN MOUSE SERUM

9.1 Introduction

Previous chapters examined the ablation of the NS1 glycosylation sites and the affects of these mutations in cell culture and in mice. Several mutant viruses were highly attenuated for neuroinvasiveness and neurovirulence in mice. The most attenuated NS1 glycosylation mutant virus in mice proved to be $NS1_{130\text{-}132QQA/175A/207A}$, which also showed decreased infectivity titre compared to the parental NY99 strain. This virus was stable in cell culture and in mice given that no reversions or putative compensating mutations were identified and the mouse experiments were highly reproducible.

The $NS1_{130A/175A.207A}$ mutant virus also proved highly attenuated for neuroinvasiveness in mice although the infectivity titre in cell culture was comparable to the parental NY99 strain. Interestingly, a reversion at $NS1_{130}$ and putative compensating mutations in the E protein were routinely observed in the viral RNA from brains of mice that succumbed to ip infection, but not in cell culture. Unlike the $NS1_{130\text{-}132QQA/175A/207A}$ mutant, however, the $NS1_{130A/175A/207A}$ mutant virus was not fully attenuated for mouse neurinvasiveness.

Previous experiments also indicated that the levels of intracellular and secreted NS1 protein (see chapters 5 and 8) and viraemia (see chapter 3) were reduced for the attenuated mutants compared to the parental NY99 strain. In order to better understand the mechanism for attenuation *in vivo,* cytokine assays were utilized to determine which, if any, cytokines were up-regulated or down-regulated in the parental NY99- and attenuated mutant-infected mice versus the mock-infected mice. Initially, the serum of parental NY99 virus-infected mice was screened using a

cytokine membrane to determine if there were differences in the levels of the cytokines between the infected and uninfected serum samples. A larger experiment involved the use of the Bioplex system to screen secreted cytokines in the serum of $NS1_{130A/175A/207A}$, $NS1_{130\text{-}132QQA/175A/207A}$, parental NY99 and mock-infected mice at three days post-ip inoculation.

Since it was also previously shown that the $NS1_{130A/175A/207A}$ mutant virus showed variable $ipLD_{50}$ values, it was hypothesized that the age of the mice may have contributed to this discrepancy. Due to the lack of available mice, the ages of the mice varied somewhat. Therefore, smaller groups of mice were obtained containing 3-week-old weanling and 5- week-old adult mice. The $ipLD_{50}$ of the $NS1_{130A/175A/207A}$ and $NS1_{130\text{-}132QQA/175A/207A}$ mutants and parental NY99 strain were examined for both age groups. At the same time, the sera of these mice were collected at one and three days post-ip infection for use with a cytokine Bioplex screening assay to determine any differences in cytokines secreted in the sera of weanling or adult mice.

9.2 Results

9.2.1 Cytokine membrane

Initial cytokine experiments involved the use of RayBiotech cytokine arrays and female 3-4 week old outbred mice. These arrays involved the use of a 62 cytokine coated membrane (see Material and Methods Fig. 2-2). Mouse blood was collected at one and two days post-ip infection from either parental NY99 virus- or mock-infected mice. The blood was allowed to coagulate at room temperature before centrifugation and collection of the serum, which was placed at -80°C before subsequent use. This serum was added to the cytokine membranes, incubated overnight before strepdavidin

incubation and chemiluminescence development of membranes. The cytokine levels were determined by a densitometer and significance ($p < 0.05$ by Students t-test) of each cytokine calculated.

9.2.1.1 New York 99- vs. Mock- infected

In this preliminary study, the effects on cytokines in the serum of mice following NY99 virus infection was determined by comparison of virus-infected versus mock-infected mice bled on one and two days post-infection. These time points were examined in this experiment since previous studies showed that high viraemia for NY99 virus-infected mice occurred on either one or two days post-ip infection, with total clearance from the serum by the fourth day (see chapter 3).

Interestingly, at one day post-infection there were no statistical differences between the NY99 virus-infected and mock-infected serum samples. At two days post-infection, the NY99 virus-infected serum samples showed significant cytokine differences compared to the mock-infected serum samples, including: eotaxin, interleukin 1 beta (IL-1β), interleukin 9 (IL-9), interleukin 17 (IL-17), lymphocyte adhesion molecule 1 (L-selectin), lymphotactin, macrophage inflammatory protein 1 gamma (MIP-1γ), macrophage inflammatory protein 3 alpha (MIP-3α) and soluble interferon receptor type 2 (sIFNrII). Although most of these cytokines were up-regulated in the virus-infected serum sample, one, eotaxin, was down-regulated compared to the mock-infected cells (Table 9-1).

9.2.2 Bioplex

The Bioplex technology differs from the cytokine membranes in that the antibodies used for the Bioplex are identified by laser capture rather than chemiluminescence. Real time fluorescence of each antibody tagged 'bead' is read for each antibody in the assay. These studies used either a mouse 23-plex kit or 32-plex (23-plex plus 9-plex) kit so that all cytokines could be assayed at one time (see Materials and Methods Table 2-3). In this larger study, all five mice in groups inoculated with either the parental NY99, $NS1_{130A/175A/207A}$ or $NS1_{130\text{-}132QQA/175A/207A}$ viruses were utilized to determine statistical ($p < 0.05$) differences in secreted cytokines between the virus-infected and mock-infected mice.

9.2.2.1 3-5-week-old mice

The initial Bioplex assay examined the extracellular cytokine expression in female outbred mice inoculated by the ip route with a dose of 1,000 PFU for the parental NY99 and $NS1_{130A/175A/207A}$ viruses and a higher dose of 10,000 PFU for the $NS1_{130\text{-}132QQA/175A/207A}$ virus. Due to the lack of availability of mice, 3-5-week-old mice were utilized. The blood from these mice was collected at three days post-infection only and the serum collected for the cytokine assay. Various virus doses were chosen for multiple reasons. Since all mice given 1,000 PFU of the parental NY99 succumbed to infection, this dose was chosen to determine the cytokine expression in mice infected with the virulent strain at the time point of high viraemia but before clearance of the virus (see Table 3-3 and Figure 3-4A). A dose of 1,000 PFU was chosen for $NS1_{130A/175A/207A}$ -infected mice since it was previously shown that mice inoculated with this dose resulted in some mice succumbing to infection while others survived

infection (see Table 3-3). It was hypothesized that differences in cytokines may be identified between mice that succumbed or survived infection. A higher dose of $NS1_{130\text{-}132QQA/175A/207A}$ virus was chosen since the $ipLD_{50}$ of this virus was higher than the other two viruses.

Similar to the preliminary cytokine membrane data, the initial Bioplex experiment revealed both up-regulation and down-regulation of various cytokines including: IL-9, IL-12p20, IL-12p40, IL-13, IL-17, monocyte chemotactic protein-1 or monocyte chemoattractant protein -1 (MCP-1) and cytokine induced neutrophil chemoattractant (KC) (Table 9-2). Of these, IL-12p20 was up regulated in $NS1_{130A/175A/207A}$, $NS1_{130\text{-}132QQA/175A/207A}$ and the parental NY99 virus-infected serum samples. In comparison interluekin-9 (IL-9), IL-13 and IL-17 were up-regulated only in the sera from $NS1_{130\text{-}132QA/175A/207A}$–infected mice, KC was up-regulated in the NY99 samples and MCP-1 was up-regulated in the sera from NY99 and $NS1_{130A/175A/207A}$ virus-infected mice. Down-regulation of cytokines was also demonstrated for IL-12p70 for the $NS1_{130\text{-}132QA/175A/207A}$ mice and for IL-17 for the $NS1_{130A/175A/207A}$ and NY99 serum samples.

The infectivity titres for the mouse serum samples used for this experiment were determined by plaque titration (Table 9-3). All five mice inoculated with the parental NY99 strain succumbed to infection and displayed infectivity titres of 4,500 to 11,000 PFU/ml. Similarly, the $NS1_{130A/175A/207A}$ mutant infected mouse serum had infectivity titres of 1,000 to 4,500 PFU/ml and all but one mouse succumbed to infection. The $NS1_{130\text{-}132QQA/175A/207A}$ mutant-infected serum samples, on the other hand, had no detectable viraemia and none of the mice succumbed to infection.

One mouse inoculated with the $NS1_{130A/175A/207A}$ mutant virus survived infection although the vireamia was high (Table 9-3). This mouse did show one significant difference in cytokine expression, a 4-fold increase of IL-10, compared to other serum samples from all viruses.

9.2.2.2 Weanling versus adult mice

Due to the lack of availability of mice, some of the previous mouse experiments utilized a mixture of weanling and adult mice. Since there was some variability in the LD_{50}'s between mouse experiments, it was hypothesized that this discrepancy was likely due to the differences in the immune response to infection. To test this hypothesis, 21 day (3 week) old weanling and 35 day (5 week) old adult mice were inoculated by the ip route with either $NS1_{130A/175A/207A}$, $NS1_{130\text{-}132QQA/175A/207A}$ or parental NY99 virus (Table 9-4). The NY99 virus-infected 3-week and 5-week-old mice showed similar $ipLD_{50}$ values of 10 and 5 PFU, respectively. There was also agreement for the $NS1_{130\text{-}132QQA/175A/207A}$ virus-infected 3- and 5-week-old mice with an $ipLD_{50}$ value of 100,000 and >500,000 PFU, respectively. The $NS1_{130A/175A/207A}$ virus-infected mice, on the other hand, showed different $ipLD_{50}$ values for the 3- and 5-week-old mice of 20 and 2,000 PFU, respectively. The sera from these mice were collected and used for subsequent Bioplex experiments. This time the 32-plex was used due to assay nine newly available cytokines; these nine cytokines were combined with the previously used 23 cytokines.

Since the $NS1_{130A/175A/207A}$ mutant virus showed differences in the $ipLD_{50}$ between the 3- and 5-week-old mice, the 100 PFU dose was selected for Bioplex cytokine screening to determine differences between mice that either succumbed or survived

infection. At this dose, four out of five 5-week-old mice survived infection whereas only one out of five 3-week-old mice survived infection. A higher dose of 10,000 PFU for the $NS1_{130\text{-}132QQA/175A/207A}$ inoculated mice was also chosen. Although highly attenuated in both the weanling and adult mice, three out of five 3-week-old mice survived infection whereas all of the 5-week-old mice survived infection. A dose of 1,000 PFU was chosen for the NY99 parental strain.

Due to the large sample volume required to test multiple time points, only the one and three day time points were utilized for the 5-week-old infected mice whereas only the three day time point was used for the 3-week-old infected mice. The time points were chosen since previous studies showed that low and high viraemia was correlated to one and three days post-infection, respectively, and the three day time point showed greater differences in preliminary studies (Figure 3-4A and Table 9-1).

Of the 32 cytokines examined in this study, 21 showed significant ($p< 0.05$) differences compared to the mock-infected serum samples including: IL-1α, IL-1β, IL-2, IL-3, IL-5, IL-9, IL-10, IL-12p40, IL-15, IL-17, IL-18, macrophage colony-stimulating factor (M-CSF), monokine induced by interferon gamma (MIG), macrophage inflammatory protein 2 (MIP-2), vascular endothelial growth factor (VEGF), eotaxin, MCP-1, MIP-1β, granulocyte colony-stimulating factor (G-CSF), granulocyte macrophage colony-stimulating factor (GM-CSF) and MIP-1α (Table 9-5). Interestingly, all of these cytokines were down-regulated in the parental NY99 virus-infected 5-week-old mice at one day post-inoculation. The 5-week-old $NS1_{130A/175A/207A}$ and $NS1_{130\text{-}132QQA/175A/207A}$ infected mouse serum samples at one day post-inoculation also showed that many cytokines down-regulated compared to the mock-infected mouse serum samples, including IL-1α, IL-3, IL-9, IL-10, IL-15, IL-

17, M-CSF, MIG, MIP-2, VEGF, MCP-1, MIP-1β and MIP-1α. At this time point, cytokines that were down-regulated in both the attenuated $NS1_{130A/175A/207A}$ and $NS1_{130\text{-}132QQA/175A/207A}$ mice were also down-regulated in the parental NY99 mice. By three days post-inoculation, the NY99 virus-infected 5-week-old mouse serum samples still showed down-regulation of most cytokines compared to the mock-infected mouse serum samples. The $NS1_{130A/175A/207A}$ virus-infected mouse sera, however, did not down-regulate any cytokines but there was up-regulation of IL-1β. At this time point, the $NS1_{130\text{-}132QQA/175A/207A}$ serum samples showed down-regulation of the IL-15 and G-CSF and up-regulation of M-CSF compared to the mock-infected serum samples.

As stated above, the sera from 3-week-old virus-infected mice was only examined at the three day time point. At this time point, the parental NY99 strain showed only three down-regulated cytokines (IL-17, IL-18 and MIP-1α) and one up-regulated cytokine (M-CSF) compared to the mock-infected mouse serum samples. The $NS1_{130A/175A/207A}$ virus-infected 3-week-old mouse serum samples also showed a combination of up- and down-regulated cytokines, including IL-15, M-CSF and MIG that were up-regulated, and IL-18 that was down-regulated. The $NS1_{130\text{-}132QQA/175A/207A}$ mutant virus showed only one difference in cytokine levels compared to the mock-infected mouse serum samples, namely M-CSF, which was up-regulated.

The infectivity titres for the serum samples used for this experiment were not determined in order to preserve the samples for future use to confirm these differences using other assays.

9.3 Discussion

Previous experiments showed that mutations in the NS1 glycosylation sites attenuated WNV for both neuroinvasiveness and neurovirulence in mice. These mutants showed decreased intracellular and secreted NS1 protein in cell culture and reduced vireamia in mice (chapters 3 to 6, 8). The NS1 protein has been implicated in severe dengue infections, including a link has been identified between high levels of circulating NS1 and life-threatening dengue hemorrhagic fever (Green and Rothman, 2006; Libraty *et al.*, 2002). Since some of the WNV NS1 mutants showed decreased levels of secreted NS1 protein in cell culture and reduced mortality in mice, it was hypothesized that levels of cytokine expression may reveal differences between the virulent and attenuated strains compared to mock-infected mice, and may contribute to the differences observed in the mouse neuroinvasive phenotype.

Cytokine expression showed several similarities among the parental NY99, $NS1_{130A/175A207A}$ and $NS1_{130\text{-}132QQA/175A/27A}$ mouse serum samples in separate experiments and demonstrated reproducible results. Some of these cytokines, such as MCP-1 and IL-12p40, were up-regulated in one experiment but down-regulated in another experiment. Since changes in the levels of these cytokines were identified in different experiments using different mice, these cytokines may be potentially important, and it is hypothesized that differences in vireamia or viral load may be, in part, due to the variability in cytokine expression. In fact, differences in cytokine expression was seen in mouse sera collected at different time points and between weanling mice, which were highly susceptible to infection, and adult mice, which were less susceptible to NS1 mutant virus infection. Although the infectivity titres were not determined for the Bioplex study of 3-and 5-week old mice, previous

infectivity titres of mouse serum samples demonstrated a correlation between vireamia and mortality where high vireamia was seen in mice that subsequently succumbed to infection and low or undetectable vireamia was seen in mice that survived infection (Table 3-3 and Table 9-3).

Other cytokines, such as IL-17, were consistent among different experiments suggesting its importance for WNV infection. Using mock-infected mouse serum samples as a baseline, IL-17 displayed down-regulation of expression in NY99 and $NS1_{130A/175A/207A}$ virus-infected mice, but not sera from $NS1_{130\text{-}132QQA/175A/207A}$ virus-infected mice. Since the $NS1_{130A/175A/207A}$ mutant virus showed high vireamia in all mice (Table 9-3) and mice that succumbed to infection often contained a reversion at $NS1_{130}$, it is hypothesized that this virus mimics virulent NY99 infection in mice that succumb to infection. Recently, IL-17 has been associated with a new subset of T helper (Th) cells eliciting a pro-inflammatory response against extracellular pathogens not efficiently cleared by Th1 or Th2 immunity (Bettelli *et al.*, 2007). Since both the NY99 and $NS1_{130A/175A/207A}$, but not $NS1_{130\text{-}132QQA/175A/207A}$ virus-infected mice showed down-regulation of IL-17, the expression of this cytokine may be suppressed by WNV infection. Unfortunately, these data do not allow conclusion that the difference in the down-regulation in the NY99-infected sera and the up-regulation of this cytokine in the $NS1_{130\text{-}132QQA/175A/207A}$ sera (Table 9-2) was due to the loss of secreted NS1. However, IL-17 may be an important factor in the clearance of this virus and, therefore, further work is needed to investigate the role of this cytokine.

Differences in the cytokine expression were seen between the 5-and 3-week-old mice. Interestingly, the 3-week-old mice did not have many changes in cytokine expression compared to the mock-infected samples despite the fact that the attenuated mutant

viruses were more lethal in the weanling mice than the adult mice. A comparison of neonate and adult mice showed that young mice have limited T-cell response including reduced ability to produce cytokines that are required for immune activation until adulthood is reached (Holladay and Smialowicz, 2000). It is, therefore, hypothesized that possible differences in the immune response to WNV in weanling and adult mice contributed to the limited immune response in the weanling mice.

One cytokine, IL-18, was down-regulated in both the virus-infected weanling and adult mice. This cytokine corresponded with a poor outcome since only groups of mice where at least four out of five mice succumbed to infection showed this down-regulation (Table 9-5). Interleukin-18 has been shown to induce Langerhans cell migration to the draining lymph node for the accumulation of dendritic cells and the reduction of major histocompatibility complex (MHC) class II (Cumberbatch *et al.*, 2001). Therefore, WNV may down-regulate IL-18 as a way of reducing the antigen presenting function of these cells, which triggers activation of T- and B-cells that may allow for immune evasion.

Although studies of cytokine expression for flavivirus infection have focused on the up-regulation of cytokines and their affects on the clearance of the virus, down-regulation of cytokines has also been noted. Down-regulation of IL-10, an anti-inflammatory cytokine, was seen in the brains of JE virus-infected mice, hypothesized to be the result of an overwhelming pro-inflammatory response (Swarp *et al.*, 2007). Down-regulation of IL-10 and IL-8 was seen by real time PCR of the RNA isolated from white blood cells of cynomolgus macaques infected with DEN-1 and DEN-4, but attributed to fluctuations in the normal response (Swarup *et al.*, 2007). Neither of these studies determined the affects of treatment with these cytokines. Interleukin-10

was down-regulated for the parental NY99, $NS1_{130A/175A/207A}$ and $NS1_{130-132QQA/175A/207A}$ infected 5-week-old mice one day post-infection and for the parental NY99 strain three days post-infection indicating it may be down-regulated in virus-infected mice early in infection and also important in the progression of infection since mice that survived infection did not show down-regulation of this cytokine at the later time points (Table 9-5). Also, a 4-fold increase in IL-10 was seen in the one mouse that survived $NS1_{130A/175A/207A}$ infection although having high viraemia (Table 9-3). These data suggest that IL-10 may be important for the progression of lethal WNV infection and experiments examining the treatment with this cytokine may be effective in clearance of the virus.

Interestingly, many of the cytokines examined showed no changes in the attenuated-infected mice samples. Since previous experiments found that the attenuated mutant viruses do not produce high viraemia, the lack of cytokine changes may be a direct result of the reduction in the multiplication of the virus in the blood. Again, this may indicate the importance of the virus to down-regulate cytokines to allow for efficient multiplication.

Although these studies did not confirm the interaction of secreted NS1 protein with cytokine expression, there was evidence that the cytokines respond differently to virulent and attenuated viruses. Also, these data showed that WNV infection results in the down-regulation of many cytokines. Published studies have focused on the up-regulated cytokines and their possible role in the clearance if WNV infection (Diamond *et al.*, 2003; Fredericksen *et al.*, 2004). Here it is suggested that WNV can suppress cytokines levels that allows for effective infection and that secreted NS1 may be involved either indirectly or directly in this process. Although no purified WNV

NS1 protein was available, future experiments examining the cytokine expression changes in mice inoculated with NS1 protein may reveal some of these changes.

Table 9-1. Cytokine changes in the parental NY99 virus-infected mouse serum samples compared to mock-infected 3-5-week-old mice at one and two days post-inoculation with 1,000 PFU using a cytokine membrane assay

Cytokine	1dpi	2dpi	p-value*
Eotaxin-2	nc	↑	0.02
IL-1β	nc	↓	0.04
IL-9	nc	↓	0.004
IL-17	nc	↓	0.04
L-selectin	nc	↓	0.03
Lymphotactin	nc	↓	0.04
MIP-1γ	nc	↓	0.02
MIP-3α	nc	↓	0.04
STNF-rII	nc	↓	0.04

Green= up-regulated and red= down-regulated, compared to mock-infected mice
dpi= days post-infection
*p-value of 2dpi of NY99 versus mock-infected serum

Table 9-2. Up- and down-regulation of cytokines in sera of 3-5-week-old mice inoculated with 1,000 PFU NY99 or $NS1_{130A/175A/207A}$ or 10,000 PFU $NS1_{130\text{-}132QQA/175A/207A}$ compared to mock-infected mouse serum three days post-infection using a Bioplex assay.

Virus	Cytokine						
	IL-9	IL-12p40	IL-12p70	IL-13	IL-17	KC	MCP-1
NY99	nc	↑ p=0.002	nc	nc	↓ p=0.04	↑ p=0.04	↑ p=0.005
$NS1_{130A/175A/207A}$	nc	↑ p=0.02	nc	nc	↓ p=o.02	nc	↑ p=0.003
$NS1_{130\text{-}132QQA/175A/207A}$	↑ p*=0.03	↑ p=0.04	↓ p=0.04	↑ p=0.02	↑ p=0.04	nc	nc

Green= up-regulated and red= down-regulated, nc= no change, compared to mock-infected mice
*p value indicates significance of up- or down-regulation compared to the mock-infected serum

Table 9-3. Infectivity titres (PFU/ml) in sera of 3-5-week-old mice infected with either NY99, $NS1_{130A/175A/207A}$ or $NS1_{130\text{-}132QQA/175A/207A}$ viruses at three days post infection.

Mouse	1	2	3	4	5
Virus					
NY99	10,000*	4,500*	8,000*	4,500*	11,000*
$NS1_{130A/175A/207A}$	4,000*	4,000	1,000*	4,500*	1,500*
$NS1_{130\text{-}132QQA/175A/207A}$	<50	<50	<50	<50	<50

* Succumbed to infection

Table 9-4. Lethality ($ipLD_{50}$) of NY99, $NS1_{130A/175A/207A}$ and $NS1_{130\text{-}132QQA/175A/207A}$-infected 3-and 5-week-old mice.

	Lethality in 3-week-old mice (PFU/LD_{50})	AST + SD*	Lethality in 5-week-old mice (PFU/LD_{50})	AST + SD
NY99	10	8.2 ± 0.9	5	9 ± 1.5
$NS1_{130A/175A/207A}$	30	9.3 ± 1.4	2,000	10 ± 1.3
$NS1_{130\text{-}132QQA/175A/207A}$	100,000	12.3 ± 4.1	>500,000	15 ± 0

*Average survival time in days ± standard deviation

Table 9-5. Cytokine expression in 3-week-old mice three days post-infection and 5-week-old mice at one and three days post-infection following inoculation with either NY99, $NS1_{130A/175A/207A}$ or $NS1_{130\text{-}132QQA/175A/207A}$ viruses.

	Dose	Surv/	IL-1α	IL-1β	IL-2	IL-3	IL-5	IL-9	IL-10	IL12-p40	IL-15	IL-17	IL-18	M-CSF	MIG	MIP-2	VEGF	Eotaxin	MCP-1	MIP-1β	G-CSF	GM-CSF	MIP-1α
5-week-old 1dpi																							
NY99	1,000	0/5	↓.003	↓.002	↓.004	↓.002	↓.04	↓.01	↓.02	↓.02	↓.03	↓.04	↓.005	↓.04	↓.04	↓.04	↓.04	↓.04	↓.006	↓.01	↓.04	↓.04	↓.02
$NS1_{130A/175A/207A}$	100	4/5	nc	nc	nc	↓.007	nc	↓.03	↓.03	nc	↓.01	↓.04	nc	↓.04	↓.02	↓.009	nc	nc	nc	nc	nc	nc	↓.03
$NS1_{130\text{-}132QQA/175A/207A}$	10,000	5/5	↓.02	nc	nc	nc	nc	nc	nc	nc	↓.04	nc	nc	↓.04	nc	nc	↓.04	nc	↓.02	↓.04	nc	nc	↓.02
5-week-old 3dpi																							
NY99	1,000	0/5	↓.005	↓.001	↓.002	↓.01	nc		↓.001	↓.01	↓.005	↓.02	↓.01	nc	nc	↓.01	↓.004		↓.003	↓.01	↓.004	↓.004	
$NS1_{130A/175A/207A}$	100	4/5	nc	↑.04	nc	nc	nc		nc	nc	nc	nc	nc	nc	nc	nc	nc		nc	nc	nc	nc	nc
$NS1_{130\text{-}132QQA/175A/207A}$	10,000	5/5	nc	nc	nc	nc	nc		nc	nc	↓.005	nc	nc	↑.04	nc	nc	nc		nc	nc	↓.04	nc	nc
3-week-old 3dpi																							
NY99	1,000	1/5	nc	nc	nc	nc	nc		nc	nc	nc	↓.04	↓.03	↑.04	nc	nc	nc		nc	nc	nc	nc	↓.04
$NS1_{130A/175A/207A}$	100	1/5	nc	nc	nc	nc	nc		nc	nc	↑.01	nc	↓.04	↑.03	↑.03	nc	nc		nc	nc	nc	nc	nc
$NS1_{130\text{-}132QQA/175A/207A}$	10,000	3/5	nc	nc	nc	nc	nc		nc	nc	nc	nc	nc	↑.04	nc	nc	nc		nc	nc	nc	nc	nc

*Survived infection over total mice. Grey=Not determined, green= up-regulated and red= down-regulated, nc=no change. Numbers under arrows indicated p value of up- or dpwn-regulation compared to mock-infected serum

Dpi=days post-infection

CHAPTER 10 : GENERAL DISCUSSION

West Nile virus is a mosquito-borne flavivirus and the causative agent of the highest numbers of human neuroinvasive cases in the United States in recent years (CDC, 2007). Before 1999, WNV was found in Europe, Asia, the Middle East and Africa (Hayes, 1989). In the summer of 1999, WNV was confined to the New York area. Subsequently, this virulent strain of WNV has spread across the United States, Canada, the Caribbean, Mexico and South America and has been responsible for thousands of human and animal deaths (Gubler, 2007). To date, no vaccine or antiviral is available for human use.

In order to develop a vaccine candidate or therapeutic target, it is necessary to understand the WNV replication cycle to effectively develop countermeasures to one or more of these steps. The flavivirus NS1 protein is a highly conserved glycoprotein whose function has not yet been fully determined; however, several studies suggest that the NS1 protein may be involved in various steps of the replication cycle (Lindenbach and Rice, 1997; Mackenzie *et al.,* 1996; Westaway *et al.,* 1997). The NS1 protein has also been shown to be associated with the cell membrane, within the cell and secreted from the cell (Winkler *et al.,* 1988). All mosquito-borne, tick-borne (TBE) and no known vector-borne (ENT) flaviviruses contain glycosylation sites in the NS1 protein, most of which are highly conserved, suggesting their importance for the function of the NS1 protein (Dalgarno *et al.,* 1986; Pryor and Wright 1994; Flamand *et al.,* 1992; Kuno *et al.,* 2006). Therefore, mutations in the WNV glycosylation sites were characterized, with the hypothesis that these mutations would attenuate the virus, lead to a better understanding of the function of this protein and potentially lead to advances in vaccine development.

The ablation of the NS1 glycosylation sites of WNV was used to generate a panel of mutants, none of which were temperature sensitive. Some of the mutant viruses displayed reduced replication in cell culture and attenuation in mice. Interestingly, an alanine, serine or glutamine substitution at the $NS1_{130}$ glycosylation site combined with an alanine substitution at $NS1_{175}$ and $NS1_{207}$ resulted in mutants ($NS1_{130A/175A/207A}$, $NS1_{130S/175A/207A}$, $NS1_{130Q/175A/207A}$, $NS1_{130\text{-}131SV/175A/207A}$ and $NS1_{130\text{-}132QQA/175A/207A}$) that displayed variable multiplication kinetics in cell culture and attenuation in mice compared to the parental NY99 strain. When the asparagine of the $NS1_{130}$ glycosylation motif was changed to an alanine in combination with the $NS1_{175}$ and $NS1_{207}$ mutations ($NS1_{130A/175A/207A}$), this virus was replication competent in cell culture, comparable to the parental NY99 strain, and highly attenuated in mice, although a reversion to asparagine or mutation to an aspartic acid at $NS1_{130}$ as well as two mutations in the E protein at E_{204} and E_{237} were commonly found in mice that succumbed following ip infection. These mutations were hypothesized to affect selective pressure since reversion and compensating mutations were found to be associated with mice that succumbed to ip inoculation, but were not found in cell culture. Also, the $NS1_{130}$ reversion to asparagine was commonly, but not exclusively, associated with the E mutations, while the E mutations were not found without the reversion at $NS1_{130}$. An alanine to aspartic acid at $NS1_{130}$ was also seen in two mice that succumbed to $NS1_{130A/175A/207A}$ infection. Aspartic acid differs from alanine by the replacement of one hydrogen with a carboxylic acid and differs from asparagine by one amide group, again suggesting that these mutations were the result of instability of the virus and not an artifact from the mutagenesis process.

This instability was not seen in any of the serine or glutamine mutant viruses and these mutants were also attenuated for mice at least 100-fold more that the $NS1_{130A/175A/207A}$ mutant virus, although the only difference was the amino acid at $NS1_{130}$ that resulted in loss of the glycosylation site. Disparate results of NS1 glycosylation mutant viruses were seen in separate studies for the related flavivirus dengue-2 (DEN-2) virus. Mutant viruses that contained an asparagine to glutamine change in the two NS1 glycosylation motifs of DEN-2 virus showed reduced replication and multiple compensating mutations in cell culture whereas changing the asparagine of the glycosylation motifs to an alanine in a chimeric DEN/TBE virus showed reduced replication competence, enhanced virulence and attenuation in mice (Crabtree *et al.*, 2005; Pletnev *et al.*, 1993). Although these studies did not compare mutant viruses with different amino acids at the NS1 glycosylation sites, the results described in previous chapters of this PhD thesis suggest that the disparities in the previous studies could be due to the differences in the amino acid substitutions used in these studies and the variable stability of the different amino acids, especially at the $NS1_{130}$ site.

Ablation of the glycosylation sites in the NS1 protein proved to be important for the virulence phenotype of WNV and is the first study to demonstrate that mutations in the NS1 protein attenuated the virus for neuroinvasiveness. In fact, these mutations completely attenuated for neuroinvasiveness in mice at the highest possible dose used and highly attenuated for mouse neurovirulence.

The NS1 glycosylation mutant viruses were highly attenuated and have potential for inclusion in candidate live attenuated vaccines; however, live-attenuated vaccine candidates should contain multiple attenuating mutations in several proteins to ensure reversion cannot occur. Therefore, mutations in the prM, E and NS4B proteins,

together with the NS1 mutations, were characterized. The prM mutant (prM_{15S}) contained a mutation at the prM glycosylation site that had not been previously described for WNV, whereas the E and NS4B mutations had previously been described as attenuating mutations for WNV (Beasley *et al.,* 2005; Wicker *et al.,* 2006). Interestingly, the mutant containing mutations in all four proteins ($prM_{15S}/E_{154S}/NS1_{130A/175A207A}/NS4B_{102S}$) was not attenuated in mice although some of the combinations of these mutations were found to be highly attenuated, indicating a delicate balance of attenuating mutations required for a successfully attenuated virus. Also of interest was the lack of attenuation following the ablation of the conserved prM glycosylation site, especially since the E and NS1 glycosylation mutant viruses were highly attenuated.

The ablation of the glycosylation site in the prM protein enhanced infectivity titre in cell culture and did not attenuate the virus in mice whereas the loss of glycosylation in the E and NS1 proteins reduced infectivity titre in cell culture and was attenuated in mice. It is unclear if this was the result of increased binding efficiency to cell receptor(s), fusion or assembly. Since WNV has been previously shown to interact with DC-SIGN, the prM_{15} mutant may be used in similar studies to determine the affects of this mutation related to DC-SIGN binding. Also altering the pH in cell culture is often an effective way to investigate mutations that affect the fusion process.

Another interesting finding was in the addition of the E_{154S} glycosylation mutation. Variable degrees of attenuation were seen in the mutants containing the E_{154S} glycosylation mutation in combination with the triple NS1 mutant viruses ($E_{154S}/NS1_{130A/175A/207A}$, $E_{154S}/NS1_{130\text{-}131SV/175A/207A}$ and $E_{154S}/NS1_{130\text{-}132QQA/175A/207A}$). Similar to the NS1 mutant viruses, the E/NS1 mutant virus with an asparagine to

alanine substitution at the $NS1_{130}$ glycosylation motif appeared less attenuated than the E/NS1 mutant with an asparagine to glutamine substitution at the $NS1_{130}$ site. Although the $E_{154S}/NS1_{130A/175A/207A}$ mutant virus was completely attenuated for neuroinvasiveness in mice at a dose >100,000 PFU, the $E_{154S}/NS1_{130\text{-}132QQA/175A/207A}$ did not multiply to >1,000 PFU/ml in cell culture indicating these mutations rendered the virus over-attenuated. These results also confirm that the amino acids at the $NS1_{130}$ site contribute to the overall fitness of the virus since these were the only amino acids different in these viruses.

The data in this thesis also suggest a possible interaction of the E and NS1 proteins. The $NS1_{130A/175A/207A}$ mutant showed reversion and mutations in the E protein in mice, yet none of the E/NS1 mutant viruses showed reversions or putative compensating mutations. In fact, the addition of the E_{154S} mutation appeared to stabilize these mutations in mice in that no mice succumbed to infection even at high doses. Further studies are necessary to identify this possible interaction.

The glycosylation of the NS1 clearly affected the virulence of WNV; however, the function(s) of this protein is(are) still unclear. Confocal microscopy showed that the intracellular NS1 was decreased in the attenuated NS1 glycosylation mutant virus infected Vero cells. Western blotting showed that secreted NS1 was also decreased independent of secreted E protein for mutant viruses that also showed the greatest reduction in infectivity titre in cell culture and attenuation in mice. Others have shown that there is a delay in the secretion of the NS1 protein compared to the release of the virus particle in cell culture (Macdonald *et al.*, 2005). These results suggest that the NS1 protein may not be involved in the release of the virus.

NS1 has been shown to colocalize with dsRNA and, therefore, is speculated to be a part of the replication complex (Mackenzie *et al.,* 1996). The deletion of the NS1 gene is lethal and therefore, the protein is necessary for replication of the virus, however, the NS1 protein may be supplied *in trans* which may indicate its function is independent of other proteins (Lindenbach and Rice, 1997). Since the NS1 protein showed differences in cell culture indicated by immunofluorescence, electron microscopy was used to further understand the affects of the NS1 glycosylation mutations in cell culture. Transmission EM of cells infected with the highly mouse attenuated NS1 glycosylation mutant virus, $NS1_{130\text{-}132QQA/175A/207A}$, showed many differences in the ultrastructure from that seen in the parental NY99-infected Vero cells. The most notable difference was the size and shape of the smooth membrane structures (SMS), previously described as flavivirus induced vesicles that contain the replication complex (Westaway *et al.,* 1997). West Nile virus-infected mosquito cells showed similar shaped SMS (Girard *et al.,* 2005). Since mosquito cells lack the enzymes required for the addition of complex carbohydrates, it is likely that the loss of NS1 glycosylation resulted in the changes of the SMS seen in Vero cells. This was the first study to identify a link in the formation of the SMS and the NS1 protein. Another interesting finding was the reduction in the presence of convoluted membranes (CM) and paracrystalline arrays (PC) in the $NS1_{130\text{-}132QQA/175A/207A}$ mutant-infected Vero cells. Although these membranes have been previously described in flavivirus-infected cells, no definitive function for these structures has been identified. The CM structures have been found to contain the protease NS3 and cofactor NS2B, and hypothesized to be the site of proteolytic cleavage (Mackenzie *et al.,* 1998). Immuno-EM of the E protein revealed the presence of this protein within the CM, suggesting a wider function for this structure (see chapter 8). The CMs were

consistently found in close proximity to the nucleus and hypothesized to be the site of virus assembly. Perhaps its location near the nucleus is necessary for assembly, and the capsid protein translocation to the nucleus may be necessary to perform assembly at this [perinuclear] location. Paracrystalline arrays are sometimes found in association with the CM and are hypothesized to be intermediate structures formed by the concentration of SMS that dissociate into CM. Given these data, the current hypothesis for virus replication in cells culture are as follows: 1) virus entry 2) fusion and disassembly 3) translation 4) formation of SMS by the NS1 protein that contains the replication complex 5) transport of the SMS in close proximity to the nucleus 6) localization of SMS near the nucleus and formation of PC 7) dissociation of PC into CM 8) virus assembly 9) maturation and release of the virus 10) secretion of NS1.

Since the NS1 protein is secreted from the cell after the release of the virus, this protein may not be involved in maturation or release of the virus. The function of this protein may be in the formation of SMS and transport of the replication complex in close proximity to the nucleus where assembly occurs. It is unclear why there would be a delay in the secretion of the NS1 protein, however, studies have shown that the majority of the NS1 remains intracellular while only a small fraction is released from the cell (Macdonald *et al.,* 2005).

A larger TEM study is necessary to understand the ultrastructural changes caused by the NS1 mutations. Other cell lines should be used to confirm the changes in the SMS structures. Also, other NS1 glycosylation mutant viruses should be used to confirm that the results seen in Chapter 8 were the result of the loss of glycosylation and not due to reduction in efficiency of virus replication. At the same time, various time points in the replication cycle of the parental NY99 and attenuated strains may also

elucidate if the ultrastructural changes are seen early and late in infection. This study may be extended to include changes in other proteins. Previous studies have shown that NS4A and NS4B proteins may be involved in the formation of virus-induced structures (Egger et al., 2002; Roosendaal et al., 2006; Miller et al., 2007). Therefore, including mutations in the NS1 and other NS proteins may lead to greater changes in the ultrastructure and could lead to a greater understanding of the synergy between proteins.

Recently the NS1 protein has been implicated in complement activation resulting in vascular leakage, which can lead to lethal dengue hemorrhagic fever (DHF) (Avirutnan *et al.,* 2006). It has been known for some time that the NS1 protein elicits a protective immune response probably due to the complement binding capabilities of NS1 antibodies (Schlesinger *et al.,* 1986; Schlesinger *et al.,* 1987; Chung *et al.,* 2006). West Nile virus-infected hamsters have been shown to secrete NS1 similar to the *in vitro* findings in that the secretion of the protein occurs after the release of mature virus and only a fraction of the NS1 was found extracellularly (Macdonald *et al.,* 2005). This systematic secretion of the NS1 protein after the release of the virus was, therefore, hypothesized to have a functional role, possibly immunomodulatory, rather than an accidental release of the protein due to cell damage (Macdonald *et al.,* 2005). NS1 has been shown to play a role in antibody dependent cellular cytoxicity and complement fixation (reviewed by Gibson et al., 1988), which is consistent with a role in the immune response. Since WNV does not cause vascular leakage like DHF, the NS1 protein may be involved in various aspects of the immune response. The NS1 glycosylation mutant viruses described in chapters 4 to 6 showed reduction of the secretion of the NS1 protein and were attenuated in mice. Viraemia studies showed

that the highly attenuated NS1 glycosylation mutant viruses displayed reduced or no viraemia, however, these viruses were replication competent in cell culture. The NS1 glycosylation mutant viruses did show a greater difference in the multiplication compared to the parental NY99 strain in the macrophage P388 D1 cells than the mammalian Vero cells, which may indicate multiple factors contributing to the attenuation of these viruses, including an immunomodulatory role. Cytokine expression assays of the parental NY99 and attenuated NS1 glycosylation mutant viruses in mice showed up- and down-regulation of several cytokines. Far more publications report the up-regulation of cytokine and their affects on the control of the virus than report down-regulation of cytokines. Chapter 9 explored the expression of secreted cytokines in the serum of infected mice and found that far more cytokines were down-regulated compared to the mock-infected mice. Some down-regulated cytokines corresponded with a poor outcome and therefore, it is hypothesized that WNV can suppress the immune response to infection, which may contribute to lethal infection. Although the down-regulation of these cytokines cannot be directly associated with the secretion, or lack of, of the NS1 protein, it is possible that the reduction of secreted NS1 did contribute to the cytokine expression.

In order to further understand the immunomodulatory capabilities of the NS1 protein, it is important to first determine that immune changes are the result of the NS1 protein. Mice given the NS1 protein alone may show some changes in the cytokine expression determined using the same assays described in Chapter 9 and inoculation of various knockout strains of mice with the NS1 mutants may help understand the interaction of NS1 with the immune system. Since mice inoculated with the attenuated strain did not show viraemia, the level of secreted NS1 cannot be

determined in these mice. However, it is hypothesized that the reduction of secreted NS1 resulted in inefficient replication and faster clearance of the virus. If correct, the induction of NS1 protein (*in trans*) simultaneous with infection of the attenuated NS1 mutant virus should result in increased mortality. Studies combining the attenuated mutant virus with wild-type NS1 protein may lead to a better understanding of the mechanism of attenuation for these mutant viruses.

These data indicate that the NS1 protein functions in various ways necessary for the replication of the virus and may have immunomodulatory capabilities. In light of these results, the NS1 protein may be a good therapeutic target for treatment of not only WNV, but also other flavivirus infections, such as DHF where high levels of circulating NS1 have been linked to a poor outcome. Finally, the ablation of the NS1 glycosylation sites in combination with the ablated E glycosylation site was replication competent in vaccine-certified Vero cells, mice showed little to no viraemia, even when inoculated with high doses of the virus, and were protected from subsequent challenge with a lethal dose of the parental strain, even in mice that were inoculated with low doses of mutant virus. In conclusion, these viruses proved to be effective components of future vaccine candidates.

BIBLIOGRAPHY

Aihara, H., Takasaki, T., Matsutani, T., Suzuki, R. and Kurane, I. 1998. Establishment and characterization of Japanese encephalitis virus-specific, human CD4(+) T-cell clones:flavivirus cross-reactivity, protein recognition and cytotoxic activity. J.Virol. 72, 8032-8036.

Alcon, S., Talarmin, A., Debruyne, M., Falconar, A., Deubel, V., Flamand, M., 2002. Enzyme-linked immunosorbent assay specific to Dengue virus type 1 nonstructural protein NS1 reveals circulation of the antigen in the blood during the acute phase of disease in patients experiencing primary or secondary infections. J.Clin.Microbiol. 40, 376-381.

Allison, S. L., Schalich, J., Stiasny, K., Mandl, C. W., Kunz, C., Heinz, F. X., 1995. Oligomeric rearrangement of tick-borne encephalitis virus envelope proteins induced by an acidic pH. J.Virol. 69, 695-700.

Alvarez, C. P., Lasala, F., Carrillo, J., Muniz, O., Corbi, A. L., Delgado, R., 2002. C-type lectins DC-SIGN and L-SIGN mediate cellular entry by Ebola virus in cis and in trans. J.Virol. 76, 6841-6844.

Amberg, S. M., Nestorowicz, A., McCourt, D. W., Rice, C. M., 1994. NS2B-3 proteinase-mediated processing in the yellow fever virus structural region: in vitro and in vivo studies. J.Virol. 68, 3794-3802.

Amberg, S. M., Rice, C. M., 1999. Mutagenesis of the NS2B-NS3-mediated cleavage site in the flavivirus capsid protein demonstrates a requirement for coordinated processing. J.Virol. 73, 8083-8094.

Anderson, J. F., Rahal, J. J., 2002. Efficacy of interferon alpha-2b and ribavirin against West Nile virus in vitro. Emerg.Infect.Dis. 8, 107-108.

Arroyo, J., Miller, C., Catalan, J., Myers, G. A., Ratterree, M. S., Trent, D. W., Monath, T. P., 2004. ChimeriVax-West Nile virus live-attenuated vaccine: preclinical evaluation of safety, immunogenicity, and efficacy. J.Virol. 78, 12497-12507.

Austin, R. J., Whiting, T. L., Anderson, R. A., Drebot, M. A., 2004. An outbreak of West Nile virus-associated disease in domestic geese (Anser anser domesticus) upon initial introduction to a geographic region, with evidence of bird to bird transmission. Can.Vet.J. 45, 117-123.

Avirutnan, P., Punyadee, N., Noisakran, S., Komoltri, C., Thiemmeca, S., Auethavornanan, K., Jairungsri, A., Kanlaya, R., Tangthawornchaikul, N., Puttikhunt, C., Pattanakitsakul, S. N., Yenchitsomanus, P. T., Mongkolsapaya, J., Kasinrerk, W., Sittisombut, N., Husmann, M., Blettner, M., Vasanawathana, S., Bhakdi, S., Malasit, P., 2006. Vascular leakage in severe dengue virus infections: a potential role for the nonstructural viral protein NS1 and complement. J.Infect.Dis. 193, 1078-1088.

Bakonyi, T., Gould, E. A., Kolodziejek, J., Weissenbock, H., Nowotny, N., 2004. Complete genome analysis and molecular characterization of Usutu virus that emerged in Austria in 2001: comparison with the South African strain SAAR-1776 and other flaviviruses. Virology 328, 301-310.

Beasley, D. W., Whiteman, M. C., Zhang, S., Huang, C. Y., Schneider, B. S., Smith, D. R., Gromowski, G. D., Higgs, S., Kinney, R. M., Barrett, A. D., 2005. Envelope

protein glycosylation status influences mouse neuroinvasion phenotype of genetic lineage 1 West Nile virus strains. J.Virol. 79, 8339-8347.

Ben-Nathan, D., Huitinga, I., Lustig, S., van, R. N., Kobiler, D., 1996. West Nile virus neuroinvasion and encephalitis induced by macrophage depletion in mice. Arch.Virol. 141, 459-469.

Bernkopf, H., Levine, S., Nerson, R., 1953. Isolation of West Nile virus in Israel. J.Infect.Dis. 93, 207-218.

Berthet, F. X., Zeller, H. G., Drouet, M. T., Rauzier, J., Digoutte, J. P., Deubel, V., 1997. Extensive nucleotide changes and deletions within the envelope glycoprotein gene of Euro-African West Nile viruses. J.Gen.Virol. 78 (Pt 9), 2293-2297.

Best, S. M., Morris, K. L., Shannon, J. G., Robertson, S. J., Mitzel, D. N., Park, G. S., Boer, E., Wolfinbarger, J. B., Bloom, M. E., 2005. Inhibition of interferon-stimulated JAK-STAT signaling by a tick-borne flavivirus and identification of NS5 as an interferon antagonist. J.Virol. 79, 12828-12839.

Bettelli, E., Korn, T., Kuchroo, V. K., 2007. Th17: the third member of the effector T cell trilogy. Curr.Opin.Immunol.

Bhatnagar, J., Guarner, J., Paddock, C. D., Shieh, W. J., Lanciotti, R. S., Marfin, A. A., Campbell, G. L., Zaki, S. R., 2007. Detection of West Nile virus in formalin-fixed, paraffin-embedded human tissues by RT-PCR: a useful adjunct to conventional tissue-based diagnostic methods. J.Clin.Virol. 38, 106-111.

Blaney, J. E., Jr., Manipon, G. G., Firestone, C. Y., Johnson, D. H., Hanson, C. T., Murphy, B. R., Whitehead, S. S., 2003. Mutations which enhance the replication of dengue virus type 4 and an antigenic chimeric dengue virus type 2/4 vaccine candidate in Vero cells. Vaccine 21, 4317-4327.

Blitvich, B. J., Mackenzie, J. S., Coelen, R. J., Howard, M. J., Hall, R. A., 1995. A novel complex formed between the flavivirus E and NS1 proteins: analysis of its structure and function. Arch.Virol. 140, 145-156.

Blitvich, B. J., Scanlon, D., Shiell, B. J., Mackenzie, J. S., Hall, R. A., 1999. Identification and analysis of truncated and elongated species of the flavivirus NS1 protein. Virus Res. 60, 67-79.

Blitvich, B. J., Scanlon, D., Shiell, B. J., Mackenzie, J. S., Pham, K., Hall, R. A., 2001. Determination of the intramolecular disulfide bond arrangement and biochemical identification of the glycosylation sites of the nonstructural protein NS1 of Murray Valley encephalitis virus. J.Gen.Virol. 82, 2251-2256.

Brinton, M. A., 2002. The molecular biology of West Nile Virus: a new invader of the western hemisphere. Annu.Rev.Microbiol. 56, 371-402.

Brinton, M. A., Dispoto, J. H., 1988. Sequence and secondary structure analysis of the 5'-terminal region of flavivirus genome RNA. Virology 162, 290-299.

Brinton, M. A., Fernandez, A. V., Dispoto, J. H., 1986. The 3'-nucleotides of flavivirus genomic RNA form a conserved secondary structure. Virology 153, 113-121.

Buckley, A., Dawson, A., Moss, SR., Hinsley, SA., Bellamy, PE., Gould EA. 2003. Serological evidence of West Nile virus, Usutu and Sindbis virus infection of birds in the UK. J.Gen. Virol. Oct;84 (Pt.10), 2807-17.

Cahour, A., Falgout, B., Lai, C. J., 1992. Cleavage of the dengue virus polyprotein at the NS3/NS4A and NS4B/NS5 junctions is mediated by viral protease NS2B-NS3, whereas NS4A/NS4B may be processed by a cellular protease. J.Virol. 66, 1535-1542.

Campbell, G. L., Ceianu, C. S., Savage, H. M., 2001. Epidemic West Nile encephalitis in Romania: waiting for history to repeat itself. Ann.N.Y.Acad.Sci. 951, 94-101.

Campbell, G. L., Marfin, A. A., Lanciotti, R. S., Gubler, D. J., 2002. West Nile virus. Lancet Infect.Dis. 2, 519-529.

Cardosa, J.M., Gordon, S., Hirsch, S., Spronger, T.A. and Porterfield, J.S. 1986. Interaction of West Nile virus with primary murine macrophages: role of cell activation and receptors for antibody amd complement. J.Virol. 57, 952-959.

Centres for Disease Control and Prevention (CDC). 2003. West Nile infection among turkey breeder farm workers-Wisconsin,2002. Morb.Mortal.Wkly.Rep.52, 1017-1019.

CDC.2007. West Nile virus activity-United States, 2006. Morb.Mortal.Wkly.Rep. 56, 556-559.

Chambers, T. J., McCourt, D. W., Rice, C. M., 1989. Yellow fever virus proteins NS2A, NS2B, and NS4B: identification and partial N-terminal amino acid sequence analysis. Virology 169, 100-109.

Chambers, T. J., McCourt, D. W., Rice, C. M., 1990. Production of yellow fever virus proteins in infected cells: identification of discrete polyprotein species and analysis of cleavage kinetics using region-specific polyclonal antisera. Virology 177, 159-174.

Chambers, T. J., Nestorowicz, A., Amberg, S. M., Rice, C. M., 1993. Mutagenesis of the yellow fever virus NS2B protein: effects on proteolytic processing, NS2B-NS3 complex formation, and viral replication. J.Virol. 67, 6797-6807.

Chambers, T. J., Nestorowicz, A., Rice, C. M., 1995. Mutagenesis of the yellow fever virus NS2B/3 cleavage site: determinants of cleavage site specificity and effects on polyprotein processing and viral replication. J.Virol. 69, 1600-1605.

Chang, H. H., Shyu, H. F., Wang, Y. M., Sun, D. S., Shyu, R. H., Tang, S. S., Huang, Y. S., 2002. Facilitation of cell adhesion by immobilized dengue viral nonstructural protein 1 (NS1): arginine-glycine-aspartic acid structural mimicry within the dengue viral NS1 antigen. J.Infect.Dis. 186, 743-751.

Chu, J. J., Ng, M. L., 2004. Infectious entry of West Nile virus occurs through a clathrin-mediated endocytic pathway. J.Virol. 78, 10543-10555.

Chu, P. W., Westaway, E. G., 1992. Molecular and ultrastructural analysis of heavy membrane fractions associated with the replication of Kunjin virus RNA. Arch.Virol. 125, 177-191.

Chung, K. M., Liszewski, M. K., Nybakken, G., Davis, A. E., Townsend, R. R., Fremont, D. H., Atkinson, J. P., Diamond, M. S., 2006. West Nile virus nonstructural protein NS1 inhibits complement activation by binding the regulatory protein factor H. Proc.Natl.Acad.Sci.U.S.A 103, 19111-19116.

Chung, K. M., Nybakken, G. E., Thompson, B. S., Engle, M. J., Marri, A., Fremont, D. H., Diamond, M. S., 2006. Antibodies against West Nile Virus nonstructural protein NS1 prevent lethal infection through Fc gamma receptor-dependent and -independent mechanisms. J.Virol. 80, 1340-1351.

Co, M. D., Terajima, M.,Cruz, J., Ennis, F.A. and Rothman,A.L. 2002. Human cytotixic T lymphocyte responses to live attenuated 17D yellow fever vaccine: identification of HLA-B35-restricted CTL epitopes on nonstructural proteins NS1, NS2b, NS3 and the structural protein E. Virology 293,151-163.

con-LePoder, S., Drouet, M. T., Roux, P., Frenkiel, M. P., Arborio, M., Durand-Schneider, A. M., Maurice, M., Le, B., I, Gruenberg, J., Flamand, M., 2005. The secreted form of dengue virus nonstructural protein NS1 is endocytosed by hepatocytes and accumulates in late endosomes: implications for viral infectivity. J.Virol. 79, 11403-11411.

Crabtree, M. B., Kinney, R. M., Miller, B. R., 2005. Deglycosylation of the NS1 protein of dengue 2 virus, strain 16681: construction and characterization of mutant viruses. Arch.Virol. 150, 771-786.

Crance, J. M., Scaramozzino, N., Jouan, A., Garin, D., 2003. Interferon, ribavirin, 6-azauridine and glycyrrhizin: antiviral compounds active against pathogenic flaviviruses. Antiviral Res. 58, 73-79.

Crooks, A. J., Lee, J. M., Easterbrook, L. M., Timofeev, A. V., Stephenson, J. R. 1994.The NS1 protein of tick-borne encephalitis virus forms multimeric species upon secretion from the host cell. J.Gen.Virol. 75, 3453-3460.

Cumberbatch, M., Dearman, R. J., Antonopoulos, C., Groves, R. W., Kimber, I., 2001. Interleukin (IL)-18 induces Langerhans cell migration by a tumour necrosis factor-alpha- and IL-1beta-dependent mechanism. Immunology 102, 323-330.

Dalgarno, L., Trent, D. W., Strauss, J. H., Rice, C. M., 1986. Partial nucleotide sequence of the Murray Valley encephalitis virus genome. Comparison of the encoded polypeptides with yellow fever virus structural and non-structural proteins. J.Mol.Biol. 187, 309-323.

Davis, B. S., Chang, G. J., Cropp, B., Roehrig, J. T., Martin, D. A., Mitchell, C. J., Bowen, R., Bunning, M. L., 2001. West Nile virus recombinant DNA vaccine protects mouse and horse from virus challenge and expresses in vitro a noninfectious recombinant antigen that can be used in enzyme-linked immunosorbent assays. J.Virol. 75, 4040-4047.

Davis, C. W., Nguyen, H. Y., Hanna, S. L., Sanchez, M. D., Doms, R. W., Pierson, T. C., 2006. West Nile virus discriminates between DC-SIGN and DC-SIGNR for cellular attachment and infection. J.Virol. 80, 1290-1301.

Deas, T. S., Binduga-Gajewska, I., Tilgner, M., Ren, P., Stein, D. A., Moulton, H. M., Iversen, P. L., Kauffman, E. B., Kramer, L. D., Shi, P. Y., 2005. Inhibition of flavivirus infections by antisense oligomers specifically suppressing viral translation and RNA replication. J.Virol. 79, 4599-4609.

Desai, A., Ravi, V., Chandramuki, A. and Gourie-Devi, M. 1995. Proliferative response of human peripheral blood mononuclear cells to Japanese encephalitis virus. Microbiol. Immunol. 39, 269-273.

Despres, P., Combredet, C., Frenkiel, M. P., Lorin, C., Brahic, M., Tangy, F., 2005. Live measles vaccine expressing the secreted form of the West Nile virus envelope glycoprotein protects against West Nile virus encephalitis. J.Infect.Dis. 191, 207-214.

Diamond, M. S., Shrestha, B., Mehlhop, E., Sitati, E., Engle, M., 2003. Innate and adaptive immune responses determine protection against disseminated infection by West Nile encephalitis virus. Viral Immunol. 16, 259-278.

Edgil, D., Harris, E., 2006. End-to-end communication in the modulation of translation by mammalian RNA viruses. Virus Res. 119, 43-51.

Egger, D., Wolk, B., Gosert, R., Bianchi, L., Blum, H. E., Moradpour, D., Bienz, K., 2002. Expression of hepatitis C virus proteins induces distinct membrane alterations including a candidate viral replication complex. J.Virol. 76, 5974-5984.

Elghonemy, S., Davis, W. G., Brinton, M. A., 2005. The majority of the nucleotides in the top loop of the genomic 3' terminal stem loop structure are cis-acting in a West Nile virus infectious clone. Virology 331, 238-246.

El Harrack, M. B., Le Guenno, Gounon, P. 1997. Isolement du virus West Nile au Maroc. Virologie. 1, 248-249.

Eliceiri, B. P., Klemke, R., Stromblad, S., Cheresh, D. A., 1998. Integrin alphavbeta3 requirement for sustained mitogen-activated protein kinase activity during angiogenesis. J.Cell Biol. 140, 1255-1263.

Elshuber, S., Allison, S. L., Heinz, F. X., Mandl, C. W., 2003. Cleavage of protein prM is necessary for infection of BHK-21 cells by tick-borne encephalitis virus. J.Gen.Virol. 84, 183-191.

Falconar, A. K., 1997. The dengue virus nonstructural-1 protein (NS1) generates antibodies to common epitopes on human blood clotting, integrin/adhesin proteins and binds to human endothelial cells: potential implications in haemorrhagic fever pathogenesis. Arch.Virol. 142, 897-916.

Falgout, B., Markoff, L., 1995. Evidence that flavivirus NS1-NS2A cleavage is mediated by a membrane-bound host protease in the endoplasmic reticulum. J.Virol. 69, 7232-7243.

Flamand, M., Deubel, V., Girard, M., 1992. Expression and secretion of Japanese encephalitis virus nonstructural protein NS1 by insect cells using a recombinant baculovirus. Virology 191, 826-836.

Flamand, M., Megret, F., Mathieu, M., Lepault, J., Rey, F. A., Deubel, V., 1999. Dengue virus type 1 nonstructural glycoprotein NS1 is secreted from mammalian cells as a soluble hexamer in a glycosylation-dependent fashion. J.Virol. 73, 6104-6110.

Fredericksen, B. L., Smith, M., Katze, M. G., Shi, P. Y., Gale, M., Jr., 2004. The host response to West Nile Virus infection limits viral spread through the activation of the interferon regulatory factor 3 pathway. J.Virol. 78, 7737-7747.

Geijtenbeek, T. B., van Duijnhoven, G. C., van Vliet, S. J., Krieger, E., Vriend, G., Figdor, C. G., van, K. Y., 2002. Identification of different binding sites in the dendritic

cell-specific receptor DC-SIGN for intercellular adhesion molecule 3 and HIV-1. J.Biol.Chem. 277, 11314-11320.

Georges, A. J., Lesbordes, J. L., Meunier, D. M. Y., Peters, C. J., Georges-Courbot, M. C., Gonzales, J. P. 1987. Fatal hepatitis from West Nile virus. Ann.Inst.Pasteur. 138, 237-244.

Gibson, C. A., Schlesinger, J. J., Barrett, A. D., 1988. Prospects for a virus non-structural protein as a subunit vaccine. Vaccine 6, 7-9.

Girard, Y. A., Popov, V., Wen, J., Han, V., Higgs, S., 2005. Ultrastructural study of West Nile virus pathogenesis in Culex pipiens quinquefasciatus (Diptera: Culicidae). J.Med.Entomol. 42, 429-444.

Goldblum, N. 1959. West Nile fever in the Middle East. Proc. 6th Int. Congr.Trop.Med.Malaria. 5,

Goto, A., Yoshii, K., Obara, M., Ueki, T., Mizutani, T., Kariwa, H., Takashima, I., 2005. Role of the N-linked glycans of the prM and E envelope proteins in tick-borne encephalitis virus particle secretion. Vaccine 23, 3043-3052.

Gould, E.A., and Buckley, A.1989. Antibody-dependent enhancement of yellow fever and Japanese encephalitis virus neurovirulence. J.Gen.Virol. 70,1605-1608.

Green, S., Rothman, A., 2006. Immunopathological mechanisms in dengue and dengue hemorrhagic fever. Curr.Opin.Infect.Dis. 19, 429-436.

Guarner, J., Shieh, W. J., Hunter, S., Paddock, C. D., Morken, T., Campbell, G. L., Marfin, A. A., Zaki, S. R., 2004. Clinicopathologic study and laboratory diagnosis of 23 cases with West Nile virus encephalomyelitis. Hum.Pathol. 35, 983-990.

Gubler, D. J., 2007. The continuing spread of West Nile virus in the western hemisphere. Clin.Infect.Dis. 45, 1039-1046.

Guirakhoo, F., Bolin, R. A., Roehrig, J. T., 1992. The Murray Valley encephalitis virus prM protein confers acid resistance to virus particles and alters the expression of epitopes within the R2 domain of E glycoprotein. Virology 191, 921-931.

Guirakhoo, F., Heinz, F. X., Mandl, C. W., Holzmann, H., Kunz, C., 1991. Fusion activity of flaviviruses: comparison of mature and immature (prM-containing) tick-borne encephalitis virions. J.Gen.Virol. 72 (Pt 6), 1323-1329.

Guo, J. T., Hayashi, J., Seeger, C., 2005. West Nile virus inhibits the signal transduction pathway of alpha interferon. J.Virol. 79, 1343-1350.

Hahn, C. S., Hahn, Y. S., Rice, C. M., Lee, E., Dalgarno, L., Strauss, E. G., Strauss, J. H., 1987. Conserved elements in the 3' untranslated region of flavivirus RNAs and potential cyclization sequences. J.Mol.Biol. 198, 33-41.

Halary, F., Amara, A., Lortat-Jacob, H., Messerle, M., Delaunay, T., Houles, C., Fieschi, F., renzana-Seisdedos, F., Moreau, J. F., chanet-Merville, J., 2002. Human cytomegalovirus binding to DC-SIGN is required for dendritic cell infection and target cell trans-infection. Immunity. 17, 653-664.

Hall, R. A., Khromykh, A. A., Mackenzie, J. M., Scherret, J. H., Khromykh, T. I., Mackenzie, J. S., 1999. Loss of dimerisation of the nonstructural protein NS1 of Kunjin virus delays viral replication and reduces virulence in mice, but still allows secretion of NS1. Virology 264, 66-75.

Halstead, S. 1989. Antibody, marophages, dengue virus infection, shock and haemorrhage: a pathogenic cascade. Rev. Infect. Dis. 11,S830-S839.

Hanley, K. A., Manlucu, L. R., Manipon, G. G., Hanson, C. T., Whitehead, S. S., Murphy, B. R., Blaney, J. E., Jr., 2004. Introduction of mutations into the non-structural genes or 3' untranslated region of an attenuated dengue virus type 4 vaccine candidate further decreases replication in rhesus monkeys while retaining protective immunity. Vaccine 22, 3440-3448.

Hanna, S. L., Pierson, T. C., Sanchez, M. D., Ahmed, A. A., Murtadha, M. M., Doms, R. W., 2005. N-linked glycosylation of west nile virus envelope proteins influences particle assembly and infectivity. J.Virol. 79, 13262-13274.

Hase, T., Summers, P. L., Eckels, K. H., Baze, W. B., 1987. An electron and immunoelectron microscopic study of dengue-2 virus infection of cultured mosquito cells: maturation events. Arch.Virol. 92, 273-291.

Hayes, C.G. 1989. West Nile Fever. The Arboviruses: Epidemiology and Ecology. T.P. Monath, Ed. Vol. V, 59-88.

Hayes, C. G., 2001. West Nile virus: Uganda, 1937, to New York City, 1999. Ann.N.Y.Acad.Sci. 951, 25-37.

Hayes, E.B., O'Leary, D.R. 2004. West Nile virus infection: a pediatric persective. Pediatrics. 113, 1375-1381.

Hayes, E. B., Sejvar, J. J., Zaki, S. R., Lanciotti, R. S., Bode, A. V., Campbell, G. L., 2005. Virology, pathology, and clinical manifestations of West Nile virus disease. Emerg.Infect.Dis. 11, 1174-1179.

Heinz, F. X., Allison, S. L., 2000. Structures and mechanisms in flavivirus fusion. Adv.Virus Res. 55, 231-269.

Heinz, F. X., Allison, S. L., 2003. Flavivirus structure and membrane fusion. Adv.Virus Res. 59, 63-97.

Higgs, S., Schneider, B. S., Vanlandingham, D. L., Klingler, K. A., Gould, E. A., 2005. Nonviremic transmission of West Nile virus. Proc.Natl.Acad.Sci.U.S.A 102, 8871-8874.

Holladay, S. D., Smialowicz, R. J., 2000. Development of the murine and human immune system: differential effects of immunotoxicants depend on time of exposure. Environ.Health Perspect. 108 Suppl 3, 463-473.

Hunsperger, E. A., Roehrig, J. T., 2006. Temporal analyses of the neuropathogenesis of a West Nile virus infection in mice. J.Neurovirol. 12, 129-139.

Hurlbut, H.S., Rizk, F., Taylor, R. M., Work, T. H., 1956. A study of the ecology of West Nile virus in Egypt. Am.J.Trop.Med.Hyg. 5, 579-620.

Iankov, I.D., Pandey, M., Harvey, M., Griesmann, G.E., Federspiel, M.J. and Russell, S.J. 2006. Immunoglobulin g antibody-mediated enhancement of measles virus infection can bypass the protective antiviral immune response. J.Virol. 80, 8530-8540.

Iglesias, M. C., Frenkiel, M. P., Mollier, K., Souque, P., Despres, P., Charneau, P., 2006. A single immunization with a minute dose of a lentiviral vector-based vaccine is highly effective at eliciting protective humoral immunity against West Nile virus. J.Gene Med. 8, 265-274.

Jacobson, E. R., Ginn, P. E., Troutman, J. M., Farina, L., Stark, L., Klenk, K., Burkhalter, K. L., Komar, N., 2005. West Nile virus infection in farmed American alligators (Alligator mississippiensis) in Florida. J.Wildl.Dis. 41, 96-106.

Jarvis, D. L., Finn, E. E., 1996. Modifying the insect cell N-glycosylation pathway with immediate early baculovirus expression vectors. Nat.Biotechnol. 14, 1288-1292.

Jeffers, S. A., Tusell, S. M., Gillim-Ross, L., Hemmila, E. M., Achenbach, J. E., Babcock, G. J., Thomas, W. D., Jr., Thackray, L. B., Young, M. D., Mason, R. J., Ambrosino, D. M., Wentworth, D. E., Demartini, J. C., Holmes, K. V., 2004. CD209L (L-SIGN) is a receptor for severe acute respiratory syndrome coronavirus. Proc.Natl.Acad.Sci.U.S.A 101, 15748-15753.

Jeha, L. E., Sila, C. A., Lederman, R. J., Prayson, R. A., Isada, C. M., Gordon, S. M., 2003. West Nile virus infection: a new acute paralytic illness. Neurology 61, 55-59.

Johansson, M., Brooks, A. J., Jans, D. A., Vasudevan, S. G., 2001. A small region of the dengue virus-encoded RNA-dependent RNA polymerase, NS5, confers interaction

with both the nuclear transport receptor importin-beta and the viral helicase, NS3. J.Gen.Virol. 82, 735-745.

Joubert, L., Oudar, J., Hannoun, C., Beytout, D., Corniou, B., Guillon, J. C., Panthier, R., 1970. [Epidemiology of the West Nile virus: study of a focus in Camargue. IV. Meningo-encephalomyelitis of the horse]. Ann.Inst.Pasteur (Paris) 118, 239-247.

Kanai, R., Kar, K., Anthony, K., Gould, L. H., Ledizet, M., Fikrig, E., Marasco, W. A., Koski, R. A., Modis, Y., 2006. Crystal structure of west nile virus envelope glycoprotein reveals viral surface epitopes. J.Virol. 80, 11000-11008.

Kapoor, H., Signs, K., Somsel, P., Downes, F. P., Clark, P. A., Massey, J. P., 2004. Persistence of West Nile Virus (WNV) IgM antibodies in cerebrospinal fluid from patients with CNS disease. J.Clin.Virol. 31, 289-291.

Kapoor, M., Zhang, L., Ramachandra, M., Kusukawa, J., Ebner, K. E., Padmanabhan, R., 1995. Association between NS3 and NS5 proteins of dengue virus type 2 in the putative RNA replicase is linked to differential phosphorylation of NS5. J.Biol.Chem. 270, 19100-19106.

Keelapang, P., Sriburi, R., Supasa, S., Panyadee, N., Songjaeng, A., Jairungsri, A., Puttikhunt, C., Kasinrerk, W., Malasit, P., Sittisombut, N., 2004. Alterations of pr-M cleavage and virus export in pr-M junction chimeric dengue viruses. J.Virol. 78, 2367-2381.

Khromykh, A.A, Westaway, E.G. 1996. RNA binding properties of core protein of the flavivirus Kunjin. Arch. Virol. 14, 685-699.

Khromykh, A. A., Sedlak, P. L., Westaway, E. G., 1999. trans-Complementation analysis of the flavivirus Kunjin ns5 gene reveals an essential role for translation of its N-terminal half in RNA replication. J.Virol. 73, 9247-9255.

Khromykh, A. A., Kondratieva, N., Sgro, J. Y., Palmenberg, A., Westaway, E. G., 2003. Significance in replication of the terminal nucleotides of the flavivirus genome. J.Virol. 77, 10623-10629.

Kinney, R. M., Butrapet, S., Chang, G. J., Tsuchiya, K. R., Roehrig, J. T., Bhamarapravati, N., Gubler, D. J., 1997. Construction of infectious cDNA clones for dengue 2 virus: strain 16681 and its attenuated vaccine derivative, strain PDK-53. Virology 230, 300-308.

Kleinschmidt-Demasters, B. K., Marder, B. A., Levi, M. E., Laird, S. P., McNutt, J. T., Escott, E. J., Everson, G. T., Tyler, K. L., 2004. Naturally acquired West Nile virus encephalomyelitis in transplant recipients: clinical, laboratory, diagnostic, and neuropathological features. Arch.Neurol. 61, 1210-1220.

Klenk, K, Snow, J., Morgan, K, Bowen, R., Stephens, M., Foster, F., Gordy, P., Beckett, S., Komar, N., Gubler, D., Bunning, M. 2004. Alligators as West Nile amplifiers. Emerg.Infect. Dis. 10, 2150-2155.

Klimstra, W. B., Nangle, E. M., Smith, M. S., Yurochko, A. D., Ryman, K. D., 2003. DC-SIGN and L-SIGN can act as attachment receptors for alphaviruses and distinguish between mosquito cell- and mammalian cell-derived viruses. J.Virol. 77, 12022-12032.

Komar, N., Langevin, S., Hinten, S., Nemeth, N., Edwards, E., Hettler, D., Davis, B., Bowen, R., Bunning, M. 2003. Experimental infection of North American birds with the New York 1999 strain of West Nile virus. Emerg.Infect.Dis.9, 311-322.

Konishi, E., Kurane, I., Mason, P.W., Innis, B.L. and Ennis, F.A. 1995. Japanese encephalitis virus-specific proliferative responses of human peripheral blood T lymphocytes, Am. J. Trop. Med.Hyg. 53,278-283.

Konan, K.V., Giddingd, T.H.Jr., Ikeda, M., Li, K., Lemon, S.M., Kirkgaard, K. 2003. Nonstructural protein precursor NS4A/B from Hepatitis C alters function and unltrastructure of host secretory apparatus. J.Virol. 77,7843-7855.

Koppel, E. A., van Gisbergen, K. P., Geijtenbeek, T. B., van, K. Y., 2005. Distinct functions of DC-SIGN and its homologues L-SIGN (DC-SIGNR) and mSIGNR1 in pathogen recognition and immune regulation. Cell Microbiol. 7, 157-165.

Kramer, L. D., Li, J., Shi, P. Y., 2007. West Nile virus. Lancet Neurol. 6, 171-181.

Kreil, T. R., Eibl, M. M., 1996. Nitric oxide and viral infection: NO antiviral activity against a flavivirus in vitro, and evidence for contribution to pathogenesis in experimental infection in vivo. Virology 219, 304-306.

Kroschewski, H., Allison, S. L., Heinz, F. X., Mandl, C. W., 2003. Role of heparan sulfate for attachment and entry of tick-borne encephalitis virus. Virology 308, 92-100.

Kuhn, R. J., Zhang, W., Rossmann, M. G., Pletnev, S. V., Corver, J., Lenches, E., Jones, C. T., Mukhopadhyay, S., Chipman, P. R., Strauss, E. G., Baker, T. S., Strauss,

J. H., 2002. Structure of dengue virus: implications for flavivirus organization, maturation, and fusion. Cell 108, 717-725.

Kumar, P., Uchil, P.D., Sulochana, P., Nirmala, G., Chandrashekar, R., Haridattatreya, M and Satchidanandam, V. 2003. Screening for T cell-eliciting proteins of Japanese encephalitis virus in a healthy JE-endemic human cohort using recombinant baculovirus-infected insect preparations. Arch.Virol. 148, 1569-1591.

Kummerer, B. M., Rice, C. M., 2002. Mutations in the yellow fever virus nonstructural protein NS2A selectively block production of infectious particles. J.Virol. 76, 4773-4784.

Kuno, G., Chang, G. J., 2006. Characterization of Sepik and Entebbe bat viruses closely related to yellow fever virus. Am.J.Trop.Med.Hyg. 75, 1165-1170.

Kurane, I., Brinton, M.A., Samson, A.L. and Ennis, F.A. 1991. Dengie virus-specific, human CD4+ CD8- cytotoxic T-cell clones:multiple patterns of virus cross-reactivity recognized by NS3-specific T-cell clones. J.Virol. 65,1823-1828.

Lanciotti, R. S., Roehrig, J. T., Deubel, V., Smith, J., Parker, M., Steele, K., Crise, B., Volpe, K. E., Crabtree, M. B., Scherret, J. H., Hall, R. A., Mackenzie, J. S., Cropp, C. B., Panigrahy, B., Ostlund, E., Schmitt, B., Malkinson, M., Banet, C., Weissman, J., Komar, N., Savage, H. M., Stone, W., McNamara, T., Gubler, D. J., 1999. Origin of the West Nile virus responsible for an outbreak of encephalitis in the northeastern United States. Science 286, 2333-2337.

Leary, K., Blair, C. D., 1980. Sequential events in the morphogenesis of japanese Encephalitis virus. J.Ultrastruct.Res. 72, 123-129.

Ledizet, M., Kar, K., Foellmer, H. G., Wang, T., Bushmich, S. L., Anderson, J. F., Fikrig, E., Koski, R. A., 2005. A recombinant envelope protein vaccine against West Nile virus. Vaccine 23, 3915-3924.

Lee, E., Stocks, C. E., Amberg, S. M., Rice, C. M., Lobigs, M., 2000. Mutagenesis of the signal sequence of yellow fever virus prM protein: enhancement of signalase cleavage In vitro is lethal for virus production. J.Virol. 74, 24-32.

Leung, D., Schroder, K., White, H., Fang, N. X., Stoermer, M. J., Abbenante, G., Martin, J. L., Young, P. R., Fairlie, D. P., 2001. Activity of recombinant dengue 2 virus NS3 protease in the presence of a truncated NS2B co-factor, small peptide substrates, and inhibitors. J.Biol.Chem. 276, 45762-45771.

Li, J., Loeb, J. A., Shy, M. E., Shah, A. K., Tselis, A. C., Kupski, W. J., Lewis, R. A., 2003. Asymmetric flaccid paralysis: a neuromuscular presentation of West Nile virus infection. Ann.Neurol. 53, 703-710.

Li, W., Brinton, M. A., 2001. The 3' stem loop of the West Nile virus genomic RNA can suppress translation of chimeric mRNAs. Virology 287, 49-61.

Libraty, D. H., Young, P. R., Pickering, D., Endy, T. P., Kalayanarooj, S., Green, S., Vaughn, D. W., Nisalak, A., Ennis, F. A., Rothman, A. L., 2002. High circulating levels of the dengue virus nonstructural protein NS1 early in dengue illness correlate with the development of dengue hemorrhagic fever. J.Infect.Dis. 186, 1165-1168.

Lin, C., Amberg, S. M., Chambers, T. J., Rice, C. M., 1993. Cleavage at a novel site in the NS4A region by the yellow fever virus NS2B-3 proteinase is a prerequisite for processing at the downstream 4A/4B signalase site. J.Virol. 67, 2327-2335.

Lin, R. J., Chang, B. L., Yu, H. P., Liao, C. L., Lin, Y. L., 2006. Blocking of interferon-induced Jak-Stat signaling by Japanese encephalitis virus NS5 through a protein tyrosine phosphatase-mediated mechanism. J.Virol. 80, 5908-5918.

Lin, Y. L., Huang, Y. L., Ma, S. H., Yeh, C. T., Chiou, S. Y., Chen, L. K., Liao, C. L., 1997. Inhibition of Japanese encephalitis virus infection by nitric oxide: antiviral effect of nitric oxide on RNA virus replication. J.Virol. 71, 5227-5235.

Lin, Y.LO., Chen, L.K., Liao, C.L., Yeh, C.T., Ma, S.H., Chen, J.L., Huang, Y.L., Chen, S.S., and Chiang, H.Y. 1998. DNA immunization with Japanese encephalitis virus nonstructural protein NS1 elicits protective immunity in mice, J.Virol. 72, 191-200.

Lindenbach, B. D., Rice, C. M., 1997. trans-Complementation of yellow fever virus NS1 reveals a role in early RNA replication. J.Virol. 71, 9608-9617.

Lindenbach, B. D., Rice, C. M., 1999. Genetic interaction of flavivirus nonstructural proteins NS1 and NS4A as a determinant of replicase function. J.Virol. 73, 4611-4621.

Liu, W. J., Chen, H. B., Khromykh, A. A., 2003. Molecular and functional analyses of Kunjin virus infectious cDNA clones demonstrate the essential roles for NS2A in virus assembly and for a nonconservative residue in NS3 in RNA replication. J.Virol. 77, 7804-7813.

Liu, W. J., Wang, X. J., Clark, D. C., Lobigs, M., Hall, R. A., Khromykh, A. A., 2006. A single amino acid substitution in the West Nile virus nonstructural protein NS2A

disables its ability to inhibit alpha/beta interferon induction and attenuates virus virulence in mice. J.Virol. 80, 2396-2404.

Liu, W. J., Wang, X. J., Mokhonov, V. V., Shi, P. Y., Randall, R., Khromykh, A. A., 2005. Inhibition of interferon signaling by the New York 99 strain and Kunjin subtype of West Nile virus involves blockage of STAT1 and STAT2 activation by nonstructural proteins. J.Virol. 79, 1934-1942.

Lo, M. K., Tilgner, M., Bernard, K. A., Shi, P. Y., 2003. Functional analysis of mosquito-borne flavivirus conserved sequence elements within 3' untranslated region of West Nile virus by use of a reporting replicon that differentiates between viral translation and RNA replication. J.Virol. 77, 10004-10014.

Lozach, P. Y., Amara, A., Bartosch, B., Virelizier, J. L., renzana-Seisdedos, F., Cosset, F. L., Altmeyer, R., 2004. C-type lectins L-SIGN and DC-SIGN capture and transmit infectious hepatitis C virus pseudotype particles. J.Biol.Chem. 279, 32035-32045.

Lundin, M., Monne, M., Widell, A., Von, H. G., Persson, M. A., 2003. Topology of the membrane-associated hepatitis C virus protein NS4B. J.Virol. 77, 5428-5438.

Lustig, S., Olshevsky, U., Ben-Nathan, D., Lachmi, B. E., Malkinson, M., Kobiler, D., Halevy, M., 2000. A live attenuated West Nile virus strain as a potential veterinary vaccine. Viral Immunol. 13, 401-410.

Macdonald, J., Tonry, J., Hall, R. A., Williams, B., Palacios, G., Ashok, M. S., Jabado, O., Clark, D., Tesh, R. B., Briese, T., Lipkin, W. I., 2005. NS1 protein

secretion during the acute phase of West Nile virus infection. J.Virol. 79, 13924-13933.

Mackenzie, J. M., Jones, M. K., Westaway, E. G., 1999. Markers for trans-Golgi membranes and the intermediate compartment localize to induced membranes with distinct replication functions in flavivirus-infected cells. J.Virol. 73, 9555-9567.

Mackenzie, J. M., Jones, M. K., Young, P. R., 1996. Immunolocalization of the dengue virus nonstructural glycoprotein NS1 suggests a role in viral RNA replication. Virology 220, 232-240.

Maier, C. C., Delagrave, S., Zhang, Z. X., Brown, N., Monath, T. P., Pugachev, K. V., Guirakhoo, F., 2007. A single M protein mutation affects the acid inactivation threshold and growth kinetics of a chimeric flavivirus. Virology 362, 468-474.

Malkinson, M., Banet, C., Khinich, Y., Samina, I., Pokamunski, S., Weisman, Y., 2001. Use of live and inactivated vaccines in the control of West Nile fever in domestic geese. Ann.N.Y.Acad.Sci. 951, 255-261.

Mandl, C. W., 2005. Steps of the tick-borne encephalitis virus replication cycle that affect neuropathogenesis. Virus Res. 111, 161-174.

Mandl, C. W., Kroschewski, H., Allison, S. L., Kofler, R., Holzmann, H., Meixner, T., Heinz, F. X., 2001. Adaptation of tick-borne encephalitis virus to BHK-21 cells results in the formation of multiple heparan sulfate binding sites in the envelope protein and attenuation in vivo. J.Virol. 75, 5627-5637.

Markoff, L., 2003. 5'- and 3'-noncoding regions in flavivirus RNA. Adv.Virus Res. 59, 177-228.

Markoff, L., Falgout, B., Chang, A., 1997. A conserved internal hydrophobic domain mediates the stable membrane integration of the dengue virus capsid protein. Virology 233, 105-117.

Martin, D.A., Biggerstaff, B.J., Allen, B., Johnson, A.J., Lanciotti, R.S., Roehrig, J.T. 2002. Use of imunoglobulin m cross-reactions in differential diagnosis of human flaviviral encephalitis infections in the United States. Clin.Diagn.Lab.Immunol. 9,544-549.

Mason, P. W., McAda, P. C., Dalrymple, J. M., Fournier, M. J., Mason, T. L. 1987. Expression of Japanese encephalitis virus antigens in Escherichia coli. Virology. 158, 361-372.

Mason, P. W., 1989. Maturation of Japanese encephalitis virus glycoproteins produced by infected mammalian and mosquito cells. Virology 169, 354-364.

Mastrangelo, E., Milani, M., Bollati, M., Selisko, B., Peyrane, F., Pandini, V., Sorrentino, G., Canard, B., Konarev, P. V., Svergun, D. I., de, L., X, Coutard, B., Khromykh, A. A., Bolognesi, M., 2007. Crystal structure and activity of Kunjin virus NS3 helicase; protease and helicase domain assembly in the full length NS3 protein. J.Mol.Biol. 372, 444-455.

Mathew, A., Kurane, I., Rothman, A.L., Zeng, L.L., Brinton, M.A. and Ennis,F,A. 1996. Dominant recognition by human CD8+ cytotoxic T lymphocytes of dengue virus nonstructural proteins NS3 and NS1.2a. J. Clin. Invest. 98,1684-1691.

Mathew, A., Kurane, I., Green, S. and 7 other authors. 1998. Predominance of HLA-restricted cytotoxic T-lymphocyte responses to serotype-cross-reactive epitopes on nonstructural proteins following natural secondary dengue virus infection. J.Virol. 72,3999-4004.

McArthur, M. A., Suderman, M. T., Mutebi, J. P., Xiao, S. Y., Barrett, A. D., 2003. Molecular characterization of a hamster viscerotropic strain of yellow fever virus. J.Virol. 77, 1462-1468.

Mehlhop, E., Diamond, M. S., 2006. Protective immune responses against West Nile virus are primed by distinct complement activation pathways. J.Exp.Med. 203, 1371-1381.

Mehlhop, E., Ansarah-Sobrinho, C., Johnson, S., Engle, M., Fremont, D.H., Pierson, T.C. and Diamond, M.S. 2007. Complement protein C1q inhibits antibody-dependent enhancement of flavivirus infection in an IgG subclass-spcific manner. Cell Host and Microbe. 2,417-426.

Melnick, J. L., Paul, J. R., Riordan, J. T., Barnett, V. H., Goldblum, N., Zabin, E., 1951. Isolation from human sera in Egypt of a virus apparently identical to West Nile virus. Proc.Soc.Exp.Biol.Med. 77, 661-665.

Miller, S., Kastner, S., Krijnse-Locker, J., Buhler, S., Bartenschlager, R., 2007. The non-structural protein 4A of dengue virus is an integral membrane protein inducing membrane alterations in a 2K-regulated manner. J.Biol.Chem. 282, 8873-8882.

Miller, S., Sparacio, S., Bartenschlager, R., 2006. Subcellular localization and membrane topology of the Dengue virus type 2 Non-structural protein 4B. J.Biol.Chem. 281, 8854-8863.

Minke, J. M., Siger, L., Karaca, K., Austgen, L., Gordy, P., Bowen, R., Renshaw, R. W., Loosmore, S., Audonnet, J. C., Nordgren, B., 2004. Recombinant canarypoxvirus vaccine carrying the prM/E genes of West Nile virus protects horses against a West Nile virus-mosquito challenge. Arch.Virol.Suppl 221-230.

Modis, Y., Ogata, S., Clements, D., Harrison, S. C., 2003. A ligand-binding pocket in the dengue virus envelope glycoprotein. Proc.Natl.Acad.Sci.U.S.A 100, 6986-6991.

Monath, T. P., Liu, J., Kanesa-Thasan, N., Myers, G. A., Nichols, R., Deary, A., McCarthy, K., Johnson, C., Ermak, T., Shin, S., Arroyo, J., Guirakhoo, F., Kennedy, J. S., Ennis, F. A., Green, S., Bedford, P., 2006. A live, attenuated recombinant West Nile virus vaccine. Proc.Natl.Acad.Sci.U.S.A 103, 6694-6699.

Mostashari, F., Bunning, M. L., Kitsutani, P. T., Singer, D. A., Nash, D., Cooper, M. J., Katz, N., Liljebjelke, K. A., Biggerstaff, B. J., Fine, A. D., Layton, M. C., Mullin, S. M., Johnson, A. J., Martin, D. A., Hayes, E. B., Campbell, G. L., 2001. Epidemic West Nile encephalitis, New York, 1999: results of a household-based seroepidemiological survey. Lancet 358, 261-264.

Mukhopadhyay, S., Kim, B. S., Chipman, P. R., Rossmann, M. G., Kuhn, R. J., 2003. Structure of West Nile virus. Science 302, 248.

Mukhopadhyay, S., Kuhn, R. J., Rossmann, M. G., 2005. A structural perspective of the flavivirus life cycle. Nat.Rev.Microbiol. 3, 13-22.

Munoz-Jordan, J. L., Laurent-Rolle, M., Ashour, J., Martinez-Sobrido, L., Ashok, M., Lipkin, W. I., Garcia-Sastre, A., 2005. Inhibition of alpha/beta interferon signaling by the NS4B protein of flaviviruses. J.Virol. 79, 8004-8013.

Munoz-Jordan, J. L., Sanchez-Burgos, G. G., Laurent-Rolle, M., Garcia-Sastre, A., 2003. Inhibition of interferon signaling by dengue virus. Proc.Natl.Acad.Sci.U.S.A 100, 14333-14338.

Murgue, B., Murri, S., Triki, H., Deubel, V., Zeller, H. G., 2001. West Nile in the Mediterranean basin: 1950-2000. Ann.N.Y.Acad.Sci. 951, 117-126.

Murray, J. M., Aaskov, J. G., Wright, P. J., 1993. Processing of the dengue virus type 2 proteins prM and C-prM. J.Gen.Virol. 74 (Pt 2), 175-182.

Muylaert, I. R., Chambers, T. J., Galler, R., Rice, C. M., 1996. Mutagenesis of the N-linked glycosylation sites of the yellow fever virus NS1 protein: effects on virus replication and mouse neurovirulence. Virology 222, 159-168.

Namba, K., Naka, K., Dansako, H., Nozaki, A., Ikeda, M., Shiratori, Y., Shimotohno, K., Kato, N. 2004. Establishment of hepatitis C virus replicon cell lines possessing interferon-resistant phenotype. Biochem.Biophys.Res.Commun. 323, 299-309.

Navarro-Sanchez, E., Altmeyer, R., Amara, A., Schwartz, O., Fieschi, F., Virelizier, J. L., renzana-Seisdedos, F., Despres, P., 2003. Dendritic-cell-specific ICAM3-grabbing non-integrin is essential for the productive infection of human dendritic cells by mosquito-cell-derived dengue viruses. EMBO Rep. 4, 723-728.

Nestorowicz, A., Chambers, T. J., Rice, C. M., 1994. Mutagenesis of the yellow fever virus NS2A/2B cleavage site: effects on proteolytic processing, viral replication, and evidence for alternative processing of the NS2A protein. Virology 199, 114-123.

Ni, H., Chang, G.J., Xie, H., Trent, D.W., Barrett, A.D. 1995. Molecular basis of attenuation of neurovirulence of wild-type Japanese encephalitis virus strain SA 14. J.Gen.Virol. 76, 409-413.

Ng, M. L., Hong, S. S., 1989. Flavivirus infection: essential ultrastructural changes and association of Kunjin virus NS3 protein with microtubules. Arch.Virol. 106, 103-120.

Ng, T., Hathaway, D., Jennings, N., Champ, D., Chiang, Y. W., Chu, H. J., 2003. Equine vaccine for West Nile virus. Dev.Biol.(Basel) 114, 221-227.

Nowak, T., Wengler, G. 1987. Analysis of disulfides present in the membrane proteins of the West Nile flavivirus. Virology. 156, 127-137.

Nowak, T., Faber, P.M., Wngler, G., Wengler, G. 1989. Analysis of the terminal sequence of West Nile virus structural proteins and of the *in vitro* translation of these proteins allows the proposal of a complete scheme of the proteolytic cleavages involved in their synthesis. Virology. 169,365-376.

Nybakken, G. E., Nelson, C. A., Chen, B. R., Diamond, M. S., Fremont, D. H., 2006. Crystal structure of the West Nile virus envelope glycoprotein. J.Virol. 80, 11467-11474.

Ogata, A., Nagashima, K., Hall, W. W., Ichikawa, M., Kimura-Kuroda, J., Yasui, K., 1991. Japanese encephalitis virus neurotropism is dependent on the degree of neuronal maturity. J.Virol. 65, 880-886.

Oliphant, T., Nybakken, G. E., Engle, M., Xu, Q., Nelson, C. A., Sukupolvi-Petty, S., Marri, A., Lachmi, B. E., Olshevsky, U., Fremont, D. H., Pierson, T. C., Diamond, M. S., 2006. Antibody recognition and neutralization determinants on domains I and II of West Nile Virus envelope protein. J.Virol. 80, 12149-12159.

Panthier, R., Hannoun, Cl., Beytout, D., Mouchet, J. 1968. Epiemiologie du virus West Nile. Etude d'un foyer en Camargue. III. Les maladies humaines. Ann.Inst. Pasteur. 115, 435-445.

Patkar, C. G., Jones, C. T., Chang, Y. H., Warrier, R., Kuhn, R. J., 2007. Functional requirements of the yellow fever virus capsid protein. J.Virol. 81, 6471-6481.

Pierson, T., Xu, Q., Nelson, S., Oliphant, T., Nybakken, G., Fremont, D. and Diamond, M. 2007. The Stoichiometry of antibody-mediated neutralization and enhancement of West Nile virus infection. Cell Host and Microbe. 1, 135-145.

Pepperell, C., Rau, N., Krajden, S., Kern, R., Humar, A., Mederski, B., Simor, A., Low, D. E., McGeer, A., Mazzulli, T., Burton, J., Jaigobin, C., Fearon, M., Artsob, H., Drebot, M. A., Halliday, W., Brunton, J., 2003. West Nile virus infection in 2002: morbidity and mortality among patients admitted to hospital in southcentral Ontario. CMAJ. 168, 1399-1405.

Pestova, T. V., Shatsky, I. N., Fletcher, S. P., Jackson, R. J., Hellen, C. U., 1998. A prokaryotic-like mode of cytoplasmic eukaryotic ribosome binding to the initiation

codon during internal translation initiation of hepatitis C and classical swine fever virus RNAs. Genes Dev. 12, 67-83.

Pletnev, A. G., Bray, M., Lai, C. J., 1993. Chimeric tick-borne encephalitis and dengue type 4 viruses: effects of mutations on neurovirulence in mice. J.Virol. 67, 4956-4963.

Pletnev, A. G., Claire, M. S., Elkins, R., Speicher, J., Murphy, B. R., Chanock, R. M., 2003. Molecularly engineered live-attenuated chimeric West Nile/dengue virus vaccines protect rhesus monkeys from West Nile virus. Virology 314, 190-195.

Pletnev, A. G., Putnak, R., Speicher, J., Wagar, E. J., Vaughn, D. W., 2002. West Nile virus/dengue type 4 virus chimeras that are reduced in neurovirulence and peripheral virulence without loss of immunogenicity or protective efficacy. Proc.Natl.Acad.Sci.U.S.A 99, 3036-3041.

Poidinger, M., Hall, R. A., Mackenzie, J. S., 1996. Molecular characterization of the Japanese encephalitis serocomplex of the flavivirus genus. Virology 218, 417-421.

Ponnuraj, E.M., Springer, J., Hayward, A.R., Wilson, H. and Simoes, E.A. 2003. Antibody-dependent enhancement, a possible mechanism in augmented pulmonary disease of respiratory syncytial virus i nthe Bonnet monkey model. J.Infect.Dis. 187, 1257-1263.

Porter, D.D., Larsen, A.E. and Porter, H.G. 1972. The pathogenesis of Aleutian disease of mink. II. Enhancement of tissue lesions following the administration of a killed virus vaccine or passive antibody. J. Immunol. 109,1-7.

Prabhakar, B.S. and Nathanson, N. 1981. Acute rabies death mediated by antibody. Nature. 290, 590-591.

Preugschat, F., Strauss, J. H., 1991. Processing of nonstructural proteins NS4A and NS4B of dengue 2 virus in vitro and in vivo. Virology 185, 689-697.

Preugschat, F., Yao, C. W., Strauss, J. H., 1990. In vitro processing of dengue virus type 2 nonstructural proteins NS2A, NS2B, and NS3. J.Virol. 64, 4364-4374.

Pruzanski, W. and Altman, R. 1962. Encephalitis due to West Nile fever virus. 1962. World Neurol. 3, 524.

Pryor, M. J., Gualano, R. C., Lin, B., Davidson, A. D., Wright, P. J., 1998. Growth restriction of dengue virus type 2 by site-specific mutagenesis of virus-encoded glycoproteins. J.Gen.Virol. 79 (Pt 11), 2631-2639.

Pryor, M. J., Wright, P. J., 1993. The effects of site-directed mutagenesis on the dimerization and secretion of the NS1 protein specified by dengue virus. Virology 194, 769-780.

Pryor, M. J., Wright, P. J., 1994. Glycosylation mutants of dengue virus NS1 protein. J.Gen.Virol. 75 (Pt 5), 1183-1187.

Qiao, M., Ashok, M., Bernard, K. A., Palacios, G., Zhou, Z. H., Lipkin, W. I., Liang, T. J., 2004. Induction of sterilizing immunity against West Nile Virus (WNV), by immunization with WNV-like particles produced in insect cells. J.Infect.Dis. 190, 2104-2108.

Ramanathan, M. P., Chambers, J. A., Pankhong, P., Chattergoon, M., Attatippaholkun, W., Dang, K., Shah, N., Weiner, D. B., 2006. Host cell killing by the West Nile Virus NS2B-NS3 proteolytic complex: NS3 alone is sufficient to recruit caspase-8-based apoptotic pathway. Virology 345, 56-72.

Reed, K. D., Meece, J. K., Henkel, J. S., Shukla, S. K., 2003. Birds, migration and emerging zoonoses: west nile virus, lyme disease, influenza A and enteropathogens. Clin.Med.Res. 1, 5-12.

Rey, F. A., Heinz, F. X., Mandl, C., Kunz, C., Harrison, S. C., 1995. The envelope glycoprotein from tick-borne encephalitis virus at 2 A resolution. Nature 375, 291-298.

Roehrig, J. T., Nash, D., Maldin, B., Labowitz, A., Martin, D. A., Lanciotti, R. S., Campbell, G. L., 2003. Persistence of virus-reactive serum immunoglobulin m antibody in confirmed west nile virus encephalitis cases. Emerg.Infect.Dis. 9, 376-379.

Roosendaal, J., Westaway, E. G., Khromykh, A., Mackenzie, J. M., 2006. Regulated cleavages at the West Nile virus NS4A-2K-NS4B junctions play a major role in rearranging cytoplasmic membranes and Golgi trafficking of the NS4A protein. J.Virol. 80, 4623-4632.

Samina, I., Khinich, Y., Simanov, M., Malkinson, M., 2005. An inactivated West Nile virus vaccine for domestic geese-efficacy study and a summary of 4 years of field application. Vaccine 23, 4955-4958.

Samuel, M. A., Diamond, M. S., 2005. Alpha/beta interferon protects against lethal West Nile virus infection by restricting cellular tropism and enhancing neuronal survival. J.Virol. 79, 13350-13361.

Samuel, M. A., Diamond, M. S., 2006. Pathogenesis of West Nile Virus infection: a balance between virulence, innate and adaptive immunity, and viral evasion. J.Virol. 80, 9349-9360.

Satchidanandam, V., Uchil, P. D., Kumar, P., 2006. Organization of flaviviral replicase proteins in virus-induced membranes: a role for NS1' in Japanese encephalitis virus RNA synthesis. Novartis.Found.Symp. 277, 136-145.

Sayao, A.L., Suchowersky,O., Al-Khathaami,A, Klassen, B., Katz, N.R., Sevick, R., Trilley, P., Fox,J., Patry,D.2004. Calgary experience with West Nile virus neurological syndrome during the late summer of 2003. Canadian J.Neurol.Sci. 31,194-203.

Schmidt, J. R., El Mansoury, H. K., 1963. Natural and experimental infection of Egyptian equines with West Nile virus. Ann.Trop.Med.Parasitol. 57, 415-427.

Schlesinger, J. J., Brandriss, M. W., Putnak, J. R., Walsh, E. E. 1990.Cell surface expression of yellow fever virus non-structural glycoprotein NS1: consequences of interaction with antibody. J.Gen.Virol. 71 (Pt 3), 593-599.

Schlesinger, J.J., Brandriss, M.W., Crop, C.B., Monath, T.P. 1986. Protection against yellow fever in monkeys by immunization with yellow fever virus nonstructural protein NS1. J.Virol. 60, 1153-1155.

Schlesinger, J.J., Brandriss, M.W., Walsh, E.E. 1987. Protection of mice against dengue 2 virus encephalitis by immunization with dengue 2 virus non-structural glycooprotein NS1. J.Gen.Virol. 68, 853-857.

Sejvar, J. J., Haddad, M. B., Tierney, B. C., Campbell, G. L., Marfin, A. A., Van Gerpen, J. A., Fleischauer, A., Leis, A. A., Stokic, D. S., Petersen, L. R., 2003a. Neurologic manifestations and outcome of West Nile virus infection. JAMA 290, 511-515.

Sejvar, J. J., Leis, A. A., Stokic, D. S., Van Gerpen, J. A., Marfin, A. A., Webb, R., Haddad, M. B., Tierney, B. C., Slavinski, S. A., Polk, J. L., Dostrow, V., Winkelmann, M., Petersen, L. R., 2003b. Acute flaccid paralysis and West Nile virus infection. Emerg.Infect.Dis. 9, 788-793.

Shimoni, Z., Niven, M. J., Pitlick, S., Bulvik, S., 2001. Treatment of West Nile virus encephalitis with intravenous immunoglobulin. Emerg.Infect.Dis. 7, 759.

Shrestha, B., Wang, T., Samuel, M. A., Whitby, K., Craft, J., Fikrig, E., Diamond, M. S., 2006. Gamma interferon plays a crucial early antiviral role in protection against West Nile virus infection. J.Virol. 80, 5338-5348.

Siger, L., Bowen, R. A., Karaca, K., Murray, M. J., Gordy, P. W., Loosmore, S. M., Audonnet, J. C., Nordgren, R. M., Minke, J. M., 2004. Assessment of the efficacy of a single dose of a recombinant vaccine against West Nile virus in response to natural challenge with West Nile virus-infected mosquitoes in horses. Am.J.Vet.Res. 65, 1459-1462.

Smithburn, K. C., Hughes, T. P., Burke, A, W., Paul, J. H., 1940. A neurotropic virus isolated from the blood of a native of Uganda. Am.J.Trop.Med.Hyg. 20, 471-492.

Southam, C. M., Moore, A. E., 1951. West Nile, Ilheus, and Bunyamwera virus infections in man. Am.J.Trop.Med.Hyg. 31, 724-741.

Southam, C. M., Moore, A. E., 1954. Induced virus infections in man by the Egypt isolates of West Nile virus. Am.J.Trop.Med.Hyg. 3, 19-50.

Speight, G., Westaway, E.G. 1989. Carboxy-terminal analysis of nine proteins specified by the flavivirus Kunjin:evidence that only the intracellular core protein is truncated. J.Gen.Virol. 70, 2209-2214.

Spigland, I., Jasinska-Klingberg, W., Hofsbi, E., Goldblum, N., 1958. Clinical and laboratory observations in an outbreak of West Nile fever in Isreal. Harefuah. 54, 275

Stadler, K., Allison, S. L., Schalich, J., Heinz, F. X., 1997. Proteolytic activation of tick-borne encephalitis virus by furin. J.Virol. 71, 8475-8481.

Sumiyoshi, H., Mori, C., Fuke, I., Morita, K., Kuhara, S., Kondou, J., Kikuchi, Y., Nagamatu, H., Igarashi, A., 1987. Complete nucleotide sequence of the Japanese encephalitis virus genome RNA. Virology 161, 497-510.

Swarup, V., Ghosh, J., Duseja, R., Ghosh, S., Basu, A., 2007. Japanese encephalitis virus infection decrease endogenous IL-10 production: correlation with microglial activation and neuronal death. Neurosci.Lett. 420, 144-149.

Takegami, T., Sakamuro, D., Furukawa, T., 1995. Japanese encephalitis virus nonstructural protein NS3 has RNA binding and ATPase activities. Virus Genes 9, 105-112.

Tassaneetrithep, B., Burgess, T. H., Granelli-Piperno, A., Trumpfheller, C., Finke, J., Sun, W., Eller, M. A., Pattanapanyasat, K., Sarasombath, S., Birx, D. L., Steinman, R. M., Schlesinger, S., Marovich, M. A., 2003. DC-SIGN (CD209) mediates dengue virus infection of human dendritic cells. J.Exp.Med. 197, 823-829.

Taylor, R. M., Work, T. H., Hurlbut, H. S., Rizk, F. 1956. A study of the ecology of West Nile virus in Egypt. Am.J.Trop.Med.Hyg. 5, 579-620.

Tber. Abdelhaq,A. 1996. West Nile fever in horses in Morocco. Bull. O.I.E. 11, 867-869.

Thurner, C., Witwer, C., Hofacker, I. L., Stadler, P. F., 2004. Conserved RNA secondary structures in Flaviviridae genomes. J.Gen.Virol. 85, 1113-1124.

Triki, H., Murri, S., Le, G. B., Bahri, O., Hili, K., Sidhom, M., Dellagi, K., 2001. [West Nile viral meningo-encephalitis in Tunisia]. Med.Trop.(Mars.) 61, 487-490.

Tsai, T. F., Popovici, F., Cernescu, C., Campbell, G. L., Nedelcu, N. I., 1998. West Nile encephalitis epidemic in southeastern Romania. Lancet 352, 767-771.

Uchil, P. D., Kumar, A. V., Satchidanandam, V., 2006. Nuclear localization of flavivirus RNA synthesis in infected cells. J.Virol. 80, 5451-5464.

Umareddy, I., Chao, A., Sampath, A., Gu, F., Vasudevan, S. G., 2006. Dengue virus NS4B interacts with NS3 and dissociates it from single-stranded RNA. J.Gen.Virol. 87, 2605-2614.

van der Most, R. G., Corver, J., Strauss, J. H., 1999. Mutagenesis of the RGD motif in the yellow fever virus 17D envelope protein. Virology 265, 83-95.

Varki, A., 1998. Factors controlling the glycosylation potential of the Golgi apparatus. Trends Cell Biol. 8, 34-40.

Varki, A. 1999. Essentials of Glycobiology: Ch. 5 Exploring the Biological Roles of Glycans, Cold Springs Harbor Laboratory Press, Edited by Ajit Varki, RichardCummings, Jeffry Esko, Hudson Freeze, Gerald Hart and Jamey Marth. Cold Harbor Springs, NY.

Wallace, M.J., Smith, D.W., Broom, A.K., Mackenzie, J.S., Hall, R.A., Shellam, G.R. and McMinn, P.C. 2003. Antibody-dependent enhancement of Murray Valley encephalitis virus virulence in mice. J.Gen.Virol. 84, 1723-1728.

Wang, E., Ryman, K.D., Jennings, A.D., Wood, D.J., Taffs,F., Minor, P.D., Sanders, P.G., Barrett, A.D. 1995. Comparison of the genomes of the wild-type French viscerotropic strain of yellow fever virus with its vaccine derivative French neurotropic vaccine. J.Gen. Virol. 76, 2749-2755.

Wang, T., Scully, E., Yin, Z., Kim, J. H., Wang, S., Yan, J., Mamula, M., Anderson, J. F., Craft, J., Fikrig, E., 2003. IFN-gamma-producing gamma delta T cells help control murine West Nile virus infection. J.Immunol. 171, 2524-2531.

Wang, W. K., Sung, T. L., Lee, C. N., Lin, T. Y., King, C. C., 2002. Sequence diversity of the capsid gene and the nonstructural gene NS2B of dengue-3 virus in vivo. Virology 303, 181-191.

Ward, M. P., Schuermann, J. A., Highfield, L. D., Murray, K. O., 2006. Characteristics of an outbreak of West Nile virus encephalomyelitis in a previously uninfected population of horses. Vet.Microbiol. 118, 255-259.

Watson, J. T., Pertel, P. E., Jones, R. C., Siston, A. M., Paul, W. S., Austin, C. C., Gerber, S. I., 2004. Clinical characteristics and functional outcomes of West Nile Fever. Ann.Intern.Med. 141, 360-365.

Wengler, G., Wengler, G., 1989. Cell-associated West Nile flavivirus is covered with E+pre-M protein heterodimers which are destroyed and reorganized by proteolytic cleavage during virus release. J.Virol. 63, 2521-2526.

Westaway, E. G., Goodman, M. R., 1987. Variation in distribution of the three flavivirus-specified glycoproteins detected by immunofluorescence in infected Vero cells. Arch.Virol. 94, 215-228.

Westaway, E. G., Khromykh, A. A., Kenney, M. T., Mackenzie, J. M., Jones, M. K., 1997. Proteins C and NS4B of the flavivirus Kunjin translocate independently into the nucleus. Virology 234, 31-41.

Wicker, J. A., Whiteman, M. C., Beasley, D. W., Davis, C. T., Zhang, S., Schneider, B. S., Higgs, S., Kinney, R. M., Barrett, A. D., 2006. A single amino acid substitution in the central portion of the West Nile virus NS4B protein confers a highly attenuated phenotype in mice. Virology 349, 245-253.

Winkler, G., Randolph, V. B., Cleaves, G. R., Ryan, T. E., Stollar, V., 1988. Evidence that the mature form of the flavivirus nonstructural protein NS1 is a dimer. Virology 162, 187-196.

Winkler, G., Maxwell, S. E., Ruemmler, C., Stollar, V. 1989.Newly synthesized dengue-2 virus nonstructural protein NS1 is a soluble protein but becomes partially hydrophobic and membrane-associated after dimerization. Virology. 171,302-305.

Wong, S. J., Demarest, V. L., Boyle, R. H., Wang, T., Ledizet, M., Kar, K., Kramer, L. D., Fikrig, E., Koski, R. A., 2004. Detection of human anti-flavivirus antibodies with a west nile virus recombinant antigen microsphere immunoassay. J.Clin.Microbiol. 42, 65-72.

Yamshchikov, G., Borisevich, V., Seregin, A., Chaporgina, E., Mishina, M., Mishin, V., Kwok, C. W., Yamshchikov, V., 2004. An attenuated West Nile prototype virus is highly immunogenic and protects against the deadly NY99 strain: a candidate for live WN vaccine development. Virology 330, 304-312.

Yamshchikov, V. F., Compans, R. W., 1994. Processing of the intracellular form of the west Nile virus capsid protein by the viral NS2B-NS3 protease: an in vitro study. J.Virol. 68, 5765-5771.

Yoshii, K., Konno, A., Goto, A., Nio, J., Obara, M., Ueki, T., Hayasaka, D., Mizutani, T., Kariwa, H., Takashima, I., 2004. Single point mutation in tick-borne encephalitis virus prM protein induces a reduction of virus particle secretion. J.Gen.Virol. 85, 3049-3058.

Young, P. R., Hilditch, P. A., Bletchly, C., Halloran, W., 2000. An antigen capture enzyme-linked immunosorbent assay reveals high levels of the dengue virus protein NS1 in the sera of infected patients. J.Clin.Microbiol. 38, 1053-1057.

Zeng, L., Kurane, I., Okamoto, Y., Ennis, F.A. and Brinton, M.A. 1996. Identification of amino acids involved in recognition by dengue virus NS3-specific, HLA-DR15-restricted cytotoxic CD4+ T-cell clones. J.Virol. 70,3108-3117.

Zhang, Y., Corver, J., Chipman, P. R., Zhang, W., Pletnev, S. V., Sedlak, D., Baker, T. S., Strauss, J. H., Kuhn, R. J., Rossmann, M. G., 2003. Structures of immature flavivirus particles. EMBO J. 22, 2604-2613.

Zhang, Y., Zhang, W., Ogata, S., Clements, D., Strauss, J. H., Baker, T. S., Kuhn, R. J., Rossmann, M. G., 2004. Conformational changes of the flavivirus E glycoprotein. Structure. 12, 1607-1618.